UNIVERSITY OF READING

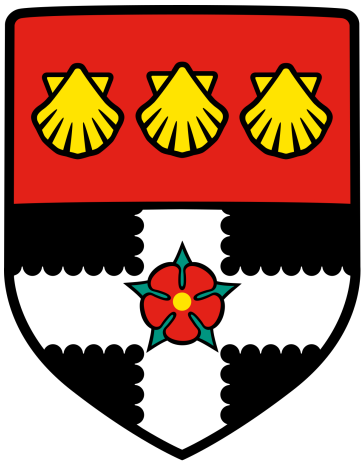

Investigation of how redox processes regulate platelet function in health and disease

A thesis submitted for the degree of Doctor of Philosophy

By

Renato Simões Gaspar

Institute for Cardiovascular and Metabolic Research

School of Biological Sciences

September 2020

Declaration

I can confirm that this is my own work and the use of all material from other sources has been properly and fully acknowledged.

Signed: Renato Simões Gaspar

Date: 23rd September 2020

Abstract

Background: Reactive oxygen species (ROS) are key signalling components in virtually all cells, acting either as second messengers or oxidants to target proteins. It has been reported that NADPH oxidase 1 (Nox-1) and the thiol isomerase protein disulphide isomerase (PDI) may interact physically and functionally to fine-tune ROS production in vascular cells. Both Nox-1 and PDI are able to individually regulate platelets, which are circulating cells of importance for thrombosis and haemostasis. However, little is known on how Nox-1 and PDI may collaborate to fine-tune platelet activity. Likewise, there is a current need to uncover novel inhibitors of these proteins and understand how ROS in platelets are implicated in metabolic diseases.

Aims: The overarching aim of this thesis is to deepen our understanding of how redox processes regulate platelets in health and disease. Redox processes include the consequences of ROS production, as well as interest in specific redox proteins, namely PDI and Nox-1.

Results: First, the flavonoid myricetin was studied and shown to be a novel inhibitor of PDI. Myricetin was able to reduce platelet aggregation, fibrinogen binding, granule exposure and *in vitro* thrombus formation, with no effect on tail bleeding *in vivo*. It is proposed that this flavonoid binds non-covalently near the active site of PDI and ERp5, which is also a thiol isomerase. Since PDI has been shown to associate with Nox-1 in vascular cells, the functional association of PDI and Nox-1 was studied. Through the use of selective inhibitors and Nox-1 deficient murine platelets, it was evident that PDI and Nox-1 collaborated to GPVI-mediated signalling in a process that involved

phosphorylation of p38 mitogen-activated kinase and p47phox, which is a cytosol organizer of Nox-1. Moreover, in a healthy population study (n=137) PDI was positively correlated with waist/hip ratio and insulinaemia, whereas Nox-1 was correlated with body mass index (BMI) and systolic blood pressure. In line with the relevance of redox proteins PDI and Nox-1 to the regulation of platelet function, the redox regulation of platelets was also shown in a murine obesity model, in which it is shown for the first time that maternal high-fat diet intake is able to programme platelets from male offspring in a process associated with higher oxidative stress. Of importance, it is described a novel 'double-hit' effect in which maternal and offspring high-fat diet ingestion results in platelet hyperactivity.

Conclusions: Altogether, data herein presented advance our understanding of how platelets are fine-tuned by redox processes. Myricetin is proposed as a novel inhibitor of thiol isomerases, while a novel mechanistic association between PDI and Nox-1 is also shown. Furthermore, it is suggested for the first time that platelets can be programmed by maternal insults. Therefore, platelets are highly regulated by redox processes and the study of these processes will contribute to improve the development of more effective anti-platelet therapy.

Acknowledgements

Jon, thank you for all your support, kindness and your thirst for extraordinary scientific ideas. You have taught me, as a supervisor, that science is full of wonders and unforeseen events – which are precisely the things that make this an exciting path. Thank you for instigating me to think bigger and through a different perspective – and for being there when I moaned and complained about how nothing is working, also an essential part of the scientific process. You have been a beacon of calmness in the midst of my anxiety. I will remember our many philosophical conversations.

Thank you Marcus, for guiding my initial steps in science and believing in me more than myself, always propelling me forward. I am extremely lucky to have you as a mentor and friend, as all my achievements have roots on the way you fostered this passion for science in me.

To everyone in the lab, I could not have found a better crew to share this experience with. Thank you Gemma and Sophie, for your trust and laughter, both in the lab and in the pub. To Alex Bye for the life advices and discussion of research work. To Tanya, the Moneybearing, the Master of All Animals and the Cheer of the Morning. To Neline, Jo, Paru, Amro and Amanda, essential support throughout my many mistakes in the lab. To Alex Stainer, Carly, Ilaria, Safa and Daniel, for being friends more than colleagues. Thanks to all my fellow PhD students and lab mates. Special thanks to my first supervisees, Yamuna, Jen, Edwin and Ashlin, for teaching me how fun it is to be a mentor.

Thank you Dyan and Craig for the immense support and the cheerful

mentoring on the maternal obesity study.

To my parents, my most sincere gratitude for the unconditional support through good and bad, through proximity and distance. I know how hard it was to see me go far away. This thesis is yours as much as mine, since you taught me the most valuable of all lessons: to always follow your dreams.

My deepest thank you for Gabriel, my brother and best friend. The PhD journey would not be the same without our countless conversations and all the help and support you have given me. Thank you for going with me in adventures and trips throughout the world. These past three years have brought us closer together and this is without a doubt the best outcome of this whole experience.

To all my friends from Brazil and the ones in the UK, thank you very much for cheering me up and enduring my lame jokes. To Zenira, thank you for your love and companionship – and for keeping me focused on writing my thesis.

Publications

Manuscripts submitted

- **Gaspar RS**, Sage T, Little G, Kriek N, Pula G, Gibbins JM. *Protein Disulphide Isomerase and NADPH oxidase 1 regulate platelet function and are associated with obesity*. Submitted to Circulation Research. **Data from this manuscript is shown in Chapter 3.**
- **Gaspar RS**, Unsworth A, Bye A, Sage T, Cox RD, Gibbins JM, Sellayah D, Hughes C. *Maternal obesity during pregnancy programs platelet hyperactivation in male mouse offspring*. Submitted to Arteriosclerosis, Thrombosis and Vascular Biology (ATVB). **Data from this manuscript is shown in Chapter 4.**

Published

- Al-Dibouni A, **Gaspar R**, Ige S, Boateng S, Cagampang FR, Gibbins J, Cox RD and Sellayah D (2020). *Unique Genetic and Histological Signatures of Mouse Pericardial Adipose Tissue*. Nutrients 2020, 12, 1855.
- Unsworth AJ, Bye AP, Sage T, **Gaspar RS**, Eaton N, Drew C, Stainer A, Kriek N, Volberding PJ, Hutchinson JL, Riley R, Jones S, Mundell SJ, Cui W, Falet H, Gibbins JM (2020). *Anti-Platelet Properties Of Pim Kinase Inhibition Is Mediated Through Disruption Of Thromboxane A2 Receptor Signalling*. Haematologica May 2020. doi.org/10.3324/haematol.2019.223529.
- **Gaspar RS**, da Silva SA, Stapleton J, Fontelles JLL, Sousa HR, Chagas

VT, Alsufyani S, Trostchansky A, Gibbins JM, Paes AMA (2020) *Myricetin, the main flavonoid in Syzygium cumini leaf, is a novel inhibitor of platelet thiol isomerases PDI and ERp5*. Frontiers in Pharmacology 31 January 2020. 10. 1678. doi.org/10.3389/fphar.2019.01678. **Data from this manuscript is shown in Chapter 2**.

- Paes AMA, **Gaspar RS**, Fuentes E, Wehinger S, Palomo I, Trostchansky A. (2019) [Review article] *Lipid metabolism and signalling in platelet function*. Advances in Experimental Medicine and Biology 2019;1127:97-115.
- Benevides ROA, Vale CC, Fontelles JLL, França LM, Teófilo TS, Silva SN, Paes AMA, **Gaspar RS** (2019) *Syzygium cumini (L.) Skeels improves metabolic and ovarian parameters in female obese rats with malfunctioning hypothalamus-pituitary-gonadal axis*. Journal of Ovarian Research 2019 Feb 4;12(1):13.
- **Gaspar RS**, Pereira MUL (2018) *Trends in reporting of sexual violence in Brazil from 2009 to 2013*. Cadernos de Saúde Pública vol.34, n.11, e00172617.
- Chagas VT, Coelho RMRS, **Gaspar RS**, da Silva SA, Mastrogiovanni M, Mendonça CJ, Ribeiro MN, Paes AMA, Trostchansky A (2018) *Protective Effects of a Polyphenol-Rich Extract from Syzygium cumini (L.) Skeels Leaf on Oxidative Stress-Induced Diabetic Rats*. Oxidative medicine and cellular longevity Article ID 5386079.

Presentations and Awards

Presentations

POSTER: Gaspar RS and Gibbins JM. *NADPH oxidase 1 and Protein Disulphide Isomerase synergize to modulate platelet function.* In: UK platelet meeting, 2019, Cambridge – UK.

POSTER: Gaspar RS, Ferreira P and Gibbins JM. *NADPH oxidase 1 and thiol isomerases regulate platelet physiology: novel insights on platelet-derived extracellular vesicles*. In: SFRR-E meeting, 2019, Ferrara – Italy.

POSTER: Gaspar RS and Gibbins JM. *Contribution of thiol isomerases and NADPH oxidases to reactive oxygen species production in platelets: old partners in a new crime.* In: EUPLAN, 2018, Bruges – Belgium.

Awards

- **Best 3rd year PhD student presentation, Biomedical Sciences division** – School of Biological Sciences Symposium 2020
- **PhD Researcher of the Year 2020 –** Biomedical Sciences division, School of Biological Sciences, University of Reading
- **Young Investigator Award 2019** –Society of Free Radicals Europe
- **Santander Academic Achievement Scholarship 2017**– Santander Bank

Table of Contents

List of Figures

List of Tables

Chapter 1

General Introduction

In this Chapter I will present overarching themes and concepts relevant to this thesis. We will start with a theoretical background on reactive oxygen species (ROS), moving on to platelet physiology and how ROS regulates platelets. I will introduce protein disulphide isomerase (PDI) and nicotinamide adenine dinucleotide phosphate (NADPH) oxidases, both of which are families of redox proteins relevant to the regulation of platelets and ROS formation and studied further within this Thesis. Furthermore, we will explore the literature on how platelets are affected by metabolic syndrome (MetS) and how platelets are incorporated within the concept of developmental origins of health and disease, which is further tested within this Thesis. Finally, an overall aim and thesis outline is presented.

All figures presented in this Chapter are original.

Please note that specific topics will be further addressed in the Introduction section of experimental Chapters: **Chapters 2, 3 and 4**.

1.1 Reactive Oxygen Species (ROS)

ROS are oxygen-containing chemicals with high reactivity, mostly due to unpaired electrons, comprising neutral, mono- or bi-electronic species. Examples include superoxide ($O_2^{\bullet -}$), hydroxyl radical ($^{\bullet}OH$), but also neutral species like hydrogen peroxide (H_2O_2) in which there is no unpaired electron. Since their discovery, ROS have been perceived as deleterious compounds, responsible for the dysregulation of cellular processes (for review, see (Ray et al., 2012)). However, these species liaise with key proteins to promote beneficial effects, such as cell growth and differentiation, immunological responses (Lander, 1997;Droge, 2002) and platelet aggregation (Qiao et al., 2018). ROS is produced mainly at the mitochondrial respiratory chain and through different Nicotinamide Adenine Dinucleotide phosphate (NADPH) oxidase (Nox) isoforms. Currently, seven different isoforms of Nox have been described: Nox-1, Nox-2, Nox3, Nox4, Nox5, Duox1 and Duox2 (Rastogi et al., 2016). Recent evidence suggests that Noxes may play a bigger role in fine-tuning ROS production in both health and disease (Qiao et al., 2018).

The main reaction precipitated by these species is oxidation, i.e. donation of an electron, which can occur to proteins, lipids or carbohydrates. Among these, perhaps the most biologically relevant reaction involves oxidation of proteins, especially those containing thiols (-SH), since thiol-containing proteins are considered major regulators of intracellular redox processes (Forman et al., 2004;Winterbourn and Hampton, 2008). Such oxidation may be divided into two distinct pathways, depending on the radical involved: the one-electron or two-electron pathways.

One-electron ROS lead to the formation of a thiyl radical (P-S$^{\bullet}$) which can then form disulphide bonds through reaction with other thiol-containing proteins or reduced glutathione (GSH). This process produces one superoxide per disulphide created, which can then react with other thiol proteins, entering the two-electron pathway, forming an intermediate chemical named sulfenic acid (P-SOH). Depending on the subcellular compartment, sulfenic acid will react with either another thiol protein or GSH to form disulphides. Alternatively, it can react with yet another bi-electric ROS, producing higher oxidation products, such as sulphinamides and sulphonic and sulphinic acids. It is important to note that regardless of the pathway involved, most oxidation reactions will generate disulphide bonds in thiol containing proteins. Still, defensive mechanisms known as regenerative systems can reverse the effects of ROS, through the actions of proteins like thioredoxin and glutaredoxin, by reducing the disulphide and restoring the protein to its initial form, i.e. before its oxidation. The oxidation pathways of ROS have been extensively reviewed elsewhere (Wang, 2017;Laurindo, 2018) and are summarized in **Figure 1.1**.

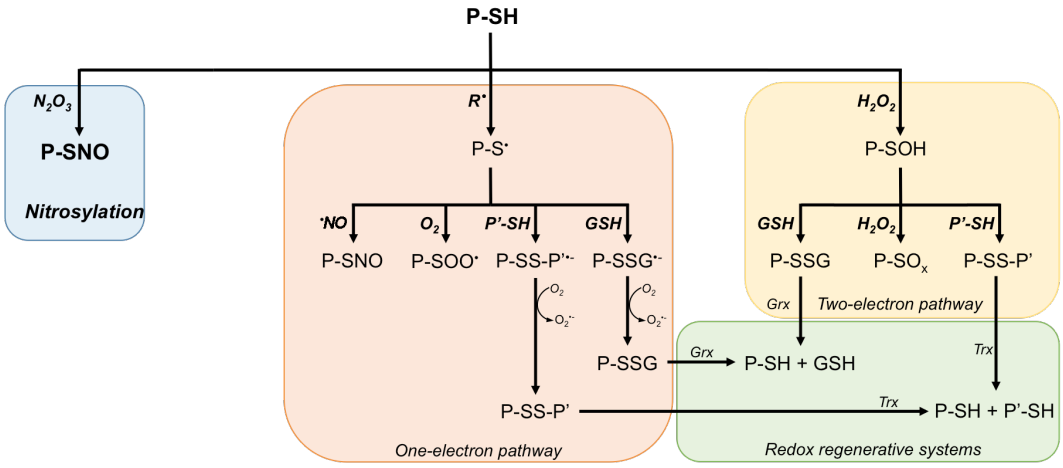

Figure 1.1. Reactive Oxygen Species' oxidation pathways. Reactive oxygen and nitrogen species (RONS) cause oxidation of thiol proteins (P-SH) through distinct mechanisms. The blue panel shows the nitrosylation of a thiol protein into a nitrosothiols (P-SNO) through the direct reaction with dinitrogen trioxide (N_2O_3). The orange panel exemplifies the one-electron pathway, in which thiyl radical (P-S•) can react with nitric oxide (NO) to form nitrosothiols through an alternative route. When in an aerobic environment, thiyl radicals react with oxygen (O_2) to form sulphinyl radical (P-SOO•), or with different thiol proteins or reduced glutathione (GSH), creating disulphide bonds in a process that generates superoxide ($O_2^{-\bullet}$). Some ROS can oxidise thiol proteins through a two-electron pathway (yellow panel), in which the initial step is the formation of sulfenic acid (P-SOH). Subsequently, sulfenic acid may react with thiol proteins or GSH to create disulphide bonds without generating superoxide. It can also further react with hydrogen peroxide (H_2O_2) generating higher oxidation products (P-SO_x). Within healthy systems, redox regenerative systems (green panel) maintain the redox balance through reconverting some dithiol proteins (P-SS-P' or P-SSG) to their initial reduced states. The two main enzymes involved in this process are glutaredoxin (Grx) and thioredoxin (Trx).

There is a constant production of different ROS in different cellular compartments, which then rapidly react with target proteins or translocate to have extended effects in other subcellular locations, e.g. H_2O_2 uses aquaporins to cross the cell membrane (Henzler and Steudle, 2000). Redox Pioneer Prof Helmut Sies coined the term *oxidative eustress* defined as regular physiological processes dependant on ROS for normal cell function. Likewise, he also defined *oxidative stress* as *an imbalance between oxidants and antioxidants in favour of the oxidants, leading to a disruption of redox signalling and control and/or molecular damage* (Sies, 2015). Interestingly, oxidative eustress and stress seem to be of seminal importance in platelet physiology and dysfunction, respectively.

1.2 Platelet physiology

Platelets were first discovered in the XIX century, being described as small plates and thought to originate from either neutrophils or red blood cells (Bizzozero, 1882). After being neglected for almost 100 years, platelets were 'rediscovered' in the 1960s, when several groups started to investigate their functions. Platelets are regarded as anucleate fractions of megakaryocytes and great scientific effort has been employed in understanding their vital task: preventing and stopping mammals from bleeding (Zahn, 1874) – making these cells a remarkable evolutionary adaptation required for human survival (for review see (de Gaetano, 2001)).

In order to maintain haemostasis, platelets rely on both blood components and endothelial cells to release several molecules to either inhibit (e.g. nitric oxide, prostaglandin I_2, etc) or induce (e.g. thromboxane, thrombin, etc) platelet aggregation (Bye et al., 2016). Thrombus formation involves exposure of the sub-endothelium of an injured vessel, thus exposing collagen, to which von Willebrand factor (VWF) binds. Platelet receptors GPVI and glycoprotein (GP) Ib-V-IX, will then bind to collagen and VWF, respectively (Savage et al., 1996;Massberg et al., 2003). Collagen binding provokes inside-out signalling that leads to activation of integrin αIIbβ3, that subsequently binds to fibrinogen and VWF irreversibly, creating a second wave of signalling events by integrins, termed outside-in signalling (for review, see (Durrant et al., 2017)). This latter chain of signals created by integrin αIIbβ3 binding and clustering results in irreversible platelet adhesion, aggregation, pseudopodia formation and reinforces degranulation of dense and α granules. Finally, through degranulation of key molecules such

as ADP and production of thromboxane A_2 (TxA_2), a positive feedback loop is initiated, culminating in successive cycles of paracrine and autocrine agonists binding to different platelet receptors, prompting more platelets to be activated and recruited, resulting in thrombus growth (for review see (Mancuso and Santagostino, 2017)).

Didactically, integrin αIIbβ3 activation occurs in a bi-directional manner, leading to platelet activation (**Figure 1.2**). The first, or inside-out signalling, starts with agonists – such as collagen, thrombin, ADP, TxA_2, adrenaline, serotonin, to cite a few – binding to their respective membrane receptors on the platelet. Of note, there has been reported synergism between agonists to activate platelets – for instance, both ADP and TxA_2 potentiate platelet aggregation induced by collagen (Atkinson et al., 2001). Agonist binding will then trigger signalling pathways, specific to each agonist, converging to activate αIIbβ3 through talin and kindlin-3 binding to integrin β_3 subunit within the cytoplasm (Tadokoro et al., 2003). Of note, kindlin-3 activates integrin αIIbβ3 independent of talin, since platelets lacking kindlin-3 failed to activate integrins despite normal talin expression levels (Moser et al., 2008). Extracellular disulphide exchange reactions between several thiol isomerases and integrins are also key to integrin activation, as demonstrated by our group (Jordan et al., 2005b;Holbrook et al., 2010;Holbrook et al., 2012;Kim et al., 2013;Holbrook et al., 2018). The contribution of thiol isomerases to platelet function will be detailed in the following section as well as in **Chapter 2** and **3**.

Initial stimulus through platelet collagen receptor GPVI is of paramount importance to platelet thrombus formation and inhibition of GPVI has been

proposed as a promising anti-platelet strategy. Indeed, GPVI deficiency leads to reduced formation of platelet aggregates, platelet aggregation and thrombus formation with no increase in primary haemostasis (Kato et al., 2003;Lockyer et al., 2006). Indeed, individuals with mutation or deficiency of GPVI show impaired platelet activation with only minor bleeding defects (Dumont et al., 2009;Hermans et al., 2009). It is possible that restricted alterations of primary haemostasis reported upon GPVI inhibition or deficiency are due to compensatory mechanisms by other agonists, for example thrombin (Mangin et al., 2006). Therefore, inhibition of GPVI or molecules downstream of this receptor is a current interest to develop more efficient anti-platelet strategies (Andrews et al., 2014;Voors-Pette et al., 2019).

Upon exposure of the sub-endothelium, GPVI binds to the Gly-Pro-Hyp (GPO) rich sequences of collagen (Jarvis et al., 2008). Other agonists include snake toxin convulxin (Atkinson et al., 2001) and synthetic ligand collagen-related peptide (CRP) that contains repeating GPO sequences (Yip et al., 2005). GPVI is associated with a FcRγ receptor (FcR) chain that contains an immunoreceptor tyrosine-based activation motif (ITAM) in the form of a homodimer (Gibbins et al., 1997). The cytosolic tail of GPVI is physically attached to the SH3 domain of Src family kinases (SFKs, fyn and lyn). These kinases are phosphorylated by GPVI clustering upon binding collagen and represent early intracellular signalling downstream of this receptor (Ezumi et al., 1998;Suzuki-Inoue et al., 2002;Schmaier et al., 2009;Poulter et al., 2017). Following this initial event, SFKs will phosphorylate the ITAM motifs in FcR, allowing binding and phosphorylation of the spleen tyrosine kinase

(Syk), which feeds back and potentiates SFKs activation. Syk has been shown to lead to activation of downstream targets linker for activated T cells (LAT), Src homology 2 domain-containing leukocyte phosphoprotein of 76-kDa (SLP-76), Vav family of guanine nucleotide exchange factors (GEF), Tec family kinases and grb2-related adapter protein (Gads), forming a LAT-signalosome that will recruit and phosphorylate phospholipase Cγ2 (PLCγ2) and phosphatidylinositol-3 kinase (PI3K) (Gibbins et al., 1998;Watson and Gibbins, 1998;Judd et al., 2002;Atkinson et al., 2003;García et al., 2006).

PI3K will subsequently evoke the conversion of phosphatidylinositol-4,5-bisphosphate (PIP2) into phosphatidylinositol-3,4,5-trisphosphate (PIP3), in a process that induces the co-localization and activation of PLCγ2 and Bruton's tyrosine kinase (Btk) (Mohamed et al., 1999;PASQUET et al., 1999a;Pasquet et al., 1999b). PLCγ2 cleaves PIP2 and leads to calcium mobilization through generation of secondary messenger inositol (1,4,5)-trisphosphate (IP3) (Chae et al., 2015). In parallel, PLCγ2 also culminates in protein kinase C (PKC) activation by diacylglycerol (DAG) in a process of fundamental importance to platelet activation (Konopatskaya et al., 2009). Finally, these pathways converge on activation of Rap1 (Stefanini et al., 2012) and Nox-1, thus leading to thromboxane A2 and ROS generation (Vara et al.;Walsh et al., 2014;Vara et al., 2019), and increasing affinity of integrin αIIbβ3 for fibrinogen binding.

Processes involved in integrin signalling, however, are less well understood than GPVI pathway. One of the earlier events on integrin binding is also tyrosine phosphorylation by SFKs, as demonstrated by SFK-deficient mice, which display impaired tyrosine phosphorylation and spreading on

fibrinogen (Obergfell et al., 2002). Syk is another kinase shown to be directly in contact with αIIbβ3, regulating integrin function (Gao et al., 1997). As a result, common downstream components such as PLCγ2 (Buensuceso et al., 2005;Pearce et al., 2007) become activated, potentiating the platelet response. Of interest, since integrin activation results in cytoskeletal rearrangements, the Rho family of small GTPases, specifically RhoA, has been shown to affect clot retraction and thrombus stability (Pleines et al., 2012). Overall, outside-in signalling results in potentiation of integrin binding and cytoskeletal changes.

Several aspects of platelet physiology will be addressed more in-depth in the Introduction and Discussion sections of **Chapters 2, 3 and 4**.

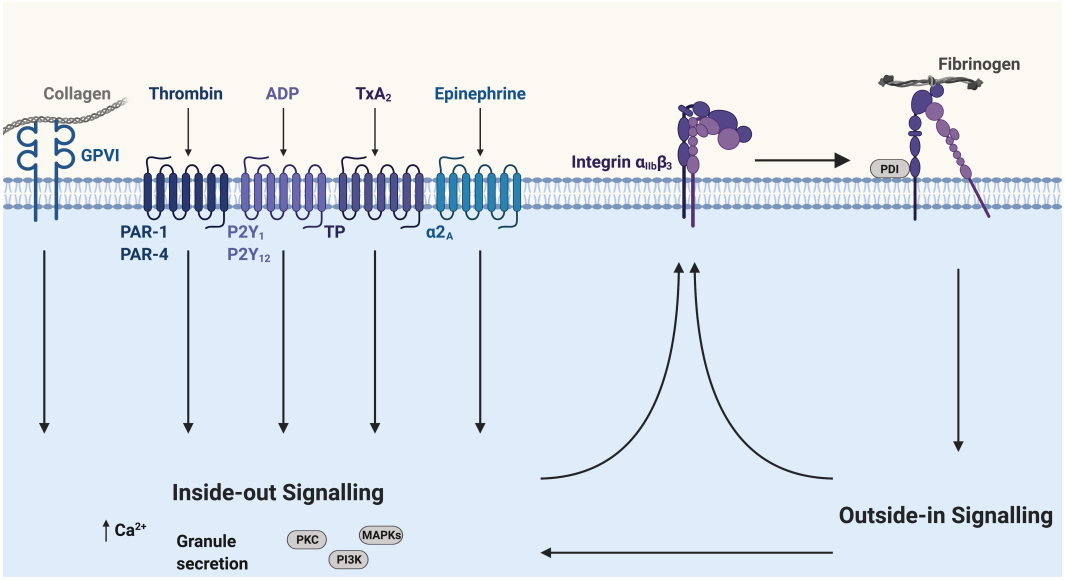

Figure 1.2. Platelet signalling. Platelet activation can be didactically divided in two pathways: inside-out and outside-in signalling. Inside-out signalling refers to binding of agonists to their respective receptors on the platelet membrane (e.g. collagen binding to GPVI). This initial binding will lead to specific pathways of each receptor that will culminate in a common pathway that involves increased intracellular Ca^{2+} mobilization, granule secretion, activation of protein kinase C (PKC), Phosphoinositide 3-kinase (PI3K) and mitogen-activated protein kinases (MAPKs). These molecules and signalling events will then activate integrin αIIbβ3 in a process that requires protein disulphide isomerase (PDI) as well as other thiol isomerases. Upon binding to fibrinogen, the integrin αIIbβ3 will cause a series of intracellular signalling events, termed outside-in signalling, that will potentiate initial response by agonists. PAR: protease-activated receptor. ADP: adenosine diphosphate. TP: thromboxane receptor. TxA_2: thromboxane A_2.

1.3 Protein disulphide isomerase and platelet function

Upon agonist binding, phosphorylation of key intracellular proteins (such as PKC) and calcium mobilization, culminate in integrin αIIbβ3 priming and activation, as described in the previous section. The activation of integrin αIIbβ3 involves a redox-regulated interaction with different protein disulphide isomerase (PDI) enzymes ((Lahav et al., 2002;Jordan et al., 2005a;Kim et al., 2013;Wang et al., 2013). PDI is the prototype of a family of thiol isomerases, also referred to as thioredoxins, capable of catalysing reduction, oxidation and isomerization of disulphide bonds, as well as nitric oxide (NO) transfer through transitrosation (**Figure 1.3**) (Schwaller et al., 2003;Jordan et al., 2005b;Gaspar et al., 2016). Initially thought to be restricted to the endoplasmic reticulum (ER) due to a KDEL retention sequence, different thiol isomerases were later identified on the surface of various cell types, including platelets (Holbrook et al., 2010). Within these, thiol isomerases are released and incorporated on to the platelet membrane upon stimulation, being important for platelet function both *in vitro* and *in vivo* and supporting thrombosis and haemostasis (Chen et al., 1995;Holbrook et al., 2010;Holbrook et al., 2012;Kim et al., 2013;Holbrook et al., 2018). The inhibition of PDI decreases platelet aggregation, whereas addition of reduced PDI potentiates platelet response (Zhou et al., 2015). PDI itself was found to modulate αIIbβ3 activation and integrin-mediated adhesion through redox exchange, possibly by isomerization of a disulphide bond within the ectodomain of the β3 chain, although the precise site of action is yet to be determined (Lahav et al., 2000). Moreover, PDI is also capable of interacting with other platelet adhesion receptors, such as integrin $\alpha_2\beta_1$ (Lahav et al.,

2003) and glycoprotein Ibα (Burgess et al., 2000). On the extracellular space, PDI enhances the coagulant function of tissue factor, thus influencing haemostasis (Versteeg and Ruf, 2007). Therefore, thiol isomerase activity is perceived as a potentiating agent of platelet function, implicated in virtually all pathways involving αIIbβ3 activation – which makes thiol isomerases promising targets to limit thrombosis. Screening of potential new drugs to inhibit thiol isomerases is an on-going drug development programme within our lab.

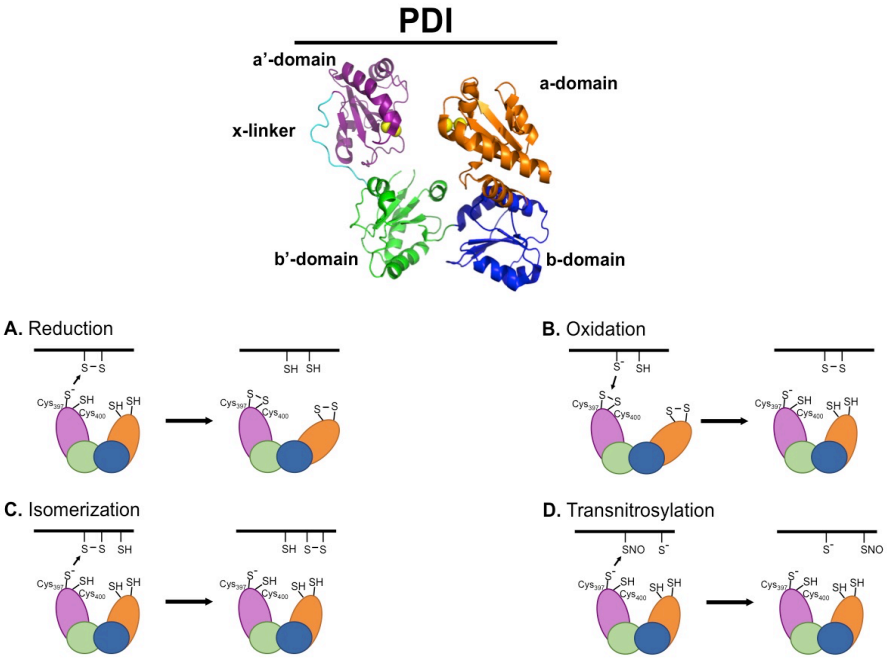

Figure 1.3. Protein disulphide isomerase catalyses redox reactions. The 3D structure of protein disulphide isomerase (PDI) was obtained from the PDB database (PDB ID: 4EL1). PDI has 5 domains, including a x-linker to promote flexibility. Its catalytic sites are located in a and a'-domains, here exemplified as dithiol (two yellow spheres). Due to its particular structure, PDI catalyses reduction of disulphide bonds into free thiols (A), oxidation of thiols into disulphide bonds (B) or isomerization of disulphide bonds (C). Alternatively, it can also transfer nitric oxide (NO) from nitrosothiols (SNO) in a process called transnitrosylation (D).

In spite of substantial evidence pointing towards pro-thrombotic effects of PDI and other thiol isomerases (Chen et al., 1995;Versteeg and Ruf, 2007;Holbrook et al., 2010;Holbrook et al., 2012;Kim et al., 2013;Holbrook et al., 2018), this enzyme also exerts paradoxical inhibition of platelet aggregation through NO transference (**Figure 1.3D**). NO is an important platelet inhibitor that acts through activating guanylate cyclase and increasing cyclic guanosine monophosphate (cGMP) levels (Radomski et al., 1990). This then induces vasodilator-stimulated phosphoprotein (VASP) phosphorylation, which will inactivate αIIbβ3 (Russo et al., 2004;Fuentes and Palomo, 2016;Kwon et al., 2016). The discovery that PDI has denitrosation activity was first reported by the Mutus laboratory that showed that S-nitrosothiols (RSNOs) inhibit platelets through a dual mechanism: first by denitrosation of RSNOs by PDI, thus releasing NO; secondly due to a direct RSNO reaction with PDI, rendering it unable to perform disulphide exchange on platelet membrane (Ramachandran et al., 2001;Root et al., 2004). This was further studied by other groups that showed that different NO donors attenuate platelet function through PDI-mediated denitrosation (Bell et al., 2007;Shah et al., 2007). Altogether, the pro-thrombotic activity of PDI seems to overcome its inhibitory effect in physiological scenarios – whether this would hold true in context of disease is yet to be uncovered.

1.4 NADPH oxidases and platelet function

Similar to PDI, the Nox system has been recently implicated as a positive regulator of platelet function (Delaney et al., 2016). This enzyme complex, which was first described in phagocytes, has been found throughout the cardiovascular system, in endothelial cells (Bayraktutan et al., 2000), vascular smooth muscular cells (Griendling et al., 1994) and platelets (Seno et al., 2001). Currently, seven different isoforms of Nox have been described: Nox-1, Nox-2, Nox3, Nox4, Nox5, Duox1 and Duox2 (Rastogi et al., 2017). Of the above, only Nox-1, Nox-2 and Nox4 have been found in platelets (Delaney et al., 2016) although the presence of Nox4 remains a matter of debate (Vara et al., 2013) and the potential presence of other Duox proteins has not been tested. The Nox complex system is comprised of transmembrane subunits (gp91-phox (Nox-2) and p22-phox) as well as cytosolic subunits ($p22^{phox}$, $p40^{phox}$, $p47^{phox}$, $p67^{phox}$, Noxo1, Noxa1, Rac1 and Rac2) that act as regulators of Nox activity (Lambeth et al., 2007). Upon activation, the cytosolic subunits are phosphorylated and bind to the transmembrane subunit, for instance $p47^{phox}$ to $p22^{phox}$, through different mechanisms, depending on the subunits involved (for review, see (Schroder et al., 2017)).

The primary goal of all Nox enzymes is to generate ROS. These proteins are thought to regulate ROS production in cardiovascular cells, being a major contributor to ROS production in health and disease (Rastogi et al., 2017). In platelets, both Nox-1 and Nox-2 regulate ROS production, although different groups have described contradictory roles for these enzymes. Using *in vivo* knockout models, Delaney et al (Delaney et al., 2016) showed that Nox-2 was of greater importance to platelet function than Nox-1, whereas the functions

of Nox-1 were restricted to effects mediated by G-protein-coupled receptors such as thrombin and thromboxane receptors. On the other hand, using pharmacological inhibition of Nox-1 and *in vivo* knockout for Nox-2, Walsh et al (Walsh et al., 2014) proposed Nox-1, but not Nox-2, mediates GPVI-induced ROS production as well as thrombus formation. Likewise, this same group later on proposed that both Nox-1 and 2 are implicated in GPVI pathway through the interaction of tumour necrosis factor receptor associated factor 4 (TRAF4) and $p47^{phox}$, which regulates the activation of both Nox-1 and 2 (Arthur et al., 2011). A recent study published by Vara et al (Vara et al., 2019) used knockout mouse models of both Nox-1 and 2 to show that Nox-1 was the primary source of superoxide produced due to GPVI stimulation, whereas Nox-2 was key for responses to thrombin. Moreover, Nox-1 was essential for thrombus formation, whilst platelets from Nox-2 knockout mice formed normal thrombus when compared to their wildtype counterparts.

It becomes evident that different labs have produced often-contradictory data with regards to which Nox isoform is important for platelet function and which processes these enzymes regulate. One source of confusion lies in the sex of animals used for deletion studies. Both Nox-1 and Nox-2 genes are located in the X chromosome, thus possibly entailing different phenotypes in male and female animals. In this regard, Sonkay et al (Sonkar et al., 2019) compared male and female Nox-2 KO mice and unequivocally showed that Nox-2 is dispensable for platelet function and thrombosis regardless of the sex of the animal used. A similar comparison is yet to be made for Nox-1. Of the abovementioned studies that used Nox-1

deficient mice, Delaney et al (Delaney et al., 2016) showed platelet Nox-1 deletion to selectively affect responses mediated by G-protein coupled receptors but not the collagen GPVI receptor, whereas Vara et al (Vara et al., 2019) showed the exact opposite using female Nox-1 KO. Therefore, the precise effect of Nox-1 in platelets and whether this is a sex-specific observation is yet to be confirmed. This topic is further discussed in **Chapter 3**, in which data are presented that reiterate the importance of Nox-1 for GPVI-mediated platelet responses using a specific pharmacologic inhibitor, ML171, and female Nox-1-deficient mice. General discussion is also provided in section **5.2** of **Chapter 5**.

Currently there are two inhibitors that exhibit a high degree of selectivity for Nox-1: NoxA1ds and ML171 (known as 2-acetylphenothiazine or 2APT). The first is a small cell permeable peptide that mimics the activation domain of the Nox-1 activator subunit (NOXA1) (Ranayhossaini et al., 2013). With an IC_{50} of 20 nM to inhibit Nox-1-derived superoxide production in a cell-free assay, NoxA1ds was shown to disrupt NOXA1 from binding to Nox-1 (Ranayhossaini et al., 2013). Of note, Nox-1 activation can involve either NOXO1 or p47phox as the organizer cytosolic subunit. It is thought that Nox-1 is constitutively active in the presence of NOXO1, whereas p47phox leads to a further enhancement of Nox-1 activity as a consequence of stimuli, such as PKC activation (Gimenez et al., 2019). The other inhibitor, ML171, is a phenothiazine derivative (some phenothiazines are currently used as antipsychotic drugs (Woods, 2003)), identified after a high-throughput screening of over 16,000 compounds (Gianni et al., 2010). Studies in which subunits of the Nox-1 activating complex were

overexpressed in the HEK293 cell line showed that only Nox-1 overexpression was able to reverse the inhibition exerted by this compound (Gianni et al., 2010). This suggests ML171 binds to Nox-1 instead of other subunits, although the precise binding site is yet to be defined (Gianni et al., 2010).

Although more evidence is needed, the general mechanism of Nox activation in platelets is thought to involve PKC activation, that results in $p47^{phox}$ phosphorylation, allowing it to translocate to the membrane, together with other cytosolic subunits, and activate Nox-1 and 2 (Qiao et al., 2018). This is further supported by recent evidence showing that p47phox indeed translocates to the surface membrane of activated platelets to interact with both Nox-1 and Nox-2 (Wang et al., 2020). The deletion of p47phox in mice resulted in impaired platelet function and thrombus formation and led to decreased activation of several MAPK proteins (Wang et al., 2020), however the precise mechanism is yet to be uncovered.

PDI has been described as an important modulator of Nox-1 activity, through a redox interaction with $p47^{phox}$ in leukocytes (de et al., 2011) and by increasing Nox-1 activation in vascular smooth muscle cells (Fernandes et al., 2009) to cite two examples. More recently, it was described that Cys400 of PDI, which is situated on the C-terminal active site of PDI (Sousa et al., 2017), forms a disulphide bond with Cys196 of $p47^{phox}$ to regulate Nox-1 assembly (Gimenez et al., 2019). This is of particular relevance to the platelet, given that others and I proposed the inhibition of the C-terminal active site of PDI as a new antithrombotic strategy (Zhou et al., 2015;Sousa et al., 2017). Despite evidence of this interaction in other cells, it remains to be established

if the same occurs in platelets and, if so, which impact this might have to platelet function. The elucidation of how PDI and Nox-1 regulate platelets will open up novel strategies to treat and prevent cardiovascular disease. A schematic representation of Nox-1 and PDI in platelets downstream of GPVI activation is shown below in **Figure 1.4**.

Here I have attempted to investigate how Nox-1 and PDI may regulate platelet function individually as well as in collaboration with one another. In **Chapter 3** I will explore how these proteins functionally interact in platelets and show an association of both Nox-1 and PDI levels with metabolic and cardiovascular disease risk factors, thus opening up a novel field of investigation.

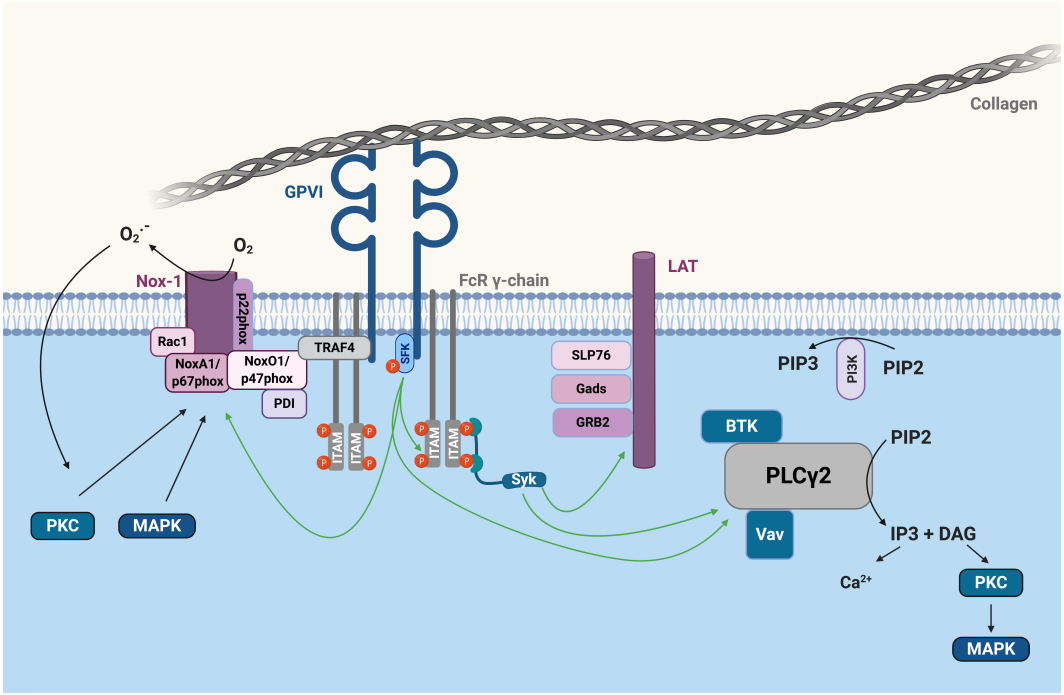

Figure 1.4. GPVI signalling in platelets. Upon collagen binding to clustered or dimeric glycoprotein VI (GPVI), the cytosolic tail of GPVI will activate Src family kinases (SFK) which phosphorylate the immunoreceptor tyrosine-based activation motif (ITAM) part of the Fc receptor γ-chain, Bruton's tyrosine kinase (BTK), and lead to activation of the Nox-1 complex that is attached to GPVI through TNF receptor-associated factor 4 (TRAF4). BTK will phosphorylate phospholipase C (PLCγ2). ITAM phosphorylation results in activation of Syk, which will phosphorylate linker for activation of T cells (LAT) protein, as well as PLCγ2, Vav and BTK. PLCγ2 will catalyse the formation of trisphosphate inositol (IP3) and diacylglycerol (DAG) from phosphatidylinositol 4,5-bisphosphate (PIP2). PIP2 may be converted to phosphatidylinositol-3,4,5-trisphosphate (PIP3) by phosphoinositide 3-kinase (PI3K). IP3 and DAG will increase intracellular Ca^{2+} and induce protein kinase C (PKC) activation, which will phosphorylate mitogen-activated protein kinases (MAPK). PKC and MAPKs may interact with p47phox to assemble the Nox-1 complex that is responsible for superoxide generation. Superoxide may then activate PKC and MAPKs in a positive feedback loop. Green lines indicate early GPVI signalling.

1.5 Obesity

Obesity can be defined as fat accumulation resulting from positive energy balance, in which one's intake of calories surpasses the amount of energy burnt (Flegal et al., 2010). Over the course of human history, people with higher fat accumulation were perceived as healthy and powerful, since the vast majority of the population suffered from food shortages, wars or debilitating illnesses. This changed between the middle of the nineteenth century and beginning of the twentieth century, when obesity started to be recognized as a disease (Beller, 1977). Therefore, the shift towards obesity being considered a negative condition with deleterious impacts to human health is very recent and many argue this disease is a side effect of the evolutionary process (Nesse, 1996), particularly in the West. For a comprehensive review of the history of obesity, please refer to (Eknoyan, 2006).

Nowadays obesity is classified as a body mass index (BMI) ≥ 30 kg/m^2. Obesity is especially challenging for Western culture given the high-calorie diet and low physical activity lifestyle of modern societies. Thus the burden of this disease is rapidly increasing, with an estimated prevalence of 50% in the adult population of USA by 2030 (Ward et al., 2019). Recently, the National Child Measurement Programme in England reported a peak of 4.4% prevalence of severe obesity in children aged 10-11 in 2018-2019 (compared to 3.4% in 2014-2015) (The, 2020). Higher rates of obesity are associated with more stress on the financial and healthcare systems (Hammond and Levine, 2010;Tsai et al., 2011). This became highly pertinent during the recent coronavirus disease 2019 (COVID-19) outbreak, in which several

reports indicated obesity as a germane risk factor for the severity and progression of this virus infection (Cai et al., 2020;Gao et al., 2020).

The basis of the socioeconomic impacts of obesity lies in its clinical repercussions to the cardiovascular system. All of the diagnostic criteria for metabolic syndrome (MetS), including obesity, are risk factors for the development of major cardiovascular ischaemic events, such as acute myocardial infarction, although obesity is by itself a risk factor for cardiovascular events, regardless of the presence of other associated factors (Arnlov et al., 2010).

1.6 Diabetes

Diabetes is a chronic and epidemic disease with high socio-economical cost worldwide, being diagnosed through fasting hyperglycaemia, increased glycated haemoglobin and/or altered oral glucose tolerance test. It is estimated that over 3 million people are diabetic in the UK alone (Holman et al., 2015) – at least 30% of these will suffer from cardiovascular disease (CVD) and ultimately die from thromboembolic events (Zhu et al., 2015). Among different types, diabetes is commonly separated in two distinct entities: type 1 and type 2 (herein defined simply as *diabetes*) (Leslie et al., 2016). The first is an autoimmune disease that kills pancreatic β cells, frequently with an onset at a young age, whereas the latter is a consequence of insulin resistance (IR), being more frequent in older, obese subjects. Regardless of the cause, all types of diabetes are characterized by lack of insulin function, be it due to deficiency of the hormone itself or defects on its actions (Leslie et al., 2016).

The importance of insulin in diabetes was not recognized until 1922, when Canadians Banting and Best gave pancreas extracts to dogs in which the pancreas have been removed, describing a striking improvement in their health (Banting et al., 1922). Before then, the term 'diabetes' was craved from ancient Egypt to describe "too great emptying of the urine", being documented as a form of polyuria (Atkinson et al., 2014;Leslie et al., 2016). After more than 3,000 years of research, which intensified exponentially in the 20th century, diabetes shifted from a death sentence to being known as a manageable chronic non-communicable disease. Such intensive scientific effort has elucidated most of its pathophysiology, with genome-wide

association studies identifying more than 50 gene loci associated with type 2 diabetes (Prasad and Groop, 2015). Despite this, we still fall short of a cure and strategies to prevent ischaemic events related to diabetes. Presently diabetes is defined as an unbalance of energy homeostasis, caused by increased energy consumption and decreased output, resulting in pancreatic β cell dysfunction, altered lipid metabolism and hyperglycaemia (Nolan et al., 2011).

With chronic surfeit of energy consumption, more fuel is available. Increased glycaemia leads to direct stimulation of insulin secretion by the pancreas, although other physiological loops have been identified – for instance, through microbiota-derived acetate production that stimulates the parasympathetic system centrally and insulin secretion peripherally (Perry et al., 2016). Once intracellular, glucose is readily metabolized through the Krebs cycle, and through the mitochondrial respiratory chain to ultimately lead to the production of ATP. This process, however, results in the generation ROS – which, as the name itself predicts, upon accumulation act as 'molecular rebels', desynchronising most cellular processes (Sies et al., 2017). Not surprisingly, increased glucose consumption results in detrimental effects caused by increased ROS production. Several other mechanisms and pathways have been shown to be up-regulated in hyperglycaemia, either as a consequence or cause of increased ROS production, namely: advanced glycation end-products (AGE) and its receptors (RAGE), hexosamine and polyol pathways, activation of protein kinase C (PKC) isoforms (Brownlee, 2001;Kitada et al., 2010), lipotoxicity (Robertson et al., 2004) and inflammatory markers (Masquio et al., 2015).

1.7 Platelet hyperactivation in metabolic syndrome

During the last 50 years, several mechanisms of platelet function in thrombosis and haemostasis have been elucidated, prompting the investigation of platelet contribution to the pathophysiology of global burden diseases, such as thrombotic events in obesity and diabetes, but also in metastasis (Gay and Felding-Habermann, 2011) and immune responses (Qu and Chaikof, 2010). Therefore, platelet function is frequently and ironically perceived as a maladaptation implicated in several public health diseases, opening up perspectives of novel scientific progress – a period described by Prof Barry Coller as the "Golden Age of Platelet Research" (Coller, 2011). Of note, Prof Coller described one of the first platelet inhibitors, a monoclonal antibody (abciximab) that targets integrin $\alpha_{IIb}\beta_3$ specifically and has been widely used to treat and prevent thrombosis (Coller, 1985). Over 35 years later, the precise binding site of abciximab to integrin $\alpha_{IIb}\beta_3$ was finally determined (Nesic et al., 2020) – evidencing the herculean endeavour that is the identification of a novel anti-platelet medication.

In the context of disease, both obesity and diabetes are integral parts of the metabolic syndrome (MetS). This syndrome is defined as the presence of at least three of the following: central obesity, hyperglycaemia, insulin resistance, hypertension and dyslipidaemia (Alberti et al., 2009). Of these, obesity is perceived as a central hub that precedes and potentiates other diagnostic criteria. Indeed, a loss of 5 – 10% of body weight through dieting and/or exercise is thought to greatly reduce the risk to develop all other diagnostic criteria for MetS, regardless of BMI (for review, see (Han and Lean, 2016)). Altogether, individuals with MetS are at a higher risk of developing

thrombotic events together with other related disorders that may entail broader social burdens such as financial stress of the health system (Hammond and Levine, 2010;Tsai et al., 2011) (**Figure 1.5**).

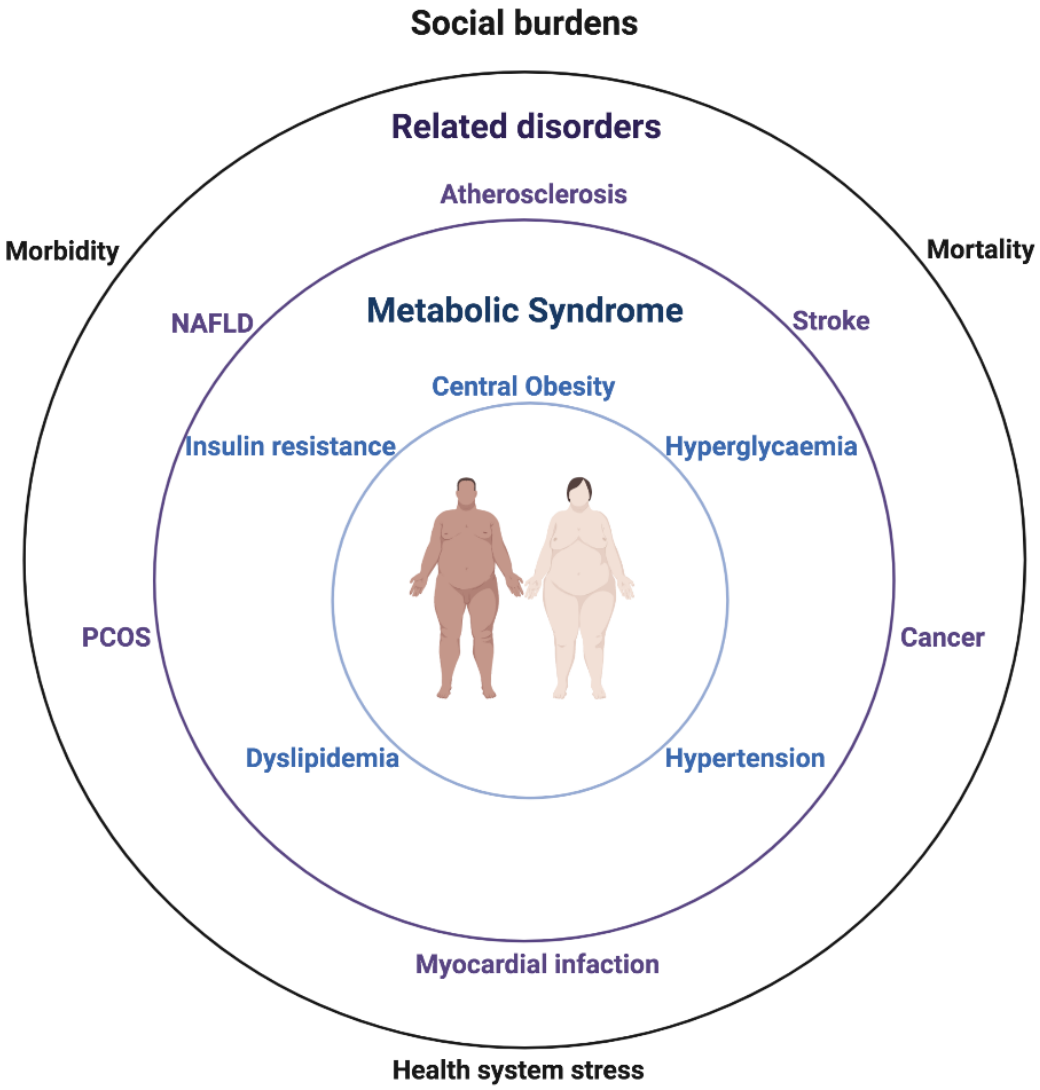

Figure 1.5. Metabolic syndrome, related disorders and social burdens. Metabolic syndrome (MetS) is defined as the presence of at least three of the following: central obesity, hyperglycaemia, insulin resistance, dyslipidaemia and hypertension. This condition is related to other diseases such as atherosclerosis, stroke, myocardial infarction, cancers, polycystic ovary syndrome (PCOS) and non-alcoholic fatty liver disease (NAFLD). Cardiovascular events are the main cause of death and contribute to a broader social impact of MetS that involves higher mortality and morbidity that will financially stress the health system.

Platelet hyperactivation is pivotal in the formation of thrombotic events, such as myocardial infarction and thrombotic stroke (Santilli et al., 2015). For this reason, anti-platelet medications, such as cyclooxygenase inhibitor aspirin or P2Y12 receptor antagonist clopidogrel, are prescribed in patients following a major ischaemic event and have been consistently shown to reduce risk of death by thrombotic events as secondary prevention (for review, see (Gremmel et al., 2018)). Whilst the benefits of anti-platelet medications are well-accepted and widely applied in the clinic, determining the pathophysiological mechanisms underlying platelet hyperactivation in MetS remains a matter of intense scientific research. There are two main components of platelet hyperactivation: increased production of pro-aggregatory stimuli and/or decreased sensitivity to inhibitory molecules – both of which are related to increased ROS production (Monteiro et al., 2012;Gaspar et al., 2016;Kobzar et al., 2017).

Obesity leads to platelet hyperactivation and consequent risk of cardiovascular events due to a prothrombotic state, which is associated with increased thrombin generation (Beijers et al., 2010) and increased platelet activity (Ranucci et al., 2019). This is associated with increased mean platelet volume (MPV) in obese individuals (Coban et al., 2005), since MPV has been shown to be an independent predictor of cardiovascular events (Vizioli et al., 2009). In spite of this, few reports have shown otherwise, suggesting platelets to function normally in obesity (Samocha-Bonet et al., 2008;Elaib et al., 2019).

In the context of platelet hyperactivation in IR and diabetes, the thromboxane pathway is one of the most studied up-regulated stimulatory

mechanisms in platelets. Thromboxane A_2 (TxA_2) is a metabolite of arachidonic acid (AA) metabolism by cyclooxygenase (COX), specifically COX-1 in platelets (Schildknecht et al., 2008), that activates these cells through its action on thromboxane (TP) receptors. Aspirin, the most disseminated anti-platelet drug, acts through irreversible inhibition of different COX isotypes. However, aspirin loses its effects in both experimental diabetes generated *in vitro* (Kobzar et al., 2017) and population studies *in vivo* (for review see (Russo et al., 2017)). This has been linked to increased ROS generation from Nox isoforms, which involves oxidised low-density lipoprotein binding to platelet CD36 (Magwenzi et al., 2015). Moreover, different ROS may act as second messengers, up-regulating different components of the thromboxane pathway (Tang et al., 2011). Finally, another feasible explanation relies on COX-1 activity, which depends on peroxide formation to be constantly activated, i.e. more peroxides tend to result in higher COX-1 activity (Schildknecht et al., 2008).

Despite the effort expended in deciphering the contribution of thromboxane to platelet hyperactivation, collagen has also been systematically shown to cause higher platelet activation in diabetes (Yamagishi et al., 2001;Haimeur et al., 2012;Siewiera et al., 2016). Albeit there is lack of evidence on how diabetes might affect the collagen pathway in platelets, Tang *et al* (2011) showed that collagen modulated platelet response through activation of platelet aldose reductase and ROS generation. Barrachina *et al* (Barrachina et al., 2019) reported increased expression levels and response of the collagen receptor GPVI in obese individuals when compared to lean ones.

As mentioned in section **1.4**, Nox-1 regulates superoxide production downstream of GPVI (Walsh et al., 2014;Vara et al., 2019). This might be of special importance since the high affinity form of GPVI appears to be a dimer, which is regulated by a disulphide bond formation at Cys_{388} on GPVI cytoplasmic tail (Arthur et al., 2007). From a pathophysiological perspective, collagen may be pivotal to increased thrombotic events in diabetes, since platelet adhesion relies heavily on platelets binding to collagen exposed upon endothelial damage. Nevertheless, the accepted working model describes both agonists as important contributors to platelet hyperactivation in diabetes and MetS.

Besides increased production or sensitivity to thromboxane and collagen, diabetic platelets are also characterized by decreased response to inhibitory NO (Williams, 1996;Rabini et al., 1998;Schaeffer et al., 1999;Tessari et al., 2010). Increased ROS, specifically superoxide, seen in diabetes, decreases NO bioavailability by converting it to peroxynitrite ($ONOO^-$), a reactive nitrogen species (RNS) that has conflicting effects on platelet function. On one side, peroxynitrite can induce P-selectin exposure and increase intracellular Ca^{2+}, while, on the other, it can be reconverted to NO and have inhibitory effects (Brown et al., 1998). Interestingly, peroxynitrite induces thiol oxidation in platelet membranes (Brown et al., 1998) while it was recently demonstrated in a cell-free environment that 57% of peroxynitrite oxidizes PDI through a 2-electron mechanism while 43% is converted to nitrate and other radicals (Peixoto et al., 2018). This opens up two hypotheses to explain decreased platelet response to NO: this is either due to its reaction with superoxide forming peroxynitrite or through

loss of the transnitrosylation activity of PDI due to oxidation caused by either peroxynitrite or superoxide (Peixoto et al., 2018). Nonetheless, no experimental work has been carried out to investigate the possible role of platelet membrane thiol isomerases in the context of diabetes.

Other factors affecting platelet hyperactivity should also be taken into account. For instance, Tamminen et al (Tamminen et al., 2003) have shown obese individuals to display lower response to the platelet-inhibitory effects of aspirin, when compared to lean adults. In line with this, increased platelet turnover has been correlated with lower response to aspirin in diabetic patients with diagnosed coronary artery disease (Neergaard-Petersen et al., 2015). Thus, both increased response and sensitivity to pro-thrombotic stimuli and less response or insensitivity to inhibitory stimuli, be them endogenous or anti-platelet medications, may play a part in the pro-thrombotic state of obesity. A summary of key mechanisms that lead to platelet hyperactivation in MetS is summarized in **Figure 1.6**.

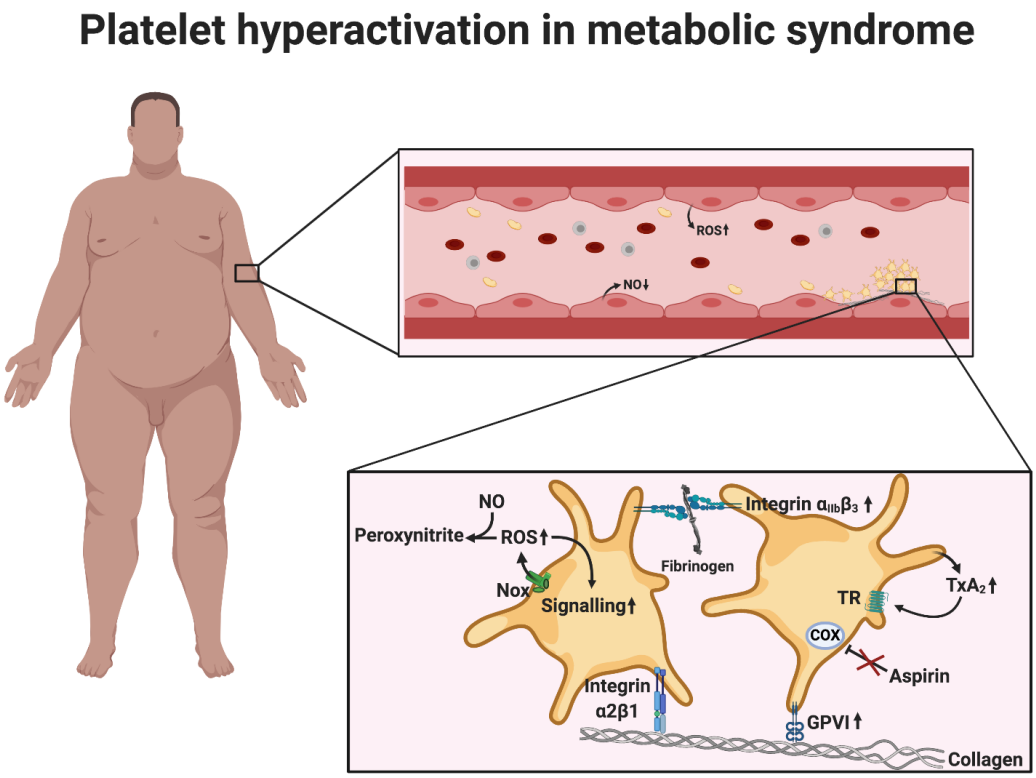

Figure 1.6. Platelet hyperactivation in metabolic syndrome. Lower circulating nitric oxide (NO) coupled with increased circulating reactive oxygen species (ROS) produced by endothelial cells will prompt platelets to activate and accumulate more upon vascular injury. Such injury will expose a collagen-enriched subendothelium to witch platelets will bind. Higher expression of GPVI coupled with increased activated integrin $\alpha_{IIb}\beta_3$ will ultimately result in hyperactive platelets. This involves increased production of reactive oxygen species (ROS) by Nox proteins. ROS can react with NO, forming peroxynitrite and consequently decreasing bioavailability of NO. These species may act as signalling molecules, thus increasing signalling inside platelets. Such signalling will result in higher thromboxane A_2 (TxA_2) production that will feed into the positive feedback loop of platelet activation through the thromboxane receptor (TR). Aspirin, on the contrary, will be less efficacious to inhibit cyclooxygenase (COX) enzymes due to various reasons, including increased ROS production.

As mentioned above, we are now entering an era of platelet research in which we are moving away from looking at the isolated cell and starting to understand its relationship to various diseases. MetS, which is often related to both obesity and diabetes, is considered a deleterious condition due to increasing rates and mortality from cardiovascular events (Han and Lean, 2016). It is clear there is much still to be discovered. The study of novel pathways upregulated in platelets from MetS individuals is therefore a pressing need in modern societies, as is decreasing the burden of metabolic diseases in both developing and developed countries. We have begun to examine this in **Chapters 3 and 4**.

1.8 Developmental origins of health and disease

In light of the increasing burden of metabolic diseases, the development of such conditions was believed to be due to a combination of inherited genetics and unhealthy lifestyle. This view has recently expanded, since common genetic variances predict only up to 10% of type 2 diabetes mellitus and 1% of increased BMI (Speliotes et al., 2010;Voight et al., 2010). Thus, epigenetics, which are the genetic changes caused by environmental factors, have been identified to be a causal factor for the rise of cardiometabolic diseases. Such changes may occur during development *in utero* and/or early childhood and may influence the predisposition of diseases later in life or even in future generations. This gave birth to a whole new area of research: the developmental origins of health and disease (DOHaD).

The first exponent of this field was Prof David Barker. Seminal work by Barker and Osmond described a positive correlation between low birth weight with increased mortality from ischaemic heart disease in adults 50 years later (Barker and Osmond, 1986;Barker and Osmond, 1987). Since then, several research groups have established that low birth weight and poor infant nutrition leads to increased risk of cardiometabolic disease (Leeson et al., 2001;Guerra et al., 2004;Smith et al., 2016). For instance, this was elegantly shown using the historical cohort from a hospital in Amsterdam during the Nazi-imposed "Dutch famine", a period of steep drops in daily rations between January 7th and December 8th 1945. Children that were born during the famine, especially those whose mothers suffered throughout the first trimester of gestation, were found to develop a higher incidence of coronary heart disease, obesity and other cardiometabolic risk

factors as adults, over 50 years later (Ravelli et al., 1998;Roseboom et al., 2000a;Roseboom et al., 2000b;Roseboom et al., 2001).

As the DOHaD theory evolved over time, several aspects and concepts were incorporated. One example is the concept of a 'second-hit' or 'double-hit' effect in which a phenotype would be observed if a given insult (i.e. undernutrition, obesity, metabolic dysfunction) is present both during developmental phases and in adult life. This concept was paramount to account for environmental and lifestyle factors during adulthood. Experimental evidence of this was shown by Hardikar et al (Hardikar et al., 2015). This study observed that over 50 generations of undernutrition in Wistar rats developed a phenotype of low birth-weight and high visceral adiposity – thus reiterating that successive insults in development and adulthood leads to greater metabolic dysfunction. These metabolic abnormalities were not reversed after two generations of unrestricted access of chow (i.e. a well-balanced diet). On the contrary, dietary recuperation of undernourished rats resulted in increased susceptibility to type 2 diabetes mellitus and greater visceral adiposity.

This latter observation extends the 'double-hit' effect to what Gluckman and Hanson defined as Predictive Adaptive Response. This postulates that the *in uterus* environment will set the adaptation of the organism for the postnatal environment (Gluckman and Hanson, 2004a). Indeed, if an organism is exposed to abundance of calories before birth such system will adapt for a similar postnatal environment of abundant calories. If the prenatal and postnatal environment do not match (for instance, prenatal undernutrition followed by postnatal nutritional abundance) the risk of

developing cardiometabolic diseases increases (Gluckman and Hanson, 2004b).

This concept has been widely criticized due to evidence showing increased risk of cardiometabolic diseases even in matching prenatal and postnatal environments (Agarwal et al., 2018). We reinforce this criticism in **Chapter 4**, with data on platelet dysfunction due to a 'double-hit' effect of maternal and offspring high-fat diet intake. Thus, the DOHaD theory currently poses that prenatal and postnatal insults may dictate disease development in adulthood – this may be a consequence of either matching or mismatching pre and postnatal environments.

Further introduction and discussion on DOHaD can be found in **Chapter 4**.

1.9 Aims and outline

The main hypothesis of this thesis is that the activation of platelets is highly regulated by redox processes, which could also be implicated in metabolic diseases and states of platelet hyperactivation. Specific hypotheses for the experimental chapters are provided at the end of the Introduction section of respective chapters. The overarching aim of this thesis is therefore to deepen our understanding of how redox processes regulate platelets in health and disease. Redox processes include the consequences of ROS production, as well as interest in specific redox proteins, namely PDI and Nox-1.

This thesis starts by describing a new inhibitor of PDI in **Chapter 2**. Since PDI has been reported to regulate Nox-1 in vascular cells (**subheading 1.4** of **Chapter 1**), I investigated how PDI and Nox-1 may contribute to platelet function (**Chapter 3**). Moreover, in **Chapter 3** I address a possible association between PDI and Nox-1 and cardiometabolic risk factors, since MetS is a state of oxidative stress (as presented in section **1.6**). In order to expand our understanding of how redox processes regulate platelets, I also hypothesized how would high-fat diet ingestion during pregnancy and lactation affect the platelet function of the offspring – and whether this process was related to oxidative stress (**Chapter 4**).

The experimental approach was as follows:

- **Chapter 2** describes the flavonoid Myricetin as a new thiol isomerase inhibitor with potent anti-platelet and anti-thrombotic properties. This consisted of an ethnopharmacological study, in which I used a polyphenol-

enriched extract of *Syzygium cumini* leaves (PESc), and tested the anti-platelet, anti-thrombotic and effects on haemostasis of the two most abundant components of PESc, myricetin and gallic acid.

- **Chapter 3** examines the functional association of PDI and Nox-1 in platelets. I have used platelet functional, biochemical and molecular biology protocols as well as an *in vivo* KO mouse model to support the conclusions. In addition, a population study addressed the correlations of platelet PDI and Nox-1 with components of MetS, such as insulin levels, BMI and systolic blood pressure.
- **Chapter 4** examines how obesity and MetS may affect platelet function through a developmental programming perspective. Here, I describe for the first time that platelets can be programmed by maternal and offspring high-fat diet-induced metabolic dysfunction. This was tested using functional, biochemical and molecular biology protocols. Metabolic parameters were also measured to assess the degree of metabolic dysfunction and aimed to pinpoint the contribution of ROS generation to the phenotype observed.

Finally, I offer a general discussion in **Chapter 5** to concatenate the scientific contributions of this Thesis and the interrelationship of the experimental chapters. Future perspectives and limitations are also discussed to suggest interesting future avenues for this research field.

1.10 References

Agarwal, P., Morriseau, T.S., Kereliuk, S.M., Doucette, C.A., Wicklow, B.A., and Dolinsky, V.W. (2018). Maternal obesity, diabetes during pregnancy and epigenetic mechanisms that influence the developmental origins of cardiometabolic disease in the offspring. *Crit Rev Clin Lab Sci* 55**,** 71-101.

Alberti, K.G., Eckel, R.H., Grundy, S.M., et al. (2009). Harmonizing the metabolic syndrome: a joint interim statement of the International Diabetes Federation Task Force on Epidemiology and Prevention; National Heart, Lung, and Blood Institute; American Heart Association; World Heart Federation; International Atherosclerosis Society; and International Association for the Study of Obesity. *Circulation* 120**,** 1640-1645.

Andrews, R.K., Arthur, J.F., and Gardiner, E.E. (2014). Targeting GPVI as a novel antithrombotic strategy. *Journal of blood medicine* 5**,** 59.

Arnlov, J., Ingelsson, E., Sundstrom, J., and Lind, L. (2010). Impact of body mass index and the metabolic syndrome on the risk of cardiovascular disease and death in middle-aged men. *Circulation* 121**,** 230-236.

Arthur, J., Shen, Y., Gardiner, E., Coleman, L., Kenny, D., Andrews, R., and Berndt, M.C. (2011). TNF receptor‐associated factor 4 (TRAF4) is a novel binding partner of glycoprotein Ib and glycoprotein VI in human platelets. *Journal of Thrombosis and Haemostasis* 9**,** 163-172.

Arthur, J.F., Shen, Y., Kahn, M.L., Berndt, M.C., Andrews, R.K., and Gardiner, E.E. (2007). Ligand binding rapidly induces disulfide-dependent dimerization of glycoprotein VI on the platelet plasma membrane. *J Biol Chem* 282**,** 30434-30441.

Atkinson, B.T., Ellmeier, W., and Watson, S.P. (2003). Tec regulates platelet activation by GPVI in the absence of Btk. *Blood* 102**,** 3592-3599.

Atkinson, B.T., Stafford, M.J., Pears, C.J., and Watson, S.P. (2001). Signalling events underlying platelet aggregation induced by the glycoprotein VI agonist convulxin. *European journal of biochemistry* 268**,** 5242-5248.

Atkinson, M.A., Eisenbarth, G.S., and Michels, A.W. (2014). Type 1 diabetes. *Lancet* 383**,** 69-82.

Banting, F.G., Best, C.H., Collip, J.B., Campbell, W.R., and Fletcher, A.A. (1922). Pancreatic Extracts in the Treatment of Diabetes Mellitus. *Can Med Assoc J* 12**,** 141-146.

Barker, D.J., and Osmond, C. (1986). Infant mortality, childhood nutrition, and ischaemic heart disease in England and Wales. *The Lancet* 327**,** 1077-1081.

Barker, D.J., and Osmond, C. (1987). Death rates from stroke in England and Wales predicted from past maternal mortality. *Br Med J (Clin Res Ed)* 295**,** 83-86.

Barrachina, M.N., Sueiro, A.M., Izquierdo, I., et al. (2019). GPVI surface expression and signalling pathway activation are increased in platelets from obese patients: Elucidating potential anti-atherothrombotic targets in obesity. *Atherosclerosis* 281**,** 62-70.

Bayraktutan, U., Blayney, L., and Shah, A.M. (2000). Molecular characterization and localization of the NAD (P) H oxidase

components gp91-phox and p22-phox in endothelial cells. *Arteriosclerosis, thrombosis, and vascular biology* 20**,** 1903-1911.

Beijers, H.J., Ferreira, I., Spronk, H.M., Bravenboer, B., Dekker, J.M., Nijpels, G., Ten Cate, H., and Stehouwer, C.D. (2010). Body composition as determinant of thrombin generation in plasma: the Hoorn study. *Arterioscler Thromb Vasc Biol* 30**,** 2639-2647.

Bell, S.E., Shah, C.M., and Gordge, M.P. (2007). Protein disulfide-isomerase mediates delivery of nitric oxide redox derivatives into platelets. *Biochem J* 403**,** 283-288.

Beller, A.S. (1977). *Fat and thin. A natural history of obesity.* Farrar, Straus and Giroux.

Bizzozero, J. (1882). Ueber einen neuen Formbestandtheil des Blutes und dessen Rolle bei der Thrombose und der Blutgerinnung. *Archiv für pathologische Anatomie und Physiologie und für klinische Medicin* 90**,** 261-332.

Brown, A.S., Moro, M.A., Masse, J.M., Cramer, E.M., Radomski, M., and Darley-Usmar, V. (1998). Nitric oxide-dependent and independent effects on human platelets treated with peroxynitrite. *Cardiovasc Res* 40**,** 380-388.

Brownlee, M. (2001). Biochemistry and molecular cell biology of diabetic complications. *Nature* 414**,** 813-820.

Buensuceso, C.S., Obergfell, A., Soriani, A., Eto, K., Kiosses, W.B., Arias-Salgado, E.G., Kawakami, T., and Shattil, S.J. (2005). Regulation of outside-in signaling in platelets by integrin-associated protein kinase C beta. *J Biol Chem* 280**,** 644-653.

Burgess, J.K., Hotchkiss, K.A., Suter, C., Dudman, N.P., Szollosi, J., Chesterman, C.N., Chong, B.H., and Hogg, P.J. (2000). Physical proximity and functional association of glycoprotein 1balpha and protein-disulfide isomerase on the platelet plasma membrane. *J Biol Chem* 275**,** 9758-9766.

Bye, A.P., Unsworth, A.J., and Gibbins, J.M. (2016). Platelet signaling: a complex interplay between inhibitory and activatory networks. *Journal of Thrombosis and Haemostasis* 14**,** 918-930.

Cai, Q., Chen, F., Wang, T., et al. (2020). Obesity and COVID-19 Severity in a Designated Hospital in Shenzhen, China. *Diabetes Care* 43**,** 1392-1398.

Chae, J.J., Park, Y.H., Park, C., Hwang, I.Y., Hoffmann, P., Kehrl, J.H., Aksentijevich, I., and Kastner, D.L. (2015). Brief report: connecting two pathways through Ca2+ signaling: NLRP3 inflammasome activation induced by a hypermorphic PLCG2 mutation. *Arthritis & Rheumatology* 67**,** 563-567.

Chen, K., Detwiler, T.C., and Essex, D.W. (1995). Characterization of protein disulphide isomerase released from activated platelets. *Br J Haematol* 90**,** 425-431.

Coban, E., Ozdogan, M., Yazicioglu, G., and Akcit, F. (2005). The mean platelet volume in patients with obesity. *Int J Clin Pract* 59**,** 981-982.

Coller, B.S. (1985). A new murine monoclonal antibody reports an activation-dependent change in the conformation and/or microenvironment of the platelet glycoprotein IIb/IIIa complex. *J Clin Invest* 76**,** 101-108.

Coller, B.S. (2011). Historical perspective and future directions in platelet research. *J Thromb Haemost* 9 Suppl 1**,** 374-395.

De, A.P.a.M., Verissimo-Filho, S., Guimaraes, L.L., Silva, A.C., Takiuti, J.T., Santos, C.X., Janiszewski, M., Laurindo, F.R., and Lopes, L.R. (2011). Protein disulfide isomerase redox-dependent association with p47(phox): evidence for an organizer role in leukocyte NADPH oxidase activation. *J Leukoc Biol* 90**,** 799-810.

De Gaetano, G. (2001). Historical overview of the role of platelets in hemostasis and thrombosis. *Haematologica* 86**,** 349-356.

Delaney, M.K., Kim, K., Estevez, B., Xu, Z., Stojanovic-Terpo, A., Shen, B., Ushio-Fukai, M., Cho, J., and Du, X. (2016). Differential Roles of the NADPH-Oxidase 1 and 2 in Platelet Activation and Thrombosis. *Arterioscler Thromb Vasc Biol* 36**,** 846-854.

Droge, W. (2002). Free radicals in the physiological control of cell function. *Physiol Rev* 82**,** 47-95.

Dumont, B., Lasne, D., Rothschild, C., Bouabdelli, M., Ollivier, V., Oudin, C., Ajzenberg, N., Grandchamp, B., and Jandrot-Perrus, M. (2009). Absence of collagen-induced platelet activation caused by compound heterozygous GPVI mutations. *Blood* 114**,** 1900-1903.

Durrant, T.N., Van Den Bosch, M.T., and Hers, I. (2017). Integrin αIIbβ3 outside-in signaling. *Blood* 130**,** 1607-1619.

Eknoyan, G. (2006). A history of obesity, or how what was good became ugly and then bad. *Adv Chronic Kidney Dis* 13**,** 421-427.

Elaib, Z., Lopez, J.J., Coupaye, M., et al. (2019). Platelet Functions are Decreased in Obesity and Restored after Weight Loss: Evidence for a Role of the SERCA3-Dependent ADP Secretion Pathway. *Thromb Haemost* 119**,** 384-396.

Ezumi, Y., Shindoh, K., Tsuji, M., and Takayama, H. (1998). Physical and functional association of the Src family kinases Fyn and Lyn with the collagen receptor glycoprotein VI-Fc receptor gamma chain complex on human platelets. *J Exp Med* 188**,** 267-276.

Fernandes, D.C., Manoel, A.H., Wosniak, J., Jr., and Laurindo, F.R. (2009). Protein disulfide isomerase overexpression in vascular smooth muscle cells induces spontaneous preemptive NADPH oxidase activation and Nox1 mRNA expression: effects of nitrosothiol exposure. *Arch Biochem Biophys* 484**,** 197-204.

Flegal, K.M., Carroll, M.D., Ogden, C.L., and Curtin, L.R. (2010). Prevalence and trends in obesity among US adults, 1999-2008. *JAMA* 303**,** 235-241.

Forman, H.J., Fukuto, J.M., and Torres, M. (2004). Redox signaling: thiol chemistry defines which reactive oxygen and nitrogen species can act as second messengers. *Am J Physiol Cell Physiol* 287**,** C246-256.

Fuentes, E., and Palomo, I. (2016). Role of oxidative stress on platelet hyperreactivity during aging. *Life Sci* 148**,** 17-23.

Gao, F., Zheng, K.I., Wang, X.B., et al. (2020). Obesity Is a Risk Factor for Greater COVID-19 Severity. *Diabetes Care* 43**,** e72-e74.

Gao, J., Zoller, K.E., Ginsberg, M.H., Brugge, J.S., and Shattil, S.J. (1997). Regulation of the pp72syk protein tyrosine kinase by platelet integrin alpha IIb beta 3. *EMBO J* 16**,** 6414-6425.

García, Á., Senis, Y.A., Antrobus, R., Hughes, C.E., Dwek, R.A., Watson, S.P., and Zitzmann, N. (2006). A global proteomics approach identifies novel phosphorylated signaling proteins in GPVI‐activated platelets: Involvement of G6f, a novel platelet Grb2‐binding membrane adapter. *Proteomics* 6**,** 5332-5343.

Gaspar, R.S., Trostchansky, A., and Paes, A.M. (2016). Potential Role of Protein Disulfide Isomerase in Metabolic Syndrome-Derived Platelet Hyperactivity. *Oxid Med Cell Longev* 2016**,** 2423547.

Gay, L.J., and Felding-Habermann, B. (2011). Contribution of platelets to tumour metastasis. *Nat Rev Cancer* 11**,** 123-134.

Gianni, D., Taulet, N., Zhang, H., et al. (2010). A novel and specific NADPH oxidase-1 (Nox1) small-molecule inhibitor blocks the formation of functional invadopodia in human colon cancer cells. *ACS Chem Biol* 5**,** 981-993.

Gibbins, J.M., Briddon, S., Shutes, A., Van Vugt, M.J., Van De Winkel, J.G., Saito, T., and Watson, S.P. (1998). The p85 subunit of phosphatidylinositol 3-kinase associates with the Fc receptor γ-chain and linker for activitor of T cells (LAT) in platelets stimulated by collagen and convulxin. *Journal of Biological Chemistry* 273**,** 34437-34443.

Gibbins, J.M., Okuma, M., Farndale, R., Barnes, M., and Watson, S.P. (1997). Glycoprotein VI is the collagen receptor in platelets which underlies tyrosine phosphorylation of the Fc receptor γ-chain. *FEBS letters* 413**,** 255-259.

Gimenez, M., Verissimo-Filho, S., Wittig, I., et al. (2019). Redox Activation of Nox1 (NADPH Oxidase 1) Involves an Intermolecular Disulfide Bond Between Protein Disulfide Isomerase and p47(phox) in Vascular Smooth Muscle Cells. *Arterioscler Thromb Vasc Biol* 39**,** 224-236.

Gluckman, P.D., and Hanson, M.A. (2004a). Developmental origins of disease paradigm: a mechanistic and evolutionary perspective. *Pediatr Res* 56**,** 311-317.

Gluckman, P.D., and Hanson, M.A. (2004b). Living with the past: evolution, development, and patterns of disease. *Science* 305**,** 1733-1736.

Gremmel, T., Michelson, A.D., Frelinger, A.L., Iii, and Bhatt, D.L. (2018). Novel aspects of antiplatelet therapy in cardiovascular disease. *Res Pract Thromb Haemost* 2**,** 439-449.

Griendling, K.K., Minieri, C.A., Ollerenshaw, J.D., and Alexander, R.W. (1994). Angiotensin II stimulates NADH and NADPH oxidase activity in cultured vascular smooth muscle cells. *Circulation research* 74**,** 1141-1148.

Guerra, A., Rego, C., Vasconcelos, C., Silva, D., Castro, E., and Guimarães, M.J. (2004). Low birth weight and cardiovascular risk factors at school age. *Revista Portuguesa De Cardiologia* 23**,** 325-339.

Haimeur, A., Ulmann, L., Mimouni, V., Gueno, F., Pineau-Vincent, F., Meskini, N., and Tremblin, G. (2012). The role of Odontella aurita, a marine diatom rich in EPA, as a dietary supplement in dyslipidemia, platelet function and oxidative stress in high-fat fed rats. *Lipids Health Dis* 11**,** 147.

Hammond, R.A., and Levine, R. (2010). The economic impact of obesity in the United States. *Diabetes Metab Syndr Obes* 3**,** 285-295.

Han, T.S., and Lean, M.E. (2016). A clinical perspective of obesity, metabolic syndrome and cardiovascular disease. *JRSM Cardiovasc Dis* 5**,** 2048004016633371.

Hardikar, A.A., Satoor, S.N., Karandikar, M.S., et al. (2015). Multigenerational Undernutrition Increases Susceptibility to Obesity and Diabetes that Is Not Reversed after Dietary Recuperation. *Cell Metab* 22**,** 312-319.

Henzler, T., and Steudle, E. (2000). Transport and metabolic degradation of hydrogen peroxide in Chara corallina: model calculations and measurements with the pressure probe suggest transport of H(2)O(2) across water channels. *J Exp Bot* 51**,** 2053-2066.

Hermans, C., Wittevrongel, C., Thys, C., Smethurst, P.A., Van Geet, C., and Freson, K. (2009). A compound heterozygous mutation in glycoprotein VI in a patient with a bleeding disorder. *Journal of Thrombosis and Haemostasis* 7**,** 1356-1363.

Holbrook, L.M., Sandhar, G.K., Sasikumar, P., Schenk, M.P., Stainer, A.R., Sahli, K.A., Flora, G.D., Bicknell, A.B., and Gibbins, J.M. (2018). A humanized monoclonal antibody that inhibits platelet-surface ERp72 reveals a role for ERp72 in thrombosis. *J Thromb Haemost* 16**,** 367-377.

Holbrook, L.M., Sasikumar, P., Stanley, R.G., Simmonds, A.D., Bicknell, A.B., and Gibbins, J.M. (2012). The platelet-surface thiol isomerase enzyme ERp57 modulates platelet function. *J Thromb Haemost* 10**,** 278-288.

Holbrook, L.M., Watkins, N.A., Simmonds, A.D., Jones, C.I., Ouwehand, W.H., and Gibbins, J.M. (2010). Platelets release novel thiol isomerase enzymes which are recruited to the cell surface following activation. *Br J Haematol* 148**,** 627-637.

Holman, N., Young, B., and Gadsby, R. (2015). Current prevalence of Type 1 and Type 2 diabetes in adults and children in the UK. *Diabetic medicine: a journal of the British Diabetic Association* 32**,** 1119.

Jarvis, G.E., Raynal, N., Langford, J.P., Onley, D.J., Andrews, A., Smethurst, P.A., and Farndale, R.W. (2008). Identification of a major GpVI-binding locus in human type III collagen. *Blood* 111**,** 4986-4996.

Jordan, P.A., Stevens, J.M., Hubbard, G.P., Barrett, N.E., Sage, T., Authi, K.S., and Gibbins, J.M. (2005a). A role for the thiol isomerase protein ERP5 in platelet function. *Blood* 105**,** 1500-1507.

Jordan, P.A., Stevens, J.M., Hubbard, G.P., Barrett, N.E., Sage, T., Authi, K.S., and Gibbins, J.M. (2005b). A role for the thiol isomerase protein ERP5 in platelet function. *Blood* 105**,** 1500-1507.

Judd, B.A., Myung, P.S., Obergfell, A., et al. (2002). Differential requirement for LAT and SLP-76 in GPVI versus T cell receptor signaling. *The Journal of experimental medicine* 195**,** 705-717.

Kato, K., Kanaji, T., Russell, S., et al. (2003). The contribution of glycoprotein VI to stable platelet adhesion and thrombus formation illustrated by targeted gene deletion. *Blood* 102**,** 1701-1707.

Kim, K., Hahm, E., Li, J., Holbrook, L.M., Sasikumar, P., Stanley, R.G., Ushio-Fukai, M., Gibbins, J.M., and Cho, J. (2013). Platelet protein disulfide isomerase is required for thrombus formation but not for hemostasis in mice. *Blood* 122**,** 1052-1061.

Kitada, M., Zhang, Z., Mima, A., and King, G.L. (2010). Molecular mechanisms of diabetic vascular complications. *J Diabetes Investig* 1**,** 77-89.

Kobzar, G., Mardla, V., and Samel, N. (2017). Glucose impairs aspirin inhibition in platelets through a NAD(P)H oxidase signaling pathway. *Prostaglandins Other Lipid Mediat* 131**,** 33-40.

Konopatskaya, O., Gilio, K., Harper, M.T., et al. (2009). PKCα regulates platelet granule secretion and thrombus formation in mice. *The Journal of clinical investigation* 119**,** 399-407.

Kwon, H.W., Shin, J.H., Cho, H.J., Rhee, M.H., and Park, H.J. (2016). Total saponin from Korean Red Ginseng inhibits binding of adhesive proteins to glycoprotein IIb/IIIa via phosphorylation of VASP (Ser(157)) and dephosphorylation of PI3K and Akt. *J Ginseng Res* 40**,** 76-85.

Lahav, J., Gofer-Dadosh, N., Luboshitz, J., Hess, O., and Shaklai, M. (2000). Protein disulfide isomerase mediates integrin-dependent adhesion. *FEBS Lett* 475**,** 89-92.

Lahav, J., Jurk, K., Hess, O., Barnes, M.J., Farndale, R.W., Luboshitz, J., and Kehrel, B.E. (2002). Sustained integrin ligation involves extracellular free sulfhydryls and enzymatically catalyzed disulfide exchange. *Blood* 100**,** 2472-2478.

Lahav, J., Wijnen, E.M., Hess, O., Hamaia, S.W., Griffiths, D., Makris, M., Knight, C.G., Essex, D.W., and Farndale, R.W. (2003). Enzymatically catalyzed disulfide exchange is required for platelet adhesion to collagen via integrin alpha2beta1. *Blood* 102**,** 2085-2092.

Lambeth, J.D., Kawahara, T., and Diebold, B. (2007). Regulation of Nox and Duox enzymatic activity and expression. *Free Radical Biology and Medicine* 43**,** 319-331.

Lander, H.M. (1997). An essential role for free radicals and derived species in signal transduction. *FASEB J* 11**,** 118-124.

Laurindo, F.R. (2018). "Redox Cellular Signaling Pathways in Endothelial Dysfunction and Vascular Disease," in *Endothelium and Cardiovascular Diseases*. Elsevier), 127-145.

Leeson, C.P., Kattenhorn, M., Morley, R., Lucas, A., and Deanfield, J.E. (2001). Impact of low birth weight and cardiovascular risk factors on endothelial function in early adult life. *Circulation* 103**,** 1264-1268.

Leslie, R.D., Palmer, J., Schloot, N.C., and Lernmark, A. (2016). Diabetes at the crossroads: relevance of disease classification to pathophysiology and treatment. *Diabetologia* 59**,** 13-20.

Lockyer, S., Okuyama, K., Begum, S., et al. (2006). GPVI-deficient mice lack collagen responses and are protected against experimentally induced pulmonary thromboembolism. *Thrombosis research* 118**,** 371-380.

Magwenzi, S., Woodward, C., Wraith, K.S., et al. (2015). Oxidized LDL activates blood platelets through CD36/NOX2-mediated inhibition of the cGMP/protein kinase G signaling cascade. *Blood* 125**,** 2693-2703.

Mancuso, M.E., and Santagostino, E. (2017). Platelets: much more than bricks in a breached wall. *Br J Haematol* 178**,** 209-219.

Mangin, P., Yap, C.L., Nonne, C., et al. (2006). Thrombin overcomes the thrombosis defect associated with platelet GPVI/FcRγ deficiency. *Blood* 107**,** 4346-4353.

Masquio, D.C., De Piano, A., Campos, R.M., et al. (2015). The role of multicomponent therapy in the metabolic syndrome, inflammation

and cardiovascular risk in obese adolescents. *Br J Nutr* 113**,** 1920-1930.

Massberg, S., Gawaz, M., Gruner, S., Schulte, V., Konrad, I., Zohlnhofer, D., Heinzmann, U., and Nieswandt, B. (2003). A crucial role of glycoprotein VI for platelet recruitment to the injured arterial wall in vivo. *J Exp Med* 197**,** 41-49.

Mohamed, A., Nore, B., Christensson, B., and Smith, C. (1999). Signalling of Bruton's tyrosine kinase, Btk. *Scandinavian journal of immunology* 49**,** 113-118.

Monteiro, P.F., Morganti, R.P., Delbin, M.A., Calixto, M.C., Lopes-Pires, M.E., Marcondes, S., Zanesco, A., and Antunes, E. (2012). Platelet hyperaggregability in high-fat fed rats: a role for intraplatelet reactive-oxygen species production. *Cardiovasc Diabetol* 11**,** 5.

Moser, M., Nieswandt, B., Ussar, S., Pozgajova, M., and Fässler, R. (2008). Kindlin-3 is essential for integrin activation and platelet aggregation. *Nature medicine* 14**,** 325-330.

Neergaard-Petersen, S., Hvas, A.M., Grove, E.L., Larsen, S.B., Gregersen, S., and Kristensen, S.D. (2015). The Influence of Haemoglobin A1c Levels on Platelet Aggregation and Platelet Turnover in Patients with Coronary Artery Disease Treated with Aspirin. *PLoS One* 10**,** e0132629.

Nesic, D., Zhang, Y., Spasic, A., Li, J., Provasi, D., Filizola, M., Walz, T., and Coller, B.S. (2020). Cryo-Electron Microscopy Structure of the alphaIIbbeta3-Abciximab Complex. *Arterioscler Thromb Vasc Biol* 40**,** 624-637.

Nesse, R.M. (1996). Evolution and healing: The new science of Darwinian medicine.

Nolan, C.J., Damm, P., and Prentki, M. (2011). Type 2 diabetes across generations: from pathophysiology to prevention and management. *Lancet* 378**,** 169-181.

Obergfell, A., Eto, K., Mocsai, A., Buensuceso, C., Moores, S.L., Brugge, J.S., Lowell, C.A., and Shattil, S.J. (2002). Coordinate interactions of Csk, Src, and Syk kinases with [alpha]IIb[beta]3 initiate integrin signaling to the cytoskeleton. *J Cell Biol* 157**,** 265-275.

Pasquet, J.-M., Bobe, R., Gross, B., Gratacap, M.-P., Tomlinson, M.G., Payrastre, B., and Watson, S.P. (1999a). A collagen-related peptide regulates phospholipase Cγ2 via phosphatidylinositol 3-kinase in human platelets. *Biochemical Journal* 342**,** 171-177.

Pasquet, J.-M., Gross, B., Quek, L., et al. (1999b). LAT is required for tyrosine phosphorylation of phospholipase Cγ2 and platelet activation by the collagen receptor GPVI. *Molecular and cellular biology* 19**,** 8326-8334.

Pearce, A.C., Mccarty, O.J., Calaminus, S.D., Vigorito, E., Turner, M., and Watson, S.P. (2007). Vav family proteins are required for optimal regulation of PLCgamma2 by integrin alphaIIbbeta3. *Biochem J* 401**,** 753-761.

Peixoto, A.S., Geyer, R.R., Iqbal, A., Truzzi, D.R., Soares Moretti, A.I., Laurindo, F.R.M., and Augusto, O. (2018). Peroxynitrite preferentially oxidizes the dithiol redox motifs of protein-disulfide isomerase. *J Biol Chem* 293**,** 1450-1465.

Perry, R.J., Peng, L., Barry, N.A., et al. (2016). Acetate mediates a microbiome-brain-beta-cell axis to promote metabolic syndrome. *Nature* 534**,** 213-217.

Pleines, I., Hagedorn, I., Gupta, S., et al. (2012). Megakaryocyte-specific RhoA deficiency causes macrothrombocytopenia and defective platelet activation in hemostasis and thrombosis. *Blood* 119**,** 1054-1063.

Poulter, N., Pollitt, A.Y., Owen, D., et al. (2017). Clustering of glycoprotein VI (GPVI) dimers upon adhesion to collagen as a mechanism to regulate GPVI signaling in platelets. *Journal of Thrombosis and Haemostasis* 15**,** 549-564.

Prasad, R.B., and Groop, L. (2015). Genetics of type 2 diabetes-pitfalls and possibilities. *Genes (Basel)* 6**,** 87-123.

Qiao, J., Arthur, J.F., Gardiner, E.E., Andrews, R.K., Zeng, L., and Xu, K. (2018). Regulation of platelet activation and thrombus formation by reactive oxygen species. *Redox Biol* 14**,** 126-130.

Qu, Z., and Chaikof, E.L. (2010). Interface between hemostasis and adaptive immunity. *Curr Opin Immunol* 22**,** 634-642.

Rabini, R., Staffolani, R., Fumelli, P., Mutus, B., Curatola, G., and Mazzanti, L. (1998). Decreased nitric oxide synthase activity in platelets from IDDM and NIDDM patients. *Diabetologia* 41**,** 101-104.

Radomski, M., Palmer, R., and Moncada, S. (1990). An L-arginine/nitric oxide pathway present in human platelets regulates aggregation. *Proceedings of the National Academy of Sciences* 87**,** 5193-5197.

Ramachandran, N., Root, P., Jiang, X.M., Hogg, P.J., and Mutus, B. (2001). Mechanism of transfer of NO from extracellular S-nitrosothiols into the cytosol by cell-surface protein disulfide isomerase. *Proc Natl Acad Sci U S A* 98**,** 9539-9544.

Ranayhossaini, D.J., Rodriguez, A.I., Sahoo, S., et al. (2013). Selective recapitulation of conserved and nonconserved regions of putative NOXA1 protein activation domain confers isoform-specific inhibition of Nox1 oxidase and attenuation of endothelial cell migration. *J Biol Chem* 288**,** 36437-36450.

Ranucci, M., Aloisio, T., Dedda, U.D., La Rovere, M.T., De Arroyabe, B.M.L., and Baryshnikova, E. (2019). Platelet reactivity in overweight and obese patients undergoing cardiac surgery. *Platelets* 30**,** 608-614.

Rastogi, R., Geng, X., Li, F., and Ding, Y. (2016). NOX Activation by Subunit Interaction and Underlying Mechanisms in Disease. *Front Cell Neurosci* 10**,** 301.

Rastogi, R., Geng, X., Li, F., and Ding, Y. (2017). NOX activation by subunit interaction and underlying mechanisms in disease. *Frontiers in cellular neuroscience* 10**,** 301.

Ravelli, A.C., Van Der Meulen, J.H., Michels, R., Osmond, C., Barker, D.J., Hales, C., and Bleker, O.P. (1998). Glucose tolerance in adults after prenatal exposure to famine. *The Lancet* 351**,** 173-177.

Ray, P.D., Huang, B.-W., and Tsuji, Y. (2012). Reactive oxygen species (ROS) homeostasis and redox regulation in cellular signaling. *Cellular signalling* 24**,** 981-990.

Robertson, R.P., Harmon, J., Tran, P.O., and Poitout, V. (2004). Beta-cell glucose toxicity, lipotoxicity, and chronic oxidative stress in type 2 diabetes. *Diabetes* 53 Suppl 1**,** S119-124.

Root, P., Sliskovic, I., and Mutus, B. (2004). Platelet cell-surface protein disulphide-isomerase mediated S-nitrosoglutathione consumption. *Biochem J* 382**,** 575-580.

Roseboom, T.J., Van Der Meulen, J.H., Osmond, C., Barker, D.J., Ravelli, A.C., and Bleker, O.P. (2000a). Plasma lipid profiles in adults after prenatal exposure to the Dutch famine. *Am J Clin Nutr* 72**,** 1101-1106.

Roseboom, T.J., Van Der Meulen, J.H., Osmond, C., Barker, D.J., Ravelli, A.C., Schroeder-Tanka, J.M., Van Montfrans, G.A., Michels, R.P., and Bleker, O.P. (2000b). Coronary heart disease after prenatal exposure to the Dutch famine, 1944-45. *Heart* 84**,** 595-598.

Roseboom, T.J., Van Der Meulen, J.H., Ravelli, A.C., Osmond, C., Barker, D.J., and Bleker, O.P. (2001). Effects of prenatal exposure to the Dutch famine on adult disease in later life: an overview. *Twin Research and Human Genetics* 4**,** 293-298.

Russo, I., Doronzo, G., Mattiello, L., De Salve, A., Trovati, M., and Anfossi, G. (2004). The activity of constitutive nitric oxide synthase is increased by the pathway cAMP/cAMP-activated protein kinase in human platelets. New insights into the antiaggregating effects of cAMP-elevating agents. *Thromb Res* 114**,** 265-273.

Russo, I., Penna, C., Musso, T., Popara, J., Alloatti, G., Cavalot, F., and Pagliaro, P. (2017). Platelets, diabetes and myocardial ischemia/reperfusion injury. *Cardiovasc Diabetol* 16**,** 71.

Samocha-Bonet, D., Justo, D., Rogowski, O., Saar, N., Abu-Abeid, S., Shenkerman, G., Shapira, I., Berliner, S., and Tomer, A. (2008). Platelet counts and platelet activation markers in obese subjects. *Mediators Inflamm* 2008**,** 834153.

Santilli, F., Simeone, P., Liani, R., and Davì, G. (2015). Platelets and diabetes mellitus. *Prostaglandins & other lipid mediators* 120**,** 28-39.

Savage, B., Saldivar, E., and Ruggeri, Z.M. (1996). Initiation of platelet adhesion by arrest onto fibrinogen or translocation on von Willebrand factor. *Cell* 84**,** 289-297.

Schaeffer, G., Wascher, T.C., Kostner, G.M., and Graier, W.F. (1999). Alterations in platelet Ca2+ signalling in diabetic patients is due to increased formation of superoxide anions and reduced nitric oxide production. *Diabetologia* 42**,** 167-176.

Schildknecht, S., Van Der Loo, B., Weber, K., Tiefenthaler, K., Daiber, A., and Bachschmid, M.M. (2008). Endogenous peroxynitrite modulates PGHS-1-dependent thromboxane A2 formation and aggregation in human platelets. *Free Radic Biol Med* 45**,** 512-520.

Schmaier, A.A., Zou, Z., Kazlauskas, A., et al. (2009). Molecular priming of Lyn by GPVI enables an immune receptor to adopt a hemostatic role. *Proceedings of the National Academy of Sciences* 106**,** 21167-21172.

Schroder, K., Weissmann, N., and Brandes, R.P. (2017). Organizers and activators: Cytosolic Nox proteins impacting on vascular function. *Free Radic Biol Med* 109**,** 22-32.

Schwaller, M., Wilkinson, B., and Gilbert, H.F. (2003). Reduction-reoxidation cycles contribute to catalysis of disulfide isomerization by protein-disulfide isomerase. *J Biol Chem* 278**,** 7154-7159.

Seno, T., Inoue, N., Gao, D., et al. (2001). Involvement of NADH/NADPH oxidase in human platelet ROS production. *Thrombosis research* 103**,** 399-409.

Shah, C.M., Bell, S.E., Locke, I.C., Chowdrey, H.S., and Gordge, M.P. (2007). Interactions between cell surface protein disulphide isomerase and S-nitrosoglutathione during nitric oxide delivery. *Nitric Oxide* 16**,** 135-142.

Sies, H. (2015). Oxidative stress: a concept in redox biology and medicine. *Redox Biol* 4**,** 180-183.

Sies, H., Berndt, C., and Jones, D.P. (2017). Oxidative Stress. *Annu Rev Biochem* 86**,** 715-748.

Siewiera, K., Kassassir, H., Talar, M., Wieteska, L., and Watala, C. (2016). Higher mitochondrial potential and elevated mitochondrial respiration are associated with excessive activation of blood platelets in diabetic rats. *Life Sci* 148**,** 293-304.

Smith, C.J., Ryckman, K.K., Barnabei, V.M., et al. (2016). The impact of birth weight on cardiovascular disease risk in the Women's Health Initiative. *Nutr Metab Cardiovasc Dis* 26**,** 239-245.

Sonkar, V.K., Kumar, R., Jensen, M., et al. (2019). Nox2 NADPH oxidase is dispensable for platelet activation or arterial thrombosis in mice. *Blood Adv* 3**,** 1272-1284.

Sousa, H.R., Gaspar, R.S., Sena, E.M., et al. (2017). Novel antiplatelet role for a protein disulfide isomerase-targeted peptide: evidence of covalent binding to the C-terminal CGHC redox motif. *J Thromb Haemost* 15**,** 774-784.

Speliotes, E.K., Willer, C.J., Berndt, S.I., et al. (2010). Association analyses of 249,796 individuals reveal 18 new loci associated with body mass index. *Nat Genet* 42**,** 937-948.

Stefanini, L., Boulaftali, Y., Ouellette, T.D., Holinstat, M., Desire, L., Leblond, B., Andre, P., Conley, P.B., and Bergmeier, W. (2012). Rap1-Rac1 circuits potentiate platelet activation. *Arterioscler Thromb Vasc Biol* 32**,** 434-441.

Suzuki-Inoue, K., Tulasne, D., Shen, Y., et al. (2002). Association of Fyn and Lyn with the proline-rich domain of glycoprotein VI regulates intracellular signaling. *Journal of Biological Chemistry* 277**,** 21561-21566.

Tadokoro, S., Shattil, S.J., Eto, K., Tai, V., Liddington, R.C., De Pereda, J.M., Ginsberg, M.H., and Calderwood, D.A. (2003). Talin binding to integrin beta tails: a final common step in integrin activation. *Science* 302**,** 103-106.

Tamminen, M., Lassila, R., Westerbacka, J., Vehkavaara, S., and Yki-Jarvinen, H. (2003). Obesity is associated with impaired platelet-inhibitory effect of acetylsalicylic acid in nondiabetic subjects. *Int J Obes Relat Metab Disord* 27**,** 907-911.

Tang, W.H., Stitham, J., Gleim, S., et al. (2011). Glucose and collagen regulate human platelet activity through aldose reductase induction of thromboxane. *J Clin Invest* 121**,** 4462-4476.

Tessari, P., Cecchet, D., Cosma, A., et al. (2010). Nitric oxide synthesis is reduced in subjects with type 2 diabetes and nephropathy. *Diabetes* 59**,** 2152-2159.

The, L.D.E. (2020). Tackling obesity in 2020-with a great resolution comes shared responsibility. *The lancet. Diabetes & endocrinology* 8**,** 89.

Tsai, A.G., Williamson, D.F., and Glick, H.A. (2011). Direct medical cost of overweight and obesity in the USA: a quantitative systematic review. *Obes Rev* 12**,** 50-61.

Vara, D., Campanella, M., and Pula, G. (2013). The novel NOX inhibitor 2-acetylphenothiazine impairs collagen-dependent thrombus formation in a GPVI-dependent manner. *Br J Pharmacol* 168**,** 212-224.

Vara, D., Cifuentes-Pagano, E., Pagano, P.J., and Pula, G. (2019). A novel combinatorial technique for simultaneous quantification of oxygen radicals and aggregation reveals unexpected redox patterns in the activation of platelets by different physiopathological stimuli. *Haematologica* 104**,** 1879-1891.

Vara, D., Tarafdar, A., Celikag, M., et al. NADPH oxidase 1 is a novel pharmacological target for the development of an antiplatelet drug without bleeding side effects. *The FASEB Journal*.

Versteeg, H.H., and Ruf, W. (2007). Tissue factor coagulant function is enhanced by protein-disulfide isomerase independent of oxidoreductase activity. *J Biol Chem* 282**,** 25416-25424.

Vizioli, L., Muscari, S., and Muscari, A. (2009). The relationship of mean platelet volume with the risk and prognosis of cardiovascular diseases. *Int J Clin Pract* 63**,** 1509-1515.

Voight, B.F., Scott, L.J., Steinthorsdottir, V., et al. (2010). Twelve type 2 diabetes susceptibility loci identified through large-scale association analysis. *Nat Genet* 42**,** 579-589.

Voors-Pette, C., Lebozec, K., Dogterom, P., et al. (2019). Safety and tolerability, pharmacokinetics, and pharmacodynamics of ACT017, an antiplatelet GPVI (glycoprotein VI) Fab: First-in-human healthy volunteer trial. *Arteriosclerosis, thrombosis, and vascular biology* 39**,** 956-964.

Walsh, T.G., Berndt, M.C., Carrim, N., Cowman, J., Kenny, D., and Metharom, P. (2014). The role of Nox1 and Nox2 in GPVI-dependent platelet activation and thrombus formation. *Redox Biol* 2**,** 178-186.

Wang, G. (2017). "Reactive Oxygen Species," in *Encyclopedia of Cancer,* ed. M. Schwab. (Berlin, Heidelberg: Springer Berlin Heidelberg), 3930-3935.

Wang, L., Wu, Y., Zhou, J., Ahmad, S.S., Mutus, B., Garbi, N., Hammerling, G., Liu, J., and Essex, D.W. (2013). Platelet-derived ERp57 mediates platelet incorporation into a growing thrombus by regulation of the alphaIIbbeta3 integrin. *Blood* 122**,** 3642-3650.

Wang, X., Zhang, S., Ding, Y., et al. (2020). p47phox deficiency impairs platelet function and protects mice against arterial and venous thrombosis. *Redox Biol* 34**,** 101569.

Ward, Z.J., Bleich, S.N., Cradock, A.L., Barrett, J.L., Giles, C.M., Flax, C., Long, M.W., and Gortmaker, S.L. (2019). Projected U.S. State-Level

Prevalence of Adult Obesity and Severe Obesity. *N Engl J Med* 381**,** 2440-2450.

Watson, S.P., and Gibbins, J. (1998). Collagen receptor signalling in platelets: extending the role of the ITAM. *Immunology today* 19**,** 260-264.

Williams, S. (1996). Cusco JA, Roddy MA, Johnstone MT, Creager MA. *Impaired nitric oxide-mediated vasodilation in patients with non-insulin-dependent diabetes mellitus. J Am Coll Cardiol* 27**,** 567-574.

Winterbourn, C.C., and Hampton, M.B. (2008). Thiol chemistry and specificity in redox signaling. *Free Radic Biol Med* 45**,** 549-561.

Woods, S.W. (2003). Chlorpromazine equivalent doses for the newer atypical antipsychotics. *J Clin Psychiatry* 64**,** 663-667.

Yamagishi, S.I., Edelstein, D., Du, X.L., and Brownlee, M. (2001). Hyperglycemia potentiates collagen-induced platelet activation through mitochondrial superoxide overproduction. *Diabetes* 50**,** 1491-1494.

Yip, J., Shen, Y., Berndt, M.C., and Andrews, R.K. (2005). Primary platelet adhesion receptors. *IUBMB life* 57**,** 103-108.

Zahn, F.W. (1874). Untersuchungen über thrombose. *Archiv für pathologische Anatomie und Physiologie und für klinische Medicin* 62**,** 81-124.

Zhou, J., Wu, Y., Wang, L., Rauova, L., Hayes, V.M., Poncz, M., and Essex, D.W. (2015). The C-terminal CGHC motif of protein disulfide isomerase supports thrombosis. *J Clin Invest* 125**,** 4391-4406.

Zhu, K., Kakehi, T., Matsumoto, M., et al. (2015). NADPH oxidase NOX1 is involved in activation of protein kinase C and premature senescence in early stage diabetic kidney. *Free Radic Biol Med* 83**,** 21-30.

Chapter 2

Myricetin is a novel inhibitor of platelet thiol isomerases PDI and ERp5

The full paper published at *Frontiers in Pharmacology* can be found in:

Front. Pharmacol. 10:1678. doi: 10.3389/fphar.2019.01678

The the anti-platelet properties of a polyphenol-enriched extract from *Syzygium cumini* (PESc), which is a common plant present in my hometown back in Brazil, were examined in this Chapter. The rationale for this project started with preliminary observations that PESc exerted some anti-platelet effect. The components of PESc were therefore isolated and identified. Myricetin and gallic acid were the main phenolic compounds of this extract found upon mass spectrometry identification. Myricetin was then showed to be a potent inhibitor of platelets, whereas gallic acid did not show any relevant inhibitory effect. Finally, it is demonstrated that low concentrations of myricetin are also able to inhibit thiol isomerases PDI and ERp5, probably through non-covalent bonds near the active site.

I have been part of designing this project, as well as collecting most experimental data, for the exception of mass spectrometry and molecular docking. Likewise, I drafted the manuscript and addressed reviewers' comments. For these reasons, it is estimated I have contributed to over 75% of all effort put into this paper.

The full paper published at *Frontiers in Pharmacology* can be found at Front. Pharmacol. 10:1678. doi: 10.3389/fphar.2019.01678

Myricetin, the main flavonoid in *Syzygium cumini* leaf, is a novel inhibitor of platelet thiol isomerases PDI and ERp5.

Running title: Myricetin is a novel inhibitor of PDI and ERp5.

Authorship

Renato Simões Gaspar [a,b]*, Samira Abdalla da Silva [b], Jennifer Stapleton [a], João Lucas de Lima Fontelles [b], Hiran Reis Sousa [b], Vinicyus Teles Chagas [b], Shuruq Alsufyani [a], Andrés Trostchansky [c], Jonathan M Gibbins [a], Antonio Marcus de Andrade Paes [b].

Affiliations

[a] Institute for Cardiovascular and Metabolic Research, School of Biological Sciences, University of Reading, Reading, UK.

[b] Laboratory of Experimental Physiology, Department of Physiological Sciences, Federal University of Maranhão, São Luís, MA, Brazil.

[c] Departamento de Bioquímica and Centro de Investigaciones Biomédicas, Facultad de Medicina, Universidad de la República, Montevideo, Uruguay.

*** Corresponding author**

Renato Simões Gaspar, M.D.

Institute of Cardiovascular and Metabolic Research, School of Biological Sciences. University of Reading - Harborne Building, Reading, RG6 6AS, UK.

E-mail: renatosgaspar@gmail.com, phone: +44 11 8378 7047

Keywords: *Syzygium cumini,* Antithrombotic Agents, Platelet, Oxidation-reduction, Platelet Aggregation Inhibitors

Full citation of this paper can be found below:

Gaspar, R.S., Da Silva, S.A., Stapleton, J., et al. (2019). Myricetin, the Main Flavonoid in Syzygium cumini Leaf, Is a Novel Inhibitor of Platelet Thiol Isomerases PDI and ERp5. *Front Pharmacol* 10**,** 1678. doi: 10.3389/fphar.2019.01678

2.1 Graphical abstract

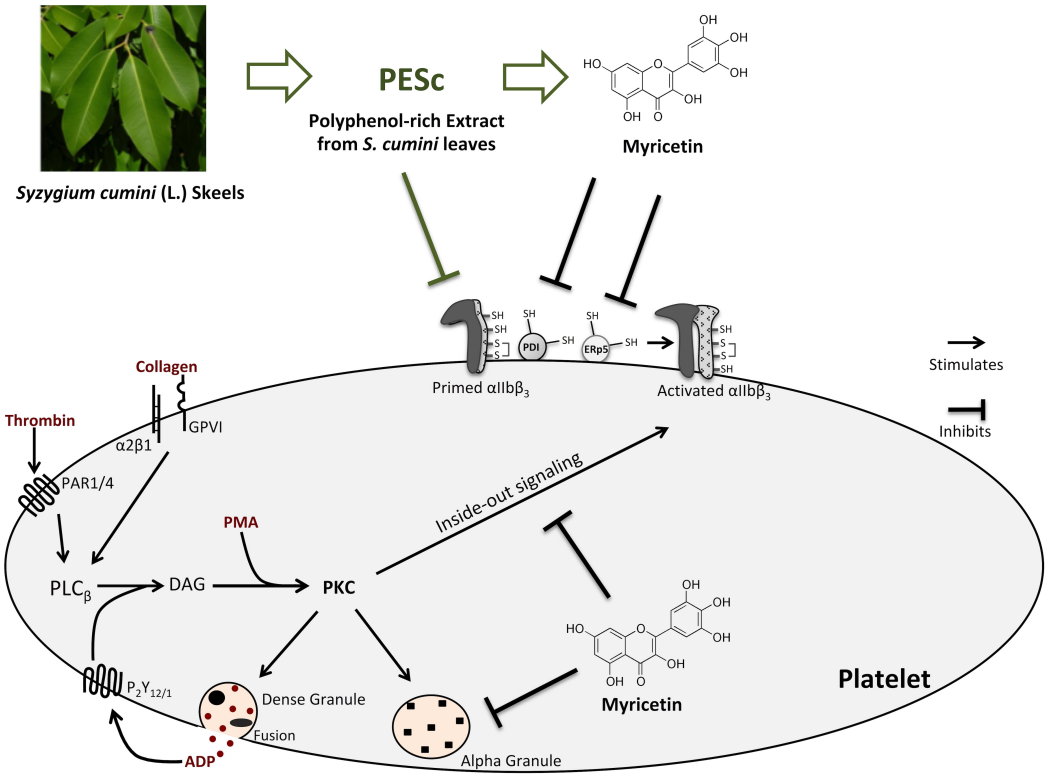

2.2 Abstract

Background: Flavonoids have been characterized as a prominent class of compounds to treat thrombotic diseases through the inhibition of thiol isomerases. *Syzygium cumini* is a flavonoid-rich medicinal plant that contains myricetin and gallic acid. Little is known about the potential anti-platelet properties of *S. cumini* and its constituent flavonoids.

Objective To evaluate the anti-platelet effects and mechanism of action of a polyphenol-rich extract (PESc) from *S. cumini* leaf and its most prevalent polyphenols, myricetin and gallic acid.

Methods PESc, myricetin and gallic acid were incubated with platelet-rich plasma and washed platelets to assess platelet aggregation and activation. *In vitro* platelet adhesion and thrombus formation as well as *in vivo* bleeding time were performed. Finally, myricetin was incubated with recombinant thiol isomerases to assess its potential to bind and inhibit these, whilst molecular docking studies predicted possible binding sites.

Results: PESc decreased platelet activation and aggregation induced by different agonists. Myricetin exerted potent anti-platelet effects, whereas gallic acid did not. Myricetin reduced the ability of platelets to spread on collagen, form thrombi *in vitro* without affecting haemostasis *in vivo*. Fluorescence quenching studies suggested myricetin binds to different thiol isomerases with similar affinity, despite inhibiting only protein disulphide isomerase (PDI) and ERp5 reductase activities (IC_{50}~3.5 μM). Finally, molecular docking studies suggested myricetin formed non-covalent bonds with PDI and ERp5.

Conclusions: PESc and its most abundant flavonoid myricetin strongly inhibit platelet function. Additionally, myricetin is a novel inhibitor of ERp5 and PDI, unveiling a new therapeutic perspective for the treatment of thrombotic disorders.

ABBREVIATIONS

CRP	collagen-related peptide
GAPDH	glyceraldehyde 3-phosphate dehydrogenase
PAR	protease-activated receptor
PDI	protein disulphide isomerase
PESc	polyphenol-rich extract of *S. cumini* leaf
PKC	protein kinase c
PMA	phorbol-12-myristate-13-acetate
PRP	platelet-rich plasma
S. cumini	*Syzygium cumini* (L.) Skeels
TxA_2	thromboxane A_2
TPR	thromboxane A_2 receptor
TRAP-6	thrombin receptor activator peptide 6
VASP	vasodilator-stimulated phospho-protein
WP	washed platelets

2.3. Introduction

Cardiovascular diseases are the leading cause of death worldwide, a scenario where thrombosis and its associated outcomes account for one in four deaths (Wendelboe and Raskob, 2016). Platelets play a key role in arterial thrombosis, due to platelet aggregation triggered by multiple agonists, such as adenosine diphosphate (ADP), thrombin and collagen. These signalling pathways will inevitably culminate in the activation of the platelet surface integrin $\alpha IIb\beta_3$ (Banno and Ginsberg, 2008;Ghoshal and Bhattacharyya, 2014), which becomes activated after the isomerization of critical disulphide bonds on its extracellular β domain. This process is thought to be mediated by protein disulphide isomerase (PDIA1, herein referred to as PDI) and sibling proteins (Essex, 2008). Therefore, PDI has been proposed as a new target to treat and prevent thrombotic diseases (Jasuja et al., 2012).

PDI is the leading member of its family, a set of thioredoxin-like thiol isomerases originally described in the endoplasmic reticulum (ER), but later found in virtually all cell compartments, including the platelet surface (Chen et al., 1995). In platelets, PDI has been shown to regulate integrins $\alpha IIb\beta_3$ and $\alpha_2\beta_1$, the latter being a collagen receptor important for platelet adhesion (Lahav et al., 2003;Essex, 2008). Besides PDI, at least three other members – ERp5 (PDIA6), ERp57 (PDIA3) and ERp72 (PDIA4) – have been demonstrated to support thrombosis (Essex and Wu, 2018). Particularly, ERp5 has been implicated in integrin $\alpha IIb\beta_3$ activation and shown to become physically associated with integrin β_3 upon platelet activation (Jordan et al., 2005). Therefore, there has been a surge of novel PDI inhibitors being

described, both synthetic (Sousa et al., 2017) and natural, such as the flavonoid quercetin and its derivatives (Lin et al., 2015). Accordingly, flavonoids and related compounds have been described as potent anti-platelet compounds, acting through diverse mechanisms (Jasuja et al., 2012;Giamogante et al., 2018).

Syzygium cumini (L.) Skeels (Myrtaceae) is a worldwide cultivated medicinal plant, popularly known as jamun, black plum, jambolan or jambolão (Ayyanar and Subash-Babu, 2012). *S. cumini* has been proposed as a prominent source of bioactive compounds against cardiometabolic disorders (Chagas et al., 2015), in accordance with its usage in the Unani medicine to "enrich blood" (Ayyanar and Subash-Babu, 2012). Indeed, *S. cumini* has been shown to inhibit the hyperactivation of platelets from diabetic patients (De Bona et al., 2010;Raffaelli et al., 2015). Recently, we characterized a polyphenol-rich extract from *S. cumini* (PESc) leaf, which consisted of gallic acid, quercetin, myricetin and its derivatives myricetin-3-α-arabinopyranoside and myricetin deoxyhexoside (Chagas et al., 2018). Out of the flavonoids identified, myricetin was the most abundant one, constituting roughly 20% of PESc weight (Chagas et al., 2018). Interestingly, this extract has been shown to improve oxidative stress and prevent the development of diabetes induced by alloxan treatment (Chagas et al., 2018). Despite this, there is scarce literature on the anti-platelet properties of *S. cumini* and its most abundant polyphenols, myricetin and gallic acid.

Therefore, in the present study, we hypothesized that PESc presents potential anti-platelet properties and that myricetin and gallic acid, as the most prevalent compounds, would be its bioactive phytochemicals.

Moreover, given the structural similarity between myricetin and quercetin, we also tested for a possible inhibition of thiol isomerases. Data herein presented endorse our hypothesis through the demonstration of PESc inhibitory effects on both platelet activation and aggregation. Assessment of gallic acid and myricetin bioactivity showed that only myricetin exerted relevant anti-platelet properties. Myricetin was then shown to be a novel inhibitor of thiol isomerases PDI and ERp5, unveiling a new therapeutic perspective for the treatment and prevention of thrombotic diseases.

2.4 Material and Methods

2.4.1. Reagents

Myricetin, gallic acid, ADP, thrombin, phorbol-12-myristate-13-acetate (PMA), Thrombin Receptor Activator Peptide 6 (TRAP-6), human fibrinogen and 1,4-Dithiothreitol (DTT) and 3,3′-Dihexyloxacarbocyanine iodide ($DIOC_6$) were purchased from Sigma-aldrich (Dorset, UK). PAPA-NONOate was purchased from Tocris (Abingdon, UK). PE/Cy5 anti human CD62P and PAC-1 FITC antibodies were purchased from BD Biosciences (Wokingham, UK). FITC-conjugated fibrinogen was purchased from Agilent (Stockport, UK). Collagen was purchased from Nycomed (Munich, Germany) whereas Collagen-Related Peptide (CRP) was obtained from Prof Richard Farndale (University of Cambridge, Cambridge, UK). Anti-phospho-vasodilator-stimulated phospho-protein (VASP) (Ser239) was purchased from Cell Signalling (Hitchin, UK), anti-glyceraldehyde 3-phosphate dehydrogenase (GAPDH) from Proteintech (Manchester, UK) and Alexa-488 conjugated phalloidin secondary antibody was bought from Life Technologies (Paisley, UK).

2.4.2. Botanical material

S. cumini leaves were collected from different trees at the campus (2º33´11.7´´S 44º18´22.7´´W) of the Federal University of Maranhão (UFMA) in São Luís, Maranhão, Brazil. Samples were identified and catalogued at the Herbarium MAR of the Department of Biology of the same institution, where a voucher specimen was deposited under nº 4573.

2.4.3. Extract preparation

The extract was prepared according to Sharma et al (Sharma et al., 2008), with modifications. Fresh leaves were dried at 38 °C in an air-flow oven, pulverized into powdered dry leaves (150g) and macerated in 70% ethanol (1:6 w/v) under constant stirring for 3 days at 25°C. The supernatant was concentrated in a rotary evaporator to obtain the crude hydroalcoholic extract (HE). HE was partitioned with chloroform (1:1 v/v, 3x) and the organic phase was washed with ethyl acetate (1:1 v/v, 3x). The ethyl acetate fraction was concentrated under vacuum (38 °C) and lyophilized, yielding the polyphenol-rich extract (PESc). For experimental procedures, PESc samples were resuspended in water, at desired concentrations, immediately before use.

2.4.4. Confirmation of polyphenolic composition of PESc

As we have previously characterized the phytochemical composition of PESc (Chagas et al., 2018), confirmatory assessment was performed by both HPLC-UV/Vis detection and LC-MS/MS to validate the lot of PESc used in this study. Methods employed were exactly the same as previously described (Chagas et al., 2018).

2.4.5. Platelet-rich plasma and washed platelets preparation

Healthy volunteers, males and females, aged 18 – 65, who did not use antiplatelet drugs and had previously provided informed consent had their blood samples collected in tubes containing 1:5 v/v acid citrate dextrose (ACD: 2.5% sodium citrate, 2% D-glucose and 1.5% citric acid) or 3.8% (w/v)

sodium citrate for platelet aggregation experiments using platelet-rich plasma (PRP). Whole blood was centrifuged at 250 x *g* for 10 minutes at 22°C to obtain PRP. To obtain washed platelets (WP), PRP was centrifuged twice (1000 x *g*, 10 min, 20°C) in the presence of 1.25 μg/mL prostacyclin. The final platelet pellet was resuspended in modified Tyrode's-HEPES buffer, (20 mM N-2-hydroxyethylpiperazine-N′-2-ethanesulfonic acid, 5 mM glucose, 134 mM NaCl, 0.34 mM Na_2HPO_4, 2.9 mM KCl, 12 mM $NaHCO_3$ and 1 mM $MgCl_2$, pH 7.3) and rested for 30 minutes at 30°C before experiments. All protocols using human blood samples were approved by the Research Ethics Committees of the Federal University of Maranhão and the University of Reading.

2.4.6. Platelet aggregation

PRP and WP aggregation assays were performed in a four-channel aggregometer (Helena Biosciences, Gateshead, England). PRP samples (2-3 x 10^8 platelets/mL) were incubated for 25 minutes at 37°C with 10, 100 or 1000 μg/mL of PESc prior to the addition of ADP (2.5 or 5 μM), thrombin (0.01 or 0.02 U/mL) or PMA (100 nM). For experiments using myricetin and gallic acid, these were incubated in PRP (10, 30 or 100 μM for myricetin and 100, 300 or 1000 μM for gallic acid) or WP (7.5, 15 or 30 μM for myricetin and 75, 150 or 300 μM for gallic acid) for 10 minutes at 37°C followed by the addition of agonists collagen (1 μg/mL) or TRAP-6 (10 μM). Aggregation traces from at least 3 different donors were recorded for 5 minutes.

2.4.7. Flow cytometry

WP (2-3 x 10^8 platelets/mL) were incubated with PESc at the same concentrations and conditions used for platelet aggregation experiments. Then WP were incubated for 10 minutes with thrombin (0.02 U/mL). FITC-conjugated PAC-1 antibody (1:10 v/v) was added for 10 minutes in the dark and fluorescence read out on a FACS Calibur (BD Biosciences, Franklin Lakes, USA). For experiments using myricetin and gallic acid, these were incubated with WP for 10 minutes at 37 °C followed by the addition of agonists CRP (1 μg/mL) or TRAP-6 (10 μM). FITC-conjugated fibrinogen (1:50 v/v) and PE/Cy5-conjugated anti-human CD62P (1:50 v/v) were incubated for 30 minutes, then platelets were read after a 25-fold dilution with Tyrodes-HEPES buffer.

2.4.8. Platelet spreading

WP (2 x 10^7 platelets/mL) were incubated in absence or presence of myricetin (7.5, 15 and 30 μM) for 10 minutes at 37°C, then 300 μL of the solution was dispensed onto a fibrinogen or collagen (100 μg/mL)-coated coverslip for 45 minutes at 37°C. Non-adhered platelets were removed and the coverslip washed three times with PBS. Adhered platelets were fixed using 0.2% paraformaldehyde for 10 minutes. This solution was then removed and coverslips washed three times with PBS before the addition of 0.1% (v/v) Triton-X to permeabilise the cells. After removal of Triton-X and further washes using PBS, platelets were stained with Alexa Fluor 488 or 647-conjugated phalloidin (1:1000 v/v) for 1 hour in the dark at room temperature. Coverslips were mounted onto microscope glass slides and

imaged using a 100x oil immersion lens on a Nikon A1-R Confocal microscope.

2.4.9. Thrombus under flow

Whole blood was pre-incubated with $DIOC_6$ (5 μM) for 30 minutes at 30°C, whilst Vena8 bio-chips (Cellix Ltd, Dublin, Ireland) were coated with collagen (100 μg/mL) for 60 minutes at 37°C. Prior to experiment, blood was pre-treated with myricetin (30 μM) or vehicle control for 10 minutes at 37°C and Vena8 bio-chips were washed with Tyrode's-HEPES buffer. Whole blood was then perfused at a shear rate of 45 dyn/cm^2 and images recorded every 4 seconds for 10 minutes using a 20x air lens on a Nikon A1-R Confocal microscope exciting at 488 nm and detecting emission at 500 to 520 nm. Fluorescence intensity was calculated using NIS Elements Software (Nikon, Tokyo, Japan).

2.4.10. Tail bleeding assay

Healthy female Swiss mice (*mus musculus)* with 10 – 12 weeks of age and 30-35 grams were acquired from the Animal Facility House of the Federal University of Maranhão (UFMA), São Luís – MA. Animals were kept under a 12 h light cycle, controlled temperature (22-24°C) and food and water *ad libitum*. Mice were given myricetin at 25 mg/kg or 50 mg/kg or vehicle control for three consecutive days through oral gavage. One hour after the last dose, animals were anesthesized with ketamine (100 mg/kg) and xylazine (10 mg/kg) and 5 mm of the tail was amputated using a sharp scissor. The bleeding tail was then placed in filtered PBS buffer at 37 °C and

bleeding time recorded for up to 20 minutes, after which mice were terminated. All procedures were done in alignment with the National Council for the Control of Animal Experimentation (CONCEA, Brazil) and approved by the local Animal Care and Welfare Committee of UFMA, under ruling number 23115.018725/2017-19.

2.4.11. Generation of full-length recombinant ERp5, ERp57, ERp72 and PDI

The generation of recombinant thiol isomerases was performed as previously described (Holbrook et al., 2018). Briefly, cDNA for ERp5, ERp57, ERp72 and PDI were subcloned into pGEX6P1 expression vector in *Escherichia coli* to generate a glutathione s-transferase (GST)-tagged fusion protein. The fusion protein was then purified by affinity chromatography using glutathione agarose and the GST cleaved using PreScision protease as per manufacturer instructions (GE Healthcare, Amersham, UK). Finally, the proteins were submitted to a gel filtration on Superdex 75 purification resin (GE Healthcare, Amersham, UK) to remove contaminants.

2.4.12. Protein quenching analysis and biochemical equations

Myricetin (0.01 – 10 μM) or vehicle (1:400 v/v DMSO:PBS) were incubated with recombinant ERp5, ERp57, ERp72 or PDI (2 μM) in PBS buffer containing ethylenediaminetetracetic acid (EDTA, 0.2mM) for 10 minutes at 25 °C in a black 96-wells plate. Fluorescence intensity was read using a Flexstation 3 fluorimeter (Molecular Devices, Wokingham, UK), with 280 nm excitation and emission scanned from 300 to 420 nm in 5nm slits, at a speed

of 0.17 seconds per well. Appropriate blanks in which no protein was added were also acquired to establish that myricetin had no autofluorescence at the specified excitation/emission wavelengths. Data obtained are the means of at least three independent experiments run at least in duplicate.

To calculate the Stern-Volmer quenching constant (K_{SV}), peak fluorescence intensity at 330 nm was used and constant determined from the following equation:

$$\frac{F_0}{F} = 1 + K_{SV}[L] \quad (1)$$

Where F_0 is the fluorescence of protein alone, F is the fluorescence in the presence of increasing concentrations of myricetin and L is the concentration of myricetin used. K_{SV} was then calculated as the slope from the linear regression of F_0/F versus [L]. Data are shown as log [L]. The quencher rate coefficient Kq was determined from the formula:

$$K\mathrm{q} = \frac{K_{SV}}{\tau_0} \quad (2)$$

Where τ_0 is the average lifetime of the emissive excited state of the protein in the absence of the inhibitor. Previous reports have determined the typical value of τ_0 to be in the order of 10^{-8} s (Lakowicz and Weber, 1973), which was also adopted for the values herein presented.

The apparent binding constant (K_b) was determined according to the equation of Bi et al(Bi et al., 2005):

$$\log\left(\frac{F_0-F}{F}\right) = n\log K_b - n\log\left(\frac{1}{[L]-n(F_0-F)[P]/F_0}\right) \quad (3)$$

In which F_0 is the fluorescence of protein alone, F is the fluorescence in the presence of increasing concentrations of myricetin, [L] is the ligand concentration and [P] is the protein concentration in M. First, the linear

regression of log ($(F_0 - F)/F$) versus log (1/ ([L] − n (F_0 − F)[P]/F_0)) was plotted and *n* determined as the slope of the regression, as described by Bi et al (Bi et al., 2005). Then, *n* was substituted back into the equation and *K*b determined for the highest concentration tested. Finally, the dissociation constant (K_d) was calculated as $K_d = 1/K_b$.

2.4.13. Reductase activity

The reductase activity of the thiol isomerases was determined through the fluorescent probe dieosin glutathione disulphide (Di-E-GssG, excitation: 510 nm, emission: 545 nm). Di-E-GssG was synthesized and assay carried as previously described(Raturi and Mutus, 2007). Myricetin (0.01 - 10 μM) was incubated for 10 minutes with recombinant proteins (2 μM) diluted in PBS and EDTA (2 mM) buffer in a 96-wells black plate. Then, DTT (5 μM) and Di-E-GssG (200 nM) were added and fluorescence intensity acquired on a Flexstation 3 fluorimeter (Molecular Devices, Wokingham, UK). Fluorescence intensity was acquired every 30 seconds for 30 minutes. Data presented are the means of at least three independent experiments run at least in duplicate.

2.4.14. Molecular docking

The predicted poses of interaction between myricetin and different thiol isomerases were assessed using AutoDock 4.2 package, similar to previously described (Wang et al., 2018). The 3D structures of proteins were obtained from the PDB database (PDB ID: 4EL1 for PDIA1 and PDB ID: 4GWR for PDIA6/ERp5). The grid box of analysis was set as a perfect cube of 20 x 20

x 20 points with 1.00 Å spacing centered at the tryptophan residue near the active site of each thiol isomerase and the exhaustiveness of the runs set to 128. The 20 predicted poses with the best binding affinity were generated for each protein and each pose was studied individually to assess if chemically sound using Pymol software (Schrodinger, Cambridge, UK).

2.4.15. Immunoblotting

WP (4 x 10^8 platelets/mL), were incubated with myricetin (7.5, 15 and 30 μM) or the nitric oxide donor PAPA-NONOate (100 μM), lysed in reducing Laemmli sample buffer (12% (w/v) Sodium Dodecyl Sulphate (SDS), 30% (v/v) glycerol, 0.15 M Tris-HCl (pH 6.8), 0.001% (w/v) Brilliant Blue R, 30% (v/v) β-mercaptoethanol) and boiled for five minutes. Samples were loaded into a 10% Mini-PROTEAN TGX precast protein gel submerged in 1X Tris/Glycine/SDS buffer (25 mM Tris, 192 mM glycine, 0.1% SDS, pH 8.3), then submitted to vertical transfer in a tetra vertical electrophoresis cell (Bio-Rad, CA, USA) using constant voltage of 150V for 45 minutes. After protein separation, semi-dry transfer was performed at 15V for 2 hours using a BioRad Trans-blot semidry blotter. Membranes were blocked with 5% bovine serum albumin (BSA) for 1 hour and incubated with primary antibodies against VASP (Ser239) or GAPDH at 1:1000 v/v dilution overnight. After washing the primary antibody off, Alexa-488 conjugated phalloidin secondary antibody was incubated for 1 hour at room temperature at 1:4000 v/v dilution. Membranes were visualised using a Typhoon imaging system (GE Healthcare, Hatfield, UK).

2.4.16. Statistical analysis

Statistical analyses were obtained from GraphPad Prism 6.0 software (GraphPad Software, San Diego, USA). Quantitative results were expressed as mean ± SEM and individual points for all bar graphs, in order to improve transparency on the variability of data. Sample size varied from 3-6 independent repeats. Statistical analysis was performed through paired one-way ANOVA and Tukey as post-test with level of significance of 5%.

2.5. Results

2.5.1. PESc inhibited platelet activation and aggregation induced by different agonists

The initial approach focused on whether PESc would inhibit platelet aggregation. Therefore, different concentrations of PESc were incubated with PRP and platelets were activated with various agonists. The composition of the batch of PESc used in this study is consistent with those previously reported (Chagas et al., 2018) (Supplementary Figure 2.1). Figure 2.1 displays the inhibitory activity of PESc in ADP-, thrombin- and PMA-induced platelet aggregation – the strongest inhibition was seen when using ADP, in which PESc promoted a 60% decrease in platelet aggregation. Increased agonist concentration partially overcame the inhibition seen in ADP- and thrombin-induced platelet aggregation (Supplementary Figure 2.2). This persuaded us to use the non-biological agonist PMA, a direct activator of protein kinase C (PKC), as a way to avoid the initial signalling processes triggered by these agonists. Interestingly, concentrations as low as 10 μg/mL of PESc were able to mitigate platelet aggregation induced by PMA by 20%.

Given that PESc inhibited platelet aggregation induced by different agonists, we hypothesized that this extract would also affect integrin $\alpha IIb\beta_3$ activation. Therefore, we incubated WP with PESc at different concentrations and used PAC-1 antibody to detect active integrin $\alpha IIb\beta_3$ by flow cytometry. Upon stimulation with thrombin, a 6- fold increase in PAC-1 binding was observed and the percentage of positive events increased from 20% to 82% (Figure 2.1G and H). Interestingly, PESc was able to decrease PAC-1 median fluorescence intensity compared to vehicle at concentrations as low as 10

μg/mL (~20% inhibition), reaching 65% inhibition at 1000 μg/mL (Figure 2.1H). Overall, our data reinforce the strong anti-platelet effects of PESc, due to the significant inhibition observed at concentrations as low as 10 μg/mL, possibly through reacting with molecules that orchestrate integrin $\alpha IIb\beta_3$ activation.

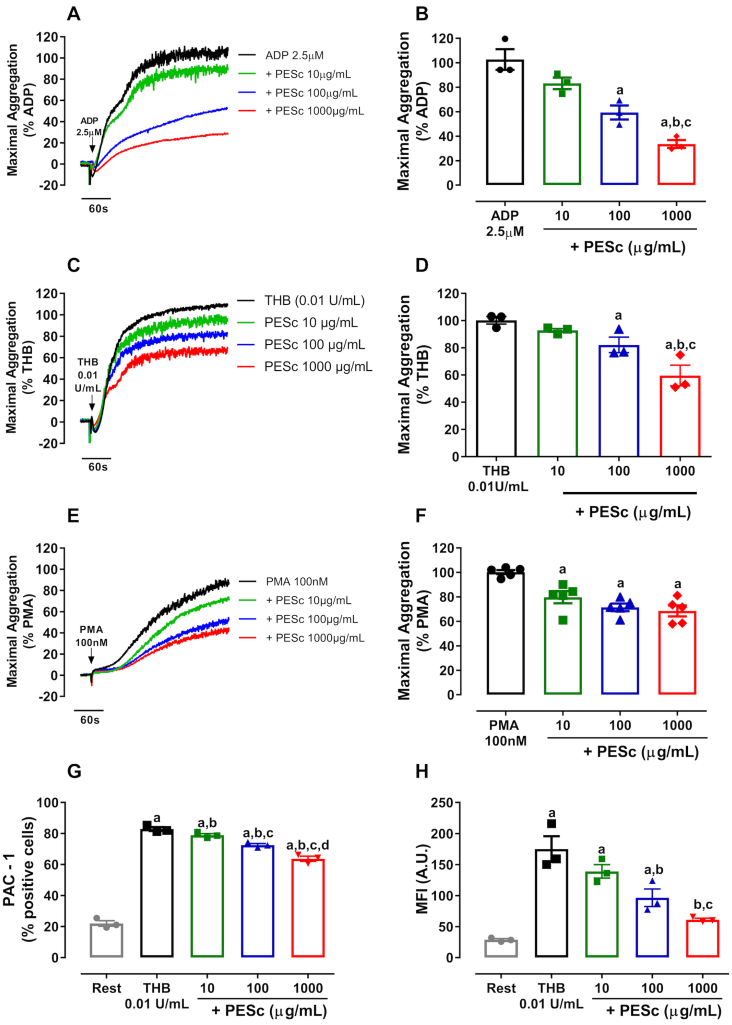

Figure 2.1. PESc inhibits platelet aggregation and integrin αIIbβ3 activation. Platelet-rich plasma was pretreated with PESc (10, 100 or 1000 µg/mL) for 25 minutes and stimulated with ADP (A), thrombin (THB, C) or PMA (E). Quantified data is shown next to representative curves for ADP (B), thrombin (D) and PMA (F) stimulated platelet aggregation. Washed platelets were pre-treated with PESc under the same conditions, stimulated with thrombin and incubated with PAC-1 antibody to measure integrin activation. (G) Percentage of PAC-1 positive events. (H) Mean fluorescence intensity (MFI) of events. a $p<0.05$ vs first column of graph. b $p<0.05$ vs second column of graph. c $p<0.05$ vs third column of graph. Data analysed by paired one-way ANOVA and Tukey as post-test. All bar graphs represent mean ± SEM and individual data points of at least 3 independent experiments. Arrows indicate when agonists were added.

2.5.2. Myricetin was more potent than gallic acid in inhibiting platelet aggregation

After establishing the antiplatelet potential of PESc and identifying its main components, we investigated the effects of myricetin (most abundant compound) and gallic acid (second most abundant compound) on platelet aggregation. Both PRP (Supplementary Figure 2.3) and WP (Figure 2.2) were incubated with different concentrations of either myricetin or gallic acid and platelets were stimulated with collagen or the thrombin-analogue TRAP-6. Myricetin at the highest concentration tested (30 μM) was able to substantially inhibit platelet aggregation induced by both agonists (~80% inhibition for collagen and ~60% inhibition for TRAP-6; Figure 2.2B and F). Gallic acid was unable to inhibit platelet aggregation, except at the highest concentration used (300 μM) in TRAP-6 activated platelets (Figure 2.2H) – an effect that is likely due to cytotoxicity of such high concentration. In fact, gallic acid has been shown to be cytotoxic to different cell lines at concentrations above 50 μM (Park et al., 2008). The effect of myricetin and gallic acid on platelet aggregation should not be compared with data on PESc as different agonists were used. Altogether, these data indicate that myricetin is a potent inhibitor of platelet aggregation at physiologically relevant concentrations, whereas gallic acid yields no inhibitory effect.

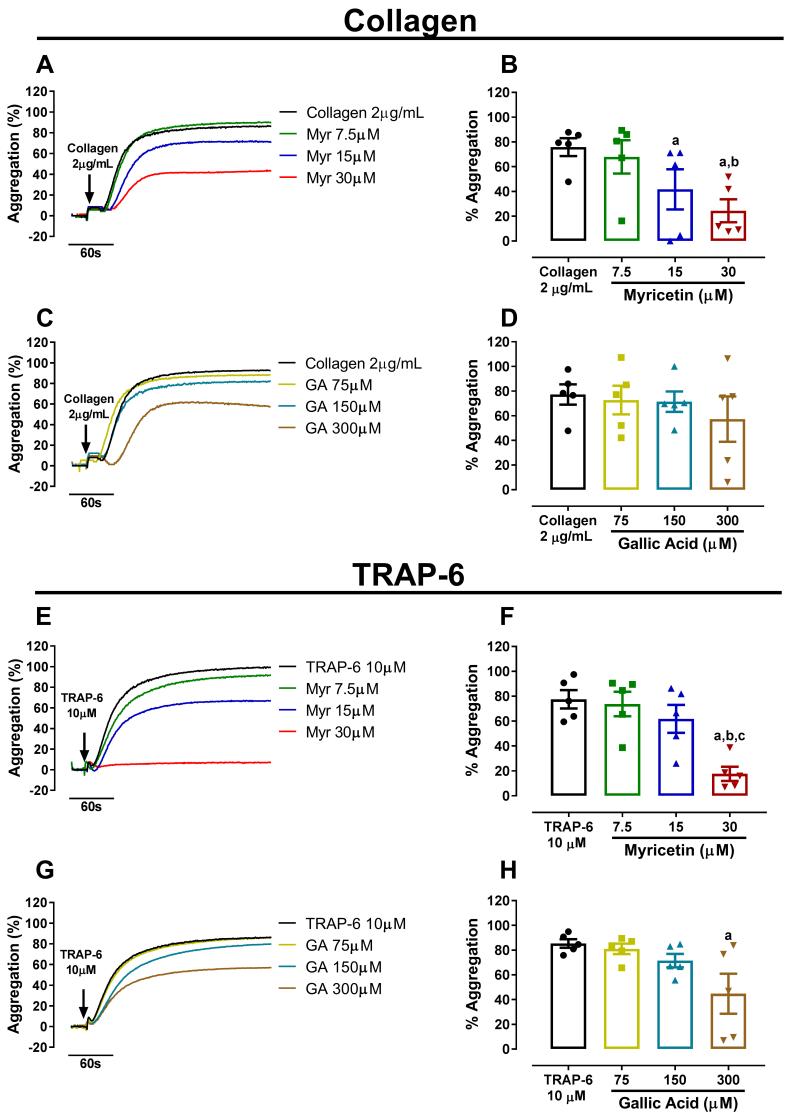

Figure 2.2. Myricetin inhibits platelet aggregation more potently than gallic acid. Washed platelets (WP) were pre-treated with myricetin (Myr) or gallic acid (GA) for 10 minutes and stimulated with collagen or TRAP-6. (A) WP treated with Myr and stimulated with collagen. (C) WP treated with GA and stimulated with collagen. (E) WP treated with Myr and stimulated with TRAP-6. (G) WP treated with GA and stimulated with TRAP-6. Quantified data is shown right next to representative curves. a $p<0.05$ vs first column of graph. b $p<0.05$ vs second column of graph. c $p<0.05$ vs third column of graph. Data analysed by paired one-way ANOVA and Tukey as post-test. All bar graphs represent mean ± SEM and individual data points of at least 3 independent experiments. Arrows indicate when agonists were added.

2.5.3. Myricetin inhibited platelet activation and alpha-granule exposure induced by different agonists

Further studies were conducted to assess the effect of both myricetin and gallic acid in platelet function through flow cytometry. Results in Figure 2.3 show that myricetin at 15 μM was able to abolish fibrinogen binding and alpha-granule exposure induced by CRP (Figure 2.3A and B). In contrast, gallic acid was only able to reduce fibrinogen binding when incubated at 150 μM, consistent with the limited potency of this phenolic compound to inhibit platelet aggregation (Figure 2.3C and D). When TRAP-6 was used as an agonist, myricetin still inhibited fibrinogen binding, whereas no effect was seen for P-selectin exposure (Figure 2.3E and F). Overall, data herein described suggest myricetin is a flavonoid with potent anti-platelet effects, whereas gallic acid only had an effect at 10x higher concentrations. Therefore, focus was given to myricetin in order to further explore its antiplatelet effects and elucidate possible mechanisms of action.

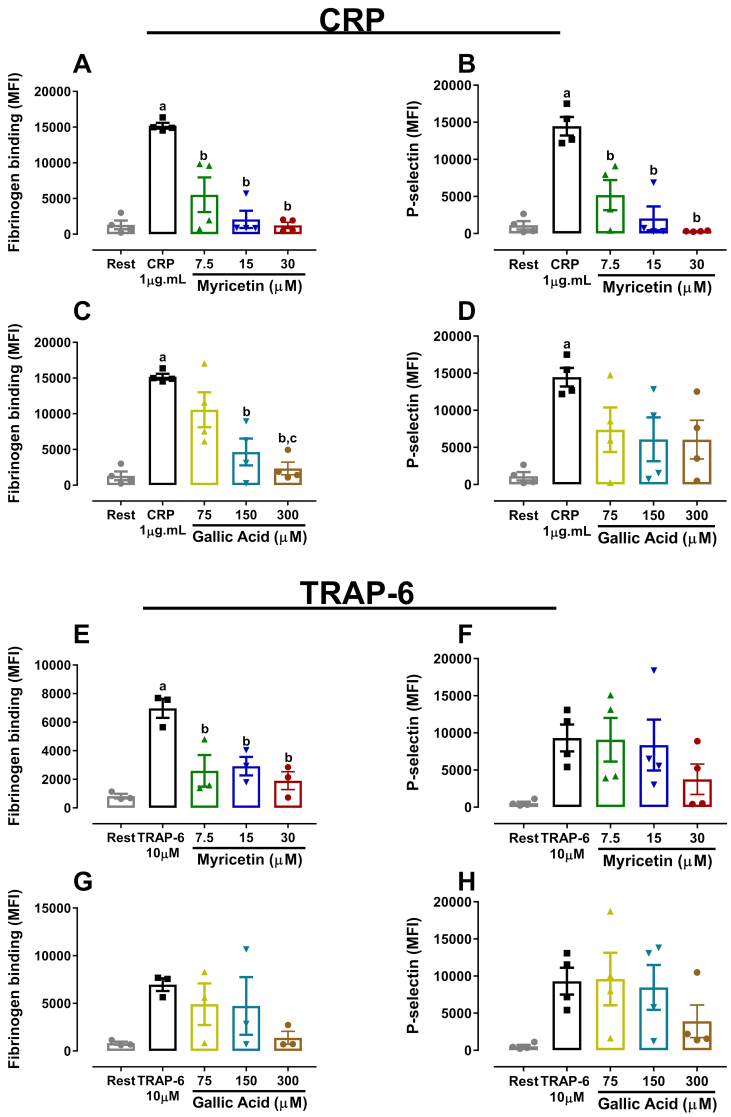

Figure 2.3. Platelet activation and alpha-granule secretion is inhibited by myricetin but not by gallic acid. Washed platelets (WP) were pre-treated with myricetin or GA for 10 minutes, stimulated with agonists and incubated with FITC-coupled fibrinogen and PE/PerCP anti-P-selectin antibodies. Fibrinogen binding (A) and P-selectin exposure (B) of CRP-activated platelets treated with myricetin. Fibrinogen binding (C) or Pselectin exposure (D) of CRP-activated platelets treated with GA. Fibrinogen binding (E) and P-selectin exposure (F) of TRAP-6-activated platelets treated with myricetin. Fibrinogen binding (G) and P-selectin exposure (H) of TRAP-6-activated platelets treated with GA. a $p<0.05$ vs first column of graph. b $p<0.05$ vs second column of graph. c $p<0.05$ vs third column of graph. Data analysed by paired one-way ANOVA and Tukey as post-test. All bar graphs represent mean ± SEM as well as individual data points of at least 3 independent experiments.

2.5.4. Myricetin inhibits platelet adhesion to collagen and thrombus formation under flow

Upon vascular injury, platelets start to adhere to components of the sub-endothelium, such as collagen and fibrinogen (Ghoshal and Bhattacharyya, 2014). In order to assess the effect of myricetin on platelet adhesion, WP were left to adhere to collagen or fibrinogen-coated coverslips in the presence or absence of different concentrations of myricetin. The area of platelets spread as well as representative images of the assay are shown in Figure 2.4. Myricetin decreased platelet spreading to collagen (~25% inhibition at 30 μM, Figure 2.4B), whereas no effect was seen on platelet spreading to fibrinogen (Figure 2.4C). This is similar to a previous report using PDI-deficient murine platelets (Chang et al., 2012).

Given the anti-platelet and inhibition of adhesion to collagen exerted by myricetin, we hypothesized this flavonoid could impact thrombus formation. Therefore, blood was perfused under physiological arterial shear rate into collagen-coated Vena8 biochips as shown in Figure 2.4E and F. It was evident that myricetin treatment decreased thrombus formation (measured as an increase in fluorescence intensity) within the first 100 seconds, persisting throughout the 10-minutes assay. This data is consistent to the platelet inhibition herein described for myricetin and expands the importance of this flavonoid to modulate thrombus formation.

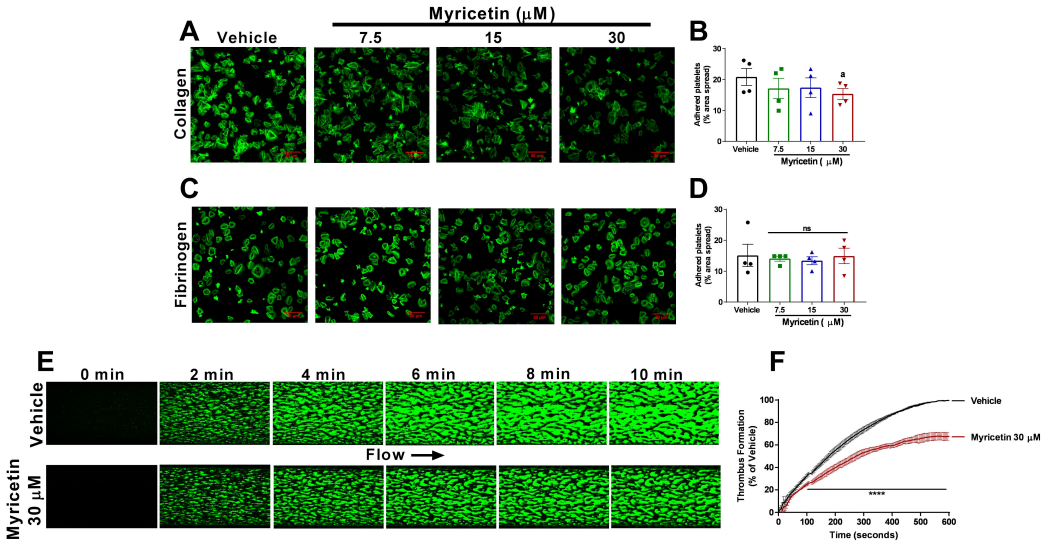

Figure 2.4. Myricetin inhibits adhesion to collagen and thrombus formation in vitro. Washed platelets (WP) were pre-treated with myricetin (7.5, 15 and 30 μM) for 10 minutes and left to adhere to coverslips coated with 100 mg/mL of collagen (A and B) or Fibrinogen (C and D) for 45 minutes. Platelets were stained with Alexa Fluor 488 or 647-conjugated phalloidin for visualization. DioC6-labelled whole blood was pre-treated with myricetin (30 μM) or vehicle control and blood perfused through collagen-coated Vena8 biochip channels at a shear rate of 45 dyn/cm2 for 10 minutes. (E) Representative image of thrombus formation assay. (F) Quantification of fluorescence normalized by vehicle control. a $p< 0.05$ vs Vehicle. **** $p<0.001$ vs Vehicle. For adhesion assay, bar graphs (B and D) represent mean ± SEM and individual data points of 4 independent experiments. For thrombus formation assay, line graph (F) represent mean ± SEM of three independent experiments.

2.5.5. Myricetin does not affect haemostasis *in vivo*

After establishing anti-platelet and anti-thrombotic properties for myricetin, we then tested its impact on haemostasis. Healthy mice (10 – 12 weeks of age) were given myricetin (25 or 50 mg/kg) orally for three consecutive days, upon which bleeding time was measured after tail tip removal. Results are shown in Figure 2.5. Mice treated with myricetin displayed similar bleeding time when compared to vehicle control. Notably Kim et al (Kim et al., 2013) have reported that genetic deletion of PDI in platelets is tolerated and bleeding time, similarly unaffected. Of note, myricetin did not induce VASP phosphorylation (Supplementary Figure 2.4).

Therefore, considering that 1) myricetin inhibited platelet aggregation induced by different agonists, 2) that PDI is a key modulator of integrin $\alpha IIb\beta_3$ function located at the end of the platelet activation pathway, 3) that myricetin inhibited platelet spreading on collagen but not on fibrinogen, similar to a PDI knockout model (Kim et al., 2013) 4) that myricetin showed no effect on haemostasis, also comparable to a platelet-specific PDI knockout model (Kim et al., 2013) and 5) that some flavonoids have been described as PDI inhibitors (Jasuja et al., 2012;Giamogante et al., 2018), we decided to investigate the biochemical effects of myricetin on PDI and other thiol isomerases important for platelet function.

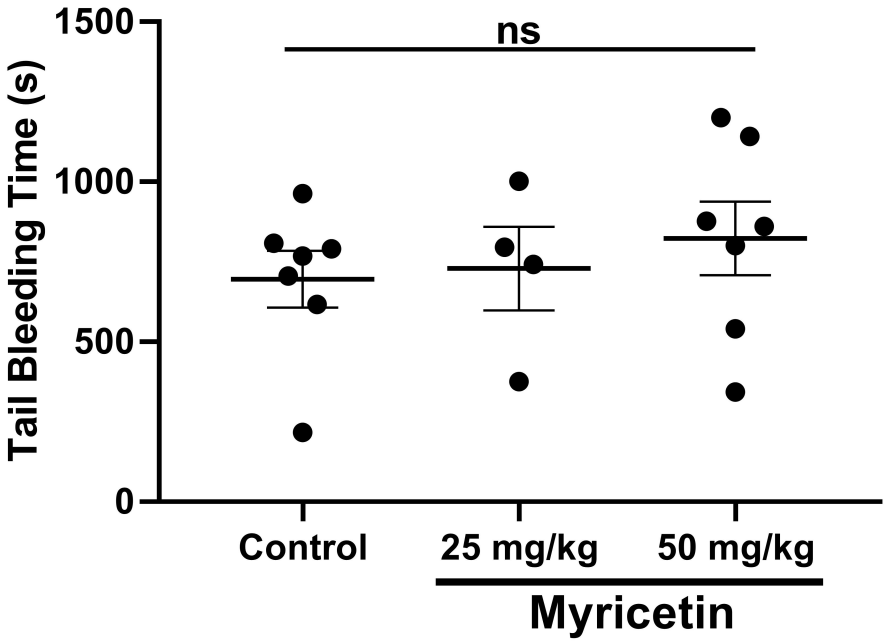

Figure 2.5. Myricetin does not affect haemostasis in vivo. Myricetin at 25 mg/kg or 50 mg/kg as well as vehicle control were administered to healthy mice by oral gavage for three consecutive days. Tail bleeding was measured after tail tip amputation. Data expressed as mean ± SEM as well as individual points. There was no statistical difference between groups.

2.5.6. Myricetin binds close to the active redox sites of PDI, ERp5, ERp57 and ERp72

The possible interaction between myricetin and PDI, ERp5, ERp57 and ERp72 was initially assessed through quenching of the fluorescence emitted by tryptophan residues exposed near the redox active site WCGHC, as described for ERp57 (Trnkova et al., 2013). Table 2.1 shows the values for the Stern-Volmer constant K_{SV}, the quencher coefficient Kq, the binding constant K_b and the dissociation constant K_d for each protein studied. Values for K_{SV} and Kq were within the same order of magnitude for all of the thiol isomerases tested, indicating a similar binding affinity between these proteins and myricetin (Table 2.1). Representative quenching curves for each protein and Stern-Volmer plot are shown in Supplementary Figure 2.5. Notwithstanding, it is possible for a compound to bind to thiol isomerases without affecting its function, as previously described for the interaction between ellagic acid and ERp57 (Giamogante et al., 2018). Therefore, the ability of myricetin to inhibit the reductase activity of these thiol isomerases was explored.

Table 2.1. Constants calculations based on protein quenching studies.

	K_{SV}(M^{-1})	Kq ($M^{-1}s^{-1}$)	K_b (M^{-1})	K_d (M)
ERp5	48,750 ± 9,554	$4.87 \cdot 10^{12}$	$5.72 \cdot 10^{5}$	$1.74 \cdot 10^{-6}$
ERp72	27,515 ± 5,675	$2.75 \cdot 10^{12}$	$3.94 \cdot 10^{5}$	$2.53 \cdot 10^{-6}$
ERp57	29,777 ± 5,966	$2.97 \cdot 10^{12}$	$5.44 \cdot 10^{5}$	$1.83 \cdot 10^{-6}$
PDI	21,207 ± 0,877	$2.12 \cdot 10^{12}$	$2.34 \cdot 10^{5}$	$4.26 \cdot 10^{-6}$

K_{SV}: Stern-Volmer constant. Kq: Quenching rate constant. K_b: Binding constant

K_d: Dissociation constant. Data presented as Mean ± SEM.

2.5.7. Myricetin inhibits the reductase activity of PDI and ERp5

The highly sensitive fluorescent probe Di-E-GssG was used to assess the reductase activity of thiol isomerase in the presence or absence of myricetin. Results shown in Figure 2.6 demonstrate the ability of myricetin to inhibit both PDI and ERp5, being more potent against PDI (Figure 2.6A and B). On the other hand, myricetin was unable to inhibit the reductase activity of ERp57 or ERp72 at the concentrations tested (Figure 2.6C and D). Therefore, we proceeded to investigate possible binding mechanisms between myricetin and PDI and ERp5 using a molecular docking approach.

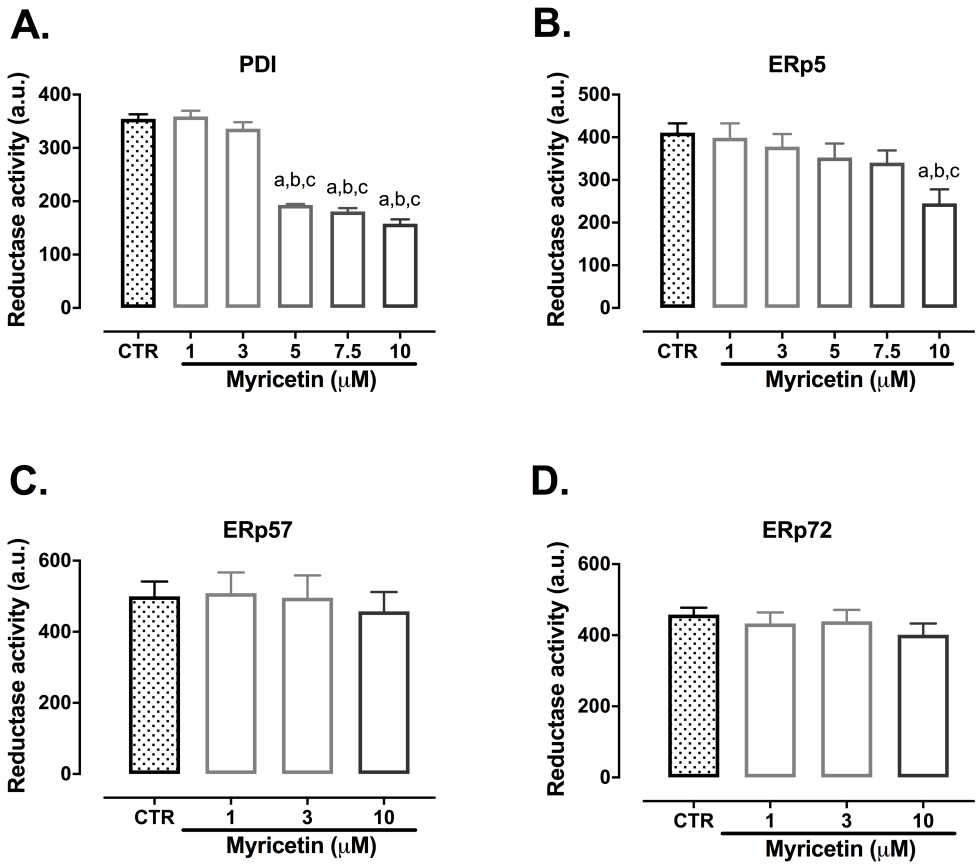

Figure 2.6. Myricetin inhibits reductase activity of PDI and ERp5. Recombinant proteins were incubated with myricetin (0.01 to 10 μM) in a black 96-wells plate for 10 minutes followed by addition of DTT (5 μM) and Di-E-GssG (200 nM). Fluorescence was read every 30 seconds for 30 minutes. Final point fluorescence at 30 minutes is shown for ERp5 (A and B), PDI (C and D), ERp72 (E and F) and ERp57 (G and H). Data represent at least three independent experiments run at least in duplicate and error bars indicate SEM. a $p<0.05$ vs first column of graph. b $p<0.05$ vs second column of graph. c $p<0.05$ vs third column of graph.

2.5.8. Myricetin is predicted to form non-covalent bonds close to the active redox sites of PDI and ERp5

To assess the nature of the interaction between myricetin and thiol isomerases ERp5 and PDI, *in silico* experiments using molecular docking were conducted. Since the protein quenching studies suggested an interaction between myricetin and the Trp residues of the thiol isomerases, the grid box of analysis for molecular docking was centred at Trp_{189} for ERp5 and Trp_{52} for PDI, which are near the active site of each protein. Results shown in Figure 2.7 provide an overview of the interactions found for the pose of highest affinity between ligand and protein, whereas the full description of interactions can be accessed on Supplementary Tables 2.1 and 2.2. It is notable that myricetin displayed similar affinity to both PDI and ERp5 (Figure 2.7), which corroborates *in vitro* findings (Table 2.1). Likewise, all of the interactions herein described are non-covalent bonds, with hydrogen bonding constituting the vast majority of these, even though it is possible for myricetin to form adducts with thiols through carbons 2' and 6' on ring B (Masuda et al., 2013).

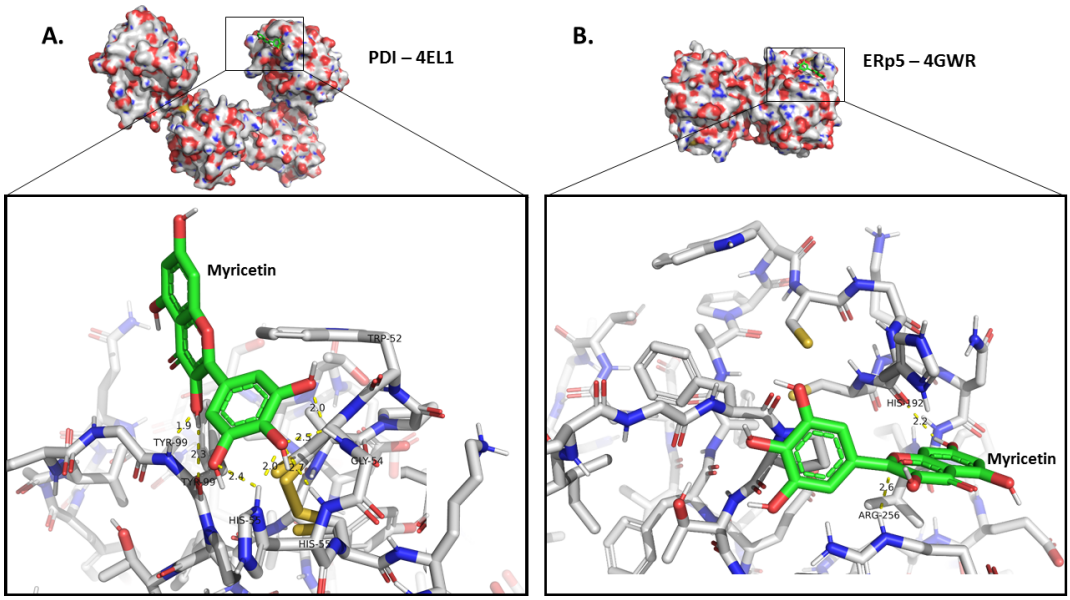

Figure 2.7. Feasible interactions for Myricetin with PDI and ERp5 predicted through molecular docking. The predicted poses of interaction between myricetin and different thiol isomerases were assessed using AutoDock 4.2 package as described in Methods. (A) Pose of highest affinity for PDI and detailed intermolecular interactions. (B) Pose of highest affinity for ERp5 and detailed intermolecular interactions. Additional information on interactions and other possible poses are described in Supplementary Tables 2.1 and 2.2.

2.6 Discussion

This study expands the applicability of PESc and myricetin, a flavonoid of widespread occurrence among plants and the most abundant in PESc, on platelet function and thrombus formation. Additionally, it offers a novel mechanism by which this flavonoid may inhibit platelets and thrombus formation. Mechanistically, it was shown that myricetin was able to bind to thiol isomerases and inhibit the reductase activity of PDI and ERp5 possibly due to non-covalent bonds between the compound and amino acids adjacent to the redox active site of these proteins.

We first showed that PESc was able to inhibit platelet function. PESc also inhibited platelet aggregation induced by PKC activator PMA (a phorbol ester that directly activates PKC), which suggests some compounds were able to cross the platelet cell membrane, probably targeting PKC or downstream molecules, i.e. signalling that occurs at the end of the platelet activation pathway. Moreover, the inhibition of platelet function herein described for PESc is in accordance with reports showing that a green tea flavonoid-rich extract reduced platelet aggregation and integrin $\alpha IIb\beta_3$ activation upon stimulus with ADP, thrombin or collagen (Kang et al., 2001). Given that myricetin and gallic acid were the two most abundant polyphenols found within PESc, we then proceeded to test these compounds individually.

Myricetin inhibited platelet aggregation and activation induced by agonists of the collagen and thrombin pathways, whereas gallic acid showed little to no effect even at 10x higher concentrations. This is in agreement with previous reports showing myricetin strongly inhibited collagen- (Dutta-Roy et al., 1999) and arachidonic acid-evoked platelet aggregation (Lescano et al.,

2018). Interestingly this latter work reported that myricetin does not inhibit cyclooxygenase activity in platelets (Lescano et al., 2018). It has been described that gallic acid is able to inhibit platelet aggregation only at exceedingly high concentrations (Chang et al., 2012) which is corroborated by our data showing no effect below 300 μM. In addition, Dang and colleagues (2014) showed that myricetin was able to reach a peak plasma concentration of 10 μM upon a single oral dose of 100 mg/kg in rats, corroborating that the concentrations tested in our study could be achievable *in vivo*. Of note, the study of Dang and colleagues (2014) reports the concentration of myricetin conjugated with glucuronic acid or sulphate, instead of the free form used in this study.

The effect of myricetin on platelet activation is also compatible with that previously shown for quercetin, a flavonoid of similar structure. Navarro-Nuñez et al (Navarro-Nunez et al., 2009) reported that quercetin was able to inhibit platelet aggregation and signalling induced by thrombin and specific agonists of the thrombin receptors protease-activated receptor 1 (PAR1) and 4 (PAR4). The ability of myricetin to inhibit platelet aggregation and activation induced by different agonists suggests this flavonoid may act on molecules common to each pathway. The lack of effect of gallic acid on platelet function, coupled with the strong inhibition exerted by myricetin prompted us to focus on myricetin to further assess its mechanisms of action.

Some flavonoids, such as nobiletin, have been shown to increase VASP phosphorylation (Jayakumar et al., 2017), which is a key inhibitory molecule in platelets. Myricetin did not induce the phosphorylation of VASP at Ser_{239} (Supplementary Figure 2.4), suggesting this is probably not the target for this

flavonoid. Likewise, quercetin has been shown to bind to the Thromboxane A_2 (TxA_2) receptor (TPR) and this could also be a potential mechanism of action for myricetin. However, previous literature has shown that SQ-29548, a specific TPR inhibitor, displayed little effect on CRP-induced platelet activation (Taylor et al., 2014) and that platelet aggregation induced by CRP was independent of TxA_2 (Jarvis et al., 2002). In addition, TRAP-induced aggregation was found to be aspirin-insensitive, suggesting a minor role for TxA_2 (Chung et al., 2002). Therefore, although the effects of myricetin on TxA_2 pathway cannot be excluded, we argue that this is likely not the main target of this flavonoid, since it was able to potently inhibit platelet aggregation and activation induced by CRP and TRAP-6.

Platelets express two principal membrane receptors that are able to bind collagen: GPVI and integrin $\alpha_2\beta_1$. Despite GPVI being considered the primary collagen receptor involved in platelet aggregation and activation (Kehrel et al., 1998), integrin $\alpha_2\beta_1$ was shown to be the main platelet adhesive receptor to collagen (Inoue et al., 2003). Moreover, it was recently shown that GPVI could also bind and contribute to platelet adhesion and spreading to immobilized fibrinogen (Mangin et al., 2018), suggesting GPVI is unlikely to be a target for myricetin since this flavonoid did not inhibit platelet spreading to fibrinogen (Figure 2.4C). Interestingly, it was demonstrated that integrin $\alpha_2\beta_1$ is in close proximity and is regulated by PDI (Lahav et al., 2003). In fact, platelet-specific PDI-deficient mice were unable to form proper thrombi on collagen-coated surfaces, even though their platelets spread normally on fibrinogen (Kim et al., 2013), similar to myricetin (Figure 2.4). This same report described no changes in bleeding

time between wildtype and platelet-PDI KO mice, also in accordance with data herein described for myricetin. Therefore, we decided to assess the interaction between myricetin and thiol isomerases.

Initially, thiol isomerases were incubated with myricetin and changes in tryptophan fluorescence were measured. Protein quenching studies showed that myricetin was able to bind to all of the thiol isomerases tested. Values of the dissociation constant *K*q greater than 2.0 x 10^{10} $M^{-1}s^{-1}$ support the formation of complexes between quencher and protein (Ware, 1962), suggesting myricetin forms a complex or complexes with the thiol isomerases tested. Interestingly, the *K*q herein reported for myricetin is one order of magnitude lower than that described for other flavonoids binding to ERp57 (Giamogante et al., 2016). Considering that the dissociation constant is inversely related to binding affinity, these results suggest myricetin has a high binding affinity to thiol isomerases, at the μM range. These results, however, do not allow the conclusion of whether the interaction between myricetin and thiol isomerases is due to static or dynamic binding.

Despite being able to bind to PDI, ERp5, ERp57 and ERp72, myricetin was only able to inhibit the reductase activity of PDI and ERp5 at concentrations able to be biologically reached. Quercetin, a structurally similar flavonoid was reported to be a weak inhibitor of PDI (Jasuja et al., 2012), whereas quercetin derivatives, such as isoquercetin (Stopa et al., 2017) and rutin (Jasuja et al., 2012), were shown to be potent inhibitors of PDI reductase activity. It is important to note that we used the fluorescent EGSH method whereas these reports used insulin turbidimetry to assess reductase activity. Thus, differing results would be anticipated since the

fluorescent EGSH method is considered to be more sensitive than insulin turbidimetry (Raturi and Mutus, 2007). This is corroborated by a recent report showing distinct behaviour of a new class of PDI inhibitors tested in both assays (Bekendam et al., 2016). Nonetheless, the inhibition exerted by myricetin is comparable to that of the flavonoid punicalagin, a non-competitive inhibitor of ERp57 (Giamogante et al., 2018).

Molecular docking studies predicted interactions between myricetin and amino acids adjacent to the tryptophan residues near the redox active sites in each thiol isomerase. This indicates that the possible quenching mechanism is unlikely to be a direct complex between ligand and tryptophan. One possibility is that the binding of myricetin to adjacent amino acids such as Tyr_{99} of PDI or His_{192} of ERp5, may induce excited-state proton or electron transfer from these amino acids to the Trp nearby, which would quench its fluorescence, as previously described (Chen and Barkley, 1998). The lack of covalent bonds predicted for myricetin and thiol isomerases suggest a weak and reversible interaction, similar to what was described for rutin and PDI (Wang et al., 2018), which makes it more difficult to assess such interaction *in vitro*. Since myricetin was predicted to bind close to the redox CGHC site of PDI and ERp5, it is also hypothesized that myricetin inhibits the reductase activity through an allosteric effect, similar to what described for rutin (Wang et al., 2018). Future studies are needed to confirm these findings.

In conclusion, this study expands the applicability of PESc as an anti-platelet extract, as well as describes myricetin as a novel inhibitor of thiol isomerases ERp5 and PDI with anti-platelet and anti-thrombotic properties. Moreover, myricetin was shown to have no effect on haemostasis, initially

suggesting lower chances of bleeding upon myricetin treatment. Nevertheless, future studies with longer treatment regimens are needed to further assess the safety and efficacy of this flavonoid, as well as the interaction of myricetin with other proteins, such as thioredoxin reductase (Lu et al., 2006) and kinases (Navarro-Nunez et al., 2009). Therefore, this study may offer new insights into the complementary use of myricetin for the treatment of thrombosis, corroborating the promising use of flavonoids to treat cardiovascular diseases with thrombotic outcomes.

AUTHOR CONTRIBUTIONS STATEMENT

RG designed the study, performed experiments, analysed data and drafted the manuscript. SS, JS, JF, HS and VC performed experiments and analysed data. SA generated recombinant proteins used in experiments. AT supervised experiments, discussed data and reviewed the manuscript. JG discussed data and reviewed the manuscript. AP designed the study, discussed the data, drafted and reviewed the manuscript.

ACKNOWLEGMENTS

The authors are grateful to the staff of the Laboratory of Immunophysiology (LIF/UFMA) and Laboratory of Experimental Physiology (LeFisio/UFMA), especially to Dr Ludmila Bezerra and Mr Victor Vieira for the technical assistance during experimental protocols execution.

SOURCES OF FUNDING

This study was funded by the British Heart Foundation (RG/15/2/31224), Medical Research Council (MR/J002666/1) and Fundação de Amparo à Pesquisa e ao Desenvolvimento Científico e Tecnológico do Maranhão, FAPEMA (PAEDT-00376/14, APCINTER 02698/14). A. Trostchansky was supported by CSIC grupos I+D 2014 and 2018 (536) and FAPEMA (PVI-05558/15). A.M.A. Paes was supported by FAPEMA (BEEP-02511/18).

DISCLOSURE OF INTEREST

The authors declare no actual or potential conflict of interest.

2.7 Supplementary Tables

Supplementary Table 2.1 Predicted interactions between Myricetin and ERp5 (4GWR) interaction

Pose	Myricetin	Distance (Å)	Intermolecular Interaction	Protein	Affinity (kcal/mol)
1	O1	2.5	= O – HN	H192	-5.3
	O1	2.6	= O – HN	R256	
	H3	2.2	OH – O =	H192	
2	O1	2.3	= O – HN	W189	-4.8
	O18	2	= O – HN	Y186	
	O21	2	HO – HN	G191	
7	O17	2.1	HO – HN	W189	-4.6
	O18	2.2	= O – HN	F237	
	O19	2.2	OH – O =	F237	
	H6	2.2	OH – O =	W189	
	O21	1.9	HO – HN	G191	
	H1	2.3	HO – HN	F237	
8	H9	2.4	OH – O =	F237	-4.4
	O19	2.7	HO – HN	G191	
	O19	2.3	HO – HN	H192	
14	O17	2.1	HO – HN	G191	-4.2
	H9	2.3	OH – O =	W189	
	O21	2.1	HO – HN	W189	
	O22	2.2	HO – HN	F237	
	H7	2.4	OH – O =	F237	
16	O22	2.4	HO – HN	F237	-4.2
	H7	2.1	OH – O =	F237	
	O21	2	HO – HN	W189	
	O1	2.2	= O – HN	G191	
	O20	2.2	HO – HN	K194	

Supplementary Table 2.2 Predicted interactions between Myricetin and PDI (4EL1) interaction

Pose	Myricetin	Distance (Å)	Intermolecular Interaction	Protein	Affinity (kcal/mol)
1	O17	1.9	HO – HN	Y99	-5.5
	H9	2.3	OH – O =	Y99	
	O21	2.4	HO – HN	H55	
	O22	2	HO – HN	H55	
	O22	2.7	HO – HN	H55	
	O22	2.5	HO – HN	G54	
	O23	2	HO – HN	G54	
3	O21	2.2	HO – HN	K81	-5.2
	O17	2.2	HO – HO	Y49	
	H9	2	OH – OH	D83	
5	O19	2.4	HO – HN	K81	-5.2
	O18	2.4	= O – HN	K81	
7	O17	2.9	HO – HN	K81	-5.1
	H9	2.2	OH – O =	E23	
	H9	2.9	OH – OH	E23	
	O22	2	HO – HN	K57	
11	O21	2	HO – HN	G54	-4.9
	O22	2.4	HO – HN	G54	
	O22	2.4	HO – HN	H55	
	O22	1.9	HO – HN	H55	
	O23	2.8	HO – HN	H55	
	O1 – C10	4 – 4,2	π – π	W52	
14	O17	2	HO – HN	G54	-4.9
	H7	2.4	OH – O =	Y99	
	O22	2.4	HO – HN	Y99	
	O21	2.3	HO – HN	Y99	
15	O19	2.3	HO – HN	Q92	-4.8
	H3	1.9	OH – O =	A84	
	C11 – C16	3.7	π – π	W52	
	O21	2.4	HO – HN	Y99	

2.8 Supplementary Figures

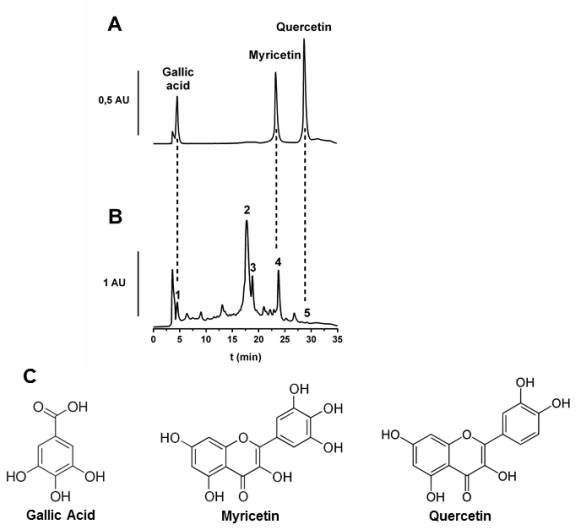

Supplementary Figure 2.1. Chromatographic fingerprint of PESc and flavonoid standards. UV detection of standards for gallic acid, myricetin and quercetin (A) or a sample of PESc (B) were analysed through LC-MS/MS as described in Methods. In addition, each fraction was purified and their identity confirmed by HPLC-MS/MS studies. Peak 1 corresponded to gallic acid, peaks 2 and 3 to myricetin glycoside derivatives, peak 4 to myricetin and peak 5 to quercetin. Structures of the identified compounds are shown in (C).

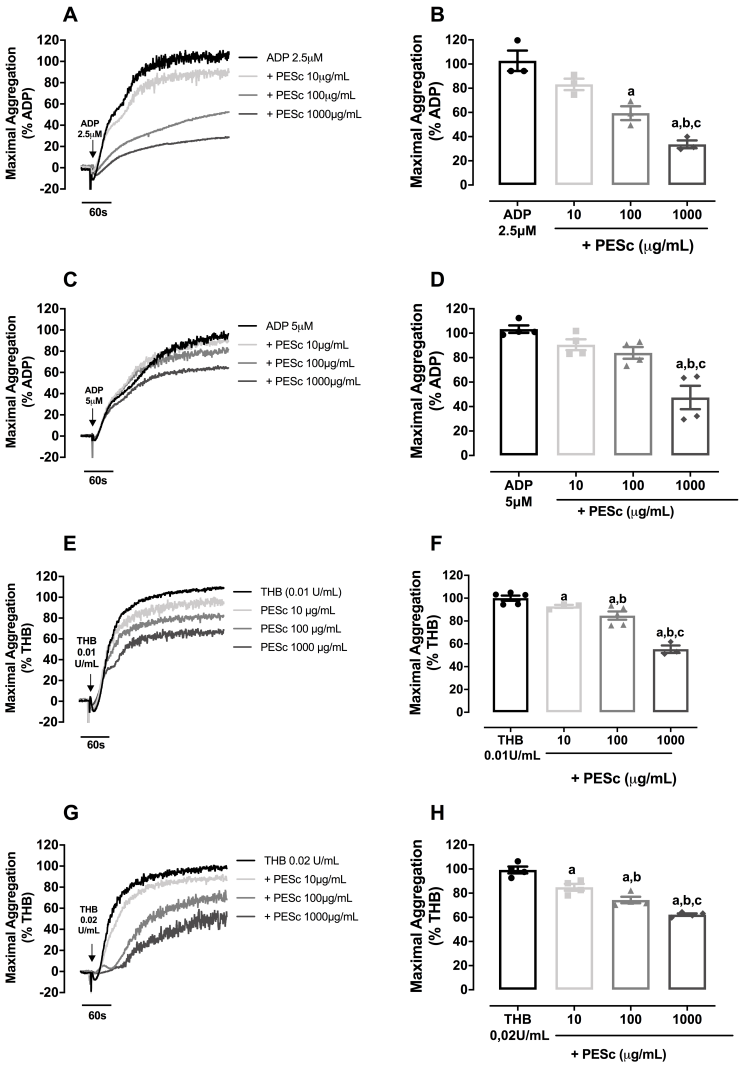

Supplementary Figure 2.2. Increased agonist concentration partially overcome anti-platelet effect of PESc. Platelet-rich plasma was pre-treated with PESc (10, 100 or 1000 μg/mL) for 25 minutes and stimulated with ADP (A-D) or thrombin (THB, E-H). Representative traces for 2.5 μM ADP (A) and 5 μM ADP (C). Representative traces for 0.01 U/mL THB (E) and 0.02 U/mL THB (G). Quantified data is shown next to representative curves. a $p<0.05$ *vs* first column of graph. b $p<0.05$ *vs* second column of graph. c $p<0.05$ *vs* third column of graph. Data analysed by paired one-way ANOVA and Tukey as post-test. All bar graphs represent mean ± SEM and individual data points of at least 3 independent experiments. Arrows indicate when agonists were added.

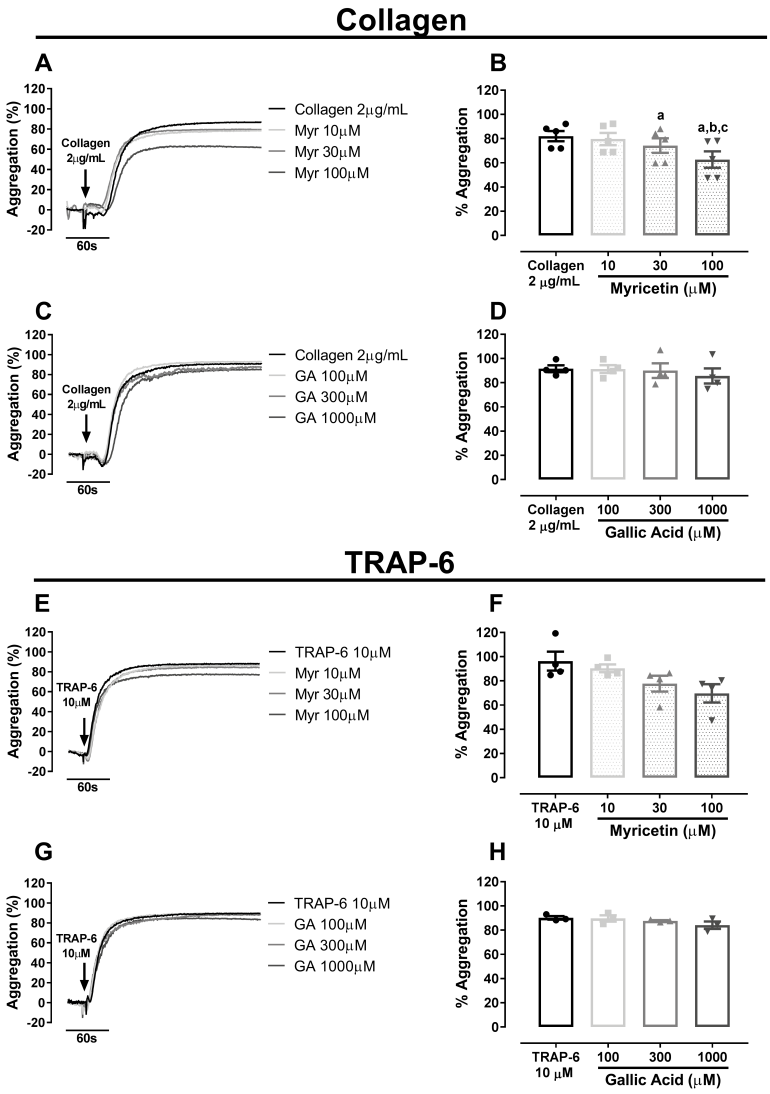

Supplementary Figure 2.3. Decreased effect of Myricetin in platelet-rich plasma. Platelet-rich plasma (PRP) was pre-treated with myricetin (Myr) or gallic acid (GA) for 10 minutes and stimulated with collagen or TRAP-6. (A) PRP treated with Myr and stimulated with collagen. (C) PRP treated with GA and stimulated with collagen. (E) PRP treated with Myr and stimulated with TRAP-6. (G) PRP treated with GA and stimulated with TRAP-6. Quantified data is shown right next to representative curves. a $p<0.05$ *vs* first column of graph. b $p<0.05$ *vs* second column of graph. c $p<0.05$ *vs* third column of graph. Data analysed by paired one-way ANOVA and Tukey as post-test. All bar graphs represent mean ± SEM and individual data points of at least 3 independent experiments. Arrows indicate when agonists were added.

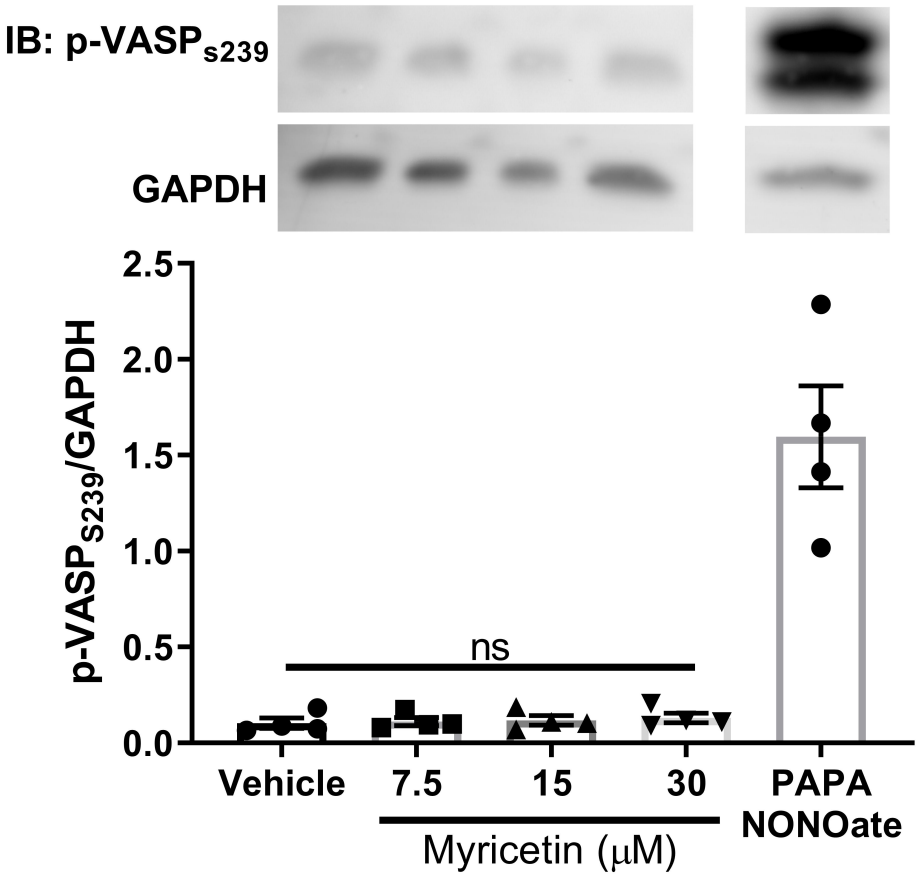

Supplementary Figure 2.4. Myricetin does not induce VASP phosphorylation. Resting WP were incubated with myricetin (7.5, 15 and 30 μM) or PAPA-NONOate (100 μM, positive control) for 10 minutes and lysed in Laemmli buffer supplemented with reducing agent. Lysed cells were processed as described in Material and Methods and probed for VASPs239 and GAPDH as loading control. Bar graph represent present the mean of four independent experiments run and error bars indicate SEM. Data compared using One-way ANOVA followed by Tukey post-test. There were no statistical differences between groups.

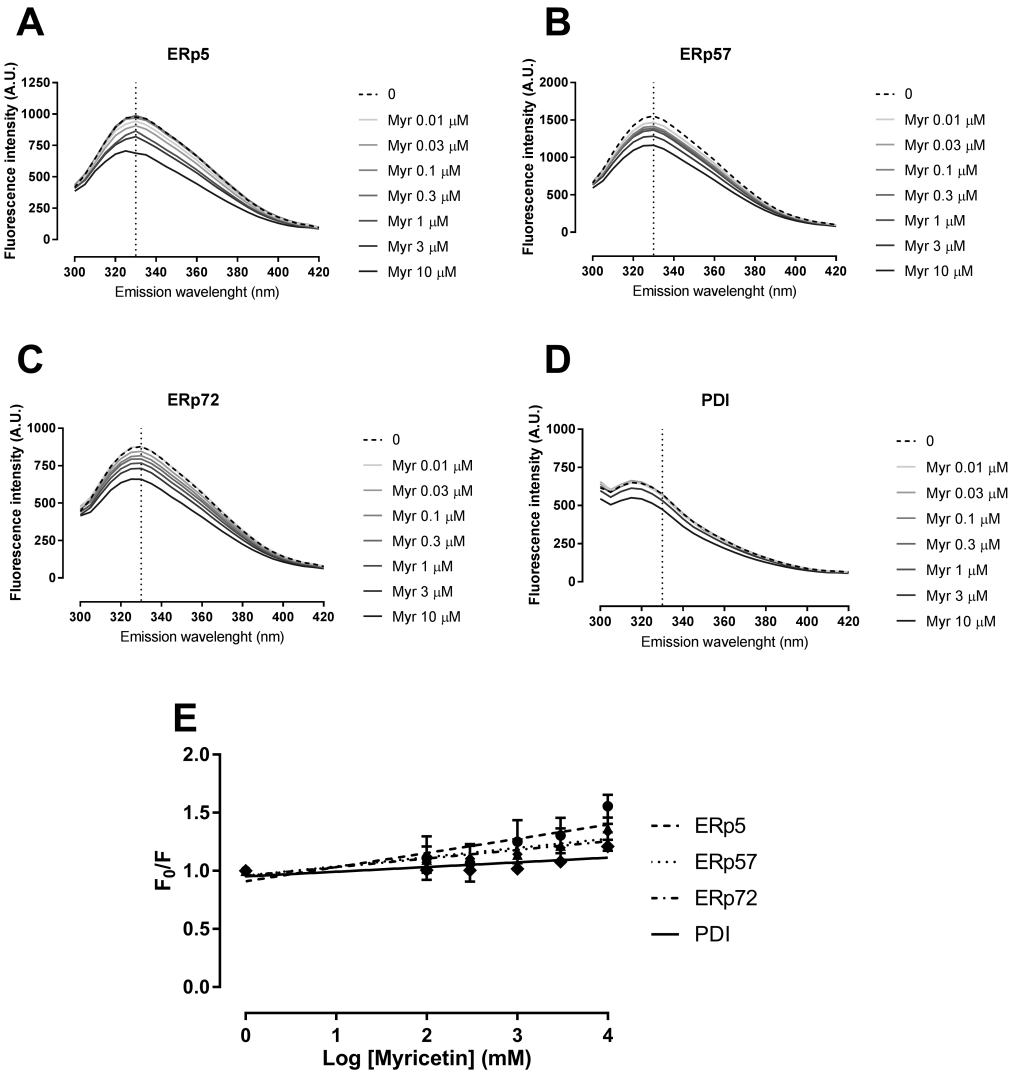

Supplementary Figure 2.5. Myricetin quenches fluorescence of ERp5, ERp57, ERp72 and PDI. Recombinant proteins were incubated with myricetin (0.01 to 10 μM) in a black 96-wells plate for 10 minutes and fluorescence spectra acquired in a fluorimeter using excitation set at 280 nm. Representative fluorescence spectra shown for ERp5 (A), ERp57 (B), ERp72 (C) and PDI (D). (E) Stern-volmer plot of quenching data is shown as the linear regression between F0/F and log of myricetin concentration in mM where F0 is the fluorescence of vehicle and F is the fluorescence in the presence of increasing concentrations of myricetin. Data represent at least three independent experiments run at least in duplicate and error bars indicate SEM.

2.9 References

Ayyanar, M., and Subash-Babu, P. (2012). Syzygium cumini (L.) Skeels: a review of its phytochemical constituents and traditional uses. *Asian Pac J Trop Biomed* 2**,** 240-246.

Banno, A., and Ginsberg, M.H. (2008). Integrin activation. *Biochemical Society transactions* 36**,** 229-234.

Bekendam, R.H., Bendapudi, P.K., Lin, L., et al. (2016). A substrate-driven allosteric switch that enhances PDI catalytic activity. *Nat Commun* 7**,** 12579.

Bi, S., Song, D., Tian, Y., Zhou, X., Liu, Z., and Zhang, H. (2005). Molecular spectroscopic study on the interaction of tetracyclines with serum albumins. *Spectrochim Acta A Mol Biomol Spectrosc* 61**,** 629-636.

Chagas, V.T., Coelho, R., Gaspar, R.S., Da Silva, S.A., Mastrogiovanni, M., Mendonca, C.J., Ribeiro, M.N.S., Paes, A.M.A., and Trostchansky, A. (2018). Protective Effects of a Polyphenol-Rich Extract from Syzygium cumini (L.) Skeels Leaf on Oxidative Stress-Induced Diabetic Rats. *Oxid Med Cell Longev* 2018**,** 5386079.

Chagas, V.T., Franca, L.M., Malik, S., and Paes, A.M. (2015). Syzygium cumini (L.) skeels: a prominent source of bioactive molecules against cardiometabolic diseases. *Front Pharmacol* 6**,** 259.

Chang, S.S., Lee, V.S., Tseng, Y.L., Chang, K.C., Chen, K.B., Chen, Y.L., and Li, C.Y. (2012). Gallic Acid Attenuates Platelet Activation and Platelet-Leukocyte Aggregation: Involving Pathways of Akt and GSK3beta. *Evid Based Complement Alternat Med* 2012**,** 683872.

Chen, K., Detwiler, T.C., and Essex, D.W. (1995). Characterization of protein disulphide isomerase released from activated platelets. *Br J Haematol* 90**,** 425-431.

Chen, Y., and Barkley, M.D. (1998). Toward understanding tryptophan fluorescence in proteins. *Biochemistry* 37**,** 9976-9982.

Chung, A.W., Jurasz, P., Hollenberg, M.D., and Radomski, M.W. (2002). Mechanisms of action of proteinase-activated receptor agonists on human platelets. *Br J Pharmacol* 135**,** 1123-1132.

Dang, Y., Lin, G., Xie, Y., Duan, J., Ma, P., Li, G., and Ji, G. (2014). Quantitative determination of myricetin in rat plasma by ultra performance liquid chromatography tandem mass spectrometry and its absolute bioavailability. *Drug Res (Stuttg)* 64**,** 516-522.

De Bona, K.S., Belle, L.P., Sari, M.H., et al. (2010). Syzygium cumini extract decrease adenosine deaminase, 5'nucleotidase activities and oxidative damage in platelets of diabetic patients. *Cell Physiol Biochem* 26**,** 729-738.

Dutta-Roy, A.K., Gordon, M.J., Kelly, C., Hunter, K., Crosbie, L., Knight-Carpentar, T., and Williams, B.C. (1999). Inhibitory effect of Ginkgo biloba extract on human platelet aggregation. *Platelets* 10**,** 298-305.

Essex, D.W. (2008). Redox Control of Platelet Function. *Antioxidants & Redox Signaling* 11**,** 1191-1225.

Essex, D.W., and Wu, Y. (2018). Multiple protein disulfide isomerases support thrombosis. *Curr Opin Hematol* 25**,** 395-402.

Ghoshal, K., and Bhattacharyya, M. (2014). Overview of platelet physiology: its hemostatic and nonhemostatic role in disease pathogenesis. *The Scientific World Journal* 2014.

Giamogante, F., Marrocco, I., Cervoni, L., Eufemi, M., Chichiarelli, S., and Altieri, F. (2018). Punicalagin, an active pomegranate component, is a new inhibitor of PDIA3 reductase activity. *Biochimie* 147**,** 122-129.

Giamogante, F., Marrocco, I., Romaniello, D., Eufemi, M., Chichiarelli, S., and Altieri, F. (2016). Comparative Analysis of the Interaction between Different Flavonoids and PDIA3. *Oxid Med Cell Longev* 2016**,** 4518281.

Holbrook, L.M., Sandhar, G.K., Sasikumar, P., Schenk, M.P., Stainer, A.R., Sahli, K.A., Flora, G.D., Bicknell, A.B., and Gibbins, J.M. (2018). A humanized monoclonal antibody that inhibits platelet-surface ERp72 reveals a role for ERp72 in thrombosis. *J Thromb Haemost* 16**,** 367-377.

Inoue, O., Suzuki-Inoue, K., Dean, W.L., Frampton, J., and Watson, S.P. (2003). Integrin alpha2beta1 mediates outside-in regulation of platelet spreading on collagen through activation of Src kinases and PLCgamma2. *J Cell Biol* 160**,** 769-780.

Jarvis, G.E., Atkinson, B.T., Snell, D.C., and Watson, S.P. (2002). Distinct roles of GPVI and integrin alpha(2)beta(1) in platelet shape change and aggregation induced by different collagens. *Br J Pharmacol* 137**,** 107-117.

Jasuja, R., Passam, F.H., Kennedy, D.R., et al. (2012). Protein disulfide isomerase inhibitors constitute a new class of antithrombotic agents. *J Clin Invest* 122**,** 2104-2113.

Jayakumar, T., Lin, K.C., Lu, W.J., Lin, C.Y., Pitchairaj, G., Li, J.Y., and Sheu, J.R. (2017). Nobiletin, a citrus flavonoid, activates vasodilator-stimulated phosphoprotein in human platelets through non-cyclic nucleotide-related mechanisms. *Int J Mol Med* 39**,** 174-182.

Jordan, P.A., Stevens, J.M., Hubbard, G.P., Barrett, N.E., Sage, T., Authi, K.S., and Gibbins, J.M. (2005). A role for the thiol isomerase protein ERP5 in platelet function. *Blood* 105**,** 1500-1507.

Kang, W.-S., Chung, K.-H., Chung, J.-H., Lee, J.-Y., Park, J.-B., Zhang, Y.-H., Yoo, H.-S., and Yun, Y.-P. (2001). Antiplatelet activity of green tea catechins is mediated by inhibition of cytoplasmic calcium increase. *Journal of cardiovascular pharmacology* 38**,** 875-884.

Kehrel, B., Wierwille, S., Clemetson, K.J., Anders, O., Steiner, M., Knight, C.G., Farndale, R.W., Okuma, M., and Barnes, M.J. (1998). Glycoprotein VI is a major collagen receptor for platelet activation: it recognizes the platelet-activating quaternary structure of collagen, whereas CD36, glycoprotein IIb/IIIa, and von Willebrand factor do not. *Blood* 91**,** 491-499.

Kim, K., Hahm, E., Li, J., Holbrook, L.M., Sasikumar, P., Stanley, R.G., Ushio-Fukai, M., Gibbins, J.M., and Cho, J. (2013). Platelet protein disulfide isomerase is required for thrombus formation but not for hemostasis in mice. *Blood* 122**,** 1052-1061.

Lahav, J., Wijnen, E.M., Hess, O., Hamaia, S.W., Griffiths, D., Makris, M., Knight, C.G., Essex, D.W., and Farndale, R.W. (2003). Enzymatically catalyzed disulfide exchange is required for platelet adhesion to collagen via integrin alpha2beta1. *Blood* 102**,** 2085-2092.

Lakowicz, J.R., and Weber, G. (1973). Quenching of fluorescence by oxygen. A probe for structural fluctuations in macromolecules. *Biochemistry* 12**,** 4161-4170.

Lescano, C.H., Freitas De Lima, F., Mendes-Silverio, C.B., et al. (2018). Effect of Polyphenols From Campomanesia adamantium on Platelet Aggregation and Inhibition of Cyclooxygenases: Molecular Docking and in Vitro Analysis. *Front Pharmacol* 9**,** 617.

Lin, L., Gopal, S., Sharda, A., et al. (2015). Quercetin-3-rutinoside Inhibits Protein Disulfide Isomerase by Binding to Its b'x Domain. *J Biol Chem* 290**,** 23543-23552.

Lu, J., Papp, L.V., Fang, J., Rodriguez-Nieto, S., Zhivotovsky, B., and Holmgren, A. (2006). Inhibition of Mammalian thioredoxin reductase by some flavonoids: implications for myricetin and quercetin anticancer activity. *Cancer Res* 66**,** 4410-4418.

Mangin, P.H., Onselaer, M.B., Receveur, N., et al. (2018). Immobilized fibrinogen activates human platelets through glycoprotein VI. *Haematologica* 103**,** 898-907.

Masuda, T., Miura, Y., Inai, M., and Masuda, A. (2013). Enhancing effect of a cysteinyl thiol on the antioxidant activity of flavonoids and identification of the antioxidative thiol adducts of myricetin. *Biosci Biotechnol Biochem* 77**,** 1753-1758.

Navarro-Nunez, L., Rivera, J., Guerrero, J.A., Martinez, C., Vicente, V., and Lozano, M.L. (2009). Differential effects of quercetin, apigenin and genistein on signalling pathways of protease-activated receptors PAR(1) and PAR(4) in platelets. *Br J Pharmacol* 158**,** 1548-1556.

Park, W., Chang, M.S., Kim, H., Choi, H.Y., Yang, W.M., Kim, D.R., Park, E.H., and Park, S.K. (2008). Cytotoxic effect of gallic acid on testicular cell lines with increasing H2O2 level in GC-1 spg cells. *Toxicol In Vitro* 22**,** 159-163.

Raffaelli, F., Borroni, F., Alidori, A., et al. (2015). Effects of in vitro supplementation with Syzygium cumini (L.) on platelets from subjects affected by diabetes mellitus. *Platelets* 26**,** 720-725.

Raturi, A., and Mutus, B. (2007). Characterization of redox state and reductase activity of protein disulfide isomerase under different redox environments using a sensitive fluorescent assay. *Free Radic Biol Med* 43**,** 62-70.

Sharma, B., Viswanath, G., Salunke, R., and Roy, P. (2008). Effects of flavonoid-rich extract from seeds of Eugenia jambolana (L.) on carbohydrate and lipid metabolism in diabetic mice. *Food Chemistry* 110**,** 697-705.

Sousa, H.R., Gaspar, R.S., Sena, E.M., et al. (2017). Novel antiplatelet role for a protein disulfide isomerase-targeted peptide: evidence of covalent binding to the C-terminal CGHC redox motif. *J Thromb Haemost* 15**,** 774-784.

Stopa, J.D., Neuberg, D., Puligandla, M., Furie, B., Flaumenhaft, R., and Zwicker, J.I. (2017). Protein disulfide isomerase inhibition blocks thrombin generation in humans by interfering with platelet factor V activation. *JCI Insight* 2**,** e89373.

Taylor, L., Vasudevan, S.R., Jones, C.I., Gibbins, J.M., Churchill, G.C., Campbell, R.D., and Coxon, C.H. (2014). Discovery of novel GPVI receptor antagonists by structure-based repurposing. *PLoS One* 9**,** e101209.

Trnkova, L., Ricci, D., Grillo, C., Colotti, G., and Altieri, F. (2013). Green tea catechins can bind and modify ERp57/PDIA3 activity. *Biochim Biophys Acta* 1830**,** 2671-2682.

Wang, X., Xue, G., Song, M., et al. (2018). Molecular basis of rutin inhibition of protein disulfide isomerase (PDI) by combined in silico and experimental methods. *RSC Advances* 8**,** 18480-18491.

Ware, W.R. (1962). OXYGEN QUENCHING OF FLUORESCENCE IN SOLUTION: AN EXPERIMENTAL STUDY OF THE DIFFUSION PROCESS. *The Journal of Physical Chemistry* 66**,** 455-458.

Wendelboe, A.M., and Raskob, G.E. (2016). Global Burden of Thrombosis: Epidemiologic Aspects. *Circ Res* 118**,** 1340-1347.

Chapter 3

Functional association of platelet PDI and Nox-1

In the previous chapter I have used part of my background to blend in previous experiences working with a plant extract with current interests in the redox physiology of platelets. As ideas developed Prof Jon Gibbins and I realized that PDI was thought to regulate the function of Nox enzymes in cardiovascular cells. Specifically, the link between PDI and Nox-1 was evidenced by the interaction between this thiol isomerase and the Nox-1 cytosolic organizer p47phox (Gimenez et al., 2019). Such connection, however, has never been made for the anucleated platelet, which prompted me to investigate this in more detail.

This Chapter examines how PDI and Nox-1 contribute to platelet activation. I have shown, by using inhibitors and a murine knockout model of Nox-1, that PDI and Nox-1 co-inhibition led to a more than additive decrease of platelet function. This seemed to be specific to responses regulated by the collagen receptor GPVI, which is itself a promising target for the development of new anti-platelet medications (Dutting et al., 2012). This response was mediated by mitogen-activated protein kinases (MAPK) and p47phox phosphorylation, both of which are downstream of Nox-1 and PDI. Moreover, platelet expression of PDI was correlated with waist/hip ratio and serum insulin levels, whereas platelet Nox-1 expression levels were correlated with body mass index (BMI) and systolic blood pressure. This was a very interesting observation that reinforced a previous hypothesis I had 4 years earlier, wherein I suggested that platelet PDI could be a culprit for platelet hyperactivation seen in individuals with metabolic syndrome (Gaspar et al., 2016).

I have drafted the manuscript, collected and analysed all of the data presented here. In addition, I have participated, together with Jon, on the design of the study. For these reasons, it is estimated I have contributed to over 80% of all effort put into this paper.

The paper has been submitted to *Circulation Research*.

Functional association of platelet Protein Disulphide Isomerase and NADPH oxidase 1: implications for cardiometabolic risk factors.

Running title: Functional association of platelet PDI and Nox-1.

Authorship

Renato Simões Gaspar [a*], Tanya Sage [a], Gemma Little [a], Neline Kriek [a], Giordano Pula [b], Jonathan M Gibbins [a]

Affiliations

[a] Institute for Cardiovascular and Metabolic Research, School of Biological Sciences, University of Reading, Reading, UK.

[b] University Medical Center Eppendorf Hamburg, Institute for Clinical Chemistry and Laboratory Medicine, Hamburg, Germany

*** Corresponding author**

Renato Simões Gaspar, M.D.

Institute for Cardiovascular and Metabolic Research, School of Biological Sciences. University of Reading - Harborne Building, Reading, RG6 6AS, UK.

E-mail: renatosgaspar@gmail.com, phone: +44 11 8378 7047

3.1 Graphical Abstract

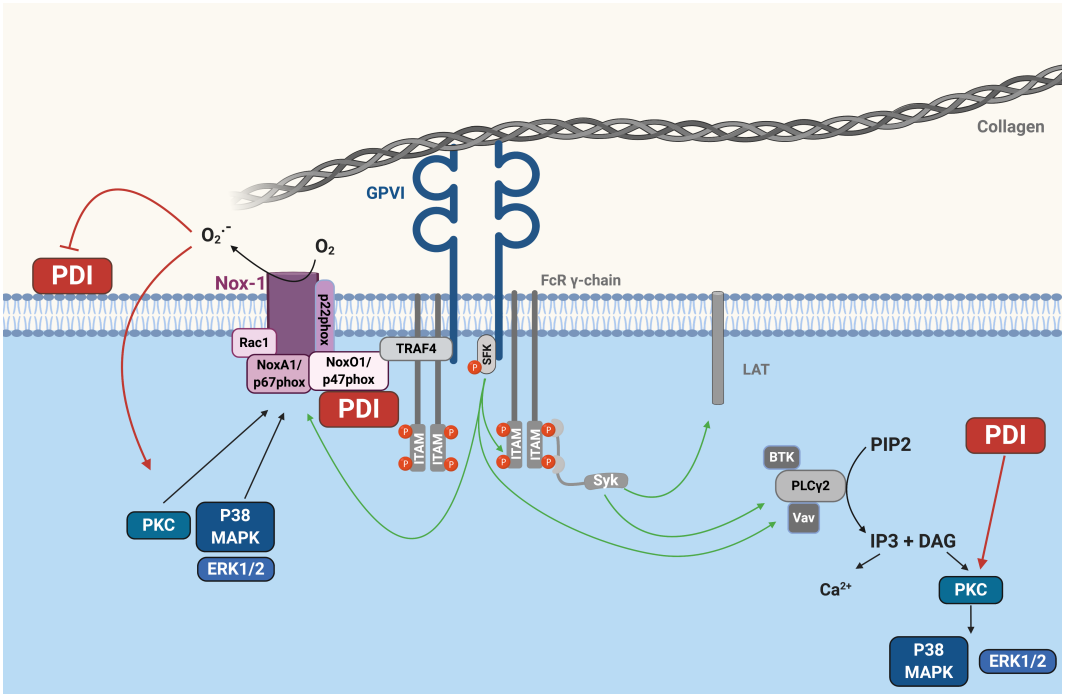

3.2 Abstract

Rationale: Metabolic syndrome (MetS) is associated with thrombotic events and increased reactive oxygen species (ROS) production. These species are key signalling components in platelets, which are pivotal to the formation of thrombotic events. Protein disulphide isomerase (PDI) and NADPH oxidase 1 (Nox-1) regulate both platelet activation and ROS production. The study of these proteins may provide novel anti-platelet strategies to reduce cardiovascular risk, particularly if associated with risk factors for MetS.

Objective: To identify how PDI and Nox-1 control platelet function and determine if these proteins are associated with risk factors for MetS.

Methods and Results: In a population study (n=137), platelet PDI levels were positively correlated with insulin levels and waist/hip ratio, while Nox-1 was correlated with BMI and systolic blood pressure. These proteins were not correlated with the same risk factors for MetS, suggesting distinct pathophysiological associations. To explore this, ROS and platelet reductase activity (surrogate for PDI activity) were measured. PDI inhibition decreased ROS production, whereas Nox-1 inhibition enhanced reductase activity. In immunofluorescence experiments, PDI and Nox-1 co-localized upon activation induced by collagen receptor GPVI agonist collagen-related peptide. Co-inhibition of PDI and Nox-1 led to an additive anti-platelet effect in GPVI-mediated platelet aggregation, activation, calcium flux and ROS production. A similar effect was observed in murine Nox-1$^{-/-}$ platelets treated with PDI inhibitor bepristat, without affecting bleeding time. PDI and Nox-1 contributed to GPVI signalling through phosphorylation of p38 MAPK and p47phox.

Conclusions: Platelet PDI levels were correlated with insulin and waist/hip ratio, while Nox-1 was correlated with BMI and systolic blood pressure. Co-inhibition of these proteins inhibited platelet function with no effects on primary haemostasis. Thus, we propose dual inhibition of PDI and Nox-1 as a novel anti-platelet strategy for the cardiovascular protection of MetS patients.

KEYWORDS: Platelets; Protein Disulphide Isomerase; NADPH Oxidase; Metabolic Syndrome; Redox biology

ABBREVIATIONS:

Akt	protein kinase B
CRP	collagen-related peptide
ERK	extracellular signal-regulated kinases
GAPDH	glyceraldehyde 3-phosphate dehydrogenase
GPVI	Glycoprotein VI
Nox	nicotinamide adenine dinucleotide phosphate oxidase
PDI	protein disulphide isomerase
PKC	protein kinase C
PMA	phorbol-12-myristate-13-acetate
PRP	platelet-rich plasma
Src	proto-oncogene tyrosine-protein kinase
Syk	spleen tyrosine kinase
TRAP-6	thrombin receptor activator peptide 6
VASP	vasodilator-stimulated phospho-protein
WP	washed platelets

3.3 Introduction

Metabolic syndrome (MetS) is defined as the presence of at least three of the following: central obesity, hyperglycaemia, insulin resistance, hypertension and dyslipidemia (Alberti et al., 2009). Individuals with MetS are under persistent oxidative stress characterized by increased production of reactive oxygen species (ROS) (Roberts and Sindhu, 2009). There is also a higher risk of developing thrombotic events partly due to platelet hyperactivation, which is pivotal to thrombus formation (Barale and Russo, 2020). Upon vascular injury, these anucleated cells become activated through adhesion receptors and secondary mediators that potentiate initial response and increase platelet recruitment to form thrombi and reduce blood loss. Of note, both ROS and enzymes that regulate ROS generation are key to platelet activation in health and disease (Qiao et al., 2018). The study of proteins that regulate ROS production in platelets may therefore be exploited to reduce cardiovascular risk in MetS patients, given their state of oxidative stress and contribution of platelets to thrombotic events.

Protein disulphide isomerase (PDI) is a redox protein and an important regulator of platelet function both *in vitro* and *in vivo* (Chen et al., 1995;Kim et al., 2013). PDI is the archetype of a family of thiol isomerases, also referred to as thioredoxins, capable of catalysing reduction, oxidation and isomerization of disulphide bonds (Schwaller et al., 2003). PDI itself is released upon platelet activation (Crescente et al., 2016) and was found to bind to integrin β3 during thrombus formation and regulate the affinity of integrin $\alpha_{IIb}\beta_3$ thereby contributing to thrombus formation (Cho et al., 2012;Kim et al., 2013). Moreover, PDI is also capable of interacting through

disulphide exchange with other platelet adhesion receptors, such as integrin $\alpha_2\beta_1$ (Lahav et al., 2003) and glycoprotein Ibα (Burgess et al., 2000).

In vascular smooth muscle cells (VSMC), PDI has been shown to regulate the production of reactive oxygen species (ROS) through aiding the assembly of nicotinamide adenine dinucleotide phosphate (NADPH) oxidase 1 (Nox-1) (Gimenez et al., 2019). Similar to PDI, Nox-1 has recently been shown to regulate platelet function (Delaney et al., 2016). This enzyme complex is responsible for the production of ROS and is expressed on the outer membrane of vascular cells, such as endothelial cells (Bayraktutan et al., 2000), vascular smooth muscular cells (VSMC) (Griendling et al., 1994) and platelets (Seno et al., 2001). Only Nox-1, Nox-2 and Nox-4 isoforms have been found in platelets (Delaney et al., 2016) although the presence of Nox-4 remains a matter of debate (Vara et al., 2013). Using both selective inhibitors and *in vivo* deletion of the Nox-1 gene, Vara et al (Vara et al., 2019) observed that Nox-1 is essential for superoxide production, platelet aggregation and thrombus formation downstream of GPVI. Meanwhile, Nox-2 was relevant to platelet responses to thrombin, with little effect on thrombus size. This suggests that Nox-1 may be of particular importance for thrombus formation.

Both PDI and Nox-1 contribute to oxidative stress observed in MetS. Indeed, we have previously proposed that platelet PDI could be implicated in platelet hyperactivation found in MetS (Gaspar et al., 2016). In addition, PDI expression has been shown to be elevated in atherosclerotic lesions (Gimenez et al., 2019) while Nox-1 is reported to be upregulated in mesenteric arteries of MetS mice and contributes to vasodilation of these vessels (Qiu et al., 2014). Despite evidence in vascular cells, there is no

literature on how platelet PDI and Nox-1 may be correlated with risk factors for MetS.

Given the critical roles of PDI and Nox-1 in the control of platelet function, and dysregulated redox processes in MetS, we hypothesized that these enzyme systems in platelets may contribute to platelet function defects associated with MetS. We therefore hypothesized that platelet PDI and Nox-1 could be correlated with risk factors for MetS. If acting through distinct mechanisms, the co-inhibition of PDI and Nox-1 could represent a promising new way to inhibit platelets. Here we investigated whether platelet PDI and Nox-1 were correlated with risk factors of MetS in humans and tested the anti-platelet effects of co-inhibition of these proteins. The co-inhibition of these proteins led to a GPVI-specific additive anti-platelet effect, suggesting that PDI and Nox-1 collaborate to fine-tune platelet activation downstream of GPVI. Indeed, in a population study, PDI levels in platelets were positively correlated with waist/hip ratio and insulinaemia, while Nox-1 levels were associated with BMI and systolic blood pressure. This indicates that dual inhibition of PDI and Nox-1 is a promising strategy for cardioprotection in individuals with risk factors for MetS.

3.4 Material and Methods

3.4.1. Washed platelets preparation

University of Reading Research Ethics Committee approved all protocols to obtain and use human blood samples. Platelet-rich plasma (PRP) and washed platelets (WP) were prepared from freshly donated blood from consenting healthy donors exactly as previously described (Gaspar et al., 2019). For more details, please refer to Supplementary Methods.

3.4.2. Collection of mouse blood and platelet preparation

Nox-1$^{-/-}$ mice originally described by Gavazzi et al (Gavazzi et al., 2006) were purchased from Jackson Laboratory (Sacramento, CA, USA) and C57BL/6 were used as controls, as recommended by the animal provider. Animals were kept under a 12 h light cycle, controlled temperature (22-24°C) and food and water *ad libitum*. The University of Reading Local Animal Welfare and Ethics Research Board approved all protocols within a license issued by the British Home Office. Mice (11 – 14 weeks, females) were culled by rising CO_2 concentration and blood collected through cardiac puncture into a syringe containing 3.2% sodium citrate at a 1:9 v/v citrate-blood ratio. Whole blood was centrifuged at 203 x *g* for 8 minutes and PRP collected. 1.25 µg/mL PGI_2 was added and PRP centrifuged at 1,028 x *g* for 5 min and pellet resuspended in modified Tyrode's-HEPES buffer (THB) to obtain WP.

3.4.3. Measurement of reactive oxygen species

Human WP (4 x 10^8 platelets/mL) were incubated with 20 μM DCF or 10 μM DHE for 15 minutes, followed by a 10 minutes incubation with Bepristat and/or ML171 or Nox2ds-tat dissolved in DMSO (vehicle). Platelets were then stimulated with CRP at 1 μg/mL for 10 minutes and events acquired on a BD Accuri C6 plus flow cytometer (BD Biosciences, Oxford, UK).

3.4.4. Reductase activity

The reductase activity of human WP was determined with the fluorescent probe dieosin glutathione disulphide (Di-E-GssG, ex/em 510/545 nm). Di-E-GssG was synthesized as previously described (Raturi and Mutus, 2007). Briefly, human WP (4 x 10^8 platelets/mL) were incubated with ML171 or vehicle for 10 minutes, and then added to a 96-well black plate in triplicates. DTT (5 μM) and Di-E-GSSG (300 nM) were added and the plate was read every 30 seconds for 1 hour, using a Flexstation 3 fluorimeter (Molecular Devices, Wokingham, UK).

3.4.5. Immunofluorescence microscopy

Human PRP was activated in the presence of 2μg/mL integrilin and fixed in 5% paraformaldehyde. Platelets were washed in 1:9 v/v ACD-phosphate buffer solution (PBS) and left to adhere onto poly-L-lysine coverslips for 90 minutes. Coverslips were blocked with 1% w/v BSA diluted in PBS and incubated with primary or IgG control antibodies overnight at 4 °C. Antibodies were washed away with PBS and secondary antibodies tagged with appropriate fluorophores added for 1 hour at room temperature. Finally, coverslips were mounted in gold anti-fade onto slides and analysed

with a 100 x magnification oil-immersion lens on a Nikon A1-R confocal microscope (Nikon Optical, Milton Keynes, UK).

3.4.6. Turbidimetry and plate-based platelet aggregation

Turbidimetry (Gaspar et al., 2019) and plate-based platelet aggregation (Bye et al., 2017) were performed using standard protocols as described previously. For more details, please refer to Supplementary Methods.

3.4.7. Fibrinogen binding and P-selectin exposure

Human WP (4 x 10^8 platelets/mL) or mouse whole blood (WB, diluted 1:25 v/v with THB) were incubated with inhibitors for 10 minutes. Platelets were then activated with CRP for 10 minutes and incubated with 1:50 v/v FITC-conjugated fibrinogen or 1:50 v/v PE/Cy5-conjugated anti-human CD62P for 30 minutes. Events were acquired using a BD Accuri C6 plus flow cytometer.

3.4.8. Calcium measurement

Human PRP was incubated with 2 μM Fura-2 AM for 1 hour at 30°C. PRP was centrifuged at 350 *g* for 20 minutes and platelets (4 x 10^8 platelets/mL) resuspended in THB. Platelets were transferred to a 96-well black plate with clear bottom and incubated with Bepristat and/or ML171 for 10 minutes and stimulated with 1 μg/mL CRP. Fluorescence was read every 5 seconds for 5 minutes using a Flexstation 3 fluorimeter (excitation 340 and

380 and emission 510 nm). Calcium signals were derived from the emission ratios following excitation: 340/380.

3.4.9. Platelet spreading

Human or mouse WP (2 x 10^7 platelets/mL) were incubated with inhibitors or vehicle for 10 minutes and left to adhere to collagen, fibrinogen, GFOGER peptide or CRP-coated surfaces for 45 minutes at 37°C. Non-adherent platelets were washed off three times with PBS. Paraformaldehyde (0.2% v/v) was added for 10 minutes to fix the platelets. Triton-X 0.01% v/v was added for 5 minutes to permeabilize the cells. Platelets were stained with Alexa Fluor 488-conjugated phalloidin (1:1000 v/v) for 1 hour in the dark at room temperature and analyzed using a 20x objective lens on a Nikon A1-R Confocal microscope.

3.4.10. Immunoblotting

Immunoblots were performed using standard protocols as previously described (Gaspar et al., 2019). For details, please refer to Supplementary Methods.

3.4.11 Tail bleeding assay

Nox-$1^{-/-}$ or C57BL/6 wildtype (WT) mice were anesthesized through an intraperitoneal injection of ketamine (100 mg/kg) and xylazine (10 mg/kg). After animals were fully anaesthetized, Bepristat (0.5 µL of a 100 µM solution diluted in 100 µL PBS per 25 g of animal; 50 µM *in vivo* concentration) was injected intravenously. Tail bleeding was performed as

described previously (Gaspar et al., 2019) and is detailed in Supplementary Methods.

3.4.12 Population study

137 volunteers aged between 30 and 65 and not using long-term medications were recruited at the University of Reading to assess physical, metabolic and platelet characteristics. Age, gender, height, weight, blood pressure (measured seated with an electronic automatic sphygmomanometer) and waist and hip circumferences were recorded. Fat mass was assessed using a body composition monitor (Tanita MC-780MA P, Tanita Europe BV, Manchester, UK). Blood was taken after overnight fasting and serum glucose, triglycerides and low-density lipoprotein (LDL) cholesterol levels measured using standard colorimetric biochemistry protocols. Insulin concentration was measured through ELISA (Crystal Chem, Zaandam, Netherlands). Platelets were washed and immunoblotting performed as above. A protein loading control, GAPDH, was measured to normalize levels of PDI and Nox-1 to protein loading in each well. The study design was approved by the University of Reading Research Ethics committee and participants have given informed consent to participate in this study.

3.4.13. Statistical analysis

Statistical analyses were performed on GraphPad Prism 8.0 software (GraphPad Software, San Diego, USA). Bar graphs and tables express individual values and mean ± SEM. Sample size varied from 4-6 independent

repeats for *in vitro* experiments, between 6 and 8 for tail bleeding experiments and 137 for population study. Statistical analysis was performed through paired one-way ANOVA and Tukey as post-test or two-way ANOVA and Sidak's multiple comparisons test for experiments using Nox-1$^{-/-}$ mice. Multiple linear regressions were run to assess the correlation between platelet expression of PDI or Nox-1 with several cardiometabolic parameters. For more details, please refer to Supplementary Methods.

3.5 Results

3.5.1. Evidence of Nox-1 and PDI mutual regulation in platelets

Previous literature has shown that PDI regulates Nox-1 activity in VSMC (Gimenez et al., 2019). Therefore we assessed if these proteins might regulate one another and co-localize in platelets. First, we incubated healthy human platelets with PDI inhibitor bepristat (100 μM) or Nox-1 inhibitor ML171 (3 μM) and measured ROS production and reductase activity. Of note, Nox-1 is the main contributor to ROS production induced by CRP in platelets (Vara et al., 2019), whereas PDI is key to the reductase activity of the platelet plasma membrane (Raturi and Mutus, 2007). Both bepristat and ML171 decreased ROS production induced by CRP (GPVI agonist) and PMA (PKC activator) by ~25% (Figure 3.1A). Of note, Nox-2 inhibitor Nox2ds-tat (3 μM) did not inhibit CRP-induced ROS production (Supplementary Figure 3.1), confirming that Nox-1 is the relevant Nox isoform downstream of GPVI. Conversely, Nox-1 inhibition led to increased platelet reductase activity (Figure 3.1B). To test whether these proteins co-localize in platelets, immunofluorescence studies were performed (Figure 3.1D) and co-localization assessed using Pearsons coefficient. PDI and p47phox, which is a cytosolic organizer of the Nox-1 complex, were localized primarily in the intracellular space in resting and TRAP-6-stimulated platelets. CRP activation induced a migration of both proteins to the plasma membrane, where Nox-1 was located – thus increasing co-localization of PDI and p47phox with Nox-1. This shift was more evident for p47phox than for PDI, probably due to PDI being highly expressed and trapped in the dense tubular system (Crescente

et al., 2016). Therefore, both PDI and p47phox translocate closer to Nox-1 in the platelet membrane upon activation with CRP.

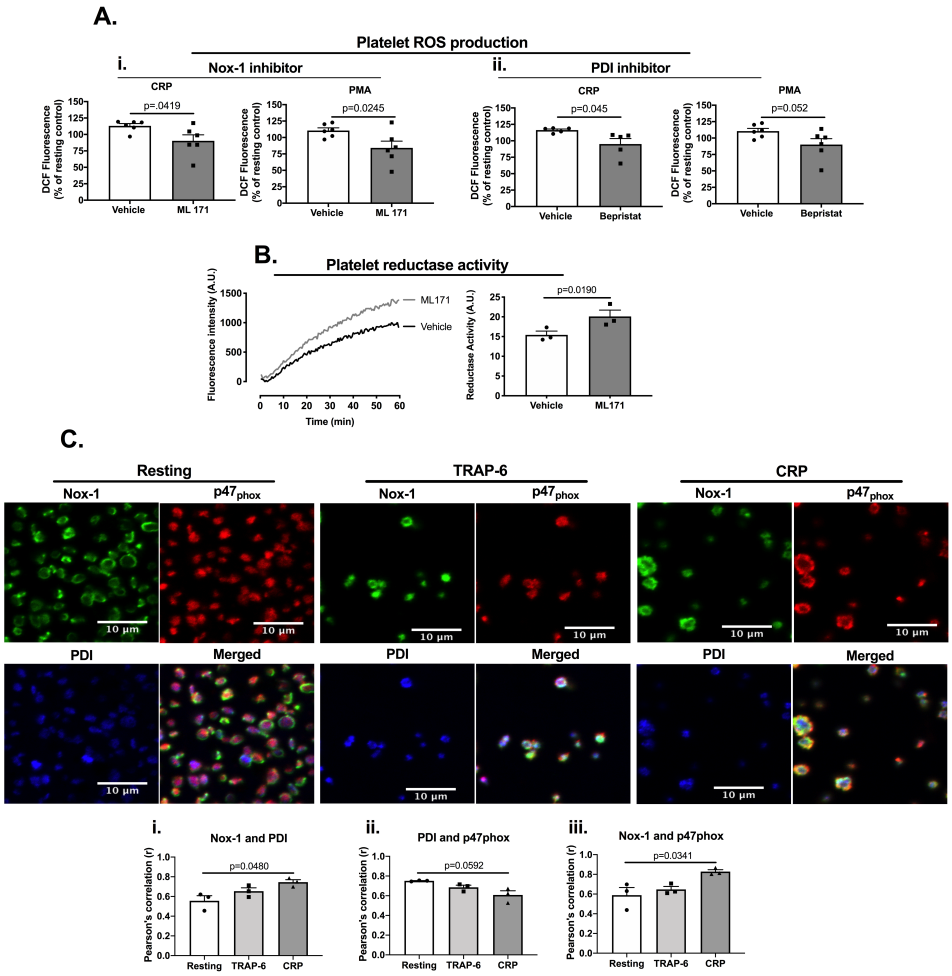

Figure 3.1. PDI and Nox-1 co-localize and may affect one another in platelets. (A) Human washed platelets (WP) at 4 x 10^8 platelets/mL were incubated with 20 µM of DCF dye for 15 minutes, then 3 µM ML171, 100 µM Bepristat or vehicle control for 10 minutes prior to addition of 1µg/mL CRP and fluorescence read using a flow cytometer. Data expressed as percentage of condition without agonist addition (resting). (B) Human WP were incubated with 3 µM ML171 for 10 minutes and reductase activity determined using Di-E-GssG dye. (C) Immunofluorescence of platelet-rich plasma (PRP) stimulated with 1 µg/mL CRP, 3 µM TRAP-6 or not stimulated (resting) for 3 minutes in the presence of 4 µg/mL integrillin. Pearson's correlation of at least 3 different fields for 3 independent donors represents the degree of co-localization of Nox-1 and PDI (i), PDI and p47phox (ii) and Nox-1 and p47phox (iii). For (A) and (B), n=5-6 donors. Bar graphs show individual values and mean ± SEM. Data in (A) analysed by Student t-test. Data in (B) and (C) analysed by paired one-way ANOVA with Tukey's post-test.

3.5.2. Bepristat and ML171 display additive inhibitory effects on platelet aggregation induced by collagen and CRP

To explore the hypothesis that PDI and Nox-1 regulate distinct processes in platelets, we assessed whether co-inhibition of these proteins would have an additive effect. Platelet aggregation was measured using a high-throughput end-point assay (Figure 3.2). ML171 decreased platelet aggregation induced by collagen and CRP, whereas 15 μM bepristat inhibited CRP-induced platelet aggregation (Figure 3.2B and D). Neither bepristat nor ML171 decreased platelet aggregation induced by TRAP-6 or PMA. Co-incubation with bepristat and ML171 led to an additive inhibitory effect in collagen and CRP-stimulated platelets (Figure 3.2A – D). Co-incubation with bepristat and ML171 did not inhibit platelet aggregation when platelets were stimulated with TRAP-6 or PMA (Figure 3.2E – H), consistent with the selective role for Nox-1 in GPVI-mediated platelet aggregation (Vara et al., 2019). Other thiol isomerase inhibitors co-incubated with ML171 yielded a similar additive inhibitory effect in collagen-stimulated platelets (Supplementary Figure 3.2). Therefore, co-inhibition of PDI (or other thiol isomerases) and Nox-1 exerts an additive inhibitory effect in GPVI-mediated platelet aggregation. Focus was given to PDI, since this protein is the archetype enzyme of thiol isomerases.

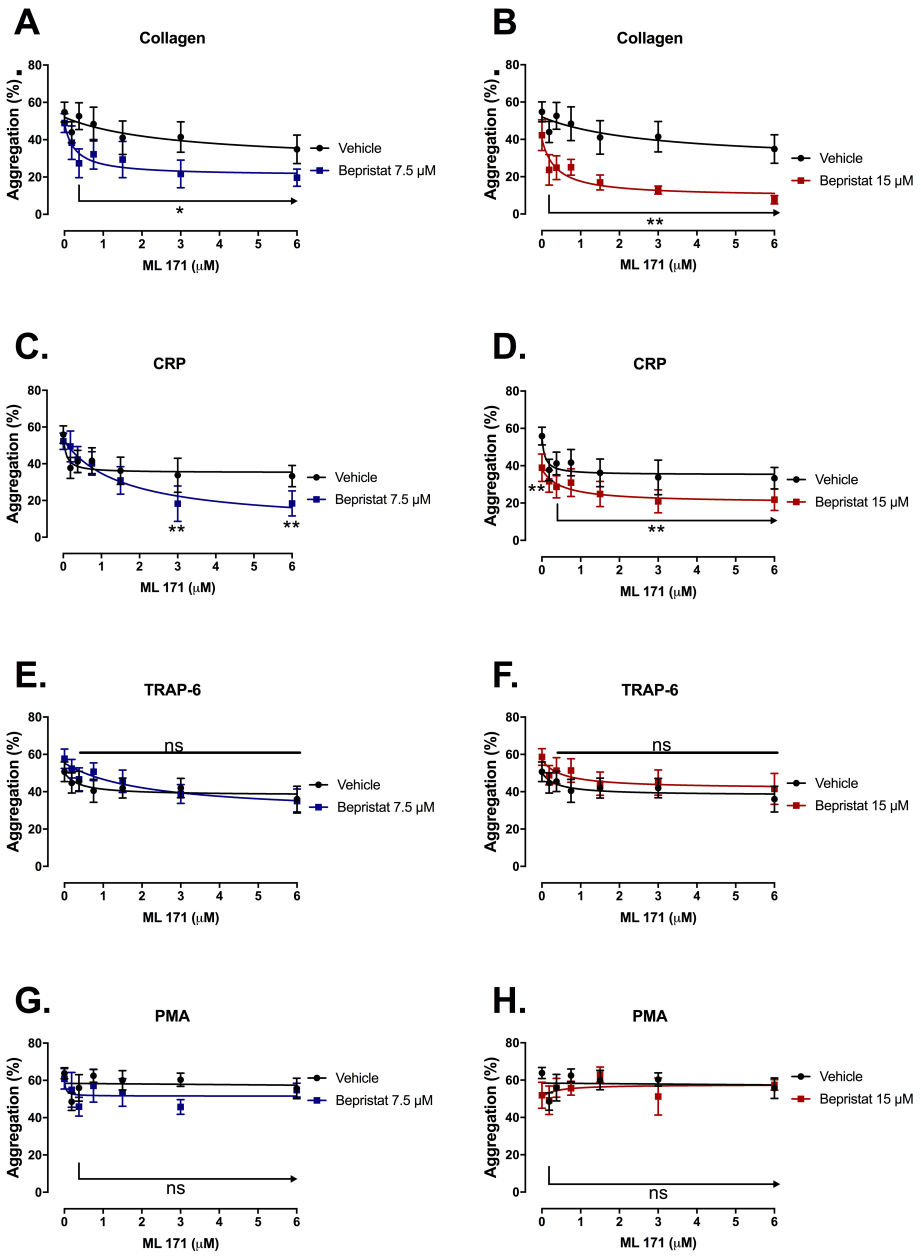

Figure 3.2. Bepristat and ML171 exert an additive inhibitory effect on platelet aggregation induced by GPVI agonists. Human WP at 4 x 10^8 platelets/mL were pre-treated with 2x serial dilution of ML171 (0.1875 to 6 µM) and 7.5 µM (A, C, E, G) or 15 µM (B, D, F, H) Bepristat for 10 minutes prior to addition of agonists: 2 µg/mL Collagen (A and B), 1 µg/mL CRP (C and D), 10 µM TRAP-6 (E and F) or 500 nM PMA. Vehicle was a condition in which Bepristat was not added. n=4-5 different donors. Data on graphs show mean ± SEM and lines are the non-linear fit of inhibitor *vs* response curve. Data analysed by paired two-way ANOVA and Tukey's multiple comparisons test. *p<0.05 and **p<0.01 *vs* equivalent ML171 concentration in Vehicle line.

3.5.3. Bepristat and ML171 display additive inhibitory effect on platelet activation and calcium mobilization induced by CRP

To test the effects of PDI and Nox-1 inhibition on other aspects of platelet function, WP were incubated with bepristat and/or ML171 and stimulated with CRP. Individually, neither bepristat nor ML171 showed inhibitory effects, however, when co-incubated these inhibitors caused a ~50% decrease in fibrinogen binding and P-selectin exposure (Figure 3.3A and B) while calcium mobilization was reduced by 33% (Figure 3.3C and D). Of note, a lower concentration of bepristat was used for calcium mobilization due to complete inhibition at higher concentrations (data not shown). No additive inhibitory effect was observed on platelet spreading on surfaces coated with collagen, CRP or fibrinogen (Supplementary Figure 3.3). Thus, the co-incubation of bepristat and ML171 inhibited platelet aggregation, activation and calcium mobilization, whilst there was no inhibition of platelet spreading. These data indicate that bepristat and ML171 have an additive effect on GPVI-evoked activation of platelets.

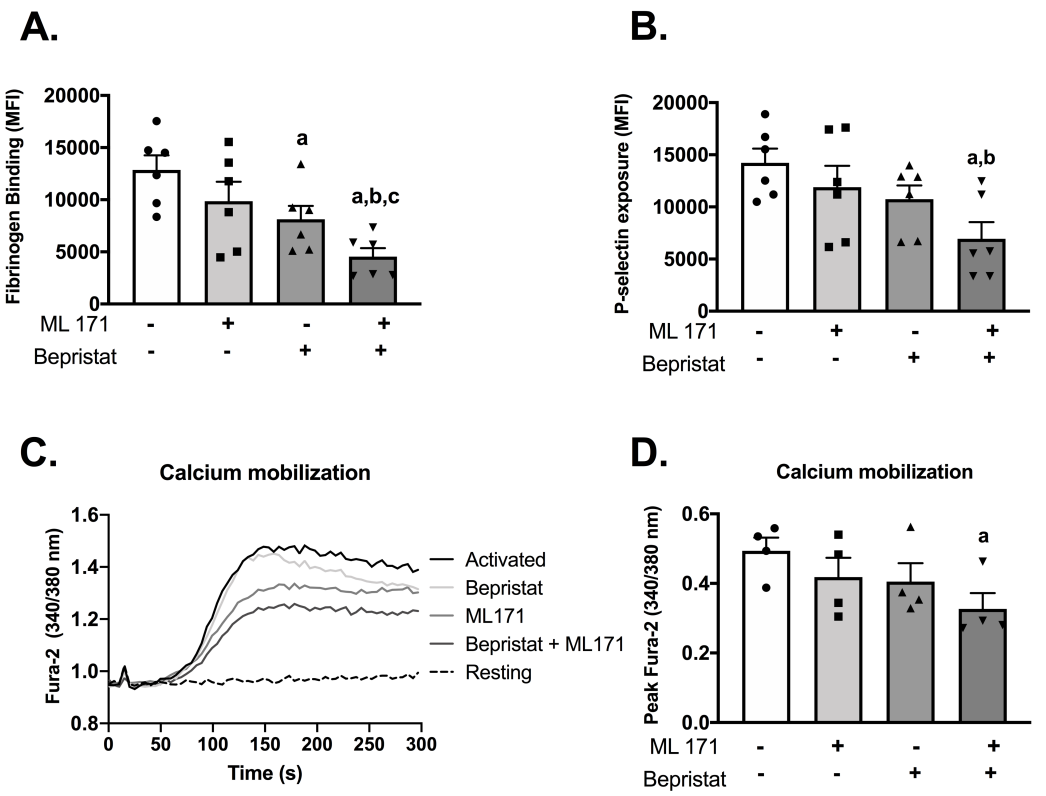

Figure 3.3. Bepristat and ML171 display additive inhibitory effects on platelet activation and calcium mobilization induced by CRP. (A) and (B): Human WP (4 x 10^7 platelets/mL) were incubated with 0.75 μM ML171 and/or 7.5 μM bepristat for 10 minutes, then 1 μg/mL CRP was added. FITC-fibrinogen and PE/Cy5-anti-P-selectin were incubated for 30 minutes and events acquired using a flow cytometer. Data expressed as median fluorescence intensity (MFI). (C): Representative curve of WP pre-incubated with calcium dye Fura-2 AM and pre-treated with 3 μM ML171 and/or 3.75 μM bepristat for 10 minutes prior to activation with 1 μg/mL CRP. Fluorescence acquired over 5 minutes using a plate reader. (D) Summary statistics for data in (C) activated with CRP. Peak Fura-2 was determined as the highest fluorescence value subtracted from baseline before agonist addition. n=6 donors for (A) and (B) and 4 donors for (C) and (D). Bar graphs show individual values, mean ± SEM. Data analysed by paired one-way ANOVA and Tukey's post-test and Tukey's multiple comparisons test. a $p<0.05$ *vs* first column; b $p<0.05$ *vs* second column and c $p<0.05$ *vs* third column of corresponding graph.

3.5.4. P38 MAPK, Akt and p47phox are important regulators of the anti-platelet effects of PDI and Nox-1 co-inhibition

Immunoblot analysis was performed to determine the effect of PDI and/or Nox-1 inhibition on several components of the collagen-stimulated signalling pathway. Initially we assessed receptor-proximal molecules such as Src and Syk, however, we found no changes (Supplementary Figure 3.4). Likewise, bepristat and ML171 exerted no effect on VASP phosphorylation, which is important in mediating the inhibitory responses to nitric oxide and PGI_2 (Supplementary Figure 3.5). Therefore, we focused on proteins regulated by ROS that signal further downstream, analysing platelets stimulated with collagen and lysed at 60 seconds (Figure 3.4). Bepristat alone was able to decrease the phosphorylation of PKC substrates, but no inhibition was observed for Akt_{S473}, $p38_{T180/Y182}$, $p47phox_{S370}$ or $ERK_{T202/Y204}$. When co-incubated, bepristat and ML171 caused decreased phosphorylation of PKC substrates, Akt_{S473}, $p38_{T180/Y182}$ and $ERK_{T202/Y204}$. We also assessed phosphorylation at 90 seconds to address delayed responses. Indeed, at 90 seconds ML171 alone was able to reduce ERK phosphorylation, while the co-incubation of PDI and Nox-1 inhibitors caused decreased phosphorylation of PKC substrates, Akt_{S473}, $p38_{T180/Y182}$ and $ERK_{T202/Y204}$, as well as $p47phox_{S370}$. Therefore, these data suggest that PDI and Nox-1 may act at distinct points within the GPVI pathway, since only the co-incubation of bepristat and ML171 was able to inhibit phosphorylation of PKC substrates, MAPKs, Akt and p47phox.

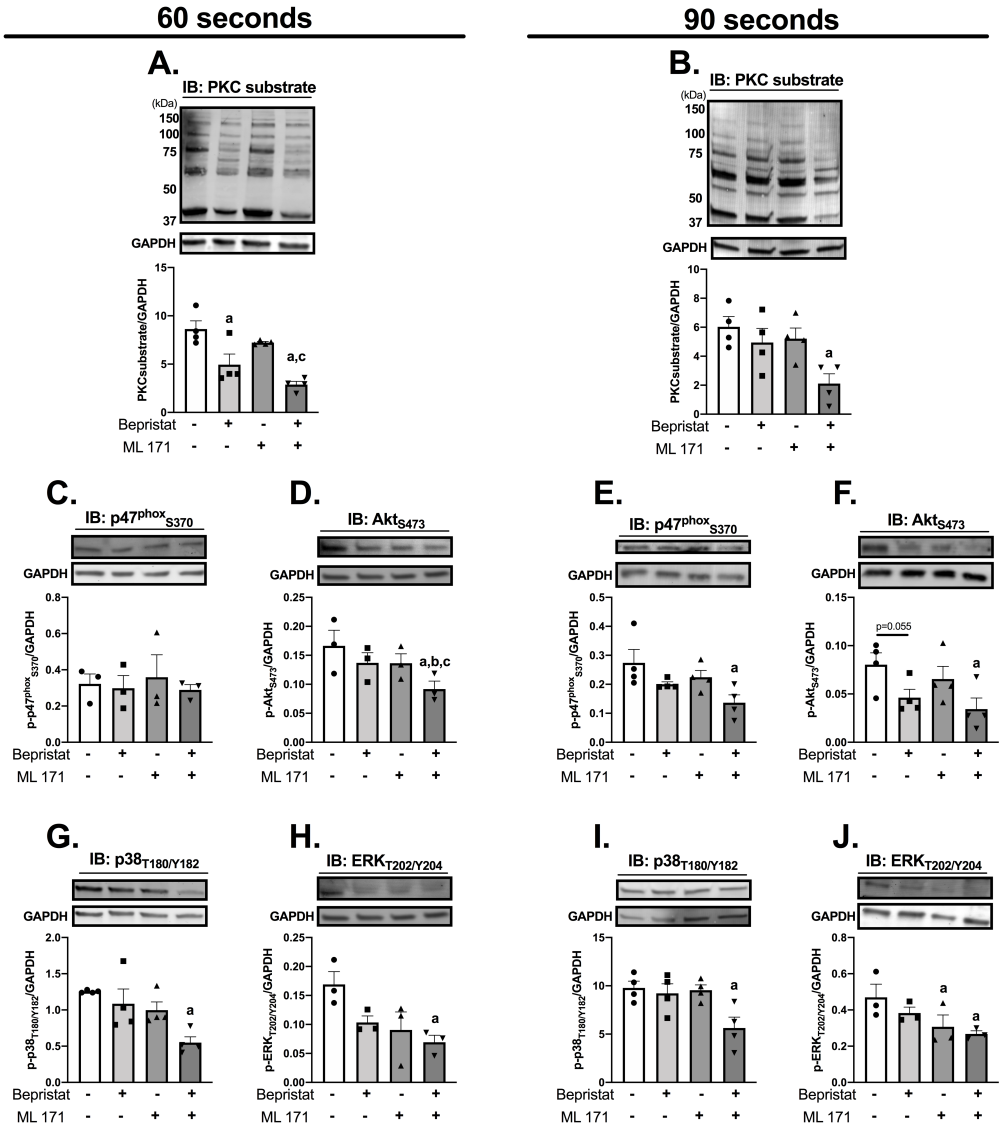

Figure 3.4. P38 MAPK and p47phox are important regulators of the anti-platelet effects of PDI and Nox-1 co-inhibition. WP at 4 x 10^8 platelets/mL were incubated with 3 µM ML171 and/or 15 µM bepristat for 10 minutes prior to adding 3 µg/mL Collagen. Platelets were lysed after 60 (left side) or 90 (right side) seconds and immunoblots performed. Samples were tested for: PKC substrate phosphorylation (A) and (B), p47phoxS370 (C) and (E), AktS473 (D) and (F), p38 MAPKT180/Y182 (G) and (I) and ERKT202/Y204 (H) and (J). GAPDH was used as a control for equal loading. Representative blot is presented above of bar graphs with summary statistics. Each lane represents the condition in graph below. n=3-4 donors. Bar graphs show individual values, mean ± SEM and were analysed by paired one-way ANOVA and Tukey's post-test. a $p<0.05$ *vs* first column; b $p<0.05$ *vs* second column and c $p<0.05$ *vs* third column of corresponding graph.

3.5.5. Nox-1$^{-/-}$ mice treated with bepristat show similar additive anti-platelet effects without increasing bleeding time

Nox-1$^{-/-}$ mice were used to further explore the contribution of Nox-1 and PDI to the regulation of platelet function. Full blood counts are provided in Supplementary Table 1. Nox-1$^{-/-}$ platelets treated with bepristat displayed diminished platelet aggregation, fibrinogen binding and PKC substrate phosphorylation; an effect not seen when platelets from WT mice were treated with the same concentration of bepristat (Figure 3.5A – D). There was no change on total protein tyrosine phosphorylation (Figure 3.5E) and no effects on platelet spreading over several surfaces (Supplementary Figure 3.6), corroborating data using human platelets. Akt$_{S473}$ phosphorylation was diminished in Nox-1$^{-/-}$ platelets treated with bepristat, although Nox-1 deletion alone was sufficient to reduce phosphorylation levels (Figure 3.5F). Nox-1$^{-/-}$ platelets displayed lower phosphorylation of ERK$_{T202/Y204}$ when compared to WT (Figure 3.5G). In contrast to data for human platelets, p38$_{T180/Y182}$ phosphorylation was also inhibited in Nox-1$^{-/-}$ platelets and no further effect was detected when these platelets were treated with bepristat (Figure 3.5H). Despite defects in platelet function and signalling, neither Nox-1 deletion nor treatment with bepristat (or both) affected bleeding times (Figure 3.5I), suggesting Nox-1 and PDI co-inhibition does not affect primary haemostasis.

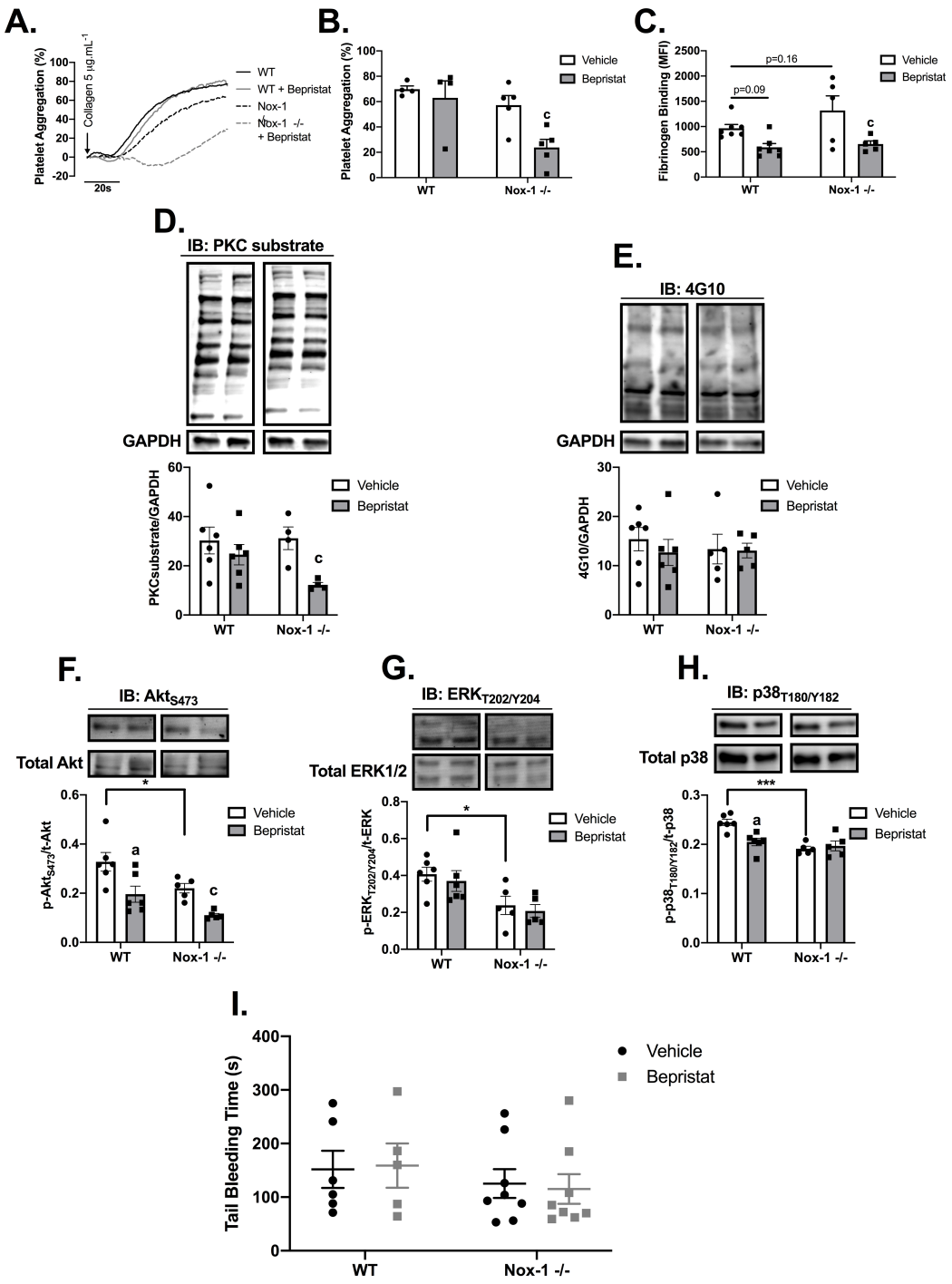

Figure 3.5. Nox-1$^{-/-}$ mice treated with bepristat showed similar additive anti-platelet effects with no repercussion in bleeding time. (A) Platelet aggregation curves of mouse wildtype (WT) and Nox-1$^{-/-}$ platelets pre-treated with 7.5 µM bepristat or vehicle for 10 minutes and activated with 5 µg/mL Collagen. (B) Summary statistics of aggregation curves. (C) Fibrinogen binding in murine platelets pre-treated with 7.5 µM bepristat or vehicle for 10 minutes and activated with 1 µg/mL CRP. Immunoblots performed in platelets pre-treated with 7.5 µM bepristat or vehicle for 10 minutes and activated with 5 µg/mL Collagen

for 90 seconds. (D) PKC substrate. (E) 4G10 total Tyr phosphorylation. (F) Akt S473 phosphorylation. (G) ERK T202/Y204 phosphorylation. (H) p38 MAPK T180/Y182 phosphorylation. Representative blot is presented on top of bar graphs with summary statistics. Each lane represents the condition in graph below. (I) Tail bleeding time in mice injected with 50 μM bepristat or vehicle control. n=5-6 mice for (A to H) and n=5-8 for (I). Data on graphs expressed as individual values, mean ± SEM analysed by unpaired two-way ANOVA and Sidak's post-test. a $p<0.05$ *vs* first column; b $p<0.05$ *vs* second column and c $p<0.05$ *vs* third column of corresponding graph.

3.5.6. Additive anti-platelet effect of PDI and Nox-1 co-inhibition is unaltered by superoxide scavenger Tiron

Next, we assessed the contribution of superoxide to the anti-platelet effect of PDI and Nox-1 inhibition. WP were incubated with 5 mM of superoxide scavenger Tiron as well as PDI and Nox-1 inhibitors. Platelet aggregation was recorded and immunoblots performed 90 seconds after collagen addition. Tiron is a widely used superoxide scavenger and has been shown to abrogate DCF fluorescence in platelets at 3 mM, which is lower than the concentration used here (Begonja et al., 2005). Tiron did not affect platelet aggregation by itself or in the presence of ML171 (Figure 3.6A and B). However, Tiron exerted an additive inhibitory effect with bepristat, while bepristat had no effect (Figure 3.2 and Supplementary Figure 3.2A). The addition of bepristat, ML171 and Tiron exerted similar additive effect as described for previous assays using only bepristat and ML171. Tiron did not affect PKC substrate and $p38_{T180/Y182}$ phosphorylation (Figure 3.6C and D). There was, however, decreased Akt_{S473} phosphorylation in the presence of Tiron (Figure 3.6E). These results suggest that the anti-platelet effects of PDI and Nox-1 co-inhibition are at least partially due to superoxide inhibition.

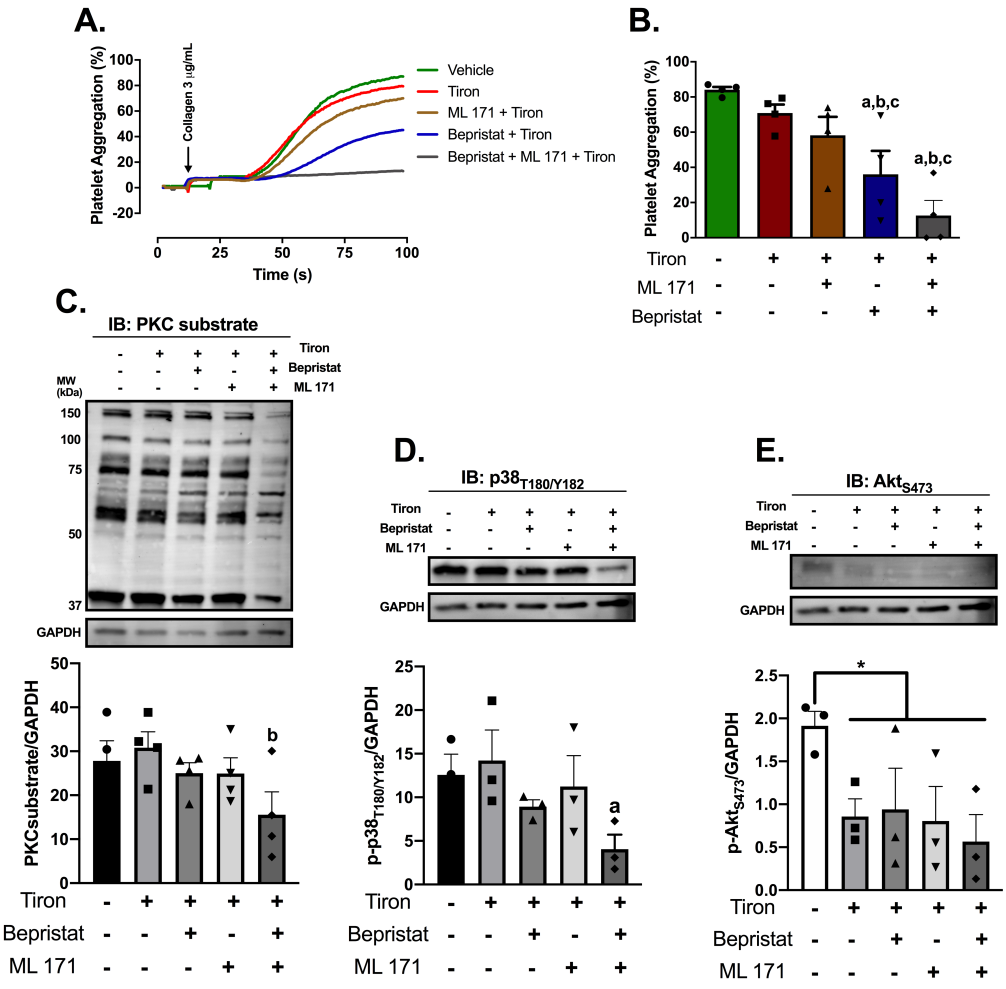

Figure 3.6. Superoxide scavenger Tiron did not affect anti-platelet effects of PDI and Nox-1 co-inhibition. WP at 4 x 10^8 platelets/mL were incubated with 5 mM Tiron, 3 µM ML171 and/or 15 µM bepristat for 10 minutes prior to adding 3 µg/mL Collagen. Platelet aggregation was measured up to 90 seconds, upon which platelets were lysed and immunoblots performed. (A) Representative aggregation curve. (B) Summary statistics of aggregation curves. (C) PKC substrate phosphorylation. (D) p38 MAPK T180/Y182 phosphorylation. (E) Akt S473 phosphorylation. Representative blot is presented on top of bar graphs with summary statistics. Each lane represents the condition in graph below. n=4 donors. Data on graphs show individual values, mean ± SEM analysed by paired one-way ANOVA and Tukey's post-test. a $p<0.05$ *vs* first column; b $p<0.05$ *vs* second column and c $p<0.05$ *vs* third column of corresponding graph.

3.5.7. Platelet PDI and Nox-1 are distinctly correlated with risk factors for MetS in a healthy population

To assess the relevance of platelet PDI and Nox-1 to MetS, the levels of both proteins were measured with several metabolic characteristics in 137 individuals not in use of long-term medications (for descriptive statistics, please see Supplementary Table 3.2). Using a multivariate regression model, we assessed the correlation between the expression levels of these proteins in platelets and several risk factors for MetS (Table 3.1). PDI levels were correlated positively with waist/hip ratio and insulin levels, whereas Nox-1 levels correlated with BMI and systolic blood pressure. There were negative correlations between PDI and mean platelet volume (MPV) and between Nox-1 and glycaemia. Interestingly, there was no correlation between the levels of PDI and Nox-1 in platelets (Supplementary Figure 3.7). Together, these data show that although both PDI and Nox-1 are correlated with risk factors for MetS, these proteins are associated with distinct risk factors. The lack of correlation between the levels of PDI and Nox-1 is consistent with the notion that different processes in platelets may regulate them.

Table 3.1. Multiple linear regression for PDI and Nox-1 expression and cardiometabolic factors.

	PDI expression			Nox-1 expression		
	Coefficient	**95% CI**	**P-value**	**Coefficient**	**95% CI**	**P-value**
BMI	-0,0015	-0,0065 to 0,0033	0,529	**0,0193**	**0,0004 to 0,0382**	**0,045***
Waist/hip	**0,3675**	**0,1085 to 0,6266**	**0,005***	-0,6286	-1,6290 to 0,3718	0,216
%FAT	0,0005	-0,0013 to 0,0024	0,550	-0,0034	-0,0108 to 0,0038	0,347
Glycaemia	0,0030	-0,0157 to 0,0219	0,745	**-0,0838**	**-0,1567 to -0,0110**	**0,024***
Insulin	**0,0048**	**0,0002 to 0,0093**	**0,037***	-0,0012	-0,0187 to 0,0162	0,891
Triglycerides	-0,0220	-0,0552 to 0,0111	0,191	-0,0048	-0,1329 to 0,1233	0,940
LDL	0,0132	-0,0012 to 0,0278	0,073	0,0114	-0,0447 to 0,0675	0,688
Systolic BP	-0,0007	-0,0017 to 0,0001	0,118	**0,0041**	**0,0004 to 0,0079**	**0,028***
MPV	**-0,0021**	**-0,0035 to -0,0008**	**0,001***	0,0031	-0,0019 to 0,0082	0,225

Data from 137 volunteers. Platelet PDI and Nox-1 expressions were determined by immunoblotting and normalized to GAPDH loading control. Body mass index (BMI) in kg/m^2, glycaemia in mmol/L, Insulin in mIU/L, triglyceridaemia in mmol/L, LDL cholesterol in mmol/L, systolic blood pressure (BP) in mmHg, mean platelet volume (MPV) in fL. Coefficient and 95% confidence interval (CI) shown. P<0.05 indicated in bold and *.

3.6 Discussion

Data herein presented suggest that platelet PDI and Nox-1 are correlated with risk factors for MetS and dual inhibition may provide a new pharmacological avenue for the development of anti-platelet medications. Using selective inhibitors in both human and murine Nox-1$^{-/-}$ platelets, we established that the co-inhibition of PDI and Nox-1 led to an additive inhibitory effect on GPVI-mediated platelet aggregation, activation, calcium flux and ROS production. Moreover, no bleeding defect was observed in Nox-1$^{-/-}$ mice treated with the PDI inhibitor bepristat, suggesting the anti-platelet effects were not correlated with defects in haemostasis.

In vascular smooth muscle cells, PDI has been reported to regulate Nox-1 activity and transcription (Fernandes et al., 2009). This involves the formation of a disulphide bond between Cys400 of PDI and Cys196 of p47phox, a cytosolic subunit of the Nox-1 complex (Gimenez et al., 2019). We note a migration of both PDI and p47phox towards the platelet membrane, where the active Nox-1 complex is located, upon activation with CRP, which is consistent with PDI and Nox-1 co-localization in HEK293 cells (Matsumoto et al., 2014). Co-migration of PDI and p47phox was not seen when TRAP-6 was used as an agonist, indicating that the co-localization of PDI and p47phox with the Nox-1 complex is GPVI-specific, which prompted us to assess the functional relevance of these observations.

Platelets pre-treated with both PDI and Nox-1 inhibitors did not aggregate, activate or signal to the same degree in GPVI-mediated responses when compared to each inhibitor alone. This was confirmed using different PDI inhibitors and in murine Nox-1 deficient platelets incubated with

bepristat. Likewise, inhibition of PDI in Nox-1$^{-/-}$ mice did not affect bleeding time. In line with our data, previous reports have shown that platelets from female Nox-1 KO mice did not respond to collagen, whilst responses to thrombin were preserved (Vara et al., 2019). It has also been reported that ML171 (also referred to as 2APT) does not affect platelet adhesion, nor does it inhibit aggregation induced by agonists other than collagen (Vara et al., 2013;Lu et al., 2019). In contrast, one study reported that male Nox-1 KO mice presented defects in thrombin-stimulated platelets (Delaney et al., 2016). The reason for this inconsistency is unclear, although since the Nox-1 gene is located on chromosome X, sex-dependent phenotypes may be observed. Nonetheless, our data using female Nox-1$^{-/-}$ mice are in agreement with the majority of the literature, and propose for the first time that PDI and Nox-1 both contribute to the regulation of platelet responses in a GPVI-specific manner.

To explore the mechanisms of action for the strong anti-platelet effects of PDI and Nox-1 dual inhibition, protein phosphorylation targets were investigated. Nox-1 activation results in increased p38 MAPK activity in CaCo-2 colonic epithelial cells (Guina et al., 2015). Furthermore, in diabetic kidney cells, Nox-1 hyperactivation induced phosphorylation of p38 MAPK through PKC (Zhu et al., 2015), suggesting the Nox-1/PKC/p38 MAPK pathway to be relevant in different cell types and diseases. PKC itself regulates p47phox phosphorylation, and thus Nox-1 activation, in platelets activated by LPS (Lopes Pires et al., 2019). It is therefore possible that PKC and Nox-1 interact in a bi-directional way.

P38 MAPK has been implicated in platelets to regulate responses to low-dose collagen and the thromboxane analogue U46619 but not thrombin (Saklatvala et al., 1996). In neutrophils, p38 and ERK have been shown to interact with p47phox directly, inducing its phosphorylation (El Benna et al., 1996). Our data show that 60 seconds after collagen addition, dual inhibition of PDI and Nox-1 decreased phosphorylation levels of p38 MAPK and ERK, whereas p47phox phosphorylation was only affected at a later time point. This suggests that, within the collagen pathway in platelets, p38 MAPK and ERK may lie upstream of p47phox. Of note, the Nox complex was postulated to be constitutively associated to the cytoplasmic tail of GPVI and its assembly may comprise an initial step of GPVI-induced platelet activation (Qiao et al., 2018). Therefore, PDI and Nox-1 are both relevant to the GPVI-induced platelet activation by acting at different points within the pathway.

The additive anti-platelet effect of PDI and Nox-1 inhibition was unaffected by a superoxide scavenger. However, addition of Tiron exerted an additive effect to bepristat in platelet aggregation, reiterating the role of superoxide to the effects herein observed. Nox-1 and PDI may therefore have different roles within the GPVI pathway, considering that the primary role of Nox-1 is to generate superoxide. Of note, a previous report using Nox-1$^{-/-}$ female mice have shown that Nox-1 deletion reduces superoxide production induced by collagen, but does not abrogate it (Vara et al., 2019). This indicates that there are other sources of superoxide downstream of GPVI. In juxtaposition, it is unlikely that the additive effect of PDI and Nox-1 co-inhibition is due to PDI regulation of integrins (Kim et al., 2013), given that 1) the additive inhibitory effects on platelet function were specific to GPVI

ligands and 2) platelet adhesion, which is mainly regulated by integrins, was not affected. Nonetheless, we show that p38MAPK and p47phox are key to signalling downstream of PDI and Nox-1.

Perhaps the most puzzling data in our study was the lack of additive inhibitory effect of bepristat and Nox-1 deficiency to platelet p38 MAPK phosphorylation in mice. This is contradictory to results measured in human platelets incubated with bepristat and ML171, since only the co-incubation of these inhibitors was able to decrease p38 MAPK phosphorylation. There has been reported a great interspecies variability of p38 MAPK inhibitors suggesting humans to be more sensitive to responses regulated by p38 MAPK in different cell types (Laufer et al., 2005;Fehr et al., 2015). It is possible that p38 is more important to the activation of human platelets than it is to murine cells, but the literature lacks a comparative analysis of the functional relevance of p38 in human and murine platelets. In addition, Nox-1$^{-/-}$ mice presented decreased p38 MAPK phosphorylation compared to WT; an effect not seen in human platelets incubated with only ML171. The specificity of ML171 for Nox-1 has been demonstrated by our group (Vara et al., 2020) and others (Gianni et al., 2010) using concentrations up to 5 times higher than used in the present report. It is possible that Nox-1 deletion in mice could lead to adaptive responses that may not be directly comparable to pharmacologic inhibition in humans. Therefore, we consider that p38 MAPK is a key target downstream of dual PDI and Nox-1 inhibition and that discrepant data on human and Nox-1$^{-/-}$ murine platelets could be due to interspecies differences.

Platelet PDI was correlated with waist/hip ratio and insulin levels, which are markers of visceral fat accumulation and insulin resistance, respectively, whereas Nox-1 was positively associated with BMI and systolic blood pressure. The negative correlation of PDI with MPV suggests that this protein may not be relevant to increased MPV observed in obese patients (Coban et al., 2005). Likewise, the negative correlation of Nox-1 with glycaemia was not expected since this protein has been implicated in diabetic vasculopathy (Gray et al., 2013). It is possible that Nox-1 is upregulated by glycaemia only in specific cell types or that Nox-1 in platelets negatively correlates with glycaemia as a compensatory mechanism. These hypotheses should be further explored in the future. Altogether, these data demonstrate the potential importance of platelet PDI and Nox-1 to MetS and suggest that distinct mechanisms control the higher expression of these proteins given distinct associations with risk factors for MetS.

In conclusion, we show that platelet PDI and Nox-1 were distinctly associated with risk factors for MetS. Dual inhibition of these proteins results in decreased platelet aggregation, fibrinogen binding, p-selectin exposure and calcium mobilization, all of which were GPVI-specific and required the phosphorylation of p38 MAPK and p47phox. This suggests PDI and Nox-1 may act at different points in the GPVI signalling pathway. Together, we propose that PDI and Nox-1 are promising targets for the development of new anti-platelet strategies as secondary prevention in chronic metabolic diseases. Future studies should address the pathophysiological relevance of these proteins in platelets to the development of MetS.

AUTHOR CONTRIBUTIONS STATEMENT

RSG designed the study, performed experiments, analysed data and drafted the manuscript. TS, GL and NK performed experiments and reviewed the manuscript. GP supervised some mouse experiments, discussed data and reviewed the manuscript. JMG designed the study, supervised protocols and reviewed the manuscript. All authors agreed on the final version submitted.

ACKNOWLEDGEMENTS

This work is part of the PhD thesis of RSG.

SOURCES OF FUNDING

This study was funded by the British Heart Foundation (RG/15/2/31224), Medical Research Council (MR/J002666/1).

DISCLOSURE OF INTEREST

The authors declare no actual or potential conflict of interest.

3.7 Supplementary Tables

Supplementary Table 3.1. Full blood count of WT and Nox-1$^{-/-}$ mice.

	WT	Nox-1$^{-/-}$
Red Blood Cells		
Hematocrit (%)	36.67±1.368	36.00±0.806
RBC (x10^3/µL)	7.76±0.278	7.67±0.192
Haemoglobin (g/dL)	12.42±0.504	12.30±0.158
MCV (fL)	47.37±0.214	47.50±0.65
MCH (pg)	15.89±0.155	16.04±0.287
MCHC (g/dL)	33.54±0.336	34.20±0.626
RDW (%)	14.64±0.148	**15.64±0.256***
White Blood Cells		
Leukocytes (x10^3 cells/µL)	6.75±0.247	**8.22±0.407***
Lymphocytes (x10^3 cells/µL)	5.47±0.337	**6.82±0.296***
Lymphocytes (%)	82.92±1.216	82.94±0.618
Monocytes (x10^3 cells/µL)	0.76±0.072	0.82±0.066
Monocytes (%)	9.52±0.571	9.98±0.392
Granulocytes (x10^3 cells/µL)	0.60±0.072	0.60±0.071
Granulocytes (%)	8.50±1.136	7.08±0.41
Platelets		
Platelet count (x10^3 cells/µL)	507.9±22.78	468.8±20.49
MPV (fL)	4.95±0.043	4.98±0.111

Data presented as mean ± SEM. N= 7 mice for WT and N=5 for Nox-1$^{-/-}$. Groups were compared by unpaired Student t-test. * $p<0.05$.

Supplementary Table 3.2. Summary statistics of study population (n=137)

Parameter	
Age (years)	48,08 ± 11,46
BMI (kg/m²)	25,09 ± 4,15
Gender (M%/F%)	(32%/68%)
Glycaemia (mmol/L)	5,36 ± 0,70
Insulinaemia (pM)	29,33 ± 21,34
MPV (fL)	8,49 ± 0,89
Systolic BP (mmHg)	128,30 ± 15,15
Triglyceridaemia (mmol/L)	0,91 ± 0,48
LDL (mmol/L)	3,16 ± 0.95
Waist/hip ratio	0,88 ± 0,05
PDI expression	0,27 ± 0,07
Nox-1 expression	0,57 ± 0,27

Data presented as mean ± SD or % for gender. BMI: body mass index. HOMA-IR: homeostatic model assessment of insulin resistance. MPV: mean platelet volume. BP: blood pressure. LDL: low-density lipoprotein cholesterol. PDI: protein disulphide isomerase.

3.8 Supplementary Figures

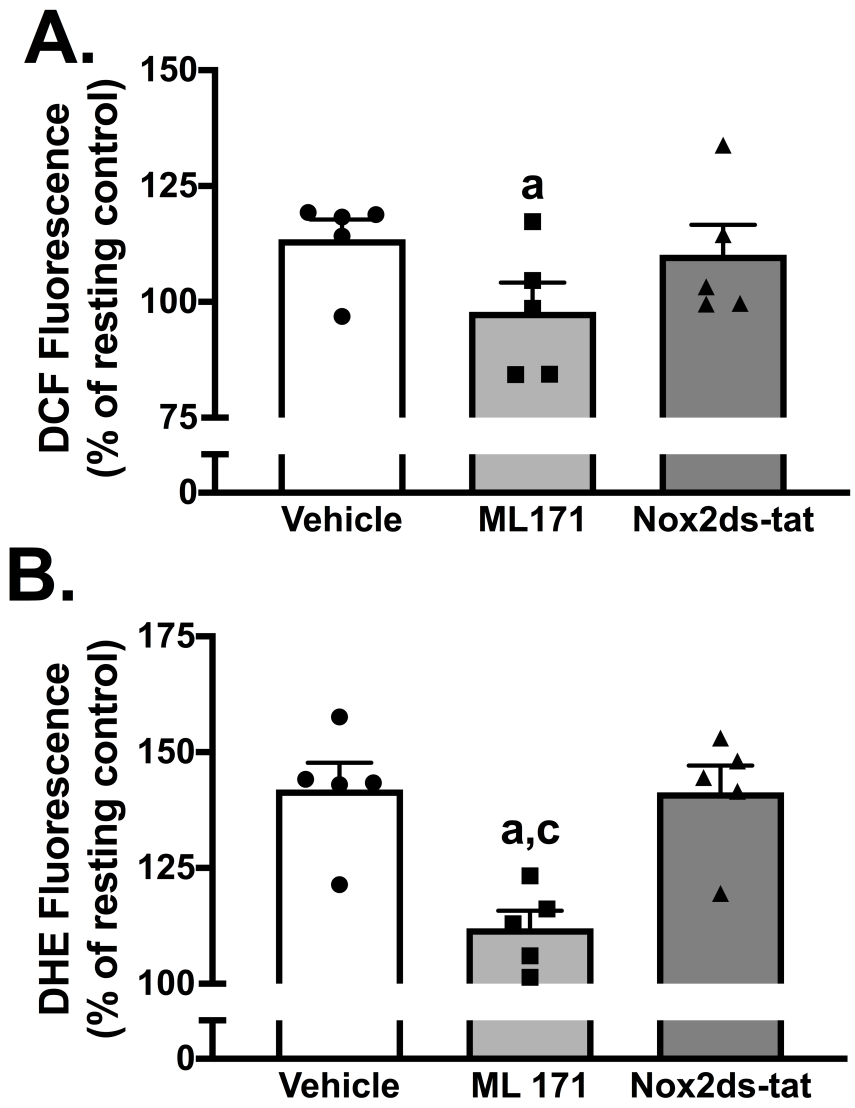

Supplementary Figure 3.1. Nox-1, but not Nox-2, is relevant for ROS generation downstream of GPVI. Nox-1 inhibitor ML171 (3 μM) or Nox-2 inhibitor Nox2ds-tat (3 μM) were incubated for 10 minutes in washed platelets loaded with 20 μM DCF or 10 μM DHE for 15 minutes. WP were stimulated with 1 μg/mL CRP and fluorescence acquired using a flow cytometer. Data on graphs show mean ± SEM as well as individual points. Data analysed by paired one-way ANOVA with Tukey's post-test. a $p<0.05$ *vs* first column and c $p<0.05$ *vs* third column of corresponding graph.

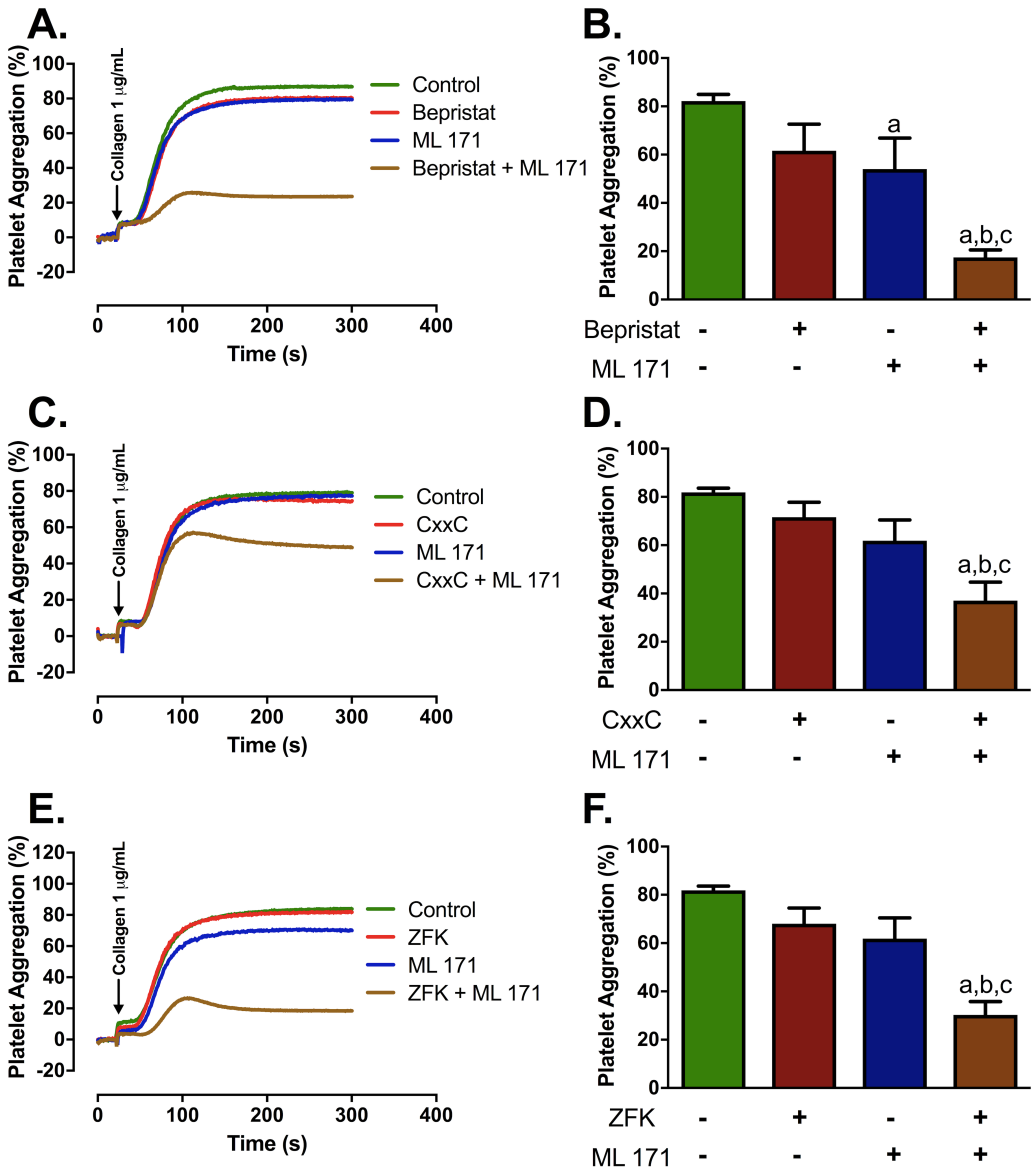

Supplementary Figure 3.2. Different PDI inhibitors exert similar additive inhibitory effect to ML171 in platelet aggregation induced by Collagen. Human WP at 4 x 10^8 platelets/mL were incubated with 0.75 µM ML171 and/or: 15 µM Bepristat (A) and (B), 50 µM CxxC peptide (C) and (D) or 1.25 µM Zafirlukast for 10 minutes, then stimulated with 1µg/mL Collagen. Aggregation traces were recorded for up to 5 minutes. Representative aggregation curves are provided in (A), (C) and (E) with corresponding summary statistics in (B), (D) and (F). n=3-5 different donors. Data on graphs show mean ± SEM. Data analysed by paired one-way ANOVA with Tukey's post-test. a $p<0.05$ *vs* first column; b $p<0.05$ *vs* second column and c $p<0.05$ *vs* third column of corresponding graph.

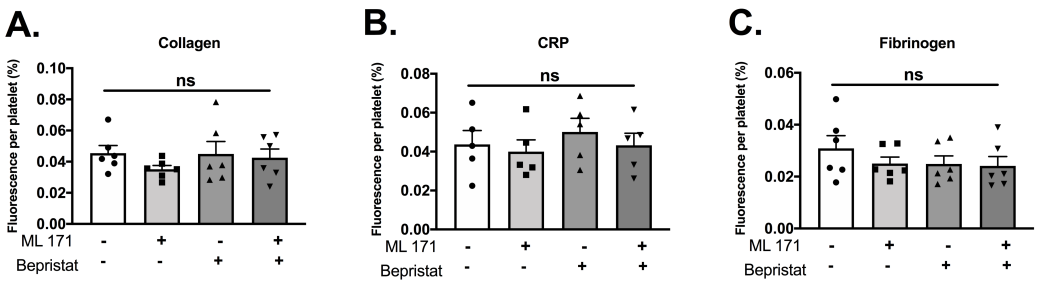

Supplementary Figure 3.3. No additive inhibitory effect of bepristat and ML171 to human platelet spreading. Human WP at 2 x 10^7 platelets/mL were incubated with ML171 (3 μM) and/or bepristat (15 μM) for 10 minutes and left to adhere and spread on Collagen- (A), CRP- (B) or Fibrinogen-coated (C) surfaces for 45 minutes. Platelets were labeled with fluorescently tagged phalloidin and visualized in a Nikon A1-R confocal microscope. Number of platelets was divided by total fluorescence of field to obtain fluorescence per platelet as a surrogate for platelet spreading. Data on graphs show mean ± SEM. Data analysed by paired one-way ANOVA with Tukey's post-test. * $p<0.05$ and ** $p<0.01$ *vs* Vehicle of corresponding ML171 concentration. Blue denotes difference from 30 μM bepristat, whereas black asterisk denotes difference from 15 μM.

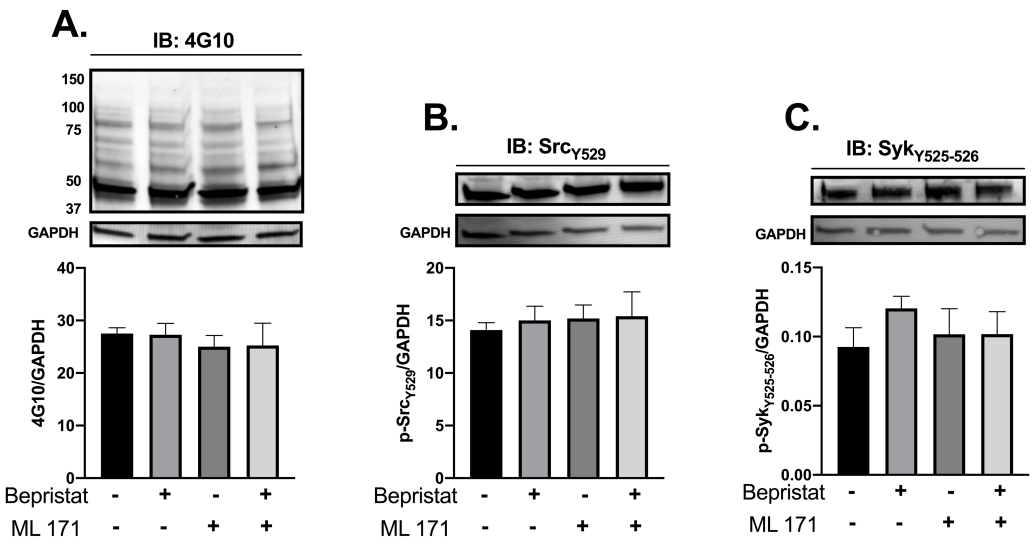

Supplementary Figure 3.4. PDI and Nox-1 co-inhibition did not affect tyrosine phosphorylation or phosphorylation of upstream GPVI proteins. WP at 4 x 10^8 platelets/mL were incubated with 3 μM ML171 and/or 15 μM bepristat for 10 minutes prior to the addition of 3 μg/mL Collagen. Platelets were lysed after 90 seconds and immunoblots performed. Samples were tested for: 4G10 total Tyr phosphorylation (A), Src Y529 (B) and Syk Y525-526 (C). Representative blot is presented on top of bar graphs with summary statistics. Each lane represents the condition in graph below. n=3-4 donors. Data on graphs show mean ± SEM and analysed by paired one-way ANOVA and Tukey's post-test.

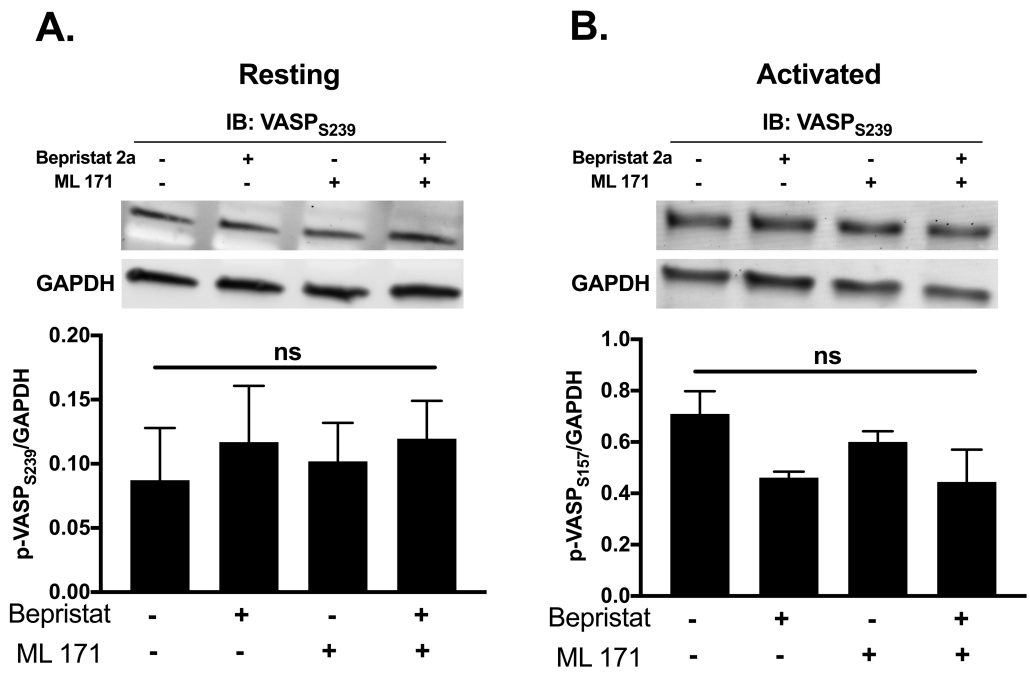

Supplementary Figure 3.5. VASP phosphorylation in resting and activated platelets was not affected by PDI and Nox-1 inhibition. WP at 4 x 10^8 platelets/mL were incubated with 3 μM ML171 and/or 15 μM bepristat for 10 minutes prior to the addition of 3 μg/mL Collagen. On some conditions, platelets were not stimulated. Platelets were lysed after 90 seconds and immunoblots performed. Samples were tested for VASP S239 phosphorylation. Representative blot is presented on top of bar graphs with summary statistics. Each lane represents the condition in graph below. n=3-4 donors. Data on graphs show mean ± SEM and analysed by paired one-way ANOVA and Tukey's post-test.

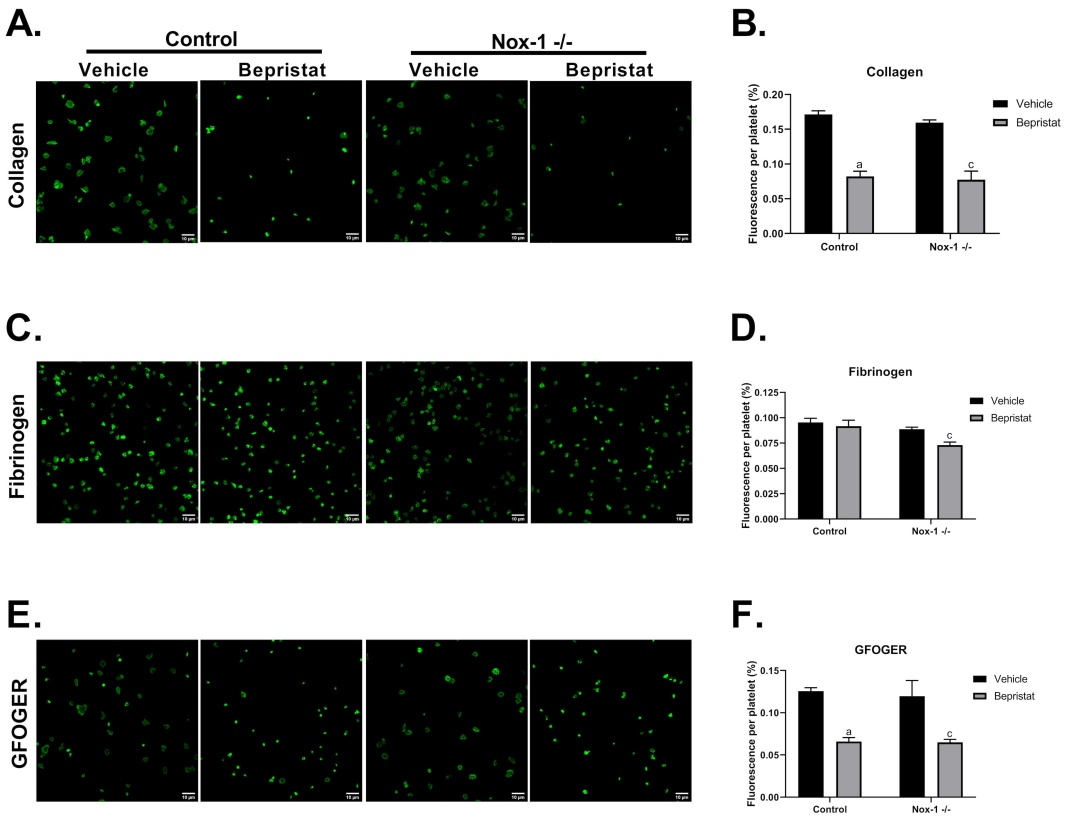

Supplementary Figure 3.6. No additive inhibitory effect of bepristat and ML171 to murine platelet spreading. Platelets from wildtype (WT) or Nox-1$^{-/-}$ mice (2 x 10^7 platelets/mL) were incubated with 30 μM bepristat or vehicle for 10 minutes and left to adhere and spread on Collagen- (A) and (B), Fibrinogen- (C) and (D) or GFOGER-coated (E) and (F) surfaces for 45 minutes. Platelets were labeled with fluorescently tagged phalloidin and visualized in a Nikon A1-R confocal microscope. Number of platelets was divided by total fluorescence of field to obtain fluorescence per platelet as a surrogate for platelet spreading. n=4-5 different mice. Data on graphs show mean ± SEM. Data analysed by two-way ANOVA with Sidak's post-test. a $p<0.05$ *vs* first column; b $p<0.05$ *vs* second column and c $p<0.05$ *vs* third column of corresponding graph.

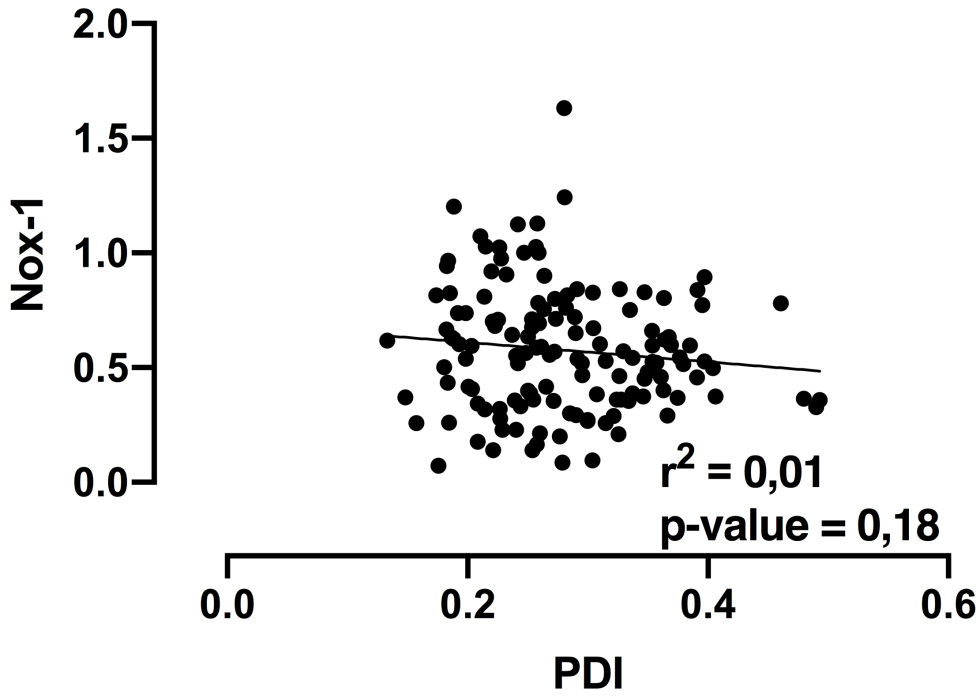

Supplementary Figure 3.7. Linear regression of PDI and Nox-1 levels in platelets. PDI and Nox-1 were measured in platelets of 137 donors and normalized by GAPDH loading control. Simple linear regression was performed. P-value and r^2 are shown in graph.

3.9 Supplementary Methods

3.8.1. Reagents

Prostacyclin (PGI_2), Bepristat 2a, Zafirlukast, Dithiotreitol (DTT), Phorbol-12-myristate-13-acetate (PMA), 2′,7′-Dichlorofluorescin diacetate (DCF), Thrombin Receptor Activator Peptide 6 (TRAP-6), human fibrinogen, 3,3′-Dihexyloxacarbocyanine iodide ($DIOC_6$) and Tiron were purchased from Sigma-Aldrich (Dorset, UK). PAPA-NONOate and ML171 (also known as 2-acetylphenothiazine or 2APT) was purchased from Tocris (Abingdon, UK). PE/Cy5 anti human CD62P antibody was purchased from BD Biosciences (Wokingham, UK). FITC-conjugated fibrinogen was purchased from Agilent (Stockport, UK). PDI inhibitor CxxC peptide (Sousa et al., 2017) was purchased from EZBiolab (Parsippany, USA). GFOGER was purchased from CambCol (Cambridge, UK). Collagen was purchased from Nycomed (Munich, Germany) whereas Collagen-Related Peptide (CRP) was obtained from Prof Richard Farndale (University of Cambridge, Cambridge, UK). Anti-PDI (NB600-1164, clone RL77), Anti-Nox-1 (NBP1-31546) were from Novus Biologicals (Bio-techne R&D Systems Europe Ltd, Abingdon, UK). Anti-p47phox, anti-phospho p47phox Ser370, 4G10 total phospho Tyr, Fura-2 AM calcium dye, Alexa-488, Alexa-568 and Alexa-647-conjugated secondary antibodies were bought from ThermoFisher (Paisley, UK). Anti-ERK1/2 and anti-p38 antibodies were purchased from Santacruz Biotechnology (Heidelberg, Germany). Anti-Akt, anti-phospho Src Tyr529, anti-phospho Syk Tyr525/526, anti-phospho vasodilator-stimulated phospho-protein (VASP) (Ser239), PKC substrate, anti-phospho-Akt Ser473, anti-phospho p38 Thr180/Tyr182, anti-phospho ERK Thr202/Tyr204 were purchased from

Cell Signalling (Hitchin, UK). Anti-glyceraldehyde 3-phosphate dehydrogenase (GAPDH) was purchased from Proteintech (Manchester, UK).

3.8.2. Washed platelets preparation

Blood was collected from healthy adult volunteers who were not using antiplatelet medication and had previously provided informed consent. Platelet-rich plasma (PRP) was obtained after centrifuging whole blood at 100 x *g*, 20 minutes, 22°C. To obtain washed platelets (WP), PRP was centrifuged twice at 1000 x *g*, 10 min, 22°C in the presence of 1.25 μg/mL prostacyclin and 1:5 v/v acid citrate dextrose (ACD: 5% sodium citrate, 2% D-glucose and 1.5% citric acid). The final platelet pellet was resuspended in modified Tyrode's-HEPES buffer, (134 mM NaCl, 20 mM N-2-hydroxyethylpiperazine-N′-2-ethanesulfonic acid, 12 mM $NaHCO_3$ 5 mM glucose, 0.34 mM Na_2HPO_4, 9 mM KCl and 1 mM $MgCl_2$, pH 7.3) and rested for 30 minutes at 30 °C before experiments. The Research Ethics Committee from the University of Reading approved all protocols to obtain and use human blood samples.

3.8.3. Collection of mouse blood and platelet preparation

Colonies of Nox-$1^{-/-}$ mice were purchased from Jackson Laboratory (Sacramento, CA, USA) and C57BL/6 were used as controls, as recommended by the animal provider. Animals were kept under a 12 h light cycle, controlled temperature (22-24°C) and food and water *ad libitum*. The University of Reading Local Ethics Review Panel approved all protocols within a license from the British Home Office. Mice (11 – 14 weeks, females)

were culled in a CO_2–filled chamber and blood collected through cardiac puncture in a syringe containing 3.2% sodium citrate at a 1:9 v/v citrate-blood ratio. Whole blood was centrifuged at 203 x *g* for 8 minutes and PRP collected. 1.25 µg/mL PGI_2 was added and PRP centrifuged at 1,028 x *g* for 5 min and pellet resuspended in modified Tyrode's-HEPES buffer to obtain WP.

3.8.4. Measurement of reactive oxygen species

Human WP (4 x 10^8 platelets/mL) were incubated with 20 µM DCF for 15 minutes, followed by a 10 minutes incubation with Bepristat (7.5 to 100 µM) and/or ML171 (0.1875 to 6 µM). Platelets were then stimulated with CRP at 1 µg/mL for 10 minutes and fluorescence read on a BD Accuri C6 plus flow cytometer (BD Biosciences, Oxford, UK).

3.8.5. Reductase activity

The reductase activity of human WP was determined through the fluorescent probe dieosin glutathione disulphide (Di-E-GssG, ex/em 510/545 nm). Di-E-GssG was synthesized as previously described (Raturi and Mutus, 2007). Briefly, human WP (4 x 10^8 platelets/mL) were incubated with ML171 for 10 minutes, and then added to a 96-well black plate in triplicates. DTT (5 µM) and Di-E-GSSG (300 nM) were added and the plate was immediately read every 30 seconds for 1 hour, using a Flexstation 3 fluorimeter (Molecular Devices, Wokingham, UK). The runs were then subtracted from a blank sample, without di-E-GSSG.

3.8.6. Immunofluorescence microscopy

Human PRP were activated with 1 μg/mL CRP or 3 μM TRAP-6 for 3 minutes in the presence of integrillin at 4 μg/mL. PRP was fixed immediately using 5% paraformaldehyde and centrifuged at 1000 x *g* for 10 minutes. The pellet was resuspended in 1:9 v/v ACD-phosphate buffer solution (PBS) and submitted to another centrifugation under the same conditions. The final pellet was resuspended in PBS containing 1% w/v BSA and left to adhere onto poly-L-lysine coverslips for 90 minutes at 37 °C. Coverslips were washed three times with PBS and blocked again in PBS containing 1% w/v BSA for 1 hour. Blocking buffer was washed away with PBS and primary or IgG control antibodies added at 1:250 v/v dilution in PBS containing 0.2% v/v Triton-X-100 and 2% v/v donkey serum and incubated at 4 °C overnight. Antibodies were washed away three times with PBS and appropriate secondary antibodies tagged with different fluorophores added for 1 hour at room temperature. Finally, coverslips were mounted in gold anti-fade onto a coverslips and analysed with a 100 x magnification oil-immersion lens on a Nikon A1-R confocal microscope (Nikon Instruments Europe BV, Amsterdam, Netherlands).

3.8.7. Turbidimetry and plate-based platelet aggregation

Platelet aggregometry was performed by turbidimetry in a four-channel AggRam aggregometer (Helena Biosciences, Gateshead, UK), as described previously (Gaspar et al., 2019). Briefly, human (4 x 10^8 platelets/mL) or mouse (2 x 10^8 platelets/mL) WP were pre-incubated with inhibitors for 10 minutes before stimulation with collagen and curves recorded for up to 300 seconds. For mouse experiments, WP were pre-

incubated with inhibitors for 10 minutes and stimulation obtained with 5 μg/mL collagen. The concentrations of inhibitors used are described in appropriate figure legend. To reconstruct the curves, 0% was set when t = 10 seconds and 100% set as blank (distilled water) placed at the end of the run in each channel for at least 15 seconds.

Platelet aggregation was also assessed through an end-point, plate-based method, as described previously (Bye et al., 2017). Briefly, human WP (4 x 10^8 platelets/mL) were added to a 96-wells half-area plate (Greiner) containing varying concentrations of PDI inhibitor Bepristat or Nox-1 inhibitor ML171 and incubated for 10 minutes. Then, agonists collagen (2 μg/mL), CRP (1 μg/mL), TRAP-6 (10 μM) or PMA (500 nM) were added and plate shaken at 1200 rpm for 5 minutes at 37°C using a plate shaker (Quantifoil Instruments). Absorbance was measured at 450 nm using a Flexstation 3 plate reader.

3.8.8. Fibrinogen binding and P-selectin exposure

Human WP (4 x 10^8 platelets/mL) were incubated with 7.5 μM Bepristat and/or 0.75 μM ML171 for 10 minutes. Platelets were activated with 1 μg/mL CRP for 10 minutes and incubated with FITC-conjugated fibrinogen or PE/Cy5-conjugated anti-human CD62P for 30 minutes. This was then diluted 25 x with Tyrodes-HEPES buffer and read using a BD Accuri C6 plus flow cytometer. Platelets were gated according to forward and size scatter and analysed using the BD Accuri software.

For mouse studies, whole blood (WB) was diluted 1:25 v/v with Tyrodes-HEPES buffer and incubated with 30 μM Bepristat. Higher

concentration of inhibitor was used in order to account for binding of plasma proteins. WB was stimulated with 3 μg/mL CRP for 10 minutes, followed by incubation of FITC-conjugated fibrinogen for 30 minutes. This solution was further diluted with Tyrodes-HEPES buffer and read using a BD Accuri C6 plus flow cytometer.

3.8.9. Calcium measurement

Human PRP was incubated with 2 μM Fura-2 AM for 1 hour at 30°C. PRP was centrifuged at 350 *g* for 20 minutes and WP (4 x 10^8 platelets/mL) resuspended in Tyrodes-HEPES buffer. Platelets were immediately placed in a 96-wells black plate with clear bottom and incubated with 3.75 μM Bepristat and/or 3 μM ML171 for 10 minutes and stimulated with 1 μg/mL CRP. Fluorescence was read every 5 seconds for 5 minutes using a Flexstation 3 fluorimeter (excitation 340 and 380 and emission 510 nm). Calcium signal was derived from the ratio of the 340 and 380 excitation beams.

3.8.10. Platelet spreading

Human WP (2 x 10^7 platelets/mL) were incubated with Bepristat (7.5 to 30 μM) and/or ML171 (0.1875 to 6 μM) for 10 minutes and left to adhere to collagen (30 μg/mL), fibrinogen (30 μg/mL) or CRP (10 μg/mL)-coated surfaces (96-wells plate) for 45 minutes at 37°C. Non-adherent platelets were washed off three times with PBS. Paraformadehyde 0.2% was added for 10 minutes to fix the platelets. Triton-X 0.01% v/v was added for 5 minutes to permeabilize the cells. After three washes with PBS to remove Triton-X,

platelets were stained with Alexa Fluor 488-conjugated phalloidin (1:1000 v/v) for 1 hour in the dark at room temperature and analyzed using a 20x lens on a Nikon A1-R Confocal microscope.

For mouse studies, the same procedure was followed, with slight alterations. WP were incubated with 30 μM Bepristat for 10 minutes and left to adhere to collagen, fibrinogen (30 μg/mL) or GFOGER (10 μg/mL)-coated coverslips and mounted onto slides instead of using a 96-wells plate.

3.8.11. Immunoblotting

Human WP (4 x 10^8 platelets/mL) were incubated with 15 μM Bepristat and/or 3 μM ML171 for 10 minutes and stimulated with 3 μg/mL collagen. On some experiments, collagen was not added in order to assess the effects of PDI and Nox-1 inhibitors in resting platelets. For mouse experiments, WP (2 x 10^8 platelets/mL) were incubated with 7.5 μM Bepristat for 10 minutes and stimulated with 5 μg/mL collagen. Platelets were lysed in reducing Laemmli buffer (12% (w/v) Sodium Dodecyl Sulphate (SDS), 30% (v/v) glycerol, 0.15 M Tris-HCl (pH 6.8), 0.001% (w/v) Brilliant Blue R, 30% (v/v) β-mercaptoethanol) and heated for five to ten minutes. SDS-PAGE and immunoblotting were performed using standard protocols exactly as described in (Gaspar et al., 2019). Specific primary phosphor-antibodies were used as described in figure legends. Mouse anti-human GAPDH was used as loading controls. Membranes were visualised using a Typhoon imaging system (GE Healthcare, Hatfield, UK).

3.8.12. Tail bleeding assay

Nox-1$^{-/-}$ or C57BL/6 wildtype (WT) mice were anesthesized through an intraperitoneal injection of ketamine (100 mg/kg) and xylazine (10 mg/kg). After animals were fully anaesthetized, Bepristat (0.5 µL of a 100 µM solution diluted in 100 µL PBS per 25 g of animal; 50 µM *in vivo* concentration) was injected intravenously. After 5 minutes, 5 mm of the tail was amputated using a sharp blade. The bleeding tail was then placed in PBS buffer kept at 37 °C and bleeding time recorded for up to 20 minutes, after which mice were terminated.

3.8.13. Population study

This study comprised of 143 volunteers aged 30 to 65 not using chronic medications that were recruited at the University of Reading to assess physical, metabolic and platelet characteristics. Volunteers answered a questionnaire about their age, gender, amongst other personal questions not included in this study. A competent researcher measured the height, weight, blood pressure (measured seated with an electronic automatic sphygmomanometer) and waist and hip circumferences. Fat mass was assessed using a body composition monitor (Tanita MC-780MA P, Tanita Europe BV, Manchester, UK). Blood was taken after overnight fasting and serum glucose, triglycerides and low-density lipoprotein (LDL) levels measured using standard biochemistry protocols. Insulin was measured through ELISA (Crystal Chem, Zaandam, Netherlands). Platelets were washed and immunoblotting performed as above. Loading control GAPDH was used to normalize levels of PDI and Nox-1 to protein loading in each well.

3.8.14. Statistical analysis

Statistical analyses were performed on GraphPad Prism 8.0 software (GraphPad Software, San Diego, USA). Bar graphs and tables express mean ± SEM. Sample size varied from 4-6 independent repeats for *in vitro* experiments and between 6 and 8 for tail bleeding experiments. Outliers were determined and excluded by ROUT test. Due to sample size, data was considered of normal distribution. For *in vitro* experiments using inhibitors, statistical analysis was performed through paired one-way ANOVA and Tukey as post-test, whereas for *in vivo* experiments using Nox-1$^{-/-}$ mice, these were analysed through two-way ANOVA and Sidak's multiple comparisons test.

For population study, 137 out of 143 individuals were included in the analysis due to occasional missing values. To assess the possible correlation of platelet Nox-1 and PDI to risk factors for metabolic syndrome, multiple linear regression models were performed using platelet protein expression as the dependent variable and a set of independent variables: BMI, waist/hip ratio, % of fat, fasting glycaemia, fasting insulinaemia, fasting triglyceridaemia, fasting LDL cholesterol levels, systolic blood pressure and MPV. The beta coefficient of each variable on the final model is presented.

3.10 References

Alberti, K.G., Eckel, R.H., Grundy, S.M., et al. (2009). Harmonizing the metabolic syndrome: a joint interim statement of the International Diabetes Federation Task Force on Epidemiology and Prevention; National Heart, Lung, and Blood Institute; American Heart Association; World Heart Federation; International Atherosclerosis Society; and International Association for the Study of Obesity. *Circulation* 120**,** 1640-1645.

Barale, C., and Russo, I. (2020). Influence of Cardiometabolic Risk Factors on Platelet Function. *Int J Mol Sci* 21.

Bayraktutan, U., Blayney, L., and Shah, A.M. (2000). Molecular characterization and localization of the NAD(P)H oxidase components gp91-phox and p22-phox in endothelial cells. *Arterioscler Thromb Vasc Biol* 20**,** 1903-1911.

Begonja, A.J., Gambaryan, S., Geiger, J., Aktas, B., Pozgajova, M., Nieswandt, B., and Walter, U. (2005). Platelet NAD(P)H-oxidase-generated ROS production regulates alphaIIbbeta3-integrin activation independent of the NO/cGMP pathway. *Blood* 106**,** 2757-2760.

Burgess, J.K., Hotchkiss, K.A., Suter, C., Dudman, N.P., Szollosi, J., Chesterman, C.N., Chong, B.H., and Hogg, P.J. (2000). Physical proximity and functional association of glycoprotein 1balpha and protein-disulfide isomerase on the platelet plasma membrane. *J Biol Chem* 275**,** 9758-9766.

Bye, A.P., Unsworth, A.J., Desborough, M.J., et al. (2017). Severe platelet dysfunction in NHL patients receiving ibrutinib is absent in patients receiving acalabrutinib. *Blood Adv* 1**,** 2610-2623.

Chen, K., Detwiler, T.C., and Essex, D.W. (1995). Characterization of protein disulphide isomerase released from activated platelets. *Br J Haematol* 90**,** 425-431.

Cho, J., Kennedy, D.R., Lin, L., Huang, M., Merrill-Skoloff, G., Furie, B.C., and Furie, B. (2012). Protein disulfide isomerase capture during thrombus formation in vivo depends on the presence of beta3 integrins. *Blood* 120**,** 647-655.

Coban, E., Ozdogan, M., Yazicioglu, G., and Akcit, F. (2005). The mean platelet volume in patients with obesity. *Int J Clin Pract* 59**,** 981-982.

Crescente, M., Pluthero, F.G., Li, L., et al. (2016). Intracellular Trafficking, Localization, and Mobilization of Platelet-Borne Thiol Isomerases. *Arterioscler Thromb Vasc Biol* 36**,** 1164-1173.

Delaney, M.K., Kim, K., Estevez, B., Xu, Z., Stojanovic-Terpo, A., Shen, B., Ushio-Fukai, M., Cho, J., and Du, X. (2016). Differential Roles of the NADPH-Oxidase 1 and 2 in Platelet Activation and Thrombosis. *Arterioscler Thromb Vasc Biol* 36**,** 846-854.

Dutting, S., Bender, M., and Nieswandt, B. (2012). Platelet GPVI: a target for antithrombotic therapy?! *Trends Pharmacol Sci* 33**,** 583-590.

El Benna, J., Han, J., Park, J.W., Schmid, E., Ulevitch, R.J., and Babior, B.M. (1996). Activation of p38 in stimulated human neutrophils: phosphorylation of the oxidase component p47phox by p38 and ERK but not by JNK. *Arch Biochem Biophys* 334**,** 395-400.

Fehr, S., Unger, A., Schaeffeler, E., Herrmann, S., Laufer, S., Schwab, M., and Albrecht, W. (2015). Impact of p38 MAP Kinase Inhibitors on LPS-Induced Release of TNF-alpha in Whole Blood and Primary Cells from Different Species. *Cell Physiol Biochem* 36**,** 2237-2249.

Fernandes, D.C., Manoel, A.H., Wosniak, J., Jr., and Laurindo, F.R. (2009). Protein disulfide isomerase overexpression in vascular smooth muscle cells induces spontaneous preemptive NADPH oxidase activation and Nox1 mRNA expression: effects of nitrosothiol exposure. *Arch Biochem Biophys* 484**,** 197-204.

Gaspar, R.S., Da Silva, S.A., Stapleton, J., et al. (2019). Myricetin, the Main Flavonoid in Syzygium cumini Leaf, Is a Novel Inhibitor of Platelet Thiol Isomerases PDI and ERp5. *Front Pharmacol* 10**,** 1678.

Gaspar, R.S., Trostchansky, A., and Paes, A.M. (2016). Potential Role of Protein Disulfide Isomerase in Metabolic Syndrome-Derived Platelet Hyperactivity. *Oxid Med Cell Longev* 2016**,** 2423547.

Gavazzi, G., Banfi, B., Deffert, C., Fiette, L., Schappi, M., Herrmann, F., and Krause, K.H. (2006). Decreased blood pressure in NOX1-deficient mice. *FEBS Lett* 580**,** 497-504.

Gianni, D., Taulet, N., Zhang, H., et al. (2010). A novel and specific NADPH oxidase-1 (Nox1) small-molecule inhibitor blocks the formation of functional invadopodia in human colon cancer cells. *ACS Chem Biol* 5**,** 981-993.

Gimenez, M., Verissimo-Filho, S., Wittig, I., et al. (2019). Redox Activation of Nox1 (NADPH Oxidase 1) Involves an Intermolecular Disulfide Bond Between Protein Disulfide Isomerase and p47(phox) in Vascular Smooth Muscle Cells. *Arterioscler Thromb Vasc Biol* 39**,** 224-236.

Gray, S.P., Di Marco, E., Okabe, J., et al. (2013). NADPH oxidase 1 plays a key role in diabetes mellitus-accelerated atherosclerosis. *Circulation* 127**,** 1888-1902.

Griendling, K.K., Minieri, C.A., Ollerenshaw, J.D., and Alexander, R.W. (1994). Angiotensin II stimulates NADH and NADPH oxidase activity in cultured vascular smooth muscle cells. *Circ Res* 74**,** 1141-1148.

Guina, T., Deiana, M., Calfapietra, S., et al. (2015). The role of p38 MAPK in the induction of intestinal inflammation by dietary oxysterols: modulation by wine phenolics. *Food Funct* 6**,** 1218-1228.

Kim, K., Hahm, E., Li, J., Holbrook, L.M., Sasikumar, P., Stanley, R.G., Ushio-Fukai, M., Gibbins, J.M., and Cho, J. (2013). Platelet protein disulfide isomerase is required for thrombus formation but not for hemostasis in mice. *Blood* 122**,** 1052-1061.

Lahav, J., Wijnen, E.M., Hess, O., Hamaia, S.W., Griffiths, D., Makris, M., Knight, C.G., Essex, D.W., and Farndale, R.W. (2003). Enzymatically catalyzed disulfide exchange is required for platelet adhesion to collagen via integrin alpha2beta1. *Blood* 102**,** 2085-2092.

Laufer, S., Thuma, S., Peifer, C., Greim, C., Herweh, Y., Albrecht, A., and Dehner, F. (2005). An immunosorbent, nonradioactive p38 MAP kinase assay comparable to standard radioactive liquid-phase assays. *Anal Biochem* 344**,** 135-137.

Lopes Pires, M.E., Antunes Naime, A.C., Oliveira, J.G.F., Anhe, G.F., Garraud, O., Cognasse, F., Antunes, E., and Marcondes, S. (2019). Signalling

pathways involved in p47(phox) -dependent reactive oxygen species in platelets of endotoxemic rats. *Basic Clin Pharmacol Toxicol* 124**,** 394-403.

Lu, W.J., Li, J.Y., Chen, R.J., Huang, L.T., Lee, T.Y., and Lin, K.H. (2019). VAS2870 and VAS3947 attenuate platelet activation and thrombus formation via a NOX-independent pathway downstream of PKC. *Sci Rep* 9**,** 18852.

Matsumoto, M., Katsuyama, M., Iwata, K., Ibi, M., Zhang, J., Zhu, K., Nauseef, W.M., and Yabe-Nishimura, C. (2014). Characterization of N-glycosylation sites on the extracellular domain of NOX1/NADPH oxidase. *Free Radic Biol Med* 68**,** 196-204.

Qiao, J., Arthur, J.F., Gardiner, E.E., Andrews, R.K., Zeng, L., and Xu, K. (2018). Regulation of platelet activation and thrombus formation by reactive oxygen species. *Redox Biol* 14**,** 126-130.

Qiu, S., Mintz, J.D., Salet, C.D., et al. (2014). Increasing muscle mass improves vascular function in obese (db/db) mice. *J Am Heart Assoc* 3**,** e000854.

Raturi, A., and Mutus, B. (2007). Characterization of redox state and reductase activity of protein disulfide isomerase under different redox environments using a sensitive fluorescent assay. *Free Radic Biol Med* 43**,** 62-70.

Roberts, C.K., and Sindhu, K.K. (2009). Oxidative stress and metabolic syndrome. *Life Sci* 84**,** 705-712.

Saklatvala, J., Rawlinson, L., Waller, R.J., Sarsfield, S., Lee, J.C., Morton, L.F., Barnes, M.J., and Farndale, R.W. (1996). Role for p38 mitogen-activated protein kinase in platelet aggregation caused by collagen or a thromboxane analogue. *J Biol Chem* 271**,** 6586-6589.

Schwaller, M., Wilkinson, B., and Gilbert, H.F. (2003). Reduction-reoxidation cycles contribute to catalysis of disulfide isomerization by protein-disulfide isomerase. *J Biol Chem* 278**,** 7154-7159.

Seno, T., Inoue, N., Gao, D., et al. (2001). Involvement of NADH/NADPH oxidase in human platelet ROS production. *Thromb Res* 103**,** 399-409.

Sousa, H.R., Gaspar, R.S., Sena, E.M., et al. (2017). Novel antiplatelet role for a protein disulfide isomerase-targeted peptide: evidence of covalent binding to the C-terminal CGHC redox motif. *J Thromb Haemost* 15**,** 774-784.

Vara, D., Campanella, M., and Pula, G. (2013). The novel NOX inhibitor 2-acetylphenothiazine impairs collagen-dependent thrombus formation in a GPVI-dependent manner. *Br J Pharmacol* 168**,** 212-224.

Vara, D., Cifuentes-Pagano, E., Pagano, P.J., and Pula, G. (2019). A novel combinatorial technique for simultaneous quantification of oxygen radicals and aggregation reveals unexpected redox patterns in the activation of platelets by different physiopathological stimuli. *Haematologica* 104**,** 1879-1891.

Vara, D., Tarafdar, A., Celikag, M., et al. NADPH oxidase 1 is a novel pharmacological target for the development of an antiplatelet drug without bleeding side effects. *The FASEB Journal*.

Zhu, K., Kakehi, T., Matsumoto, M., et al. (2015). NADPH oxidase NOX1 is involved in activation of protein kinase C and premature senescence in early stage diabetic kidney. *Free Radic Biol Med* 83**,** 21-30.

Chapter 4

Maternal obesity alters platelet function in obese offspring

In **Chapters 2 and 3**, I have demonstrated the relevance of Nox-1 and PDI to platelets, first by describing a new PDI inhibitor, myricetin, then by showing the functional association of these enzymes in healthy platelets. Moreover, PDI and Nox-1 were correlated with components of MetS, thus suggesting possible pathophysiological relevance of these proteins to the platelet hyperactivation described for MetS patients.

Meanwhile, as described in the Introduction (**Chapter 1, section 1.7)** platelets are thought to be hyperactive in MetS, whilst MetS itself is a multifactorial disorder. One aspect of this syndrome is its interdependence with environmental insults *in utero* or during early childhood. My background working in the DOHaD field, coupled with current interests in platelet redox physiology, made me realize there were no studies assessing whether platelets could be programmed by maternal insults. Conversations held with Jon and Craig (my co-supervisor) led to Dr Dyan Sellayah, who was carrying out an ambitious project investigating how maternal obesity would affect adipocyte function in the offspring. Coincidentally, Dyan was also part of my assessing committee for the PhD. Craig and Dyan put together a project to address whether platelet function of the offspring would be affected by maternal obesity, and that was when I was invited to take part in this study.

Here I have shown that offspring born to dams fed a high-fat diet displayed enlarged and more reactive platelets. This was potentiated if offspring also received a high-fat diet. This seems to be a 'double-hit' effect, in which the insult (high-fat diet ingestion) in both dams and offspring has an additive effect for the overall phenotype of platelet hyperactivation. Platelets from these animals were larger, more active both at basal and when

stimulated with different agonists, with decreased expression of collagen receptors and increased phosphorylation of key processes downstream of GPVI. Likewise, platelets from these animals exhibited increased oxidative stress. Altogether, these data provide pathophysiological insights on previous observations in humans showing increased cardiovascular events in offspring born from obese mothers, since platelet function is a key driver of thrombosis. Moreover this study adds yet another layer of evidence to the deleterious effects of maternal obesity to the cardiovascular health of the offspring.

For this work I have contributed with the design, collection and analysis of data as well as drafting the manuscript. This was a joint effort from various individuals in the lab and from MRC Harwell and without them this would not be possible. For these reasons, it is estimated I have contributed to over 70% of all effort put into this paper.

The paper in its current form is under review at *Arteriosclerosis Thrombosis and Vascular Biology (ATVB)*.

Maternal high-fat diet during pregnancy and lactation contributes to platelet hyperactivation in male mouse offspring.

Running title: Maternal high-fat diet alters platelet function in obese offspring.

Authorship

Renato S. Gaspar [a*], Amanda J. Unsworth [b], Alex Bye [a], Tanya Sage [a], Michelle Stewart [c], Sara Wells [c], Roger D. Cox [d], Jonathan M. Gibbins [a], Dyan Sellayah [a#], Craig Hughes [a#]

Affiliations

[a] Institute for Cardiovascular and Metabolic Research, School of Biological Sciences, University of Reading, Reading, UK.

[b] Department of Life Sciences, Faculty of Science and Engineering, John Dalton Building, Manchester Metropolitan University, Manchester, UK, M1 5GD

[c] MRC Harwell Institute, Mary Lyon Centre, Harwell Campus, Oxfordshire, OX11 0RD, UK.

[d] MRC Harwell Institute, Genetics of type 2 diabetes, Mammalian Genetics Unit, Harwell Campus, Oxfordshire, OX11 0RD, UK.

Joint senior authors

*** Corresponding author**

Renato Simões Gaspar, M.D.

Institute of Cardiovascular and Metabolic Research, School of Biological Sciences. University of Reading - Harborne Building, Reading, RG6 6AS, UK.

E-mail: renatosgaspar@gmail.com, phone: +44 11 8378 7047

Keywords: Platelet; Developmental Biology; Oxidative stress; Metabolic Syndrome; .

Subject terms: Developmental Biology, Metabolism, Oxidant Stress, Platelets, Pathophysiology.

Word count: 6,238

Number of Figures/Tables: 6 Figures, 2 Tables and 3 Supplementary Figures

TOC category: Basic

TOC subcategory: Thrombosis

4.1 Graphical Abstract

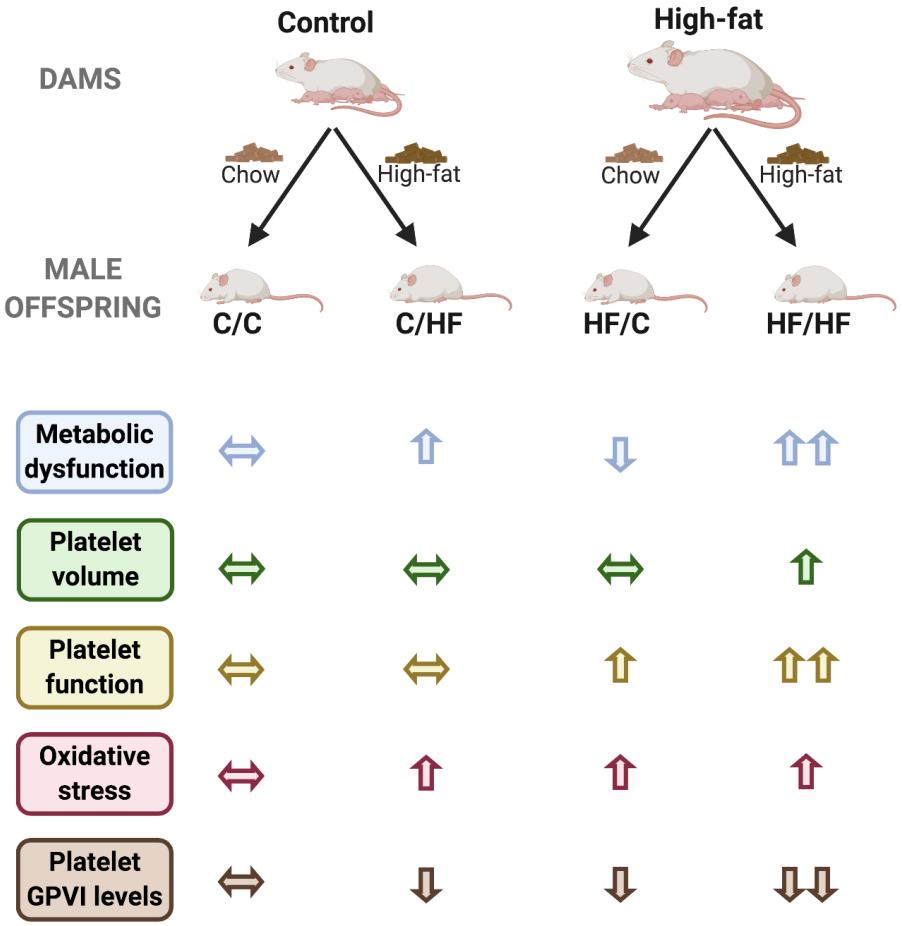

4.2 Abstract

Objective: Maternal over-nutrition increases the risk of diabetes and cardiovascular events in offspring. While prominent effects on cardiovascular health are observed, the impact of this on platelet physiology has not been studied. Here, we determined whether maternal high-fat diet (HF) ingestion can affect the platelet function in offspring.

Approach and Results: C57BL6/N mice dams were given a HF or control (C) diet for 8 weeks prior to and during pregnancy. Male offspring also received either C or HF diets for 26 weeks. Experimental groups were: C/C, dam and offspring fed chow; C/HF dam fed chow and offspring fed high-fat diet; HF/C and HF/HF. Phenotypic (body weight, % of body fat, etc) and metabolic (glycaemia, triglyceridemia, etc) tests were performed and blood collected for platelet studies. Compared to C/C, offspring HF groups were obese, with fat accumulation, hyperglycaemia and insulin resistance. Maternal obesity led to an overall effect of increased mean platelet volume and reactivity in offspring. Platelets from HF/HF mice were hyperreactive, displaying higher fibrinogen binding after stimulation with different agonists, and increased platelet adhesion and spreading on collagen. Both maternal and offspring HF groups presented decreased levels of collagen receptor GPVI with increased oxidative stress. HF/HF mice had increased phosphorylation of PKC substrates, total tyrosine and AKT at Ser473 compared to C/C.

Conclusions: Maternal HF diet ingestion programmes platelet hyperactivation in male mouse offspring. Since platelet function can be programmed by early developmental periods, it is possible to use this window of intervention to reduce the risk of thrombotic events.

LIST OF ABBREVIATIONS

AKT – Protein Kinase B

CRP - Collagen-related Peptide

DCFDA – 2′,7′-Dichlorofluorescin diacetate

FFA – Free Fatty Acids

GPVI – Glycoprotein VI

ipGTT – intraperitoneal Glucose Tolerance Test

NO – Nitric Oxide

PAPA-NONOate – Propylamine Propylamine NONOate

PKC – Protein Kinase C

PRP - Platelet-Rich Plasma

RER – Respiratory Exchange Rate

ROS – Reactive Oxygen Species

VASP – Vasodilator-Stimulated Phospho-protein

WB – Whole blood

WP - Washed Platelets

4.3. Introduction

The concept that the *in utero* environment impacts long-term metabolic health was first introduced in the late 1980s by Prof David Barker at the University of Southampton (Barker and Osmond, 1986). Analysing data from large cohort studies, he noted that infants of low birth weight (a proxy for *in utero* malnutrition), had increased risk of developing cardiovascular disease and dying of acute thrombotic events (such as stroke and myocardial infarction) in adulthood (Barker et al., 1993;Osmond et al., 1993). This concept of developmental programming of cardiovascular disease has since been expanded to include maternal over-nutrition, which is more reflective of Western lifestyles. Both epidemiological and animal studies have established unequivocally that maternal diabetes, obesity or maternal high-fat (HF) diet during pregnancy is associated with increased susceptibility to cardiovascular disease in offspring (reviewed by Williams et al (Williams et al., 2014)), although the precise mechanisms underlying this observation remain to be established.

A key component of cardiovascular disease pathophysiology is platelet reactivity, which has been somewhat neglected in the developmental programming field. Platelets contribute to the initiation and development of atherosclerosis through their interaction with activated endothelium and inflammatory cells (Massberg et al., 2002;Huo et al., 2003;Lindemann et al., 2007). From a clinical perspective however, their major role is at the later stages of disease when platelets can form unwanted thrombi on atherosclerotic plaques, or when unstable plaques rupture. These acute thrombotic events cause stenosis or occlusion of vessels supplying the heart

or brain resulting in myocardial infarction (MI) or stroke respectively (for review see (Schafer and Bauersachs, 2008)). To this end, a recent cohort study has documented that increased platelet activation in participants before the onset of cardiovascular disease, was a major risk factor and predictor for myocardial infarction and stroke events later in life (Puurunen et al., 2018).

Various components of the cardiovascular system of offspring appear to be negatively affected by *in utero* over-nutrition. Studies in sheep and rodents documented that maternal diet-induced obesity during pregnancy led to endothelial dysfunction, cardiac remodelling, cardiac inflammation and fibrosis, cardiac hypertrophy and impaired cardiac contractility in offspring (Samuelsson et al., 2008;Huang et al., 2010;Fan et al., 2011;Fan et al., 2013). No measurement of platelet function was reported in those studies. The concept that cardiovascular disease in later life might be programmed during development by maternal over-nutrition is particularly alarming given that the UK has the highest rate of obesity amongst women of reproductive age in Europe (Poston et al., 2011). Likewise, maternal diabetes during pregnancy increased early onset of cardiovascular disease in offspring (Yu et al., 2019).

Despite strong evidence for developmental programming of cardiovascular disease and the key role of platelets on cardiovascular disease pathophysiology, there is currently no literature assessing the effects of maternal metabolic dysfunction on the platelet reactivity of the offspring. Using a mouse model, we set out to examine the effects of maternal HF diet ingestion on the platelet function of 30-week-old male offspring mice. Our data showed an overall effect of increased platelet reactivity on offspring

born to HF dams and a worsened phenotype if offspring were also fed HF. This suggests 1) that platelet function is programmed by maternal obesity and 2) that there is a 'double-hit' effect in which metabolic dysfunction in both mother and offspring potentiate platelet reactivity. This is the first study to describe the deleterious impact of maternal HF ingestion on the platelet reactivity of the offspring and offer a possible pathophysiological mechanism to previous reports showing increased cardiovascular events related to maternal metabolic dysfunction.

4.4 Material and Methods

4.4.1. Reagents

Prostacyclin (PGI_2), Adenosine Diphosphate (ADP), thrombin and 2′,7′-Dichlorofluorescin diacetate (DCFDA) were purchased from Sigma-Aldrich (Dorset, UK). PAPA-NONOate was purchased from Tocris (Abingdon, UK). FITC-conjugated fibrinogen was purchased from Agilent (Stockport, UK). Collagen was purchased from Nycomed (Munich, Germany) and Collagen-Related Peptide (CRP) was obtained from Prof Richard Farndale (University of Cambridge, Cambridge, UK). Alexa-488 conjugated phalloidin was purchased from Life Technologies (Paisley, UK). Rat anti-mouse GPVI, α2 integrin, GpIbα and appropriate IgG controls were purchased from Emfret (Emfret Analytics GmbH & Co, Eibelstadt, Germany). Goat anti-mouse CD36 was purchased from R&D Systems (R&D Systems Inc, Abingdon, UK). Anti-phospho Tyr 4G10 antibody was purchased from Merck Millipore (Watford, UK). Polyclonal goat anti-β-Actin antibody was purchased from Abcam (Cambridge, UK). Anti-phospho-vasodilator-stimulated phospho-protein (VASP) Ser239 and anti-protein kinase B (Akt) Ser473 were purchased from Cell Signalling (Hitchin, UK) and Alexa-488 and Alexa-647-conjugated secondary antibodies were bought from Life Technologies (Paisley, UK).

4.4.2. Animal and experimental design

All animal studies were approved by the Medical Research Council Harwell Institute Animal Welfare and Ethical Review Board, and all procedures were carried out within project license restrictions (PPL 30/3146) under the UK

Animals (Scientific Procedures) Act 1986 and conform to the guidelines from Directive 2010/63/EU of the European Parliament on the protection of animals used for scientific purposes. Female C57BL6/N mice at 8 weeks old were fed either a control diet (C, 10% kCal fat) or a high-fat diet (HF, 60% kCal fat) for 6 weeks before pregnancy. They were then mated at 14 weeks of age with chow-fed males and maintained on their respective diets during pregnancy (3 weeks) and lactation (4 weeks), totalling 13 weeks of dietary intervention on the dams. Litter size was standardized to 6 pups per litter. Upon weaning at 4 weeks, male offspring were randomly assigned by a technician, a control or high-fat diet for 26 weeks. Therefore, there were 4 experimental groups: C-fed dam and C-fed offspring (C/C), C-fed dam and HF-fed offspring (C/HF), HF/C and HF/HF. The four offspring groups (HF/C, HF/HF, C/HF and C/C) were represented by 3-4 distinct litters and often more than one pup per litter was used to compose groups. There were 11 dams to derive the offspring groups. Throughout dietary intervention, mice were weighed weekly, metabolic cage analysis performed at 22 weeks whilst body composition and intraperitoneal glucose tolerance test (ipGTT) were measured at 26 weeks of age. At 30 weeks of age, blood was collected through retro-orbital sinus with mice under terminal anaesthesia, which consisted of inhalation of 5% isoflurane until full anaesthesia was achieved, determined by loss of pedal reflex. Death was confirmed by cessation of the circulation and neck dislocation. For serological analysis, blood was allowed to clot, then centrifuged at 3000 x g for 3 min and sera frozen at -80°C until analysis. For platelet studies, blood was collected in 1:9 v/v acid citrate dextrose (ACD: 2.5% sodium citrate, 2% D-glucose, and 1.5% citric acid) and

analysed after 1 hour of resting. A schematic diagram of the animal model can be found in Supplementary Figure 4.1.

4.4.3. Serological analyses and full blood count

All samples for serological analyses and full blood count were processed by the MRC Clinical Chemistry core facility, MRC Harwell Institute (Oxfordshire, UK) using an AU680 Clinical Chemistry Analyser (Beckman Coulter, High Wycombe, UK) and performed as per manufacturer (Cambridge Biomedical Research Centre, Cambridge, UK). Full blood count was determined using mice-specific settings on an Advia 2120 dedicated veterinary blood counter (Siemens Healthcare, Surrey, UK). TyG index was calculated as: Ln [triglyceridaemia (mg/dL) x glycaemia (mg/dL)]/2.

4.4.4. Body composition analysis

Body composition was measured at 26 weeks of age by nuclear magnetic resonance (EchoMRI™, Houston, Texas, USA), which determined total body fat, lean mass and free water in grams. The percentage of each component was then calculated based on the total body weight of the animal.

4.4.5. Intraperitoneal glucose tolerance test

Intraperitoneal glucose tolerance tests were performed at 26 weeks following a 16 hour fast. Specifically, fasted mice received an i.p. administration of 2g/kg glucose and blood sampled under a local anesthetic at 0 min (baseline), 15, 30, 60 and 120 min post glucose injection. Whole

blood glucose was measured using an AlphaTRAK meter and test strips (Abbott Animal Health, UK).

4.4.6. Indirect calorimetry

Indirect calorimetry was performed in 22 weeks old mice using a TSE PhenoMaster system (TSE Systems GmbH, Hamburg, Germany). Animals were individually placed in metabolic cages for 1 hour to acclimatize. Measurements started at 15:00 and finished at 11:00 of the next day. VO_2, VCO_2, respiratory exchange rate (RER), energy expenditure rate and locomotor activity were measured every 15 minutes under constant temperature of 20°C.

4.4.7. Platelet activation and membrane receptor studies

Blood was collected through retro-orbital sinus in 1:9 v/v ACD tubes and centrifuged at 203 x *g* for 8 minutes to separate the platelet-rich plasma (PRP). PRP was then incubated in a 96-well plate with or without NO donor PAPA-NONOate at 100 μM for 10 minutes prior to addition of agonists ADP, CRP or thrombin at specified concentrations. FITC-labelled fibrinogen was incubated for 30 minutes in the dark followed by dilution (25X) with Tyrodes-HEPES buffer (134 mM NaCl, 20 mM N-2-hydroxyethylpiperazine-N′-2-ethanesulfonic acid, 12 mM $NaHCO_3$ 5 mM glucose, 0.34 mM Na_2HPO_4, 2.9 mM KCl and 1 mM $MgCl_2$, pH 7.3). In order to measure platelet membrane receptor expression, whole blood was incubated with antibodies specific to membrane receptors or control IgG at the concentrations specified by the manufacturer for 30 minutes in the dark. In both assays, events were

acquired using a BD Accuri C6 Plus flow cytometer (BD Biosciences, Oxford, UK) and platelets gated by forward and side scatter.

4.4.8. Platelet spreading

PRP was supplemented with 1.25 μg/mL PGI_2 and further centrifuged at 1,028 x g for 5 minutes and washed platelets (WP) pellet resuspended in Tyrodes-HEPES buffer. WP (2 x 10^7 platelets/mL) were added to a coverslip coated with 100 μg/mL collagen and left to adhere for 45 minutes at 37°C. Non-adherent platelets were washed off with PBS, and adherent platelets fixed with 0.2% paraformaldehyde, permeabilized with Triton-X 0.01% v/v for 10 minutes and subsequently stained with Alexa Fluor 488-conjugated phalloidin (1:1000 v/v) for 1 hour in the dark at room temperature. Images were acquired using a Nikon A1-R Confocal microscope (Nikon Instruments Europe BV, Amsterdam, Netherlands).

4.4.9. Reactive oxygen species (ROS) measurement

Whole blood (WB) was incubated with 20 μM ROS-detecting fluorescent dye DCFDA for 30 minutes in the dark and events acquired using a BD Accuri C6 Plus flow cytometer. Platelet and red blood cells populations were separated by forward and side scatter.

4.4.10. Immunoblotting

WP (2 x 10^8 platelets/mL) incubated with or without PAPA-NONOate at 100 μM for 10 minutes prior to addition of 1μg/mL CRP. Reduced Laemmli buffer was added 90 seconds after CRP addition to lyse platelets and stop

reaction. This solution was heated for 10 minutes and processed exactly as previously described (Gaspar et al., 2019).

4.4.11. Statistical analysis

Statistical analyses were run in GraphPad Prism 8.0 software (GraphPad Software, San Diego, USA). Quantitative results in figures and tables were expressed as mean ± SD and individual values. Overall, n=17 for C/C, n=10 for C/HF, n=16 for HF/C and n=13 for HF/HF. However, n number varied across assays. For metabolic and phenotypic studies n=10-17 per group except for indirect calorimetry experiments, which had n=3-8 due to low availability of metabolic cages and time-constraints. Functional platelet studies had n=5-13 and immunoblots had n=3-7 due to high blood volume needed per animal to perform all experiments. Outliers were identified and excluded using ROUT method. Data were considered of normal distribution due to sample size. Equal variance (sphericity) was not assumed since samples were independent and analysed through unpaired two-way ANOVA for bar graphs with Dunnett's post-test to test differences *vs* C/C. Overall effect of maternal, offspring or the interaction of these are presented and interpreted throughout text. Data in XY graphs were assessed by repeated measures two-way ANOVA and Dunnett's as post-test with level of significance of 5%.

4.5 Results

4.5.1. Maternal high-fat diet programmed phenotypic and metabolic parameters differently in lean and obese offspring

Several aspects of the metabolic phenotype as well as serum biochemistry were assessed in 30 weeks old male mice (Table 4.1). It was evident that both offspring HF groups presented significant increases in body weight, fat mass, total cholesterol, fasting glucose, TyG Index which is a surrogate for insulin resistance, as well as HDL and LDL levels when compared to offspring C groups. Interestingly, HF/C animals were lighter and had increased lean mass as percentage of body weight when compared to C/C. HF/HF, but not C/HF, showed increased serum levels of triglycerides when compared to C/C group. Lack of interaction between maternal and offspring diet indicates an additive effect of these dietary interventions leads to elevated serum triglyceride levels.

Table 4.1. Maternal and offspring high-fat diet have additive effects on triglycerides and free fatty acid levels.

	C/C n=17	C/HF n=10	HF/C n=16	HF/HF n=13	MD	OD	MD x OD
					p-values		
Final weight (g)	35.51 ±4.299	**51.21 ±3.713***	**32.17 ±4.138***	**49.96 ±2.436***	**0.0312**	**<0.0001**	0.3205
Lean weight (%)	72.34 ±7.028	**57.58 ±4.045***	**79.07 ±7.378***	**56.98 ±4.590***	0.0808	**<0.0001**	**0.0380**
Fat mass (%)	28.62 ±11.43	**48.01 ±3.738***	26.55 ±6.789	**48.02 ±4.339***	0.6296	**<0.0001**	0.6253
Total Cholesterol (mmol/L)	3.991 ±1.035	**6.809 ±1.732***	3.653 ±0.5534	**6.928 ±0.8321***	0.7154	**<0.0001**	0.4472
HDL (mmol/L)	2.439 ±0.6491	**3.839 ±0.8223***	2.254 ±0.3639	**3.858 ±0.3213***	0.6031	**<0.0001**	0.5217
LDL (mmol/L)	1.12 ±0.2372	**1.97 ±0.5949***	0.8256 ±0.2875	**1.768 ±0.4475***	**0.0240**	**<0.0001**	0.6650
Triglycerides (mmol/L)	1.22 ±0.2862	1.418 ±0.3338	1.283 ±0.4205	**1.661 ±0.6094***	0.1940	**0.0166**	0.4432
Free fatty acids (mmol/L)	0.6994 ±0.1426	**0.881 ±0.1246***	0.7888 ±0.1991	**0.9338 ±0.2455***	0.1657	**0.0021**	0.7197
Fasting glucose (mmol/L)	7.435 ±1.362	**11.21 ±1.176***	6.613 ±1.027	**9.717± 2.041***	**0.0049**	**<0.0001**	0.3985
TyG index	8.842 ±0.3315	**9.419 ±0.2772***	8.756 ±0.3506	**9.378 ±0.3953***	0.5063	**<0.0001**	0.8101

Data presented as mean ± SD. N= 10-17 animals for each group. Groups were analyzed by Two-way ANOVA and Dunnet post-test for multiple comparisons *vs* C/C. * p<0.05 *vs* C/C.

C/C. dam and offspring fed chow; C/HF. dam fed chow and offspring fed high-fat diet; HF/C dam fed high-fat diet and offspring fed chow; HF/HF dam and offspring fed high fat diet. MD: Maternal diet. OD: Offspring diet.

All groups were also assessed for their body weight growth, glucose homeostasis and indirect calorimetry to further characterize the model (Figure 4.1). Both HF offspring groups presented increased body weight compared to C/C. HF/HF animals were consistently heavier than C/C starting at 7 weeks ($p<0.01$), whereas C/HF started at 8 weeks of age (Figure 4.1A). Of note, HF/C mice were lighter than C/C over the last 4 weeks of the study (Figure 4.1A), in agreement with the increased lean weight described in Table 4.1. To assess glucose homeostasis of these animals, ipGTT was performed and evidenced that both offspring HF groups were glucose intolerant, whereas HF/C showed improved glucose homeostasis compared to C/C (Figure 4.1B). Overall, both HF/C and HF/HF presented severe metabolic dysfunction since these mice were obese, had increased accumulated fat, were insulin resistant and glucose intolerant.

Indirect calorimetry was measured from individual animals placed in a metabolic cage. Due to restricted cage availability, sample size was reduced. Offspring HF groups showed a lower RER coupled with decreased energy expenditure, suggesting increased burning of fat and diminished metabolic activity respectively (Figure 4.1C – G), which would contribute to the other metabolic dysfunctions present in these animals. Surprisingly, HF/C also showed lower RER compared to C/C, though not as pronounced as offspring HF groups. Total ambulatory activity was not changed across groups, likely due to the high variability of the assay (Figure 4.1H). In summary, maternal HF programmed the offspring differently, depending on the diet given to the offspring: if given a high-fat diet, offspring presented more severe metabolic dysfunctions in terms of triglycerides levels; if given standard chow,

offspring burned more fat, were lighter and had improved glucose homeostasis.

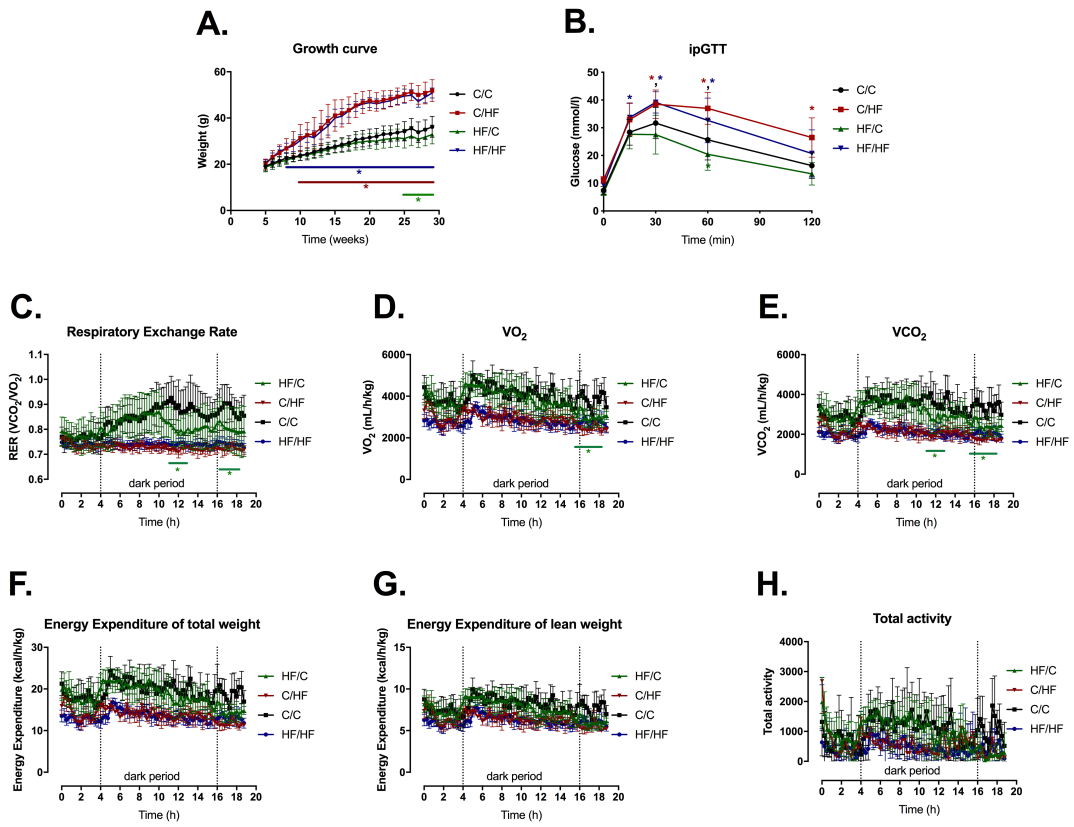

Figure 4.1. Metabolic effects of maternal obesity depend on offspring diet. (A) Growth curve with weekly weight measures. (B) Intraperitoneal glucose tolerance test (ipGTT) with glucose measured at 0, 15, 30, 60 and 120 min after glucose injection. (C) Respiratory exchange rate (RER), (D) maximum rate of oxygen consumption (VO_2), (E) maximum rate of carbon dioxide consumption (VCO_2), (F) energy expenditure of total weight, (G) energy expenditure of lean weight and (H) total ambulatory activity were measured in individual mice placed in a metabolic cage for 20 hours. C/C, dam and offspring fed chow; C/HF dam fed chow and offspring fed high-fat diet; HF/C dam fed high-fat diet and offspring fed chow; HF/HF dam and offspring fed high-fat diet. For (A) and (B), n=10-17 mice per group. For (C–H), n=4 for C/C, n=3 for C/HF, n=8 for HF/C and n=8 for HF/HF. Data on graphs show mean ± SD. Data analysed by repeated measures two-way ANOVA with Dunnett's multiple comparisons test *vs* C/C. *p<0.05 and colour of stars indicate significance of the group against C/C.

4.5.2. Maternal and offspring high-fat diet ingestion led to increased platelet volume

It has been shown that increased mean platelet volume (MPV) is correlated with cardiovascular events (Chu et al., 2010), therefore full blood count was performed (Table 4.2). There was a 30% decrease in total leukocytes on the HF/C group compared to C/C, which suggests leukocytes could be programmed by maternal high-fat diet ingestion, although there was no overall effect (two-way ANOVA, p=0.06). HF/HF animals had a significant 0.7 fL increase in MPV when compared to C/C. Indeed, MPV was significantly increased by maternal (two-way ANOVA, maternal diet effect p=0.01) and offspring (p=0.02) high-fat diet. The effect of maternal and offspring high-fat diet were independent since there was no interaction, indicating an additive effect between maternal and offspring diet on platelet size.

Table 4.2 Maternal and offspring high-fat diet leads to increased platelet volume.

	C/C n=17	C/HF n=10	HF/C n=16	HF/HF n=13	MD	OD	MD x OD
					P-values		
Red blood cells							
Hematocrit (L/L)	0.483 ±0.017	0.478 ±0.040	0.500 ±0.020	0.492 ±0.047	0.089	0.494	0.892
RBC (x10^6 cells/µL)	9.382 ±0.491	9.462 ±0.633	9.715 ±0.392	9.612 ±1.095	0.219	0.953	0.639
Hbg (g/dL)	13.81 ±0.487	12.78 ±1.925	13.69 ±0.680	13.41 ±1.377	0.450	0.056	0.266
MCV (fL)	51.05 ±1.161	51.24 ±1.413	51.39 ±1.611	51.12 ±1.180	0.781	0.923	0.541
MCH (pg)	14.38 ±0.683	**13.14 ±1.840***	13.95 ±0.903	14.08 ±0.735	0.389	0.064	**0.022**
MCHC (g/dL)	28.19 ±1.131	**25.94 ±2.742***	27.35 ±1.070	27.42 ±1.003	0.462	**0.013**	**0.009**
CHCM (g/dL)	26.29 ±0.848	**25.12 ±1.863***	25.73 ±0.947	25.63 ±0.637	0.931	**0.039**	0.080
RDW (%)	13.57 ±1.086	**15.29 ±2.687***	13.08 ±0.637	13.97 ±0.451	**0.019**	**0.001**	0.269
White blood cells							
Leukocytes (x10^3 cells/µL)	6.099 ±2.536	5.297 ±1.589	**4.322 ±1.457***	5.189 ±0.580	0.068	0.949	0.105
Neutrophils (x10^3 cells/µL)	0.590 ±0.221	0.524 ±0.188	0.534 ±0.221	0.503 ±0.0857	0.477	0.367	0.736
Neutrophils (%)	12.59 ±3.966	9.456 ±3.429	11.56 ±3.141	**8.946 ±1.799***	0.398	**0.002**	0.774

Lymphocytes (x10³ cells/µL)	4.086 ±1.071	4.256 ±1.213	3.673 ±1.406	4.853 ±1.119	0.784	**0.049**	0.137
Lymphocytes (%)	80.19 ±5.129	83.63 ±5.021	82.09 ±3.750	84.00 ±3.440	0.358	**0.034**	0.532
Monocytes (x10³ cells/µL)	0.19 ±0.072	0.167 ±0.088	**0.1013 ±0.043***	0.19 ±0.059	0.078	0.078	**0.003**
Monocytes (%)	3.194 ±0.863	3.18 ±1.538	2.294 ±0.921	3.354 ±1.116	0.224	0.082	0.075
Eosinophils (x10³ cells/µL)	0.103 ±0.051	0.095 ±0.054	0.138 ±0.114	0.096 ±0.039	0.372	0.220	0.402
Eosinophils (%)	1.813 ±1.063	1.82 ±0.921	2.619 ±1.506	1.754 ±0.913	0.250	0.184	0.177
Platelets							
Platelet count (x10³ cells/µL)	1530 ±341.7	1366 ±384.3	1468 ±466.2	1308 ±264.4	0.560	0.120	0.986
MPV (fL)	8.112 ±0.711	8.46 ±0.371	8.513 ±0.444	**8.8 ±0.378***	**0.011**	**0.029**	0.831
PDW (%)	48.04 ±3.707	49.71 ±2.823	48.00 ±2.369	**51.88 ±3.309***	0.231	**0.002**	0.216
PCT (%)	1.245 ±0.311	1.158 ±0.336	1.253 ±0.403	1.151 ±0.243	0.999	0.301	0.936

Data presented as mean ± SD. N= 10-17 animals for each group. Groups were analyzed by Two-way ANOVA and Dunnet post-test for multiple comparisons *vs* C/C. * $p<0.05$ *vs* C/C.

C/C. dam and offspring fed chow; C/HF. dam fed chow and offspring fed high-fat diet; HF/C dam fed high-fat diet and offspring fed chow; HF/HF dam and offspring fed high fat diet. MD: Maternal diet. OD: Offspring diet. RBC: red blood cells. Hbg: haemoglobin. MCV: mean corpuscular volume. MCH: mean corpuscular haemoglobin. MCHC: mean corpuscular hemoglobin concentration. CHCM: cellular hemoglobin concentration mean. RDW: red cell distribution width. MPV: mean platelet volume. PDW: platelet distribution width. PCT: plateletcrit.

4.5.3. Maternal high-fat diet ingestion increases offspring platelet adhesion and spreading to collagen

Upon vascular injury, platelets are exposed and adhere to collagen. Therefore, we assessed the ability of platelets from all groups to adhere and spread to immobilized collagen and undergo cytoskeletal reorganisation, referred to as spreading (Figure 4.2). When compared to C/C, platelets from HF/HF group exhibited a 9 and 1.5 fold increase in platelet adherence and spreading, respectively. This effect was not seen in C/HF, whilst there was an increase in adherence in the HF/C group. The overall effect of maternal high-fat diet ingestion led to increased adhesion (two-way ANOVA, $p<0.0001$) and spreading ($p=0.0012$) independent of offspring diet, since there was no interaction between maternal and offspring diet.

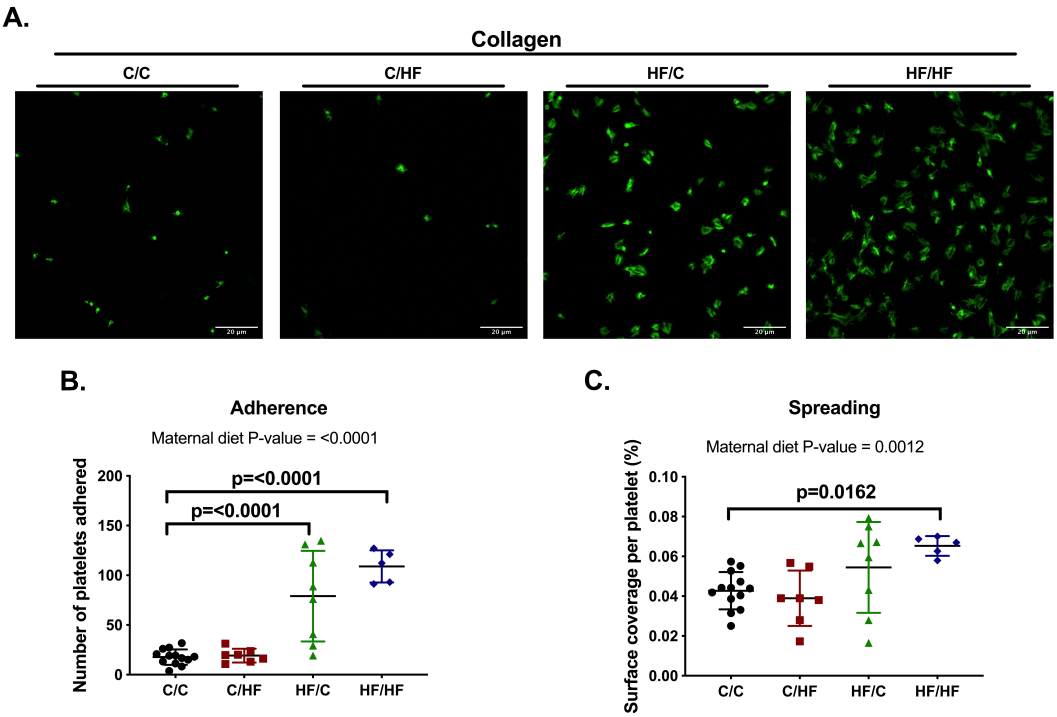

Figure 4.2. Maternal high-fat diet increased platelet spreading over collagen. WP (2 x 10^7 platelets/mL) was left to adhere to coverslips coated with collagen and platelets fluorescently labelled for visualization. (A) Representative images of platelet spreading of each group. (B) Quantification of platelet adherence as number of platelets per field. (C) Platelet spreading as the total fluorescence of the field divided by the number of platelets. C/C, dam and offspring fed chow; C/HF dam fed chow and offspring fed high-fat diet; HF/C dam fed high-fat diet and offspring fed chow; HF/HF dam and offspring fed high-fat diet. N=5-13 mice per group. Graphs show mean ± SD as well as individual values. Data analysed by two-way ANOVA with Dunnett's multiple comparisons test *vs* C/C. The overall effects of maternal and offspring diet are reported where significant.

4.5.4. High-fat diet ingestion in both offspring and dams let to platelet hyperactivity and decreased surface expression levels of collagen receptors

Given the severe metabolic dysfunction, increased adhesive potential and increased platelet size found in HF/HF animals, we assessed platelet activation by measuring fibrinogen binding to platelet integrin αIIbβ3 using FITC-conjugated fibrinogen (Figure 4.3). PRP was isolated from whole blood and stimulated with different concentrations of the platelet activators ADP, CRP (a GPVI collagen receptor agonist) or thrombin. Platelets of HF/HF animals bound to fibrinogen 3x more than C/C when stimulated with ADP and 2x more when stimulated with CRP (Figure 4.3A and B), however, for ADP there was an interaction between maternal and offspring diet. This indicates that the increase in fibrinogen binding seen in HF/HF is dependent on both maternal and offspring high-fat diet ingestion, thus not being an effect solely due to maternal diet. Interestingly, there was no increase when platelets were stimulated with thrombin (Figure 4.3C), suggesting that rises in fibrinogen binding are specific to some agonists and are unlikely to be due to increased MPV in HF/HF. The abovementioned effects were similar when different doses of agonists were used or when platelets were resting (Supplementary Figure 4.2).

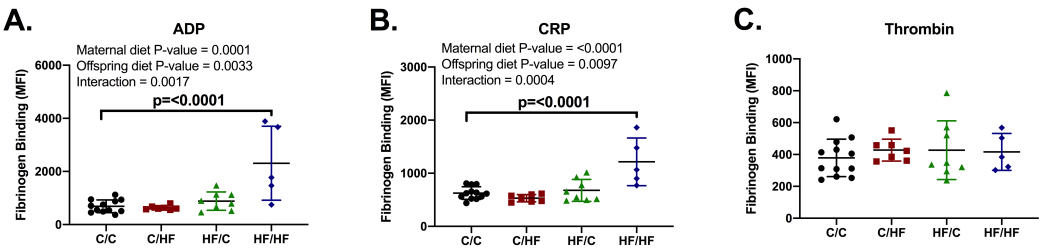

Figure 4.3. Maternal and offspring high-fat diet ingestion resulted in platelet hyperactivation. Platelet-rich plasma (PRP) was stimulated with 10 µM ADP (A), 3 µg/mL CRP (B) or 0.1 U/mL Thrombin (C) and FITC-conjugated fibrinogen binding measured through flow cytometry. C/C, dam and offspring fed chow; C/HF dam fed chow and offspring fed high-fat diet; HF/C dam fed high-fat diet and offspring fed chow; HF/HF dam and offspring fed high-fat diet. N=5-13 mice per group. Graphs show mean ± SD as well as individual values. Data analysed by two-way ANOVA with Dunnett's multiple comparisons test *vs* C/C. The overall effects of maternal and offspring diet are reported where significant.

Surface expression levels of key platelet receptors were measured through flow cytometry. Both offspring HF groups showed decreased levels of GPVI and integrin α2 compared to C/C (Figure 4.4A and B), indicating increased spreading on collagen and CRP-induced activation observed in HF/HF platelets was not due to upregulated GPVI surface expression. Interestingly, maternal obesity resulted in decreased expression levels of collagen receptors, suggesting possible epigenetic regulation. There were no differences between groups on surface levels of oxidized LDL receptor CD36 or von willebrand factor receptor CD42b (Figure 4.4C and D), despite overall effects of maternal and offspring diets.

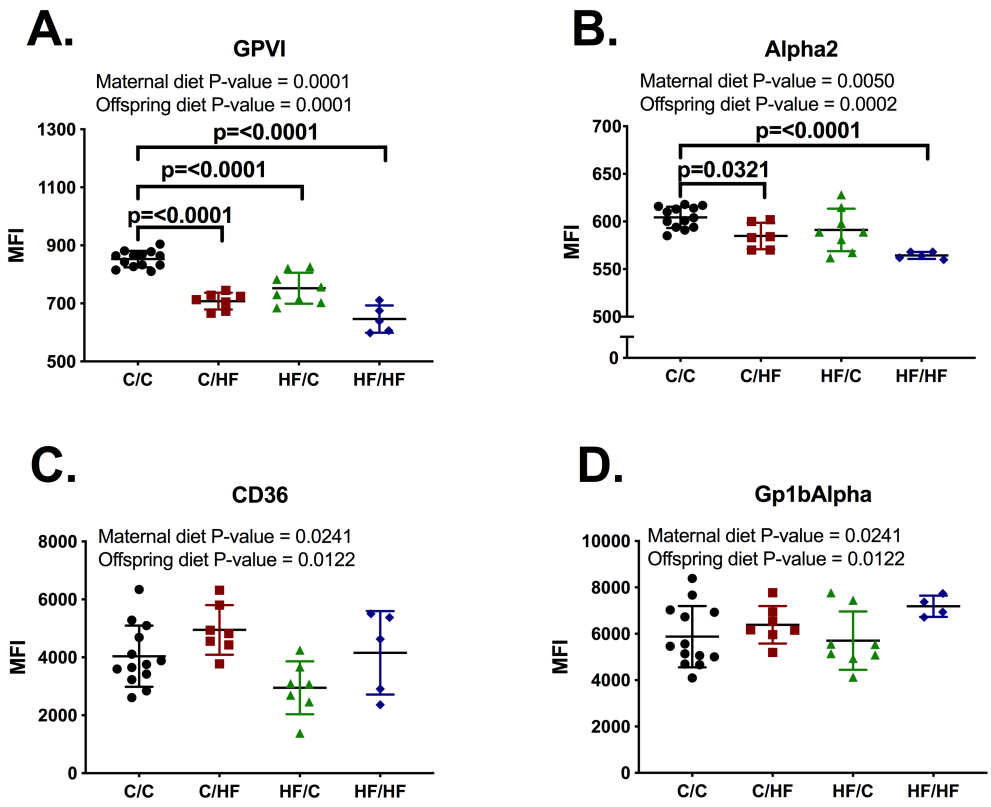

Figure 4.4. Maternal and offspring high-fat diet ingestion decreased surface expression levels of collagen receptors. Platelet-rich plasma (PRP) was incubated with antibodies for GPVI (A), α2 integrin (B), CD36 (C) and Gp1bα (D) receptors and measured using flow cytometry. C/C, dam and offspring fed chow; C/HF dam fed chow and offspring fed high-fat diet; HF/C dam fed high-fat diet and offspring fed chow; HF/HF dam and offspring fed high-fat diet. N=5-13 mice per group. Graphs show mean ± SD as well as individual values. Data analysed by two-way ANOVA with Dunnett's multiple comparisons test *vs* C/C. The overall effects of maternal and offspring diet are reported where significant.

4.5.5. Both maternal and offspring high-fat diet induce increased oxidative stress in whole blood

We measured unspecific ROS production in whole blood to test the hypothesis that oxidative stress, often associated with metabolic dysfunction, could contribute to the observed platelet hyperreactivity (Figures 2 and 3). Both maternal and offspring HF groups presented an increase in oxidative stress of ~100% in platelets and ~50% in red blood cells when compared to C/C. These effects were dependent on both maternal and offspring dietary intervention, since there was interaction of terms (Figure 4.5A and B). This increase in ROS may contribute to the increase platelet functional effects observed so far, although further experiments are needed to show a causal link.

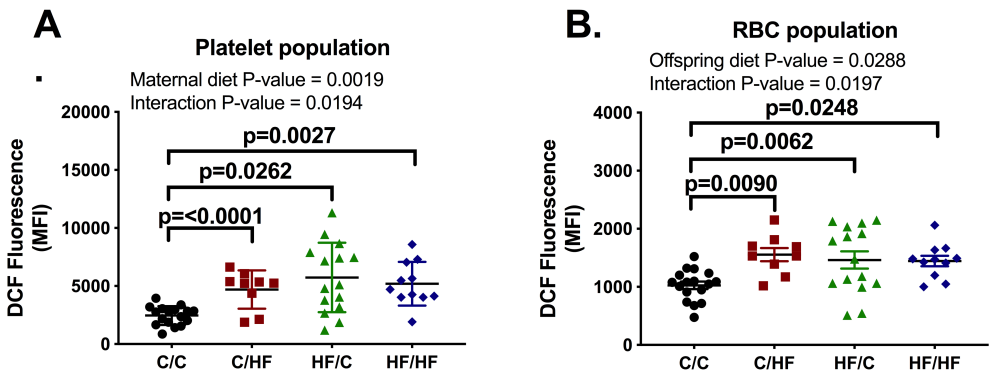

Figure 4.5. Maternal or offspring high-fat diet induced increased oxidative stress in whole blood. Whole blood was diluted 25 times with Tyrodes-HEPES buffer and incubated with 20 µM ROS-detecting fluorescent dye DCFDA. Events acquired using a flow cytometer and platelet (A) or red blood cells (RBC, B) populations separated by forward and side scatter. C/C, dam and offspring fed chow; C/HF dam fed chow and offspring fed high-fat diet; HF/C dam fed high-fat diet and offspring fed chow; HF/HF dam and offspring fed high-fat diet. N=10-17 mice per group. Graphs show mean ± SD as well as individual values. Data analysed by two-way ANOVA with Dunnett's multiple comparisons test *vs* C/C. The overall effects of maternal and offspring diet are reported where significant.

4.5.6. Increased signalling in platelets from HF/HF animals

Following the observation that GPVI levels were reduced, but GPVI-mediated platelet function was increased in HF-HF mice, we stimulated platelets with CRP for 90 seconds and performed immunoblots to characterize the effects on intracellular signalling downstream of GPVI (Figure 4.6). Compared to C/C, platelets from HF/HF animals presented increased Akt phosphorylation at Ser473 (Figure 4.6A), as well as increased tyrosine (4G10 antibody, Figure 4.6B) and PKC substrate phosphorylation (Figure 4.6C). Out of these, maternal diet led to increased Akt phosphorylation independent of offspring diet (two-way ANOVA, $p=0.02$), since there was no interaction. The responses to nitric oxide donor PAPA-NONOate were also assessed. VASP phosphorylation was unchanged across groups, although C/HF mice presented slightly increased PAPA-NONOate inhibition in ADP-stimulated platelets and slightly decreased inhibition in CRP-stimulated ones (Supplementary Figure 4.3). These data indicate that the hyperactivation of HF/HF platelets were associated to increased signalling downstream of GPVI.

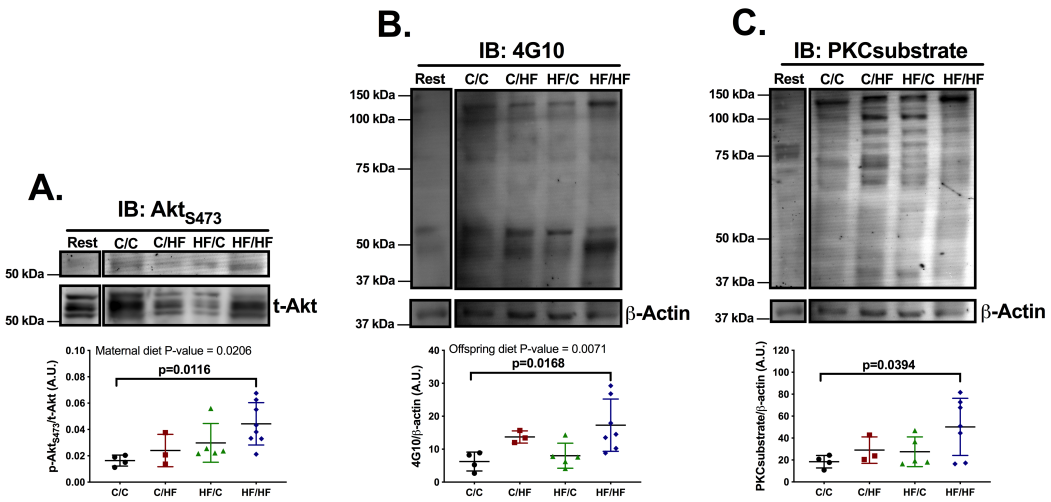

Figure 4.6. Maternal and offspring high-fat diet ingestion enhanced platelet signalling. Washed platelets (WP) were stimulated with CRP for 90 seconds and lysed. Representative immunoblot and summarized data are shown for phosphorylation of Akt at Ser473 (A), 4G10 total tyrosine phosphorylation (B) and PKC substrate serine phosphorylation (C). C/C, dam and offspring fed chow; C/HF dam fed chow and offspring fed high-fat diet; HF/C dam fed high-fat diet and offspring fed chow; HF/HF dam and offspring fed high-fat diet. N=3-7 mice per group. Graphs show mean ± SD as well as individual values. Data analysed by two-way ANOVA with Dunnett's multiple comparisons test *vs* C/C. The overall effects of maternal and offspring diet are reported where significant.

4.6 Discussion

This is the first study to describe the impacts of maternal metabolic dysfunction on the platelet activity of the offspring. We show that HF animals born from HF dams presented metabolic dysfunction, with higher serum levels of triglycerides, as well as developed heavier body weight earlier than HF offspring whose mothers were lean ($p<0.01$ at week 7). Maternal obesity led to increased spreading over collagen, decreased surface expression of collagen receptors and increased oxidative stress. Platelets from HF/HF animals were larger, hyper-reactive and with increased signalling, suggesting multiple mechanisms leading to increased platelet activation. Therefore, we suggest a novel 'double-hit' effect of maternal and offspring high-fat diet ingestion that causes platelet hyperactivation in the offspring.

To begin with, we assessed metabolic and phenotypic parameters to characterize our model. Our data show that maternal high-fat diet decreased body weight of chow-fed offspring after 18 weeks of age, when HF/C animals began to gain less weight than C/C animals. The majority of studies assessing effects of maternal obesity on offspring have used offspring at a younger age and showed increased or unchanged body weight and adiposity in chow-fed male offspring born to obese dams (Simar et al., 2012;Ribaroff et al., 2017). Similar to our data, Blackmore et al (2014) showed male mice born to obese dams to have a trend towards lighter body weight and improved metabolic parameters at 12 and 8 weeks of age, respectively. They have also described an increased sympathetic activity in the heart of these mice, compared to mice born to lean dams. It is possible that maternal obesity may programme the offspring to adapt to a fat-rich environment through higher adrenergic

discharge, potentially explaining the increased tendency to burn fat in HF/C offspring. This may represent an adaptive response to perceived nutritional stress such as those termed 'predictive adaptive responses' (Bateson et al., 2014), however it is not clear why these potential adaptive changes occur at a delayed point during the life-course of the offspring. Further work is necessary to examine this potential adaptive response and indeed to confirm whether higher sympathetic activity may account for the effects on body weight.

Our results showed that if mice born to HF dams were weaned onto an obesogenic diet, these mice displayed increased body weight, adiposity and serum cholesterol levels as well as glucose intolerance, decreased RER and energy expenditure compared C/C mice. Increased body weight was comparable between HF/HF and C/HF, similar to a previous report by Loche et al (Loche et al., 2018). The effects of maternal and offspring high-fat diet were additive on serum triglycerides levels. This is in agreement with previous reports describing a consistent (Sheen et al., 2018) or a trend (Simar et al., 2012) towards increased serum levels of triglycerides in similar murine models, albeit using younger mice. Increased triglyceredaemia have been shown to aggravate other metabolic functions, such as insulin resistance (for review see (Sears and Perry, 2015)). Likewise, hypertriglyceredaemia was correlated with increased platelet activity both after acute intralipid injection (Aye et al., 2014) and in chronic obese patients (Bordeaux et al., 2010). Therefore, it is possible that the additive effect of maternal and offspring obesity on serum triglycerides may be correlated with altered platelet function and increased cardiovascular risk.

In agreement with increased serum triglycerides levels, HF/HF mice presented altered platelet size and function. These mice had larger platelets with enhanced spreading on collagen as well as activation induced by two agonists that act through distinct mechanisms. Interestingly, maternal or offspring high-fat diet ingestion had an overall effect of increasing MPV in offspring. In contrast, only maternal obesity led to increased platelet spreading over collagen, suggesting that increased platelet size does not fully explain this result. In line with this, platelets from HF/HF mice were hyperreactive to ADP and CRP, but not to thrombin. Therefore, agonist-specific effects reiterates that increased platelet function consequent of maternal high-fat diet ingestion is not fully explained by increased MPV alone.

The fact that only HF/HF mice presented increased platelet activation suggests a previously undescribed 'double-hit' effect of maternal and offspring obesity, in which both insults are needed to alter platelet function. This is in line with a previous epidemiological report describing an association between maternal obesity and premature mortality from cardiovascular events (Reynolds et al., 2013), to which platelets are intrinsically related (Willoughby et al., 2002). Therefore, it is possible that the platelet hyperactivation herein observed in HF offspring born to HF dams can be a key pathophysiological component of the cardiovascular consequences of maternal obesity described in humans. Future research will explore epigenetic changes in platelets and megakaryocytes to better understand this phenomenon.

Platelet GPVI and integrin α2 expression was decreased due to maternal high-fat diet ingestion. We believe these alterations could be a consequence of shedding, in case of GPVI (Bender et al., 2010) or epigenetic changes in case of integrin α2. Considering that all HF groups presented increased levels of circulating ROS and that GPVI activation is both cause and consequence of increased ROS production in platelets (Qiao et al., 2018), it is possible that oxidative stress interferes with GPVI expression and response to CRP. This, however, may not be the only pathway involved, given that HF/C and C/HF mice had normal platelet function, highlighting the potential for developmental programming at the epigenetic level based on the metabolic profile of the mother.

Barrachina et al have recently shown that platelets from obese individuals are hyperresponsive to CRP and that they express higher levels of GPVI when compared to non-obese individuals (Barrachina et al., 2019). Using non-human primates, Arthur et al (2013) demonstrated that platelets from diabetic monkeys produce more ROS and are more responsive to CRP despite having unaltered levels of GPVI. There is a lack of reports assessing platelet GPVI levels in obesity and, although not directly comparable, the abovementioned studies flag the importance of the GPVI signalling pathway to the platelet dysfunction observed metabolic diseases. We argue that this might also be true for the consequences of maternal obesity on the platelet hyperactivation seen in obese offspring.

Besides differently expressed receptor levels, platelets from HF/HF mice also showed increased PKC substrate, total tyrosine and Akt phosphorylation; an effect not seen in other groups. Although we only

studied these following GPVI activation, they are all key signalling events common to a range of agonists (for review, see (Bye et al., 2016)), therefore it will be interesting to extend this work to identify whether other signalling pathways are affected or whether this is a GPVI-specific effect. Moreover, it has been shown that platelets from obese individuals are less sensitive to inhibitory molecules such as NO (Russo et al., 2010). Our data do not support differences in NO sensitivities, suggesting that metabolic dysfunction in both maternal and offspring favours platelet dysfunction through higher sensitivity to stimulatory signals rather than lower responsiveness to inhibitory ones. Nevertheless, this should be further explored in the future with the use of other inhibitors, such as aspirin and PGI_2.

We acknowledge several limitations in this study. As this is the first report on the effect of maternal obesity on platelet function, we did not exhaust all aspects of platelet function. Future research could use different approaches, such as: platelet aggregation, calcium mobilization, and thrombus formation *in vitro*. Likewise, epigenetic changes due to maternal obesity were not explored and could provide interesting insights on the precise mechanism of the phenotype herein observed. We recognize that data *in vitro* do not always translate in functional consequences *in vivo* and therefore encourage future reports to assess the effects of maternal obesity on thrombus formation *in vivo* and link animal data with human studies to support or discard our hypothesis. Finally, we believe that future studies should address sex-specific effects of maternal metabolic dysfunction on platelet function.

To summarize, we propose that platelets can be programmed by metabolic dysfunction in mothers and that there is a 'double-hit' effect that leads to platelet hyperactivity. The molecular mechanisms involved decreased GPVI expression, increased ROS production and enhanced phosphorylation levels of key stimulatory signalling proteins. Also, maternal high-fat diet ingestion per se seemed to induce a pro-adaptive metabolic response in chow-fed offspring, since these animals were leaner and tended to burn more fat than their counterparts born to lean dams. This should be further explored due to the lack of literature assessing offspring as old as those used in this report. These findings shed light on possible pathophysiological explanations to the increased risk of cardiovascular events in individuals born to mothers with metabolic dysfunction and add yet another layer of evidence to the deleterious effects of maternal obesity to the health of their offspring.

ACKNOWLEDGMENTS

The authors are grateful to Prof Marcus Paes for relevant scientific discussion of data at preliminary stages of this manuscript. We would like to thank the animal phenotypers and managers at the Mary Lyon Centre, especially Becky Starbuck, Lee Kent, Marie Hutchison and Maz Yon for supervising and performing the metabolic phenotyping experiments and for help with designing the study. The data underlying this article will be shared on reasonable request to the corresponding author.

SOURCES OF FUNDING

This work was supported by the Medical Research Council (MRC) [MR/P011683/1 to D.S., MR/J002666/1 to J.M.G, MC/U142661184 to R.D.C]; the British Heart Foundation **[**RG/15/2/31224 to J.M.G]; and the Royal Society Research Grant [RG170398 to C.H].

DISCLOSURES

The authors declare that they have no competing interests. This manuscript is part of the PhD Thesis of RSG.

4.7 Supplementary Figures

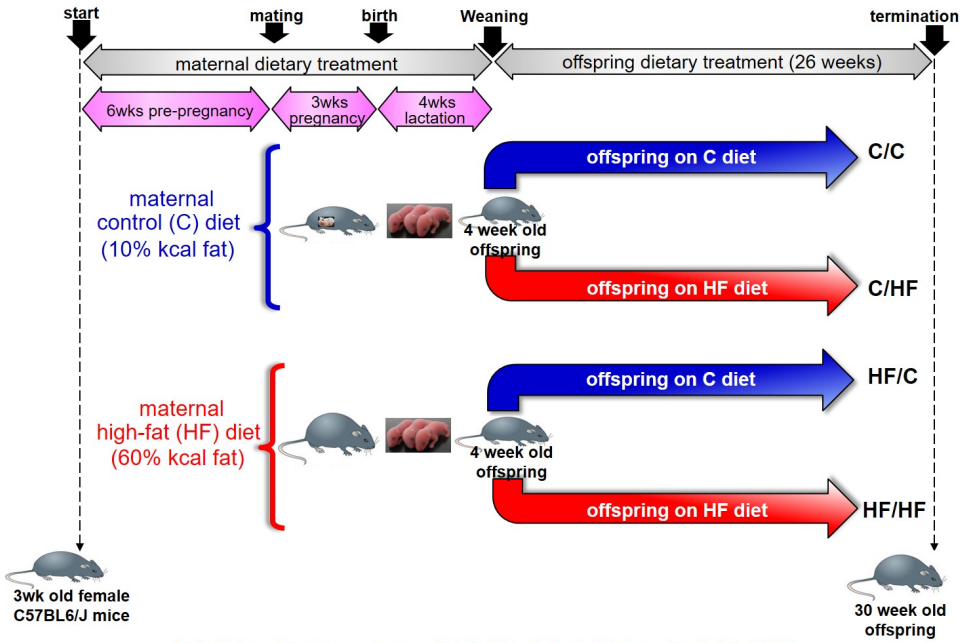

Supplementary Figure 4.1. Design of animal experiments. 3 weeks old female C57BL6/J mice were fed a control chow (C) or high-fat (HF) diet for 6 weeks before pregnancy, as well as the whole duration of pregnancy and lactation. Offspring was then subdivided to receive C or HF for 26 weeks after weaning, constituting four experimental groups: C/C, dam and offspring fed chow; C/HF dam fed chow and offspring fed high-fat diet; HF/C dam fed high-fat diet and offspring fed chow; HF/HF dam and offspring fed high-fat diet. Offspring was terminated at 30 weeks of age.

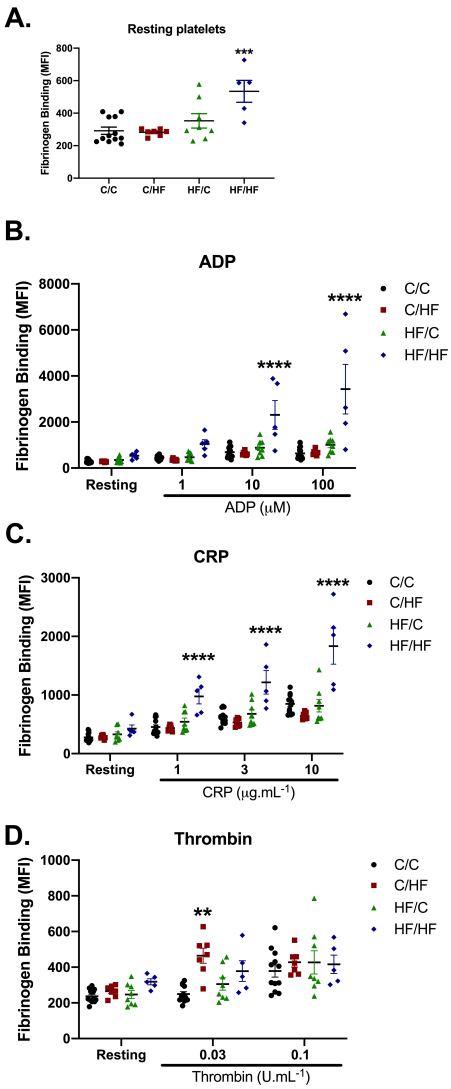

Supplementary Figure 4.2. Platelet hyperactivation of HF/HF mice is maintained throughout different doses of ADP and CRP, but not thrombin. Platelet-rich plasma (PRP) was incubated with FITC-conjugated fibrinogen and binding was measured in resting (A) or ADP (B), CRP (C) or Thrombin (D) stimulated platelets. C/C, dam and offspring fed chow; C/HF dam fed chow and offspring fed high-fat diet; HF/C dam fed high-fat diet and offspring fed chow; HF/HF dam and offspring fed high-fat diet. N=5-13 mice per group. Graphs show mean ± SEM as well as individual values. ** p<0.01 *vs* C/C; *** p<0.001 *vs* C/C; **** p<0.0001 *vs* C/C. Data analysed by repeated-measures two-way ANOVA with Dunnett's multiple comparisons test *vs* C/C. The overall effects of maternal and offspring diet are reported where significant.

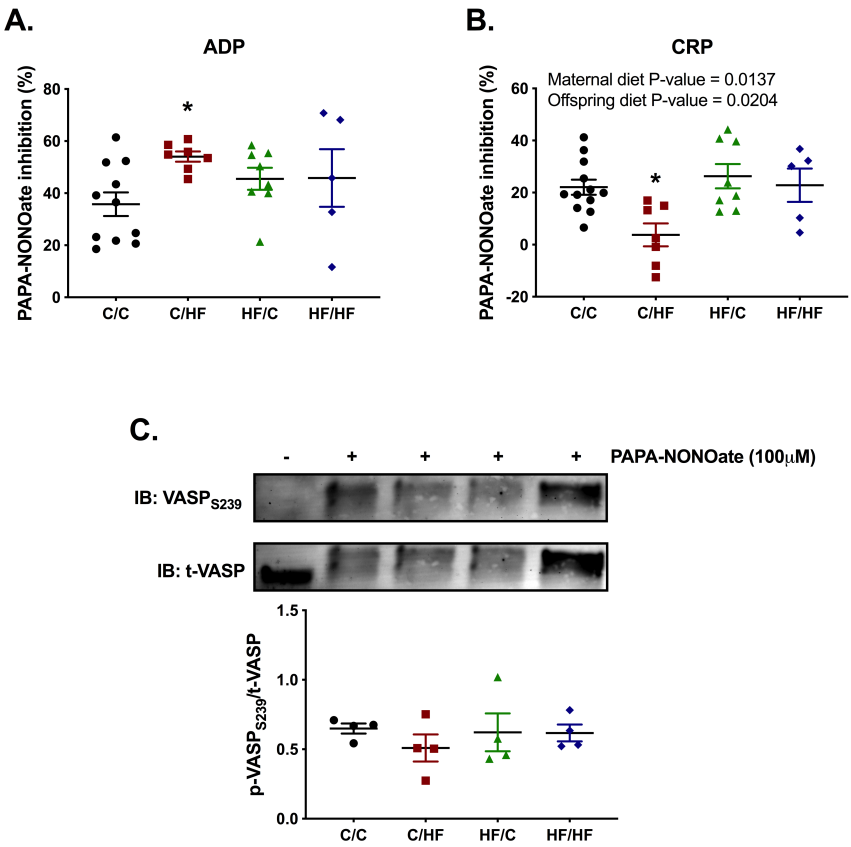

Supplementary Figure 4.3. Maternal obesity does not influence response to nitric oxide donor PAPA-NONOate. Platelet-rich plasma (PRP) was incubated with 100 μM PAPA-NONOate for 10 minutes and stimulated with 10 μM ADP (A) or 3 μg/mL CRP (B) and fibrinogen binding measured. PAPA-NONOate inhibition was calculated in comparison to stimulated platelets incubated with vehicle control. (C) Washed platelets (WP) were incubated with 100 μM PAPA-NONOate for 10 minutes and lysed. Representative immunoblot and summarized data are shown for VASP phosphorylation at Ser239 (C). C/C, dam and offspring fed chow; C/HF dam fed chow and offspring fed high-fat diet; HF/C dam fed high-fat diet and offspring fed chow; HF/HF dam and offspring fed high-fat diet. N=5-12 mice per group for (A) and (B) and n=4 mice per group for (C). Graphs show mean ± SEM as well as individual values. * $p<0.05$ *vs* C/C. Data analysed by two-way ANOVA with Dunnett's multiple comparisons test *vs* C/C. The overall effects of maternal and offspring diet are reported where significant.

Major Resources Table

In order to allow validation and replication of experiments, all essential research materials listed in the Methods should be included in the Major Resources Table below. Authors are encouraged to use public repositories for protocols, data, code, and other materials and provide persistent identifiers and/or links to repositories when available. Authors may add or delete rows as needed.

Animals (in vivo studies)

Species	**Vendor or Source**	**Background Strain**	**Sex**	**Persistent ID / URL**
M.musculus	In house	C57BL6/N	F/M	

Antibodies

Target antigen	**Vendor or Source**	**Catalog #**	**Working concentration**	**Lot # (preferred but not required)**	**Persistent ID / URL**
F-actin	Life Technology	#8878	1:1000 v/v		https://www.cellsignal.com/products/buffers-dyes/alexa-fluor-488-phalloidin/8878
GPVI	Emfret	M011-1	5 µL per 10^6 platelets		https://www.emfret.com/uploads/tx_beproducts/M011-1_JAQ1.pdf
α2 integrin	Emfret	M070-1	5 µL per 10^6 platelets		https://www.emfret.com/uploads/tx_beproducts/M070-1_SamG4.pdf
GpIbα	Emfret	M040-2	5 µL per 10^6 platelets		https://www.emfret.com/uploads/tx_beproducts/M040-2_XiaG5.pdf
Negative control (Rat IgG)	Emfret	P190-2	5 µL per 10^6 platelets		https://www.emfret.com/uploads/tx_beproducts/P190-2_rat_IgG.pdf
Negative control	Emfret	P190-1	5 µL per 10^6 platelets		https://www.emfret.com/upl

(Rat IgG)					oads/tx_beproducts/P190-1_rat_IgG.pdf
CD36	R&D Systems	AF2519	2.5 µg per 10^6 platelets		https://www.rndsystems.com/products/mouse-cd36-sr-b3-antibody_af2519
Tyrosine phosphorylation (4G10 antibody)	Merck Millipore	05-321	1:1000 v/v		https://www.merckmillipore.com/GB/en/product/Anti-Phosphotyrosine-Antibody-clone-4G10,MM_NF-05-321?ReferrerURL=https%3A%2F%2Fwww.google.com%2F
Actin	Abcam	ab8229	1:1000 v/v		https://www.abcam.com/beta-actin-antibody-loading-control-ab8229.html
$VASP_{S239}$	Cell Signaling	#3114	1:1000 v/v		https://www.cellsignal.com/products/primary-antibodies/phospho-vasp-ser239-antibody/3114
Akt_{S473}	Cell Signaling	#9271	1:1000 v/v		https://www.cellsignal.com/products/primary-antibodies/phospho-akt-ser473-antibody/9271?site-search-type=Products

4.8 References

1. Barker DJ, Osmond C. Infant mortality, childhood nutrition, and ischaemic heart disease in england and wales. *The Lancet*. 1986;327:1077-1081
2. Barker DJ, Godfrey KM, Gluckman PD, Harding JE, Owens JA, Robinson JS. Fetal nutrition and cardiovascular disease in adult life. *The Lancet*. 1993;341:938-941
3. Osmond C, Barker D, Winter P, Fall C, Simmonds S. Early growth and death from cardiovascular disease in women. *Bmj*. 1993;307:1519-1524
4. Williams L, Seki Y, Vuguin PM, Charron MJ. Animal models of in utero exposure to a high fat diet: A review. *Biochimica et Biophysica Acta (BBA)-Molecular Basis of Disease*. 2014;1842:507-519
5. Massberg S, Brand K, Gruner S, Page S, Muller E, Muller I, Bergmeier W, Richter T, Lorenz M, Konrad I, Nieswandt B, Gawaz M. A critical role of platelet adhesion in the initiation of atherosclerotic lesion formation. *J Exp Med*. 2002;196:887-896
6. Lindemann S, Kramer B, Seizer P, Gawaz M. Platelets, inflammation and atherosclerosis. *J Thromb Haemost*. 2007;5 Suppl 1:203-211
7. Huo Y, Schober A, Forlow SB, Smith DF, Hyman MC, Jung S, Littman DR, Weber C, Ley K. Circulating activated platelets exacerbate atherosclerosis in mice deficient in apolipoprotein e. *Nat Med*. 2003;9:61-67
8. Schafer A, Bauersachs J. Endothelial dysfunction, impaired endogenous platelet inhibition and platelet activation in diabetes and atherosclerosis. *Curr Vasc Pharmacol*. 2008;6:52-60
9. Puurunen MK, Hwang SJ, Larson MG, Vasan RS, O'Donnell CJ, Tofler G, Johnson AD. Adp platelet hyperreactivity predicts cardiovascular disease in the fhs (framingham heart study). *Journal of the American Heart Association*. 2018;7:e008522
10. Fan L, Lindsley S, Comstock S, Takahashi D, Evans A, He G, Thornburg K, Grove K. Maternal high-fat diet impacts endothelial function in

nonhuman primate offspring. *International journal of obesity*. 2013;37:254-262

11. Fan X, Turdi S, Ford SP, Hua Y, Nijland MJ, Zhu M, Nathanielsz PW, Ren J. Influence of gestational overfeeding on cardiac morphometry and hypertrophic protein markers in fetal sheep. *The Journal of nutritional biochemistry*. 2011;22:30-37
12. Huang Y, Yan X, Zhao JX, Zhu MJ, McCormick RJ, Ford SP, Nathanielsz PW, Ren J, Du M. Maternal obesity induces fibrosis in fetal myocardium of sheep. *American Journal of Physiology-Endocrinology and Metabolism*. 2010;299:E968-E975
13. Samuelsson A-M, Matthews PA, Argenton M, Christie MR, McConnell JM, Jansen EH, Piersma AH, Ozanne SE, Twinn DF, Remacle C. Diet-induced obesity in female mice leads to offspring hyperphagia, adiposity, hypertension, and insulin resistance: A novel murine model of developmental programming. *Hypertension*. 2008;51:383-392
14. Poston L, Harthoorn LF, Van Der Beek EM. Obesity in pregnancy: Implications for the mother and lifelong health of the child. A consensus statement. *Pediatric research*. 2011;69:175-180
15. Yu Y, Arah OA, Liew Z, Cnattingius S, Olsen J, Sorensen HT, Qin G, Li J. Maternal diabetes during pregnancy and early onset of cardiovascular disease in offspring: Population based cohort study with 40 years of follow-up. *BMJ*. 2019;367:l6398
16. Gaspar RS, da Silva SA, Stapleton J, Fontelles JLL, Sousa HR, Chagas VT, Alsufyani S, Trostchansky A, Gibbins JM, Paes AMA. Myricetin, the main flavonoid in syzygium cumini leaf, is a novel inhibitor of platelet thiol isomerases pdi and erp5. *Front Pharmacol*. 2019;10:1678
17. Chu SG, Becker RC, Berger PB, Bhatt DL, Eikelboom JW, Konkle B, Mohler ER, Reilly MP, Berger JS. Mean platelet volume as a predictor of cardiovascular risk: A systematic review and meta-analysis. *J Thromb Haemost*. 2010;8:148-156
18. Simar D, Chen H, Lambert K, Mercier J, Morris MJ. Interaction between maternal obesity and post-natal over-nutrition on skeletal muscle metabolism. *Nutr Metab Cardiovasc Dis*. 2012;22:269-276

19. Ribaroff GA, Wastnedge E, Drake AJ, Sharpe RM, Chambers TJG. Animal models of maternal high fat diet exposure and effects on metabolism in offspring: A meta-regression analysis. *Obes Rev*. 2017;18:673-686
20. Blackmore HL, Niu Y, Fernandez-Twinn DS, Tarry-Adkins JL, Giussani DA, Ozanne SE. Maternal diet-induced obesity programs cardiovascular dysfunction in adult male mouse offspring independent of current body weight. *Endocrinology*. 2014;155:3970-3980
21. Bateson P, Gluckman P, Hanson M. The biology of developmental plasticity and the predictive adaptive response hypothesis. *J Physiol*. 2014;592:2357-2368
22. Loche E, Blackmore HL, Carpenter AA, Beeson JH, Pinnock A, Ashmore TJ, Aiken CE, de Almeida-Faria J, Schoonejans JM, Giussani DA, Fernandez-Twinn DS, Ozanne SE. Maternal diet-induced obesity programmes cardiac dysfunction in male mice independently of post-weaning diet. *Cardiovasc Res*. 2018;114:1372-1384
23. Sheen JM, Yu HR, Tain YL, Tsai WL, Tiao MM, Lin IC, Tsai CC, Lin YJ, Huang LT. Combined maternal and postnatal high-fat diet leads to metabolic syndrome and is effectively reversed by resveratrol: A multiple-organ study. *Sci Rep*. 2018;8:5607
24. Sears B, Perry M. The role of fatty acids in insulin resistance. *Lipids Health Dis*. 2015;14:121
25. Aye MM, Kilpatrick ES, Aburima A, Wraith KS, Magwenzi S, Spurgeon B, Rigby AS, Sandeman D, Naseem KM, Atkin SL. Acute hypertriglyceridemia induces platelet hyperactivity that is not attenuated by insulin in polycystic ovary syndrome. *J Am Heart Assoc*. 2014;3:e000706
26. Bordeaux BC, Qayyum R, Yanek LR, Vaidya D, Becker LC, Faraday N, Becker DM. Effect of obesity on platelet reactivity and response to low-dose aspirin. *Prev Cardiol*. 2010;13:56-62
27. Reynolds RM, Allan KM, Raja EA, Bhattacharya S, McNeill G, Hannaford PC, Sarwar N, Lee AJ, Bhattacharya S, Norman JE. Maternal obesity

during pregnancy and premature mortality from cardiovascular event in adult offspring: Follow-up of 1 323 275 person years. *BMJ*. 2013;347:f4539

28. Willoughby S, Holmes A, Loscalzo J. Platelets and cardiovascular disease. *European Journal of Cardiovascular Nursing*. 2002;1:273-288
29. Bender M, Hofmann S, Stegner D, Chalaris A, Bosl M, Braun A, Scheller J, Rose-John S, Nieswandt B. Differentially regulated gpvi ectodomain shedding by multiple platelet-expressed proteinases. *Blood*. 2010;116:3347-3355
30. Qiao J, Arthur JF, Gardiner EE, Andrews RK, Zeng L, Xu K. Regulation of platelet activation and thrombus formation by reactive oxygen species. *Redox Biol*. 2018;14:126-130
31. Barrachina MN, Sueiro AM, Izquierdo I, Hermida-Nogueira L, Guitian E, Casanueva FF, Farndale RW, Moroi M, Jung SM, Pardo M, Garcia A. Gpvi surface expression and signalling pathway activation are increased in platelets from obese patients: Elucidating potential anti-atherothrombotic targets in obesity. *Atherosclerosis*. 2019;281:62-70
32. Arthur JF, Shen Y, Chen Y, Qiao J, Ni R, Lu Y, Andrews RK, Gardiner EE, Cheng J. Exacerbation of glycoprotein vi-dependent platelet responses in a rhesus monkey model of type 1 diabetes. *J Diabetes Res*. 2013;2013:370212
33. Bye AP, Unsworth AJ, Gibbins JM. Platelet signaling: A complex interplay between inhibitory and activatory networks. *J Thromb Haemost*. 2016;14:918-930
34. Russo I, Traversa M, Bonomo K, De Salve A, Mattiello L, Del Mese P, Doronzo G, Cavalot F, Trovati M, Anfossi G. In central obesity, weight loss restores platelet sensitivity to nitric oxide and prostacyclin. *Obesity (Silver Spring)*. 2010;18:788-797

Arthur, J.F., Shen, Y., Chen, Y., Qiao, J., Ni, R., Lu, Y., Andrews, R.K., Gardiner, E.E., and Cheng, J. (2013). Exacerbation of glycoprotein VI-dependent platelet responses in a rhesus monkey model of Type 1 diabetes. *J Diabetes Res* 2013**,** 370212.

Aye, M.M., Kilpatrick, E.S., Aburima, A., et al. (2014). Acute hypertriglyceridemia induces platelet hyperactivity that is not attenuated by insulin in polycystic ovary syndrome. *J Am Heart Assoc* 3**,** e000706.

Barker, D.J., Godfrey, K.M., Gluckman, P.D., Harding, J.E., Owens, J.A., and Robinson, J.S. (1993). Fetal nutrition and cardiovascular disease in adult life. *The Lancet* 341**,** 938-941.

Barker, D.J., and Osmond, C. (1986). Infant mortality, childhood nutrition, and ischaemic heart disease in England and Wales. *The Lancet* 327**,** 1077-1081.

Barrachina, M.N., Sueiro, A.M., Izquierdo, I., et al. (2019). GPVI surface expression and signalling pathway activation are increased in platelets from obese patients: Elucidating potential anti-atherothrombotic targets in obesity. *Atherosclerosis* 281**,** 62-70.

Bateson, P., Gluckman, P., and Hanson, M. (2014). The biology of developmental plasticity and the Predictive Adaptive Response hypothesis. *J Physiol* 592**,** 2357-2368.

Bender, M., Hofmann, S., Stegner, D., Chalaris, A., Bosl, M., Braun, A., Scheller, J., Rose-John, S., and Nieswandt, B. (2010). Differentially regulated GPVI ectodomain shedding by multiple platelet-expressed proteinases. *Blood* 116**,** 3347-3355.

Blackmore, H.L., Niu, Y., Fernandez-Twinn, D.S., Tarry-Adkins, J.L., Giussani, D.A., and Ozanne, S.E. (2014). Maternal diet-induced obesity programs cardiovascular dysfunction in adult male mouse offspring independent of current body weight. *Endocrinology* 155**,** 3970-3980.

Bordeaux, B.C., Qayyum, R., Yanek, L.R., Vaidya, D., Becker, L.C., Faraday, N., and Becker, D.M. (2010). Effect of obesity on platelet reactivity and response to low-dose aspirin. *Prev Cardiol* 13**,** 56-62.

Bye, A.P., Unsworth, A.J., and Gibbins, J.M. (2016). Platelet signaling: a complex interplay between inhibitory and activatory networks. *J Thromb Haemost* 14**,** 918-930.

Chu, S.G., Becker, R.C., Berger, P.B., Bhatt, D.L., Eikelboom, J.W., Konkle, B., Mohler, E.R., Reilly, M.P., and Berger, J.S. (2010). Mean platelet volume as a predictor of cardiovascular risk: a systematic review and meta-analysis. *J Thromb Haemost* 8**,** 148-156.

Fan, L., Lindsley, S., Comstock, S., Takahashi, D., Evans, A., He, G., Thornburg, K., and Grove, K. (2013). Maternal high-fat diet impacts endothelial function in nonhuman primate offspring. *International journal of obesity* 37**,** 254-262.

Fan, X., Turdi, S., Ford, S.P., Hua, Y., Nijland, M.J., Zhu, M., Nathanielsz, P.W., and Ren, J. (2011). Influence of gestational overfeeding on cardiac morphometry and hypertrophic protein markers in fetal sheep. *The Journal of nutritional biochemistry* 22**,** 30-37.

Gaspar, R.S., Da Silva, S.A., Stapleton, J., et al. (2019). Myricetin, the Main Flavonoid in Syzygium cumini Leaf, Is a Novel Inhibitor of Platelet Thiol Isomerases PDI and ERp5. *Front Pharmacol* 10**,** 1678.

Huang, Y., Yan, X., Zhao, J.X., Zhu, M.J., Mccormick, R.J., Ford, S.P., Nathanielsz, P.W., Ren, J., and Du, M. (2010). Maternal obesity induces fibrosis in fetal myocardium of sheep. *American Journal of Physiology-Endocrinology and Metabolism* 299**,** E968-E975.

Huo, Y., Schober, A., Forlow, S.B., Smith, D.F., Hyman, M.C., Jung, S., Littman, D.R., Weber, C., and Ley, K. (2003). Circulating activated platelets exacerbate atherosclerosis in mice deficient in apolipoprotein E. *Nat Med* 9**,** 61-67.

Lindemann, S., Kramer, B., Seizer, P., and Gawaz, M. (2007). Platelets, inflammation and atherosclerosis. *J Thromb Haemost* 5 Suppl 1**,** 203-211.

Loche, E., Blackmore, H.L., Carpenter, A.A., et al. (2018). Maternal diet-induced obesity programmes cardiac dysfunction in male mice independently of post-weaning diet. *Cardiovasc Res* 114**,** 1372-1384.

Massberg, S., Brand, K., Gruner, S., et al. (2002). A critical role of platelet adhesion in the initiation of atherosclerotic lesion formation. *J Exp Med* 196**,** 887-896.

Osmond, C., Barker, D., Winter, P., Fall, C., and Simmonds, S. (1993). Early growth and death from cardiovascular disease in women. *Bmj* 307**,** 1519-1524.

Poston, L., Harthoorn, L.F., and Van Der Beek, E.M. (2011). Obesity in pregnancy: implications for the mother and lifelong health of the child. A consensus statement. *Pediatric research* 69**,** 175-180.

Puurunen, M.K., Hwang, S.J., Larson, M.G., Vasan, R.S., O'donnell, C.J., Tofler, G., and Johnson, A.D. (2018). ADP platelet hyperreactivity predicts cardiovascular disease in the FHS (Framingham Heart Study). *Journal of the American Heart Association* 7**,** e008522.

Qiao, J., Arthur, J.F., Gardiner, E.E., Andrews, R.K., Zeng, L., and Xu, K. (2018). Regulation of platelet activation and thrombus formation by reactive oxygen species. *Redox Biol* 14**,** 126-130.

Reynolds, R.M., Allan, K.M., Raja, E.A., et al. (2013). Maternal obesity during pregnancy and premature mortality from cardiovascular event in adult offspring: follow-up of 1 323 275 person years. *BMJ* 347**,** f4539.

Ribaroff, G.A., Wastnedge, E., Drake, A.J., Sharpe, R.M., and Chambers, T.J.G. (2017). Animal models of maternal high fat diet exposure and effects on metabolism in offspring: a meta-regression analysis. *Obes Rev* 18**,** 673-686.

Russo, I., Traversa, M., Bonomo, K., et al. (2010). In central obesity, weight loss restores platelet sensitivity to nitric oxide and prostacyclin. *Obesity (Silver Spring)* 18**,** 788-797.

Samuelsson, A.-M., Matthews, P.A., Argenton, M., et al. (2008). Diet-induced obesity in female mice leads to offspring hyperphagia, adiposity, hypertension, and insulin resistance: a novel murine model of developmental programming. *Hypertension* 51**,** 383-392.

Schafer, A., and Bauersachs, J. (2008). Endothelial dysfunction, impaired endogenous platelet inhibition and platelet activation in diabetes and atherosclerosis. *Curr Vasc Pharmacol* 6**,** 52-60.

Sears, B., and Perry, M. (2015). The role of fatty acids in insulin resistance. *Lipids Health Dis* 14**,** 121.

Sheen, J.M., Yu, H.R., Tain, Y.L., Tsai, W.L., Tiao, M.M., Lin, I.C., Tsai, C.C., Lin, Y.J., and Huang, L.T. (2018). Combined maternal and postnatal high-fat diet leads to metabolic syndrome and is effectively reversed by resveratrol: a multiple-organ study. *Sci Rep* 8**,** 5607.

Simar, D., Chen, H., Lambert, K., Mercier, J., and Morris, M.J. (2012). Interaction between maternal obesity and post-natal over-nutrition on skeletal muscle metabolism. *Nutr Metab Cardiovasc Dis* 22**,** 269-276.

Williams, L., Seki, Y., Vuguin, P.M., and Charron, M.J. (2014). Animal models of in utero exposure to a high fat diet: a review. *Biochimica et Biophysica Acta (BBA)-Molecular Basis of Disease* 1842**,** 507-519.

Willoughby, S., Holmes, A., and Loscalzo, J. (2002). Platelets and cardiovascular disease. *European Journal of Cardiovascular Nursing* 1**,** 273-288.

Yu, Y., Arah, O.A., Liew, Z., Cnattingius, S., Olsen, J., Sorensen, H.T., Qin, G., and Li, J. (2019). Maternal diabetes during pregnancy and early onset of cardiovascular disease in offspring: population based cohort study with 40 years of follow-up. *BMJ* 367**,** l6398.

Chapter 5

General Discussion

Platelets are key for haemostasis and thrombus formation (Stevens and McFadyen, 2019). These processes are highly regulated by redox process, as shown throughout this thesis and in previous literature. Both ROS and the enzymatic systems that generate ROS have been shown to be relevant to the proper function of platelets. For instance, over 30 years ago Salvemini et al (Salvemini et al., 1989) demonstrated that addition of superoxide dismutase (SOD), an enzyme that catalyses the dismutation of superoxide radicals (McCord and Fridovich, 1969), inhibited platelet aggregation induced by thrombin. These authors also showed that incubation with pyrogallol, a chemical that generates superoxide radicals through auto-oxidation (Marklund and Marklund, 1974), increased platelet aggregation induced by thrombin. More recently, Vara et al (Vara et al., 2019) explored how ROS-generating enzymes regulate platelet function and showed that Nox-1 regulates superoxide production and platelet activation downstream of GPVI, while Nox-2 regulates these functions downstream of the thrombin receptors.

Despite substantial progress made throughout the last decades, the redox processes that regulate platelets are still in need of further investigation. The endpoint goal of understanding such fundamental processes in platelets is to develop more efficient anti-platelet medications to treat and prevent thrombotic disorders. Therefore, the broad aim of this thesis was to investigate how redox processes regulate platelets in health and disease.

This was first shown in **Chapter 2** through the identification of myricetin as a novel inhibitor of thiol isomerases, which are redox proteins of

paramount importance to platelets (Jordan et al., 2005;Holbrook et al., 2010;Holbrook et al., 2012;Jasuja et al., 2012;Crescente et al., 2016). Myricetin exhibited potent anti-platelet and anti-thrombotic activities, with no effect on haemostasis. The fact that this flavonoid was able to inhibit PDI and ERp5 at similar concentrations to those that achieved platelet inhibition (i.e. around 10 μM) suggests thiol isomerase inhibition may be a feasible mechanism of action for the anti-platelet and anti-thrombotic effects observed. Of note, the study of Dang and colleagues (2014) reports a peak plasma concentration of 10 μM myricetin conjugated with glucuronic acid or sulphate, instead of the unconjugated form used in **Chapter 2**. Despite this, it is possible that myricetin has targets other than thiol isomerases that modulate the anti-platelet and anti-thrombotic effects exerted by this flavonoid (as argued in the **Discussion** section of **Chapter 2**).

In **Chapter 3** I examined the functional association between PDI and Nox-1 and investigated how PDI and Nox-1 contribute to platelet function, both individually and in collaboration with one another. PDI inhibition led to decreased levels of platelet aggregation, activation, degranulation, ROS production and other GPVI-mediated processes. Similarly, inhibition of Nox-1 with ML171 was also able to decrease platelet aggregation, activation and ROS generation. When both PDI and Nox-1 were blocked, there was an additive inhibitory effect that was selective to GPVI-mediated processes. PDI and Nox-1 co-localised when platelets were activated by the GPVI agonist CRP. The additive anti-platelet effect of PDI and Nox-1 co-inhibition affected several aspects of platelet function such as calcium mobilization and ROS generation, but did not interfere with adhesion assays. This indicates that the

additive inhibitory effect of PDI and Nox-1 co-inhibition was independent of integrin function and outside-in signalling (as introduced in **section 1.2** of **Chapter 1**), since platelet adhesive assays are principally regulated by integrins. Therefore, PDI and Nox-1 co-inhibition may affect events that occur before integrin activation, i.e. inside-out signalling (as introduced in **section 1.2** of **Chapter 1**). This process may be of relevance to the development of anti-platelet medications, given that both PDI and Nox-1 were found to be positively correlated with cardiometabolic risk factors.

Finally, in **Chapter 4**, I have reported for the first time that platelets can be programmed by maternal and offspring high-fat diet ingestion, leading to a phenotype of platelet hyperactivity. This involved enlarged and more reactive platelets that exhibited higher levels of oxidative stress. These observations add yet another layer of evidence to the deleterious effects of maternal metabolic dysfunction to the cardiovascular outcomes of their offspring. In particular, increased platelet activity in offspring may be related to higher cardiovascular events reported later in life in offspring born to obese mothers (Reynolds et al., 2013). Description of this novel phenomenon emphasizes future work needed to understand the cellular and pathophysiological mechanisms underlying increased platelet activity.

In light of the lines of investigation presented in this Thesis, we can conclude platelets are highly regulated by redox proteins PDI and Nox-1 and this may be of relevance to cardiometabolic diseases.

The studies included in this thesis are interconnected through several links – these will be further explored in this Chapter. Future perspectives,

speculations, limitations and an overarching conclusion of the work will also be presented in the following sections.

5.1 Hormesis

Initial experiments with a polyphenolic extract of *S. cumini*, PESc, demonstrated that concentrations up to 1000 μg/mL PESc inhibited platelet aggregation up to 60%, depending on the agonist used (**Figure 2.1** of **Chapter 2**). Previously I have shown that 1000 μg/mL PESc abrogated proliferation of a mouse insulinoma cell line, INS-1E (Chagas et al., 2018). It is likely that the inhibition of platelet aggregation induced by 1000 μg/mL PESc was at least partially due to toxicity. On the other hand, 10 μg/mL PESc did not exert effects on platelet aggregation, suggesting that there is a range of concentration, between 10 and 1000 μg/mL, in which PESc is able to exert its anti-platelet effect without becoming toxic. Within this preclinical pharmacological study, I aimed to find a physiologically relevant effect of PESc, i.e. inhibition of platelets, without exerting toxicity.

In parallel, current anti-platelet therapies aim to decrease platelet function and the deleterious effects of thrombosis, while keeping haemostasis intact to avoid bleeding as a side effect. Thus fine-tuning is required in the development of new anti-platelet medications in order to reduce side effects. Both **Chapter 2** and **Chapter 3** explore this using PDI and Nox-1 inhibitors. In **Chapter 2**, I showed that the flavonoid myricetin has promising anti-platelet (80% inhibition of TRAP-6-induced platelet aggregation at 30 μM myricetin, **Figure 2.2** of **Chapter 2**) and anti-thrombotic (40% decreased thrombus formation at 30 μM myricetin, **Figure 2.4** of **Chapter 2**) properties without detectable effects on bleeding time (**Figure 2.5** of **Chapter 2**) when given orally to healthy female mice. Data contained in **Chapter 3** explore how the PDI inhibitor bepristat and Nox-1

inhibitor ML171 promote an additive inhibitory effect to one another in GPVI-mediated responses. Co-incubation of these inhibitors abrogated platelet aggregation induced by collagen (**Figure 3.2B** of **Chapter 3**, at 15 μM bepristat and 3 μM ML171), while bleeding time was preserved in female Nox-1$^{-/-}$ mice injected with 50 μM final concentration of bepristat (**Figure 3.5I** of **Chapter 3**). These data collectively indicate that targeting PDI or PDI together with Nox-1 are promising strategies to develop more efficient anti-platelet drug therapies with reduced impact on haemostasis. This reinforces the current goal within the platelet field of finding a physiologically relevant effect with limited adverse outcomes, i.e. reduced platelet function and thrombus formation without increased bleeding time.

While **Chapter 2 and 3** explore novel ways to reduce platelet function, data in **Chapter 4** investigate how platelets become more reactive upon maternal intervention. In **Chapter 4**, the deleterious impacts of maternal high-fat (HF) diet ingestion to the platelet function of the offspring were studied. Maternal metabolic dysfunction induced platelet hyperactivation in male offspring regardless of the offspring diet (**Figure 4.2** of **Chapter 4**), albeit additional feeding a HF diet to the offspring had an additive effect to maternal HF diet ingestion (**Figure 4.3** of **Chapter 4**). This is the first study to report that platelets can be programmed by maternal insult. While here I have focused on harmful effects caused by maternal metabolic dysfunction induced by HF diet, it is possible that other maternal interventions are able to improve platelet function on the offspring (this will be further discussed below). The modulation of platelet function by maternal dietary

interventions is a novel concept and is similar to the fine-tuning of platelet function by inhibitors.

Therefore the idea of fine-tuning platelet function is presented throughout the experimental chapters of this thesis. First by identifying novel anti-platelet compounds that exert a physiologically relevant effect without inducing toxicity (**Chapter 2**), next by describing a novel additive anti-platelet effect when PDI and Nox-1 were inhibited simultaneously (**Chapter 3**) and finally by showing how platelets can be programmed by maternal HF ingestion (**Chapter 4**) and the possibilities of programming platelets to become more or less reactive depending on maternal diet. These data collectively describe a concept of paramount importance to many biological systems, namely Hormesis.

Hormesis is defined as a biological process that leads to a concentration-response curve, in which there is a stimulatory response at low concentrations and an inhibitory response at high doses (Calabrese and Baldwin, 1997;Calabrese, 2008). Within an hormetic curve there is an ideal intermediate effect which is the peak of maximal stimulatory response before the decay (Calabrese, 2008). Pathologist Virchow first described this concept in 1854 (Henschler, 2006) when he described that low concentrations of sodium and potassium hydroxide increased beating activity of tracheal ciliae whilst high concentrations led to a concentration-dependent decrease in ciliae activity. However, the term hormesis started to be applied to the observations of Virchow only in 1943 by Southam and Ehrlich (Southam, 1943), being widely used by 2006 (Calabrese, 2008).

Hormesis was first applied within the toxicology field to explain the effects of chemical compounds, radiation and other environmental factors on biological systems (Calabrese, 2008). The concept was then extended to other aspects of biology and throughout different scientific fields under different names, such as the Yerkes–Dodson Law in experimental psychology, subsidy-gradient in ecology and U-shaped curves in epidemiology. In 2008 Prof Calabrese amalgamated these different concepts as hormesis and convincingly showed that the biphasic response was not restricted to a cellular-specific process, but was rather a more fundamental aspect of the biological, social and mental capacities of mammals (Calabrese, 2008).

I would argue that the concept of hormesis is perhaps more enrooted in how modern scientists perceive biological processes than proposed by Prof Calabrese. For instance, this concept can be found in the work of Greek philosopher Aristotle's "doctrine of the mean", over 2,000 years ago. Aristotle was a prolific thinker that, amongst other things, conceived the field of ethical theory (Kraut, 2001). He studied ethics as an attempt to improve our lives, being primarily concerned with the nature of human well-being. Within this field, he developed the concept of ethical virtues, which are complex rational, social and emotional traits to which one should aspire – such as justice and courage – in order to achieve one's well-being. These ethical virtues lie in the intermediate condition between two states of vice, excess and deficiency (Kraut, 2001), thus introducing the perception of an ideal intermediate effect way before Science was conceptualized. The idea of Aristotle's ethical virtues is therefore applicable to the concept of hormesis, since there will always be an ideal intermediate condition before the phase

change within the bi-phasic response and fine-tuning is necessary to identify this intermediate condition (Calabrese, 2008).

Such an enrooted concept can therefore be applied to a wide range of biological phenomena. As discussed above, the discovery that platelets can be programmed by maternal insults (**Chapter 4**) opens up windows of intervention to possibly revert the deleterious effects of maternal HF ingestion. The basis of such hypothesis can be found on previous literature (cited below) within the developmental programming field that reiterate the concept of hormesis on the developmental origins of health and disease.

Several studies have addressed life-long impacts of being born small for gestational age (SGA) or large for gestational age (LGA), i.e. both ends of the birth weight curve. Barker, for instance, observed a positive correlation between low birth weight and increased mortality from ischaemic heart disease in adults 50 years later (Barker and Osmond, 1986;Barker and Osmond, 1987). More recently, it was shown that being born LGA was associated with cardiometabolic risk factors as early as 6 years of age (Evagelidou et al., 2010). Both SGA and LGA births are linked with cardiometabolic risk factors, such as obesity, hypertension and hyperglycaemia, in childhood and adolescence (Chiavaroli et al., 2014). Similarly, both low and high birthweight were associated with higher prevalence of diabetes in women aged 15 to 34 in Pima Indian individuals, a population that has been of interest to the DOHaD field due to very high prevalence of gestational diabetes (Pettitt and Knowler, 1998). This also holds true for other diseases in other populations, such as autism in childhood, where published studies suggest increased risk of development in

both SGA and LGA (Moore et al., 2012) when compared to children born at an appropriate size for gestational age. Therefore, there is a bi-phasic curve applicable to weight at birth, in which both edges of the curve, i.e. small and large newborn babies, have long-term deleterious effects. These data reinforce the concept of fine-tuning intrauterine environment to identify an ideal intermediate effect wherein the intrauterine environment is neither in excess nor in lack of nutrients.

If excessive or deficient prenatal nutritional environment is deleterious, one could speculate that interventions aiming to normalize intrauterine environment could lead to beneficial outcomes to the offspring. One such intervention is exercise. Laker et al (Laker et al., 2014) have shown in mice that exercise before and during pregnancy normalized offspring glucose homeostasis and peroxisome proliferator activated receptor γ co-activator-1α (Pgc-1α) hypermethylation induced by maternal HF diet ingestion. In line with these observations, Stanford et al (Stanford et al., 2017) showed that maternal exercise prevented the deleterious effects of maternal HF diet on glucose tolerance and hepatocyte glucose metabolism in female mice offspring. These studies indicate that maternal exercise may prevent the development of metabolic disturbances in offspring caused by maternal HF diet ingestion in rodents. Due to similarities and translational perspectives between humans and rodents (McMullen and Mostyn, 2009), it is possible that maternal exercise interventions may revert the increased platelet reactivity phenotype described in **Chapter 4**. Definitive proof of this in humans will be of paramount importance to understand the extent to which increased platelet function contributes to cardiovascular outcomes later in

life in offspring born to obese mothers. Additionally, it remains to be explored whether low birthweight affects platelet function later in life and whether it is possible to fine-tune the intrauterine environment to develop healthier offspring. These lines of investigation should be further explored in the future.

It is possible that the concept of hormesis may not be applicable to platelets individually. Upon vascular injury, the sub-endothelium exposes collagen and Von Willebrand Factor (VwF), to which platelets bind to via collagen receptors GPVI and integrin $\alpha_2\beta_1$ and VwF receptors GPIbα and $\alpha_{IIb}\beta_3$ (for review, see (van der Meijden and Heemskerk, 2019)). Binding to these proteins will activate platelets leading to the secretion of several molecules, such as ADP and the release of thromboxane A_2 (TxA_2), that potentiate the initial response and recruit more platelets and leukocytes (for more detailed information, please refer to section **1.2** of **Chapter 1**). The intra-platelet machinery is thus composed of several positive feedback loops that lead to full platelet activation when confronted with an agonist, i.e. collagen, TxA_2. One may speculate that this "all or nothing" effect is needed for effective haemostasis.

In spite of the "all or nothing" aspect of platelet activation, data presented throughout this thesis reiterate that it is possible to fine-tune platelet function when these are integrated to the complex system of thrombosis and haemostasis. This may involve the use of inhibitors to develop more effective anti-platelet strategies with minimal bleeding defects (**Chapter 2** and **3**). Likewise, platelet fine-tuning may also involve a broader

feedback loop with metabolic components of mother and offspring affecting the function of platelets (**Chapter 4**).

5.2 Sex-specific effects on platelet function

The second overarching concept embroidered in the studies herein presented is how platelets are regulated differently according to sex. It is well established that the cardiovascular risk is greater for men when compared to pre-menopausal women and that this difference decreases with age (Jousilahti et al., 1999). The decreased risk in pre-menopausal women is thought to be at least partially dependant on circulating levels of oestrogen and progesterone, as it has been suggested previously that these hormones inhibit platelet aggregation elicited by a range of agonists (Nakano et al., 1998;Bar et al., 2000) and induce NO release by the endothelium (Nakano et al., 1998;Selles et al., 2001). In addition, 17β-estradiol has been consistently shown to mitigate endothelial dysfunction (Somani et al., 2019). For instance, Collins et al (Collins et al., 1995) have shown that estradiol attenuates endothelial dysfunction caused by atherosclerotic lesions in women. Furthermore, dual treatment with estradiol and progesterone was shown to decrease coronary vasospasm in hypercholesterolemic ovariectomized non-human primates (Miyagawa et al., 1997). Therefore, the protective effects of estradiol and progesterone have been described throughout different components of the cardiovascular system, including platelets and the endothelium.

In spite of the data mentioned above, the cardioprotective effects of estradiol and progesterone remain an area of debate as some studies do not support anti-platelet effects of these hormones proposed in other studies. Previous literature shows that 17β-estradiol may potentiate platelet activation following sub-threshold concentrations of thrombin (Moro et al.,

2005). Notably, progesterone metabolites have also been reported to stimulate platelets and induce rapid calcium influx (Blackmore, 2008). Thus, it is not fully understood why there is a sex-specific difference in cardiovascular risk, since female reproductive hormones or the lack of these do not fully explain the phenotype.

The difference in platelet function between males and females may involve genetic and nongenetic determinants. Indeed, Panova-Noeva et al (Panova-Noeva et al., 2016) evaluated single nucleotide polymorphisms related to mean platelet volume (MPV) in 4,175 individuals and concluded that MPV is determined by different factors between sexes. Higher MPV was associated with cardiovascular risk factors such as hypertension and smoking in males only, whereas pre-menopausal women or women in use of oral contraceptives presented higher MPV than post-menopausal or those not in use of oral contraceptives. Of note, higher MPV was associated with increased overall mortality only in males, probably due to the correlation between MPV and independent cardiovascular risk factors (hypertension and smoking).

In addition to differing determinants of MPV, there are also sex-specific differences in platelet function and responses to aspirin. Platelets from females have been reported to exhibit higher levels of aggregation induced by a range of agonists (ADP, epinephrine, collagen and arachidonic acid) when compared to males, regardless of ethnicity (Otahbachi et al., 2010). This was corroborated by Becker et al (Becker et al., 2006) who showed increased platelet reactivity and resistance to aspirin in women. In spite of these observations, it is still unclear why platelets from men and women

seem to behave differently and which mechanisms are responsible for such changes.

Therefore there is a need for studies focusing on women and female laboratory animals to optimize clinical therapy in a gender-specific strategy, as pointed out previously (Fareed and Hoppensteadt, 1996;Zuern et al., 2009). This notion has been reinforced more recently by funding agencies, as an attempt to balance sex in preclinical and *in vitro* studies and question the general perception that male-centric preclinical studies are less variable and thus more scientifically sound (Clayton and Collins, 2014). In line with this, only female mice were used for tail bleeding assays in **Chapter 2 and 3** as an attempt to foster the use of female subjects in preclinical cardiovascular research.

Data presented throughout **Chapters 2** and **3** were obtained from a mixture of healthy men and women. Although a direct comparison of the effects of myricetin (**Chapter 2**) or bepristat and ML171 (**Chapter 3**) was not made between males and females, all experiments were performed in a paired manner. Therefore conditions with inhibitors/compounds were always compared within each individual experiment, i.e. compared with the vehicle from the same donor. This decreased the likelihood that sex-specific differences were relevant to the effects herein observed. One could speculate that even if sex-specific effects cannot explain the differences herein observed, the degree of inhibition may differ between men and women. This possibility was not explored and poses as a limitation of the current study. More details on why one could observe sex-specific differences in the works presented in this Thesis are provided below.

In fact, the importance of considering gender as a relevant variable to preclinical studies is strengthened by the very biology of the proteins of interest in this Thesis: PDI and Nox-1. PDI has been shown to interact with oestrogen receptor α (ERα) in MCF-7 cells, acting as a molecular chaperone and assisting on the binding of 17β–estradiol to ERα through a thiol-disulphide exchange reaction (Schultz-Norton et al., 2006).

The importance of the redox state of PDI is corroborated by observations that S-glutathionylation of PDI abolishes the interaction of this protein with ERα, thus decreasing the effects of estradiol in a breast cancer cell line (Xiong et al., 2012). Notwithstanding, the possibility has also been raised that estradiol, but not progesterone, directly binds to PDI, since this hormone was reported to decrease the reductase activity of PDI *in vitro* (Tsibris et al., 1989). One could speculate that platelet PDI could mediate the effects of estradiol and investigation of how PDI contributes to estradiol-mediated effects in platelets could clarify contradictory findings of the past with regards to the anti- or pro-aggregatory effects of 17β–estradiol.

Notably, the human Nox-1 gene is located on the X chromosome and therefore the effects of this protein may differ in males and females, as previously shown for other genes also located on the X chromosome (AlSiraj et al., 2019). Nox-1 expression and activity are selectively regulated by G protein-coupled estrogen receptor 1 (GPER) and blockade of this receptor is a promising strategy to inhibit Nox-1 with no detected effects on other isoforms (for review, see (Barton et al., 2019)). Indeed, chronic exposure to 17β–estradiol in adult female rats increased mRNA levels of Nox-1 in the nervous system (Subramanian et al., 2015). Taken together, both PDI and

Nox-1 are regulated by and/or regulate the actions of estradiol. Future studies should focus on the contribution of these proteins to the actions of this hormone in platelets. This will shed light on possible mechanisms to explain differences in cardiovascular function with implication for differential risk described for men and women.

Future work should therefore explore the sex-specific effects of PDI and Nox-1 in cardiovascular disease. Notwithstanding, a similar argument is made for data shown in **Chapter 4**, in which only male offspring were used to investigate the maternal programming of platelet function. The rationale for using males was due to lack of resources to study both sexes, since preliminary data suggested the platelet and metabolic phenotypes were more prominent in male offspring of high-fat fed dams. Additional work is planned on this front, to further develop data contained in **Chapter 4** which supports a grant application to thoroughly examine the epigenetic effects of maternal obesity in platelets and megakaryocytes, as well as better characterize the model *in vivo* and study sex-specific differences.

5.3 Reactive oxygen species

The third overarching theme presented in this Thesis is ROS generation. ROS were introduced in the first section of **Chapter 1** as second messengers of ubiquitous presence in eukaryotic cells. These reactive species may function as contributors to healthy cell function in a process named *oxidative eustress*, for instance, by potentiating platelet activation (Masselli et al., 2020); but may also serve as disease markers when in excess, in a processed named *oxidative stress*, for instance in MetS (Vona et al., 2019). Thus, *oxidative eustress* encompasses the physiological regulatory roles of ROS, while *oxidative stress* is an imbalance between oxidant and antioxidant responses in favour of the oxidant agents (Sies, 2015). ROS measurements were made in **Chapter 2** (data not shown), **3** and **4** and their results, limitations and future perspectives were explored within experimental chapters and will be further discussed below.

The generation of ROS is a complex process within cells and has been proven to be a clear example of a hormetic response. This is exemplified by H_2O_2, which at low concentrations leads to increased expression and activities of antioxidant defences while at high concentrations culminates in cell death (Luna-Lopez et al., 2010;Luna-Lopez et al., 2014). In L929 mouse fibroblast cell line model, this hormetic response has been shown to be regulated by B-cell lymphoma 2 (Bcl-2) that sustains nuclear factor erythroid 2–related factor 2 (Nrf2) activation (Luna-Lopez et al., 2010). Of note, Nrf2 is one of the most studied transcription factors that induce antioxidant responses in cells and activation of Nrf2 has been proposed to be beneficial in a range of diseases (Ma, 2013;Luna-Lopez et al., 2014). Therefore, as

mentioned above, there is an ideal intermediate effect for ROS within cells in which excess or deficiency are deleterious.

ROS are important signalling molecules within platelets and liaise with other signalling molecules to fully activate platelets, for instance downstream of GPVI (as mentioned in sections **1.1** and **1.2** of **Chapter 1** and throughout **Chapters 3** and **4**). When in excess, ROS have been proposed to be implicated in platelet hyperactivity reported in MetS, since this condition is characterized by increased oxidative stress (for review, see (Whaley-Connell et al., 2011)). Indeed, Monteiro et al (Monteiro et al., 2012) showed that increased platelet activity in high-fat-fed rats correlated with higher intraplatelet production of ROS. The authors suggest that such increased ROS generation in rats fed a high-fat diet led to lower nitric oxide (NO) availability since NO donors inhibited platelet activation with lower efficacy when compared to lean animals. Redondo et al (Redondo et al., 2005) made similar observations in platelets from patients with type 2 diabetes. These authors showed that diabetes led to higher ROS production and calcium mobilization in platelets stimulated with thrombin and attributed this to increased generation of H_2O_2 since addition of catalase, an enzyme that depletes H_2O_2 (Kirkman et al., 1987), reverted these effects.

In **Chapter 4** murine offspring fed a high-fat (HF) diet or whose mothers were fed a high-fat diet exhibited higher levels of ROS in both platelets and other blood cells. This was accompanied by increased platelet size and reactivity for mice born to HF dams, but did not fully explain the metabolic programming effects of platelets since HF offspring born to lean dams also experienced increased ROS production, even though their platelet

function was unaltered compared to lean mice born to lean dams. One key limitation of this dataset is the absence of protein levels or gene expression of PDI and Nox-1 in platelets from these animals. Unfortunately there were technical difficulties with protein concentrations of samples and sample availability after several attempts and therefore I was unable to present this dataset. Notwithstanding, data contained in **Chapter 4** form the basis of a grant application to further explore how maternal MetS programmes platelet function in the offspring.

Maternal HF induced increased platelet size in male offspring, as presented in **Chapter 4**. ROS in the bone marrow induce megakaryocyte maturation and platelet production (for review, see (Chen et al., 2013)). Of interest to this thesis, Nox-1 is highly expressed in megakaryocytes and proposed to be the main source of ROS generation in these cells (McCrann et al., 2009), however it is unclear the relevance of Nox-1 in megakaryocyte differentiation and platelet production. Nox-1 has been reported to be more highly expressed in renal arteries and cortex of obese rats and to contribute to renal endothelial dysfunction in these animals (Munoz et al., 2020). In spite of this, it is yet to be determined whether Nox-1 expression in megakaryocytes is changed upon MetS onset and whether the activity of this enzyme would affect platelet count or MPV. This was partly explored in **Chapter 3** since I showed that Nox-1$^{-/-}$ female mice had unaltered MPV and platelet count when compared to age-matched wildtype mice. It is possible, however, that other Nox isoforms compensate for Nox-1 deletion in healthy animals or that Nox-1 is differentially regulated in health and disease. One future approach would be to attempt to induce MetS in Nox-1$^{-/-}$ mice through

feeding a calorie-enriched diet (e.g. high-fat, high-sucrose or cafeteria diet) and compare to wildtype obese animals in order to assess the contribution of Nox-1 to the platelet phenotype observed upon MetS. This is of particular interest considering data in **Table 3.1** of **Chapter 3** showing that human platelet Nox-1 levels are positively correlated with BMI. This same rationale can be applied to Nox-1$^{-/-}$ mice born to obese dams to determine how Nox-1 contributes to maternal programming of platelets. Therefore future studies should explore whether maternal metabolic dysfunction leads to increased ROS production in megakaryocytes of the offspring and if Nox-1 contributes to the phenotype observed.

PDI has also been implicated in the development of MetS. A study carried out by Chien et al (Chien et al., 2017) studied 669 adults to determine whether serum levels of ERp72, a thiol isomerase, would be correlated with markers of MetS. They suggest that serum ERp72 could be used as a potential biomarker for the diagnosis of MetS. In 2016, I proposed that platelet PDI could be an important contributor to the platelet hyperactivation seen in individuals with MetS (Gaspar et al., 2016), although at the time this was only a speculation based on indirect evidence from the literature. It is therefore an immense pleasure to finally address this question in **Chapter 3**. Here I showed that PDI expression levels in platelets were positively correlated with serum insulin and waist/hip ratio, which are surrogates for insulin resistance and central adiposity, respectively. Nox-1 was correlated with different components of MetS, namely BMI and systolic blood pressure. This, coupled with a lack of correlation between the expression of these proteins in platelets, suggest that PDI and Nox-1 are regulated by different processes

in platelets and may contribute to MetS through different pathways. Indeed, when PDI and Nox-1 were co-inhibitted, there was a more than additive effect in GPVI-mediated responses, including ROS generation. This involved phosphorylation of MAPKs, which are highly regulated by ROS (Son et al., 2011), and p47phox, which has been shown to interact directly with PDI (Gimenez et al., 2019) and orchestrate Nox-1 activation (Gimenez et al., 2019). Collectively, these data show that both PDI and Nox-1 are key for ROS production in platelets and may be implicated in platelet hyperactivation observed in MetS.

Throughout the experimental Chapters of this Thesis I propose that PDI is central for ROS production in platelets and that ROS is a key signalling event downstream of GPVI. In **Chapter 2** I show that myricetin is a flavonoid with potent anti-platelet properties that also inhibits thiol isomerases PDI and ERp5 at concentrations able to inhibit platelets, thus suggesting that PDI inhibition is a feasible mechanism of action for this flavonoid. ROS measurements in the presence of myricetin were not presented in **Chapter 3** as this dataset was not included on the final version of the manuscript. However, myricetin was able to inhibit CRP-induced ROS production measured as DCF fluorescence by approximately 35% at concentrations as low as 7.5 μM (data not shown). This could be due to antioxidant activity of myricetin (Chagas et al., 2018) or due to PDI inhibition and this should be further explored in the future.

One key point of discussion of these datasets is the use of DCF as a tool to measure ROS. This fluorescent dye has been used for over 30 years to measure ROS production in biological systems (Swann and Acosta, 1990) and

thus far is the most widely used ROS-detecting probe. In spite of this, there are several restraints to the use of DCF that should be taken into account. Firstly, this dye auto-oxidizes in several buffers and when diluted. For instance, Lu et al ((Lu et al., 2020), Figure 1B) have shown that DCF auto-oxidizes when measured in cardiomyocytes diluted in Tyrode's buffer (similar to the buffer used throughout this Thesis to resuspend platelets). Indeed, I have obtained similar curves when measuring a time-course of DCF fluorescence in platelets using a fluorimeter (data not shown). Due to the auto-oxidation of DCF I have only used paired samples, i.e. compared an experimental condition with a control (vehicle) from the same day and same donor and normalised all data to a resting control of that same donor. This approach decreased the likelihood that the differences observed were due to changes in auto-oxidation of DCF across samples, since all samples had the same rate of auto-oxidation given they were all obtained from the same donor and originated from the same solution in which the dye was incubated.

In addition to auto-oxidation, DCF faces criticism because it reacts with several ROS, reactive nitrogen species (RNS) and cellular antioxidants (for review, see (Chen et al., 2010)) and depends on esterases to become trapped within cells (Afzal et al., 2003). This criticism is reinforced by current needs to uncover the specific roles of different ROS within biological systems (Egea et al., 2017), thus prompting the development of probes to identify ROS selectively. In light of this, I have been careful with conclusions regarding the use of DCF in platelets and have referred to these datasets as ROS or oxidative stress instead of speculating which species is being measured. Notwithstanding, I argue that while it is important to understand the specific

roles of each ROS, the use of DCF should not be disregarded and that, by following strict scientific procedures, one can reliably measure unspecific ROS production using this probe.

Several attempts were made to use other probes and techniques to measure ROS. These included the fluorescent dye dihydroethidium (DHE), which has been proposed as an alternative for DCF to measure superoxide selectively (Zhao et al., 2003), pyrogallol red, which also reacts with superoxide selectively (Faundez et al., 2011) as well as electron paramagnetic resonance (EPR) to measure intracellular superoxide as shown previously (Vara et al., 2019). Measures of DHE, pyrogallol red and EPR were attempted in **Chapters 3** and **4**, however these were not successful due to technical difficulties. DHE fluorescence levels were not reliably detected in whole blood, platelet-rich plasma or washed platelets, probably due to antioxidant defence systems or low photo-stability. In addition, I have unsuccessfully tried to replicate an assay using DHE to measure superoxide production in platelets (Abubaker et al., 2019) due to lack of fluorescence at the excitation and emission wavelengths described in the above paper. Likewise, pyrogallol red oxidation also proved to be an unreliable way to measure superoxide formation in platelets since this is an absorbance assay and platelet aggregation changes the absorbance at the same wavelength in which pyrogallol red oxidation is measured. EPR measurements were performed, but due to lack of stability of one of the compounds used, these results were also discarded.

Therefore, DCF measurements were employed throughout experimental Chapters as a surrogate of ROS production and oxidative stress

due to stability, reliable protocols and replicable data using this dye. Future studies should use other techniques to selectively measure superoxide, hydrogen peroxide and other ROS as well as focus on specific sources of ROS within platelets, such as Nox enzymes and mitochondria.

5.4 Conclusion

The results collected within this thesis support strongly the notion that platelets are highly regulated by redox processes. This was shown by describing a novel PDI and ERp5 inhibitor, myricetin, which presented strong anti-platelet and anti-thrombotic properties with no effects on haemostasis (**Chapter 2**). This was reiterated by data in **Chapter 3** showing that inhibition of PDI using bepristat or co-inhibition of PDI and Nox-1 also promoted a strong anti-platelet effect while preserving haemostasis. Both PDI and Nox-1 were correlated with risk factors for MetS in a healthy population, suggesting these platelet proteins may be relevant to the increased platelet activity observed in chronic diseases, such as obesity and MetS. Still, this should be further explored in the future to determine whether inhibition of PDI and/or Nox-1 is indeed beneficial to patients with MetS. Finally, it is shown here that platelets can be programmed by maternal metabolic dysfunction, since male offspring born to dams fed a high-fat presented increased platelet size and reactivity (**Chapter 4**). This adds yet another layer of evidence to the deleterious effects of metabolic dysfunction during gestation and lactation. One interesting future line of investigation would be to test if interventions, such as maternal exercise (as discussed in section **5.1**), aimed to abrogate or reduce the metabolic dysfunctions induced by high-fat diet ingestion on mothers, are able to restore the platelet phenotype on the offspring. In addition, due to increased circulating ROS levels in offspring born to obese dams, it is possible that PDI and/or Nox-1 are relevant to the phenotype observed. Epigenetic changes in

megakaryocytes should also be explored. A summary of key findings is provided below in **Figure 5.1**.

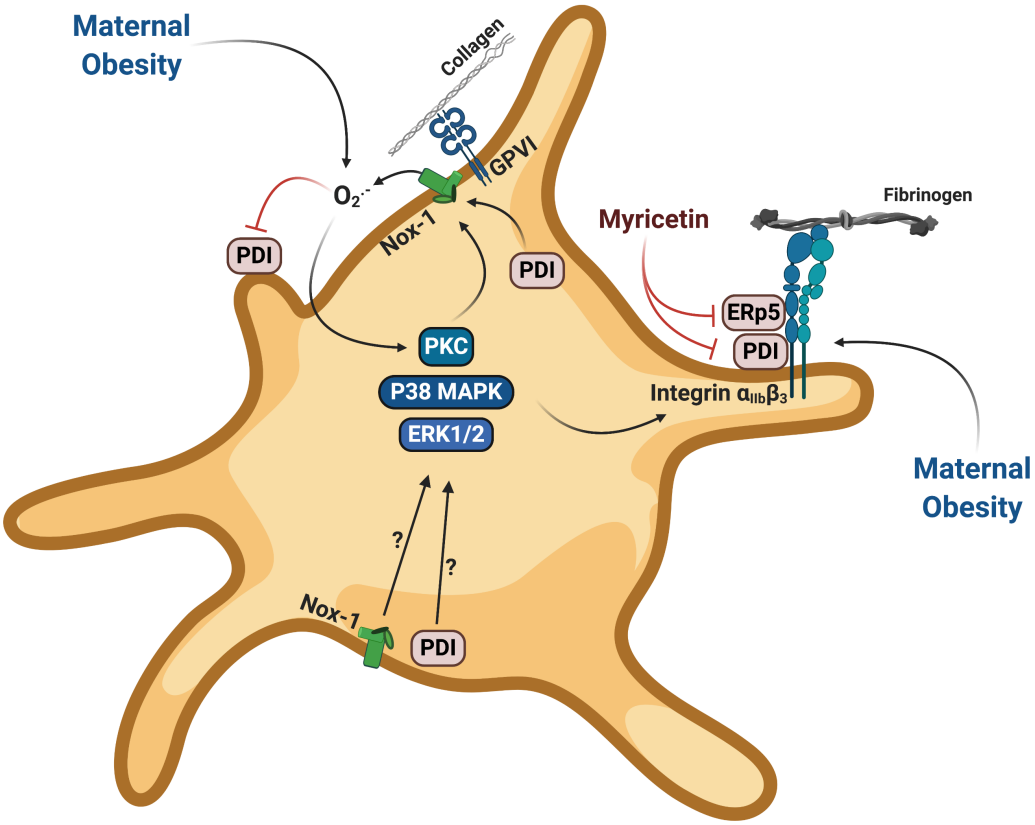

Figure 5.1. Platelets are regulated by redox processes. Upon collagen binding to clustered or dimeric glycoprotein VI (GPVI), NADPH oxidase 1 (Nox-1) will be activated by assembly of cytosolic components, which include protein disulphide isomerase (PDI). Nox-1 generates superoxide that will: 1) inhibit reductase activity of the platelet membrane, possibly through PDI inhibition (flat-head line) and 2) activate (arrow-head line) protein kinase C (PKC), p38 mitogen-activated protein kinase (p38MAPK) and extracellular signal-regulated kinase 1/2 (ERK1/2). PKC, p38MAPK and ERK1/2 will lead to the assembly of more Nox-1 in a positive feedback loop. Data gathered in this thesis suggest an alternative, yet unknown mechanism, by which PDI and Nox-1 induce activation of PKC, p38MAPK and ERK1/2. These proteins will activate integrin $\alpha_{IIb}\beta_3$ that will bind fibrinogen. This integrin is regulated by extracellular thiol isomerases, such as PDI and endoplasmic reticulum protein 5 (ERp5). Of note, the flavonoid myricetin was shown to inhibit both PDI and ERp5, thus reducing platelet function. In a broader feedback loop, this thesis has shown that maternal obesity leads to increased fibrinogen binding to platelets, which was correlated with increased reactive oxygen species (ROS) generation.

Altogether, data contained in this thesis support that PDI and Nox-1 are redox proteins of paramount importance to platelet activation and might also be relevant in metabolic dysfunction and that platelets can be programmed by maternal insults – an effect that is correlated with oxidative stress. These findings reinforce that platelets are highly regulated by redox processes.

5.5 References

Abubaker, A.A., Vara, D., Eggleston, I., Canobbio, I., and Pula, G. (2019). A novel flow cytometry assay using dihydroethidium as redox-sensitive probe reveals NADPH oxidase-dependent generation of superoxide anion in human platelets exposed to amyloid peptide β. *Platelets* 30**,** 181-189.

Afzal, M., Matsugo, S., Sasai, M., Xu, B., Aoyama, K., and Takeuchi, T. (2003). Method to overcome photoreaction, a serious drawback to the use of dichlorofluorescin in evaluation of reactive oxygen species. *Biochemical and biophysical research communications* 304**,** 619-624.

Alsiraj, Y., Chen, X., Thatcher, S.E., et al. (2019). XX sex chromosome complement promotes atherosclerosis in mice. *Nat Commun* 10**,** 2631.

Bar, J., Lahav, J., Hod, M., Ben-Rafael, Z., Weinberger, I., and Brosens, J. (2000). Regulation of platelet aggregation and adenosine triphosphate release in vitro by 17β-estradiol and medroxyprogesterone acetate in postmenopausal women. *Thrombosis and haemostasis* 84**,** 695-700.

Barker, D.J., and Osmond, C. (1986). Infant mortality, childhood nutrition, and ischaemic heart disease in England and Wales. *The Lancet* 327**,** 1077-1081.

Barker, D.J., and Osmond, C. (1987). Death rates from stroke in England and Wales predicted from past maternal mortality. *Br Med J (Clin Res Ed)* 295**,** 83-86.

Barton, M., Meyer, M.R., and Prossnitz, E.R. (2019). Nox1 downregulators: A new class of therapeutics. *Steroids* 152**,** 108494.

Becker, D.M., Segal, J., Vaidya, D., Yanek, L.R., Herrera-Galeano, J.E., Bray, P.F., Moy, T.F., Becker, L.C., and Faraday, N. (2006). Sex differences in platelet reactivity and response to low-dose aspirin therapy. *JAMA* 295**,** 1420-1427.

Blackmore, P.F. (2008). Progesterone metabolites rapidly stimulate calcium influx in human platelets by a src-dependent pathway. *Steroids* 73**,** 738-750.

Calabrese, E.J. (2008). Converging concepts: adaptive response, preconditioning, and the Yerkes-Dodson Law are manifestations of hormesis. *Ageing Res Rev* 7**,** 8-20.

Calabrese, E.J., and Baldwin, L.A. (1997). The dose determines the stimulation (and poison): development of a chemical hormesis database. *International Journal of Toxicology* 16**,** 545-559.

Chagas, V.T., Coelho, R., Gaspar, R.S., Da Silva, S.A., Mastrogiovanni, M., Mendonca, C.J., Ribeiro, M.N.S., Paes, A.M.A., and Trostchansky, A. (2018). Protective Effects of a Polyphenol-Rich Extract from Syzygium cumini (L.) Skeels Leaf on Oxidative Stress-Induced Diabetic Rats. *Oxid Med Cell Longev* 2018**,** 5386079.

Chen, S., Su, Y., and Wang, J. (2013). ROS-mediated platelet generation: a microenvironment-dependent manner for megakaryocyte proliferation, differentiation, and maturation. *Cell Death Dis* 4**,** e722.

Chen, X., Zhong, Z., Xu, Z., Chen, L., and Wang, Y. (2010). 2',7'-Dichlorodihydrofluorescein as a fluorescent probe for reactive oxygen species measurement: Forty years of application and controversy. *Free Radic Res* 44**,** 587-604.

Chiavaroli, V., Marcovecchio, M.L., De Giorgis, T., Diesse, L., Chiarelli, F., and Mohn, A. (2014). Progression of cardio-metabolic risk factors in subjects born small and large for gestational age. *PLoS One* 9**,** e104278.

Chien, C.Y., Hung, Y.J., Shieh, Y.S., Hsieh, C.H., Lu, C.H., Lin, F.H., Su, S.C., and Lee, C.H. (2017). A novel potential biomarker for metabolic syndrome in Chinese adults: Circulating protein disulfide isomerase family A, member 4. *PLoS One* 12**,** e0179963.

Clayton, J.A., and Collins, F.S. (2014). Policy: NIH to balance sex in cell and animal studies. *Nature* 509**,** 282-283.

Collins, P., Rosano, G.M., Sarrel, P.M., Ulrich, L., Adamopoulos, S., Beale, C.M., Mcneill, J.G., and Poole-Wilson, P.A. (1995). 17β-Estradiol attenuates acetylcholine-induced coronary arterial constriction in women but not men with coronary heart disease. *Circulation* 92**,** 24-30.

Crescente, M., Pluthero, F.G., Li, L., et al. (2016). Intracellular Trafficking, Localization, and Mobilization of Platelet-Borne Thiol Isomerases. *Arterioscler Thromb Vasc Biol* 36**,** 1164-1173.

Egea, J., Fabregat, I., Frapart, Y.M., et al. (2017). European contribution to the study of ROS: A summary of the findings and prospects for the future from the COST action BM1203 (EU-ROS). *Redox Biol* 13**,** 94-162.

Evagelidou, E.N., Giapros, V.I., Challa, A.S., Cholevas, V.K., Vartholomatos, G.A., Siomou, E.C., Kolaitis, N.I., Bairaktari, E.T., and Andronikou, S.K. (2010). Prothrombotic state, cardiovascular, and metabolic syndrome risk factors in prepubertal children born large for gestational age. *Diabetes Care* 33**,** 2468-2470.

Fareed, J., and Hoppensteadt, D.A. (Year). "Pharmacology of the low-molecular-weight heparins", in: *Seminars in thrombosis and hemostasis*), 13-18.

Faundez, M., Rojas, M., Bohle, P., Reyes, C., Letelier, M., Aliaga, M., Speisky, H., Lissi, E., and López-Alarcón, C. (2011). Pyrogallol red oxidation induced by superoxide radicals: Application to evaluate redox cycling of nitro compounds. *Analytical biochemistry* 419**,** 284-291.

Gaspar, R.S., Trostchansky, A., and Paes, A.M. (2016). Potential Role of Protein Disulfide Isomerase in Metabolic Syndrome-Derived Platelet Hyperactivity. *Oxid Med Cell Longev* 2016**,** 2423547.

Gimenez, M., Verissimo-Filho, S., Wittig, I., et al. (2019). Redox Activation of Nox1 (NADPH Oxidase 1) Involves an Intermolecular Disulfide Bond Between Protein Disulfide Isomerase and p47(phox) in Vascular Smooth Muscle Cells. *Arterioscler Thromb Vasc Biol* 39**,** 224-236.

Henschler, D. (2006). The origin of hormesis: historical background and driving forces. *Hum Exp Toxicol* 25**,** 347-351.

Holbrook, L.M., Sasikumar, P., Stanley, R.G., Simmonds, A.D., Bicknell, A.B., and Gibbins, J.M. (2012). The platelet-surface thiol isomerase enzyme ERp57 modulates platelet function. *J Thromb Haemost* 10**,** 278-288.

Holbrook, L.M., Watkins, N.A., Simmonds, A.D., Jones, C.I., Ouwehand, W.H., and Gibbins, J.M. (2010). Platelets release novel thiol isomerase enzymes which are recruited to the cell surface following activation. *Br J Haematol* 148**,** 627-637.

Jasuja, R., Passam, F.H., Kennedy, D.R., et al. (2012). Protein disulfide isomerase inhibitors constitute a new class of antithrombotic agents. *J Clin Invest* 122**,** 2104-2113.

Jordan, P.A., Stevens, J.M., Hubbard, G.P., Barrett, N.E., Sage, T., Authi, K.S., and Gibbins, J.M. (2005). A role for the thiol isomerase protein ERP5 in platelet function. *Blood* 105**,** 1500-1507.

Jousilahti, P., Vartiainen, E., Tuomilehto, J., and Puska, P. (1999). Sex, age, cardiovascular risk factors, and coronary heart disease: a prospective follow-up study of 14 786 middle-aged men and women in Finland. *Circulation* 99**,** 1165-1172.

Kirkman, H.N., Galiano, S., and Gaetani, G. (1987). The function of catalase-bound NADPH. *Journal of Biological Chemistry* 262**,** 660-666.

Kraut, R. (2001). Aristotle's ethics.

Laker, R.C., Lillard, T.S., Okutsu, M., Zhang, M., Hoehn, K.L., Connelly, J.J., and Yan, Z. (2014). Exercise prevents maternal high-fat diet-induced hypermethylation of the Pgc-1alpha gene and age-dependent metabolic dysfunction in the offspring. *Diabetes* 63**,** 1605-1611.

Lu, S., Liao, Z., Lu, X., et al. (2020). Hyperglycemia acutely increases cytosolic reactive oxygen species via O-linked GlcNAcylation and CaMKII activation in mouse ventricular myocytes. *Circulation Research* 126**,** e80-e96.

Luna-Lopez, A., Gonzalez-Puertos, V.Y., Lopez-Diazguerrero, N.E., and Konigsberg, M. (2014). New considerations on hormetic response against oxidative stress. *J Cell Commun Signal* 8**,** 323-331.

Luna-Lopez, A., Triana-Martinez, F., Lopez-Diazguerrero, N.E., Ventura-Gallegos, J.L., Gutierrez-Ruiz, M.C., Damian-Matsumura, P., Zentella, A., Gomez-Quiroz, L.E., and Konigsberg, M. (2010). Bcl-2 sustains hormetic response by inducing Nrf-2 nuclear translocation in L929 mouse fibroblasts. *Free Radic Biol Med* 49**,** 1192-1204.

Ma, Q. (2013). Role of nrf2 in oxidative stress and toxicity. *Annu Rev Pharmacol Toxicol* 53**,** 401-426.

Marklund, S., and Marklund, G. (1974). Involvement of the superoxide anion radical in the autoxidation of pyrogallol and a convenient assay for superoxide dismutase. *European journal of biochemistry* 47**,** 469-474.

Masselli, E., Pozzi, G., Vaccarezza, M., Mirandola, P., Galli, D., Vitale, M., Carubbi, C., and Gobbi, G. (2020). ROS in Platelet Biology: Functional Aspects and Methodological Insights. *Int J Mol Sci* 21.

Mccord, J.M., and Fridovich, I. (1969). Superoxide dismutase an enzymic function for erythrocuprein (hemocuprein). *Journal of Biological chemistry* 244**,** 6049-6055.

Mccrann, D.J., Eliades, A., Makitalo, M., Matsuno, K., and Ravid, K. (2009). Differential expression of NADPH oxidases in megakaryocytes and their role in polyploidy. *Blood* 114**,** 1243-1249.

Mcmullen, S., and Mostyn, A. (2009). Animal models for the study of the developmental origins of health and disease: Workshop on 'Nutritional models of the developmental origins of adult health and disease'. *Proceedings of the Nutrition Society* 68**,** 306-320.

Miyagawa, K., Rösch, J., Stanczyk, F., and Hermsmeyer, K. (1997). Medroxyprogesterone interferes with ovarian steroid protection against coronary vasospasm. *Nature medicine* 3**,** 324-327.

Monteiro, P.F., Morganti, R.P., Delbin, M.A., Calixto, M.C., Lopes-Pires, M.E., Marcondes, S., Zanesco, A., and Antunes, E. (2012). Platelet hyperaggregability in high-fat fed rats: a role for intraplatelet reactive-oxygen species production. *Cardiovasc Diabetol* 11**,** 5.

Moore, G.S., Kneitel, A.W., Walker, C.K., Gilbert, W.M., and Xing, G. (2012). Autism risk in small- and large-for-gestational-age infants. *Am J Obstet Gynecol* 206**,** 314 e311-319.

Moro, L., Reineri, S., Piranda, D., et al. (2005). Nongenomic effects of 17beta-estradiol in human platelets: potentiation of thrombin-induced aggregation through estrogen receptor beta and Src kinase. *Blood* 105**,** 115-121.

Munoz, M., Lopez-Oliva, M.E., Rodriguez, C., et al. (2020). Differential contribution of Nox1, Nox2 and Nox4 to kidney vascular oxidative stress and endothelial dysfunction in obesity. *Redox Biol* 28**,** 101330.

Nakano, Y., Oshima, T., Matsuura, H., Kajiyama, G., and Kambe, M. (1998). Effect of 17beta-estradiol on inhibition of platelet aggregation in vitro is mediated by an increase in NO synthesis. *Arterioscler Thromb Vasc Biol* 18**,** 961-967.

Otahbachi, M., Simoni, J., Simoni, G., Moeller, J.F., Cevik, C., Meyerrose, G.E., and Roongsritong, C. (2010). Gender differences in platelet aggregation in healthy individuals. *J Thromb Thrombolysis* 30**,** 184-191.

Panova-Noeva, M., Schulz, A., Hermanns, M.I., et al. (2016). Sex-specific differences in genetic and nongenetic determinants of mean platelet volume: results from the Gutenberg Health Study. *Blood* 127**,** 251-259.

Pettitt, D.J., and Knowler, W.C. (1998). Long-term effects of the intrauterine environment, birth weight, and breast-feeding in Pima Indians. *Diabetes care* 21**,** B138.

Redondo, P.C., Jardin, I., Hernandez-Cruz, J.M., Pariente, J.A., Salido, G.M., and Rosado, J.A. (2005). Hydrogen peroxide and peroxynitrite enhance Ca2+ mobilization and aggregation in platelets from type 2 diabetic patients. *Biochem Biophys Res Commun* 333**,** 794-802.

Reynolds, R.M., Allan, K.M., Raja, E.A., et al. (2013). Maternal obesity during pregnancy and premature mortality from cardiovascular event in adult offspring: follow-up of 1 323 275 person years. *Bmj* 347**,** f4539.

Salvemini, D., De Nucci, G., Sneddon, J.M., and Vane, J.R. (1989). Superoxide anions enhance platelet adhesion and aggregation. *Br J Pharmacol* 97**,** 1145-1150.

Schultz-Norton, J.R., Mcdonald, W.H., Yates, J.R., and Nardulli, A.M. (2006). Protein disulfide isomerase serves as a molecular chaperone to maintain estrogen receptor alpha structure and function. *Mol Endocrinol* 20**,** 1982-1995.

Selles, J., Polini, N., Alvarez, C., and Massheimer, V. (2001). Progesterone and 17 β-estradiol acutely stimulate nitric oxide synthase activity in rat aorta and inhibit platelet aggregation. *Life sciences* 69**,** 815-827.

Sies, H. (2015). Oxidative stress: a concept in redox biology and medicine. *Redox Biol* 4**,** 180-183.

Somani, Y.B., Pawelczyk, J.A., De Souza, M.J., Kris-Etherton, P.M., and Proctor, D.N. (2019). Aging women and their endothelium: Probing the relative role of estrogen on vasodilator function. *American Journal of Physiology-Heart and Circulatory Physiology* 317**,** H395-H404.

Son, Y., Cheong, Y.K., Kim, N.H., Chung, H.T., Kang, D.G., and Pae, H.O. (2011). Mitogen-Activated Protein Kinases and Reactive Oxygen Species: How Can ROS Activate MAPK Pathways? *J Signal Transduct* 2011**,** 792639.

Southam, C.M. (1943). *Effects of Extract of Western Red-cedar Heartwood on Certain Wood-decaying Fungi in Culture.*

Stanford, K.I., Takahashi, H., So, K., et al. (2017). Maternal Exercise Improves Glucose Tolerance in Female Offspring. *Diabetes* 66**,** 2124-2136.

Stevens, H., and Mcfadyen, J.D. (Year). "Platelets as Central Actors in Thrombosis—Reprising an Old Role and Defining a New Character", in: *Seminars in thrombosis and hemostasis*: Thieme Medical Publishers), 802-809.

Subramanian, M., Hahn-Townsend, C., Clark, K.A., Mohankumar, S.M., and Mohankumar, P.S. (2015). Chronic estrogen exposure affects gene expression in the rostral ventrolateral medulla of young and aging rats: Possible role in hypertension. *Brain Res* 1627**,** 134-142.

Swann, J.D., and Acosta, D. (1990). Failure of gentamicin to elevate cellular malondialdehyde content or increase generation of intracellular reactive oxygen species in primary cultures of renal cortical epithelial cells. *Biochemical pharmacology* 40**,** 1523-1526.

Tsibris, J.C., Hunt, L., Ballejo, G., Barker, W., Toney, L., and Spellacy, W. (1989). Selective inhibition of protein disulfide isomerase by estrogens. *Journal of Biological Chemistry* 264**,** 13967-13970.

Van Der Meijden, P.E.J., and Heemskerk, J.W.M. (2019). Platelet biology and functions: new concepts and clinical perspectives. *Nat Rev Cardiol* 16**,** 166-179.

Vara, D., Cifuentes-Pagano, E., Pagano, P.J., and Pula, G. (2019). A novel combinatorial technique for simultaneous quantification of oxygen radicals and aggregation reveals unexpected redox patterns in the activation of platelets by different physiopathological stimuli. *haematologica* 104**,** 1879-1891.

Vona, R., Gambardella, L., Cittadini, C., Straface, E., and Pietraforte, D. (2019). Biomarkers of Oxidative Stress in Metabolic Syndrome and Associated Diseases. *Oxid Med Cell Longev* 2019**,** 8267234.

Whaley-Connell, A., Mccullough, P.A., and Sowers, J.R. (2011). The role of oxidative stress in the metabolic syndrome. *Rev Cardiovasc Med* 12**,** 21-29.

Xiong, Y., Manevich, Y., Tew, K.D., and Townsend, D.M. (2012). S-Glutathionylation of Protein Disulfide Isomerase Regulates Estrogen Receptor alpha Stability and Function. *Int J Cell Biol* 2012**,** 273549.

Zhao, H., Kalivendi, S., Zhang, H., Joseph, J., Nithipatikom, K., Vásquez-Vivar, J., and Kalyanaraman, B. (2003). Superoxide reacts with hydroethidine but forms a fluorescent product that is distinctly different from ethidium: potential implications in intracellular fluorescence

detection of superoxide. *Free Radical Biology and Medicine* 34**,** 1359-1368.

Zuern, C.S., Lindemann, S., and Gawaz, M. (2009). Platelet function and response to aspirin: gender-specific features and implications for female thrombotic risk and management. *Semin Thromb Hemost* 35**,** 295-306.